NOTICE

The quality of this microform is heavily dependent upon the quality of the original thesis submitted for microfilming. Every effort has been made to ensure the highest quality of reproduction possible

If pages are missing, contact the university which granted the degree.

Some pages may have indistinct print especially if the original pages were typed with a poor typewriter ribbon or if the university sent us an inferior photocopy.

Reproduction in full or in part of this microform is governed by the Canadian Copyright Act, R.S.C 1970, c. C-30, and subsequent amendments.

AVIS

La qualité de cette microforme dépend grandement de la qualité de la thèse soumise au microfilmage Nous avons tout fait pour assurer une qualité supérieure de reproduction.

S'il manque des pages, veuillez communiquer avec l'université qui a conféré le grade.

La qualité d'impression de certaines pages peut laisser à désirer, surtout si les pages originales ont été dactylographiées à l'aide d'un ruban usé ou si l'université nous a fait parvenir une photocopie de qualité inférieure

La reproduction, même partielle, de cette microforme est soumise à la Loi canadienne sur le droit d'auteur, SRC 1970, c. C-30, et ses amendements subséquents.

ISBN 0-315-56097-5

Doppler Effects and Coding Performance of Hybrid Spread Spectrum Systems

Ali Hassan M. Targi

A Thesis

in

The Department

of

Electrical and Computer Engineering

Presented in Partial Fulfillment of the Requirements
for the Degree of Master of Enginneering at
Concordia University
Montréal, Québec, Canada

April, 1990

ABSTRACT

Doppler Effects and Coding Performance of Hybrid Spread Spectrum Systems

Ali Hassan M. Targi

The bit error probability is evaluated for a Hybrid Chirp/Direct sequence spread spectrum communication system. The received signal is received in Doppler, the channel is contaminated by pulsed barrage jammer with a varying duty factor. Moreover, the Direct Sequence DS correlation loss due to imperfect code synchronization is taken into account. The tradeoffs involved in dividing the total RF bandwidth into the DS and chirp bandwidths to combat both the jamming and the Doppler are discussed.

A new DS/TH spread spectrum (SS) system is also proposed in this thesis. The system is intended to increase the multiaccess efficiency of a SS system by employing time diversity and a new class (multi decoding-erasure-error) forward error correction scheme. Bose Chaudhuri Hocquenghem (BCH) code is employed and an algorithmic demodulation rule is used in conjunction with a modified majority vote among the outputs of many decoders to finally yield a superior error and throughput performance. We also show in this thesis that the extra side information represented by the DS preample acquisition matched filter output can be used to adjust the thresholds in the demodulation erasure generation process to reflect the instantaneous format condition of multi-access interference.

ACKNOWLEDGEMENTS

I would like to express my deep gratitude to my thesis supervisor Dr. A. K. Elhakeem, for his continuous encouragement, advices and guidance during the course of this thesis.

LIST OF FIGURES

LIST OF PRINCIPAL SYMBOLS

F	chirp signal bandwidth
Δ	frequncy doppler
T_b	time bamdwith product of the chirp signal
ϕ_o	arbitrary phase angle
T	the duration of bit
MF	matched filter
S_l	the probability of l users selecting the same TH slot
m_p	data bits constitute the preample length
N_b	data bit constitute the remander of the TH slot
PG	processing gain
C_p	the cross-correlation based on the preample period
C_b	the cross-correlation based on one data bit period
σ_l^2	the equavelent noise variance given l users
R_b^l	sourse rate
λ_l^j	the probability of the threshoul TH_j being selected
$\xi_{K/l}^i$	the probability of having K erasures in a record of N_b demodulated bits in a certain TH slot
θ_l	the single bit eresure probability averagd over all thresholds
q_e^l	the bit error probability on the channel
P_1^l	the probability of decoding bit error from the first decoder
P_2^l	the probability of decoding bit error from the seconde decoder

P_3^l	the probability of decoding bit error from the thired decoder
P_4^l	the probability of decoding bit error from the fourth decoder
T_F	the frame length
N_F	the number of TH slots
e	number of errors that can be corrected
i^{th}	the selected i^{th} code out of U codes for transmission
TH_j	erasure threshold
P_h	probability that any one user select a specific TH slot for transmission
S_l	probability of l users selecting the same TH slot
$\overline{n}$	the length of the feedback shift registers used to generate the code
L	the code length of each number of the RS family
T_c	the chip period
T_b	the data bit length on the channel
$P_h^l(r)$	the envelope of the branch not containing the signal
$P_{s+n}^l(r)$	the envelope of the branch containing the signal
σ^2	the equivalent noise variance
R_b	the data rate
$A^2/2$	transmitted power of each interfering user
μ_l	probability of error given l
γ'	the eresure probability of a single bit of a TH slot
JJ	MF equalization levels
K	number of errors in a record of N_b demodulated bits in a certain TH slot

$f_{1,l}$ the probability of BCH decoding symbol error if there is no more than $(n - k)$ erasures occure in the decoding input

$f_{2,l}$ the probability of BCH decoding symbol error if the applicable TH slot has a high amaunt of meltiaccess interfarence such that the number of arasurs is $> e$

S/N signal to noise ratio

TABLE OF CONTENTS

CHAPTER 1

INTRODUCTION

The demand of more telecommunication capacity, to serve the world's need has grown normally in the past ten decades to provide a broad range of services required by modern civilization. From here, there is a need for more efficient ways of sharing the radio spectrum. The conventional way of allocating the spectrum is frequency division, however, for many kinds of services this is inefficient. Spread spectrum techniques seem to offer benefits for spectrum sharing, for some applications, superior to those of frequency division [30]. The technique is based upon a principle which is a direct antithesis of reducing bandwidth, for it utilizes modulated signal spectra that deliberately employ large emission bandwidths to send information requiring a bandwidth much less than is transmitted [30]. Spread spectrum techniques, through the properties of coded modulation, can provide systems which produce low interface to other systems, have high interference rejection capability, provide multiple access capability, antijam capability, improved spectral efficiency, and have other useful capabilities.

Spread spectrum techniques are divided into four basic types.

1- Direct Sequence DS.

2- Frequency Hopping FH.

3- Time Hopping TH.

4- Chirp.

Combining two or more of the four techniques results in a technique called hybrid system. One reason for using hybrid techniques is that some of the advan-

tages of types of systems are combined in a single system. Hybrid techniques are widely used in military spread spectrum systems and are currently the only practical way of achieving extremely wide spectrum spreading.

In this thesis we start in Chapter 2 by providing a tutorial summary of some of the principles of the spread spectrum techniques.

We will study two hybrid techniques. One is DS/Chirp signals under Doppler and pulsed jamming. The chirp signals (pulse compression) offer an increase in the average power available, to illuminate radar targets without any loss at the receiver of the resolution needed for the tactical requirement of the system. The signals used are simple, they are just sweep-frequency. The secret is in the receiver which employs a dispersive filter to match the swept signal and to compress it into a much narrower time slot.

For the DS/chirp signals under Doppler and pulsed jamming spread spectrum system the signal is received in Doppler, the channel is contaminated by a pulsed jammer. The bit error probability of this system with varying duty factor, and the DS correlation loss due to interface code synchronization was considered. Also the trade-off in valued in dividing the total radio-frequency bandwidth into the DS and chirp bandwidths to combat both the jamming and Doppler are discussed.

The second hybrid techniques we will study here is DS/TH, where we study a new proposed DS/TH spread spectrum system. The system is intended to increase the multi-access efficiency of the spread spectrum system by employing time diversity and a new class (multi-decoding-erasure-error) for word error correction scheme. A BCH code is the basic code employed and an algorithmic demodulation rule is used in conjunction with a modified majority rate among

the outputs of many decoders to finally yield a superior error and throughput performance. In this thesis we also show that the extra side information represented by DS preample acquisition matched filter output can be used to adjust the thresholds on the demodulation erasure generation process to reflect the instantaneous condition of multi-access interface.

CHAPTER 2

SPREAD SPECTRUM TECHNIQUES FOR COMMUNICATION

2.1 Direct Sequence Systems (DS)

Direct Sequence (also called pseudo-noise or direct spread), in which a carrier is modulated by a digital code sequence having a bit rate much higher than the information signal bandwidth. The classical concept of modulation involves the variation of one of the three parameters (amplitude, frequency, or phase) associated with a pure sine wave so as to carry information. In the digital communications, the digital signal may be regarded conceptually as a sequence of ones and zeros. In practice, these include a pulse train in which one is a pulse and zero is a no-pulse, or using a high frequency CW signal for which a phase shift of 0^0 is a one and 180^0 a zero , each lasting a unit of duration. The pulse sequence train can be viewed as a kind of amplitude-modulated square wave, while the 0_0 , 180_0 sequence may be regarded either as a phase modulated sine wave or as balanced, amplitude-modulated sine wave.

Direct sequence spread spectrum systems are so called because they employ a high-speed code sequence (the high-speed code sequences are just long binary sequences of ones and zeros at bit rates usually in the range from one to a few hundred MHz), in addition to the basic information being sent, to double-sideband suppressed modulate their radio-frequency carrier. Binary code sequences as short as a few hundred bits or as long as 2^{89} (and longer) have been employed for this purpose, at code rates from fractions of a bit per second to several gigabit per second [29]. Fig. 2.1 shows the block diagram of a simplified

direct sequence PN system, the message to be transmitted can be considered to be first modulated on a carrier resulting in a signal with a spectral width that is proportional to the message bandwidth. The signal is then phase modulated by a code generator which has a specific phase pattern. The code generator is a binary M-sequence generator which has the desirable properties that it can be constructed from binary shift register stages and that it produces a stream of binary shift register stages and that it produces a stream of binary digits that are uncorrelated [43].

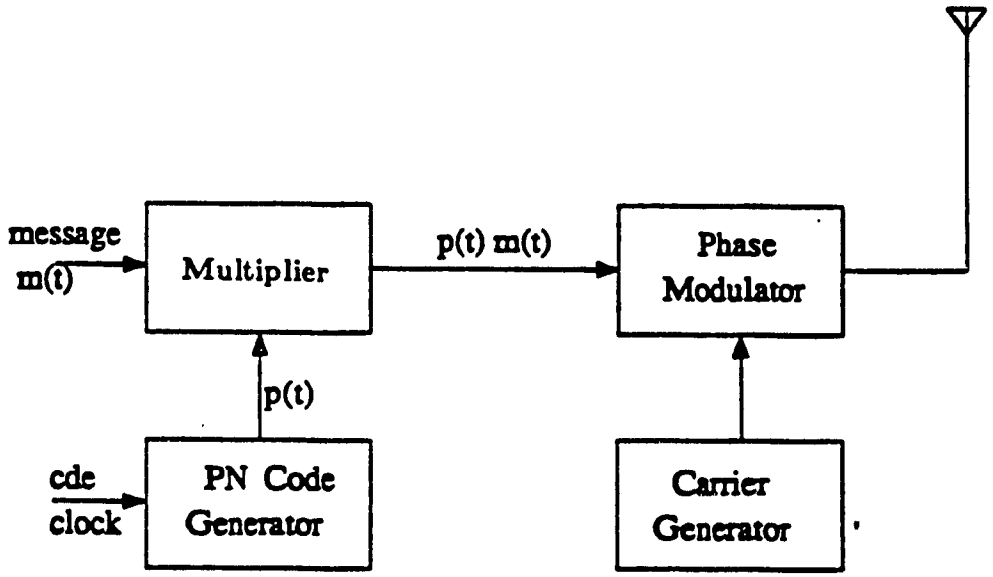

Fig.(2. 1a):- Block digram of a direct sequence transmitter

To derive the shape of the transmitted spectrum, let's consider the message signal to be m(t), p(t) is the PN binary sequence, and the two binary states of the waveforms to be +1 and -1, $m_1(t)$ represent the reclocked message (assume that the binary message is reclocked sequence transitions) the transmitted signal is given by

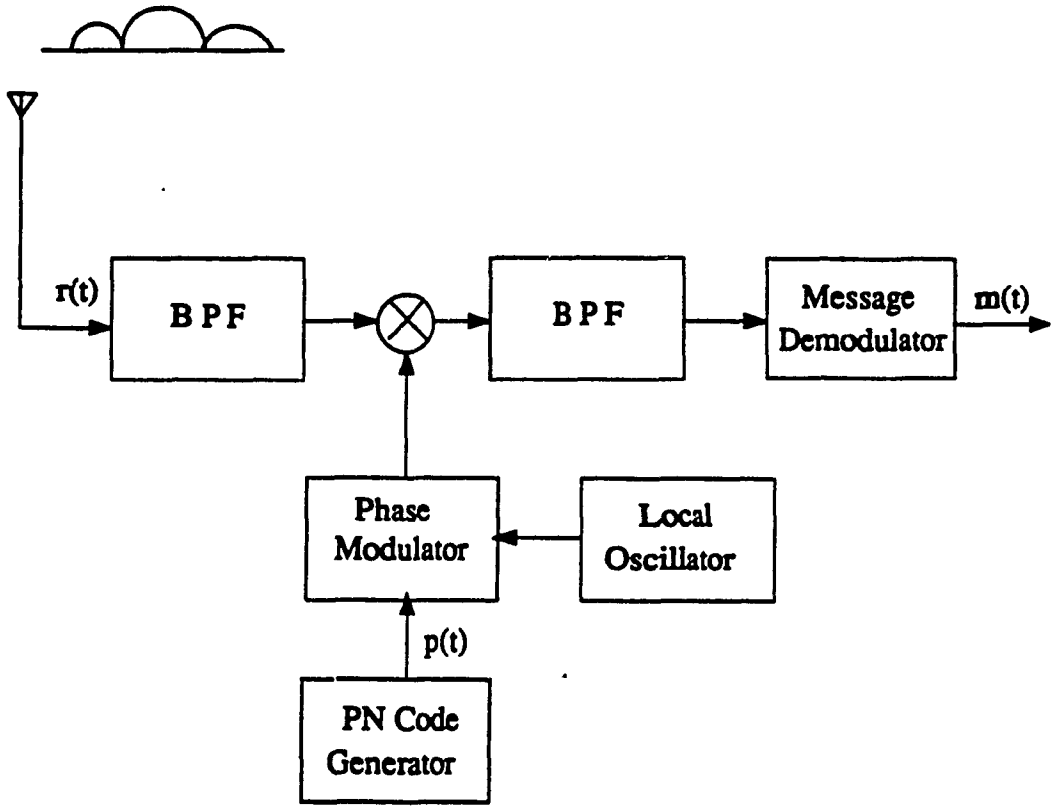

Fig.(2. 1b):- Block digram of a direct sequence receiver

$$s(t) = m_1(t)\, p(t) \sin(\omega_o + \phi_o), \tag{2.1}$$

where ϕ_o is an arbitrary phase angle. Since $m_1(t)\, p(t)$ is a sequence of ± 1 levels, s(t) may also given by

$$s(t) = \sin(\omega_o t + \phi_{pm}(t) + \phi_o), \tag{2.2}$$

where

$$\phi_{pm} = \begin{cases} 0\ , & when \quad m_1(t)\, p(t) = 1 \\ \\ \pi\ , & when \quad m_1(t)\, p(t) = -1 \end{cases} \tag{2.3}$$

Using the relation that the power spectrum is the Fourier transform of the autocorrelation function, the spectrum can be defined from that

$$S(\omega) = \frac{1}{2\pi} \int_{-\infty}^{\infty} R_s(\tau)\, e^{-j\omega\tau}\, d\tau \tag{2.4}$$

and

$$R_s(\tau) = \frac{1}{2T_1} \int_{-T_1}^{T_1} s(t)\, s(t+\tau)\, dt \tag{2.5}$$

$$= R_{mp}(\tau) \cos(\omega\tau)$$

and $R_{mp}(\tau)$ is the autocorrelation function of the binary signal, and this autocorrelation function and its corresponding power spectrum $P(\omega)$ are shown in Fig. 2.2. The power spectrum $P(\omega)$ is

$$P(\omega) = T\left[\frac{\sin(\omega T/2)}{\omega T/2}\right]^2 \tag{2.6}$$

where T is the duration of bit (chip) of the sequence. The transmitted signal has a spectrum with a shape of $(\frac{\sin x}{x})^2$, so

$$S(\omega) = T\left[\frac{\sin(\omega - \omega_o)T/2}{(\omega - \omega_o)T/2}\right]^2 \tag{2.7}$$

At the receiver end the signal $s(t)$ is received with power S then it is multiplied by a locally generated reference signal $2p(t)\cos\omega_1 t$, the resultant signal $r(t)$ is

$$r(t) = \sqrt{2S}\,p(t)\,m_1(t)\,\cos(\omega_o + \phi)\,2p(t)\,\cos(\omega_1 t) \tag{2.8}$$

Since

$p(t).p(t) = 1$ then

$$r(t) = \sqrt{2S}\;\; m_1(t)\,\cos(\omega_2 t + \phi) \tag{2.9}$$

centered at $\omega_2 = \omega_o - \omega_1$. Then $r(t)$ can be demodulated in a conventional way to get the original signal $m_1(t)$. In case of interference and noise the effect of multiplication by the reference signal $2p(t)\cos(\omega_1 t)$ can be seen by assumed $i(t)$ to be other signals, and also $i(t)$ and $p(t)$ are not related. The output of the multiplier is

$$r(t) = i(t)\,2p(t)\,\cos(\omega_1 t) \tag{2.10}$$

The power spectrum of this product signal can be obtained, as follows. Let

$$p_1(t) = 2p(t)\cos(\omega_1 t) \tag{2.11}$$

so the autocorrelation function of $r(t)$ is

$$R_r(\tau) = \frac{1}{2T}\int_{-T}^{T} i(t)\, i(t+\tau)\, p_1(t)\, p_1(t+\tau)\, dt \tag{2.12}$$

the power spectrum of the signal is the transformation of $R_r(\tau)$. since the $i(t)$ and $p_1(t)$ are uncorrelated,

$$R_r(\tau) = R_i(\tau)\, R_{p_1}(\tau) \tag{2.13}$$

and so

$$R(\omega) = I(\omega) * P_1(\omega) \tag{2.14}$$

this is the convolution of the spectra of the two signals (the reference and the interference signal). The output of the band-pass filter can be demodulated by a conventional demodulation.

An important parameter that is sometimes useful in specifying the performance of a spread spectrum signal in the presence of interference is known as the processing gain. This processing gain, P_G is frequently defined as the ratio of the signal bandwidth to the message bandwidth that is

$$P_G = \frac{B_S}{B_m} = 2\frac{t_m}{t_1} \tag{2.15}$$

where t_m is the message bit duration and t_1 is the chip duration [17].

After the IF/RF conversion, the RF power density of the transmitted signal, compared to a conventional narrow-band transmission, is reduced according to ratio f_c / f_m, for high values of the process gain the spectral power density of the received signal could be below the noise power.

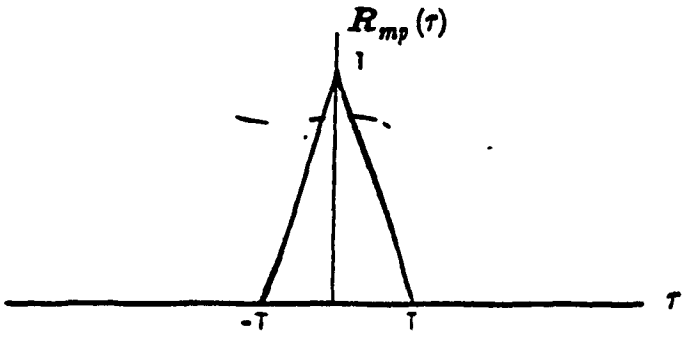

$T = \frac{1}{f_c}$ period of code clock

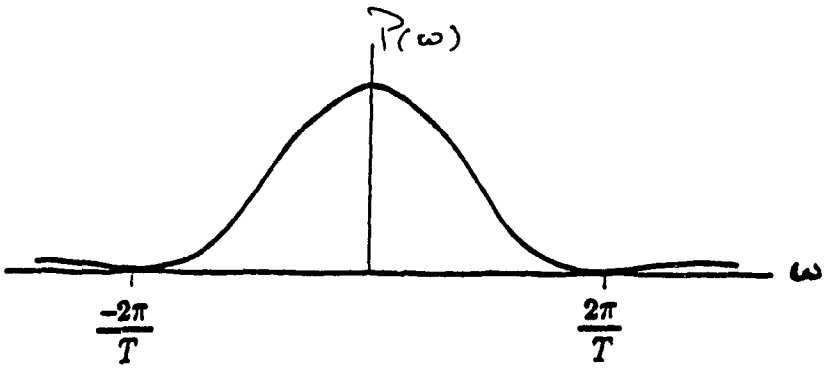

Fig.(2. 2):- Spectrum of PN signal

2.2 Frequency Hopping (FH)

Frequency hopping, in which the carrier is frequency shifted in discrete increments in a pattern determined by a digital code sequence. Frequency hopping it does first what its name implies that is, it "hops" from frequency to frequency over a wide band. The specific order in which frequencies are occupied is a function of a code sequence, and the rate of hopping from one frequency to another is a function of the rate at which information is to be sent. This code sequence are the same type as those used by the direct sequence system, with the exception that the code clock rate is usually low (where direct sequence code rates are usually in the 1Mbit/s to 100Mbit/s range, frequency hopping codes do not normally exceed a few hundred kilobits per second) [16].

The rate of hopping from frequency to frequency and the number of frequency choices in any frequency hopping system is governed by the requirements placed on it for a particular use. Fig. 2.3 shows a simplified block diagram of a frequency hopping system. The working principle of this system is quite simple; spreading of the spectrum is obtained by changing the carrier frequency f_i over the whole available band, according to a pseudo- noise multilevel sequence (PN code). The set of frequencies (or narrow-band channels) used by the frequency hopping is called "hop-set". The bandwidth over which the energy is spread is essentially independent of the code clock rate and can be chosen by a combination of the number and size of frequency hops. An ideal spectrum for a FH spread-spectrum method is shown in Fig. 2.4. It has a rectangular envelope and extends over a bandwidth $B_{RF} = (2^n - 1)\,\Delta f$, where n is the number of stages used in the shift register to generate the frequency hopping code and Δf is the frequency separation discrete frequencies, which must be at least as wide as the information

bandwidth, B_m [30]. The transmitter should be designed to transmit, to a degree as close as practical, the same amount of power in every channel.

At the receiver a frequency synthesizer driven by a PN code generator, this generate a logically frequency-shifting reference signal which is multiplied by the incoming signal in a mixer, any signal that is not a replica of the local reference is spread by multiplication with the local reference. Bandwidth of an undesired signal after multiplication with the local reference is equal to the covariance of the two signals. A signal with the same bandwidth as the local reference (but nonsynchronous) would have twice the reference bandwidth at the IF. The IF then can reject all of the undesired signal power that lies outside its bandwidth. Because this IF bandwidth is only a fraction of the bandwidth of the local reference, almost all the undesired signal's power is rejected, whereas a desired signal is enhanced by being correlated with the local reference.

As in direct sequence spread spectrum modulation, a meaningful parameter, with respect to interference spread uniformly across the RF band, is the processing gain, which for an FH system is

$$G_P = \frac{B_{RF}}{B_m} \tag{2.16}$$

when several frequency-hopping signals occupy a common RF channel, simultaneous occupancy of a given frequency slot may result in message errors. This is the basic reason why error-correction coding is needed in a frequency-hopping system since the error-correction capability of the code can restore the message that are destroyed by mutual interference.

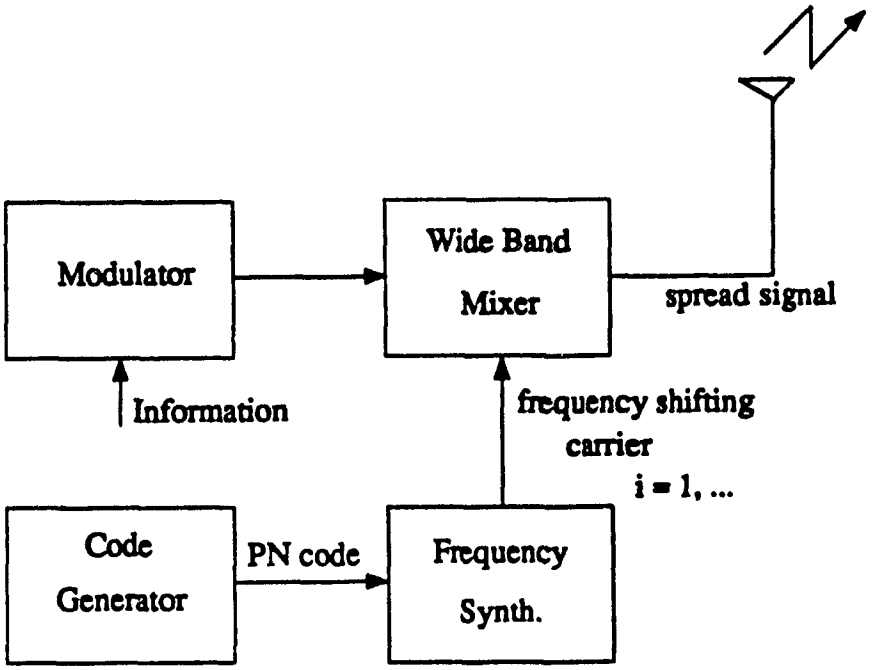

a, Transmitter

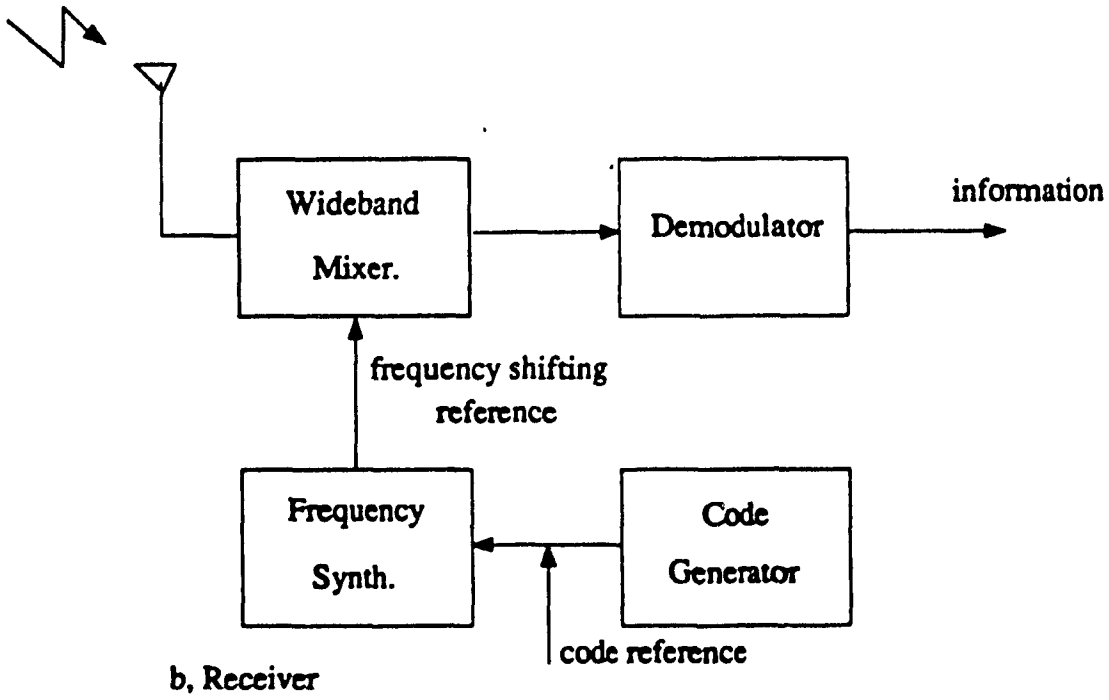

b, Receiver

Fig.(2. 3):- Block digram of frequency hopping system, (a) transmitter, (b) receiver.

Frequency-hopping system advantages:

- Create amount of spreading.
- Can be programmed to avoid portions of the spectrum.
- Relatively short acquisition time.
- Less affected by near-far problem.

Disadvantages:

- Complex frequency synthesizer.
- Not useful for range and range-rate measurement.
- Error-correction required.

2.3 Time Hopping (TH)

In time hopping systems spreading of the spectrum is achieved by compressing the information signal in the time domain. That is, the time hopping systems control their transmission time and period with a code sequence in the same way that frequency hoppers control their frequency. In fact, time hopping can be viewed as pulse modulation under code sequence control, and diagram for a time hopper can be generated by adding carrier- on-off control to the direct sequence diagram. A typical sample time-hopping system is shown in Fig. 2.5. A time-hopping waveform is given in Fig. 2.6, where the time axis is divided into intervals known as frames, and each one of these frames is subdivided into M time slots. During each frame one and only one time slot will be modulated with a message by any reasonable modulation method [17]. Time slot is chosen for a given frame is selected by means of a PN code generator.

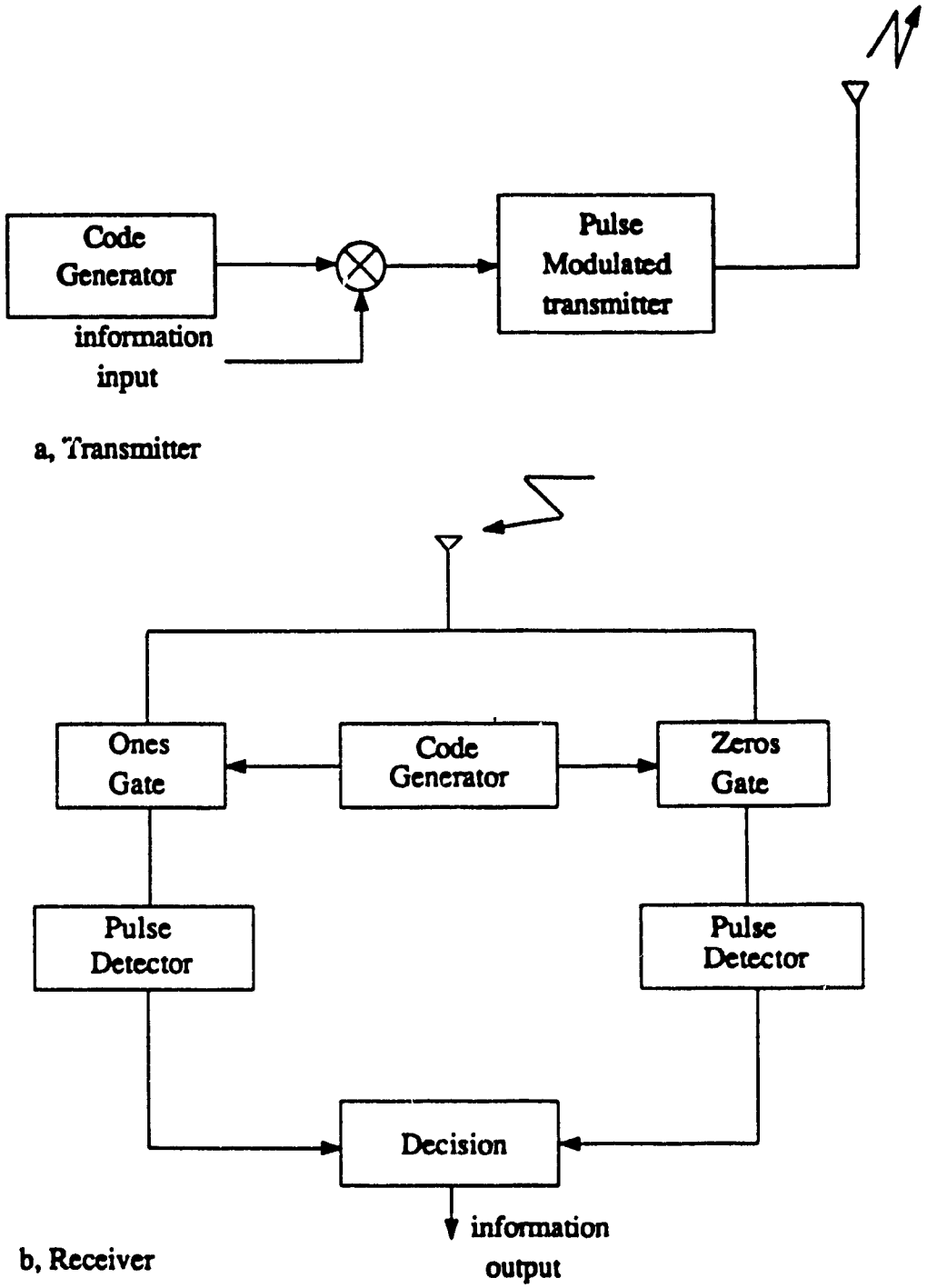

Fig.(2. 5):- Simple time hopping system block digram,
(a) transmitter, (eceiver [18].

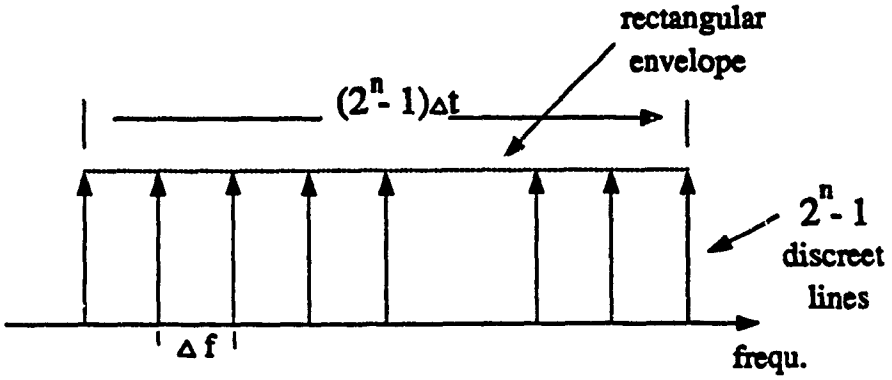

Fig.(2. 4):- Power spectrum of FH spread spectrum signal

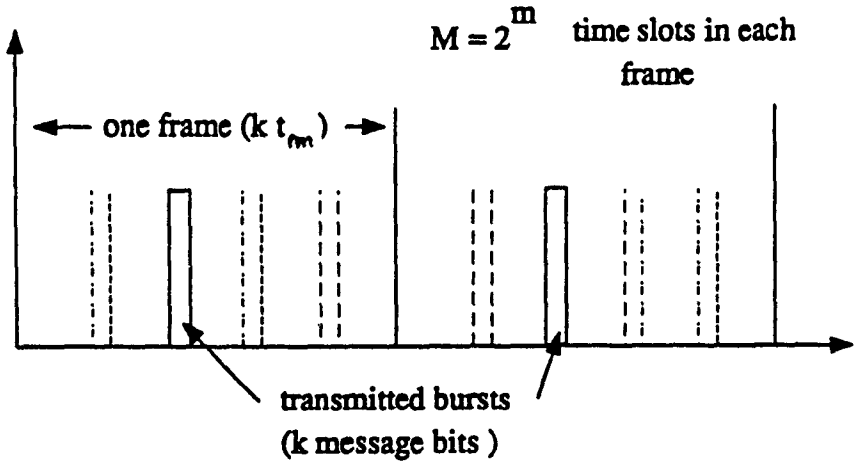

Fig.(2. 6):- Time-hopping waveform

Time hopping may be used to aid in reducing interference between systems in TDM. Interference among simultaneous users in a time-hopping system can be minimized by coordinating the times at which each user can transit a signal, which also avoid the problem of very strong signals at a receiver swamping out the effects of weaker signals. In a non-coordinated system, overlapping transmission bursts will result in message errors, and for this it will normally require the use of error-correction coding to restore the proper message bits.

Time Hopping Advantages

- High bandwidth efficiency
- Implementation simpler than FH

Time Hopping Disadvantages

- Long acquisition time
- Error correction needed

2.4 Chirp Spread Spectrum Systems

Frequency-modulation pulse compression, or chirp, is a technique in which a carrier is swept linearly over a wide band of frequencies during a given pulse. This technique of spectrum spreading was developed a number of years ago to improve radar operation by obtaining the resolution of a short pulse, but with the detection capability of a long pulse. A long transmitted pulse is suitably modulated and the receiver is designed to act on the modulation to compress the pulse into a much shorter one. In this technique each transmitted signal element gives a linear change of frequency with time. Each received signal element is operated on by a matched filter, which coherently combines the signal spectral components

into a narrower signal of increased amplitude. The advantage of this technique for radar systems is that significant power reduction is possible, also chirp waveforms are in general less affected by Doppler shifts due to motion of the target relative to the radar, and this is often significant when high-velocity targets must be catered for. Specifically, the chirps waveforms suffers very little from Doppler-induced correlation loss relative to PN-spread symbols of the same time duration. However, the chirp waveforms does have the property that the apparent time- of-arrival shifts as a function of Doppler offset, for this chirp modulation is used in jam-resistant communication and pulse-compression radars.

The receiver used for chirp signals is a matched filter, matched to the angular rate of change of the transmitting frequency-sweep signal. The transmitted frequency-swept-signal chirp signal is like that produced by common laboratory sweep generator, that is because most chirp systems use a linear sweep pattern. Any pattern suitable to the requirement that a matching receive filter must be built, is suitable. Let us consider a linear swept signal or leaner FM chirp modulation. The transmitted waveform is designed consists of a rectangular pulse of constant amplitude A and duration T, as in Fig. 2.7. The transmitted signal can be written

$$f(t) = \begin{cases} cos\,(\omega_o\, t + \frac{1}{2}\mu t^2), & -T/2 \leq t \leq T/2 \\ 0 & , \ elswher \end{cases} \tag{2.17}$$

where μ is the FM slope ($\mu = 2\pi B/T$, and ω_o is the angular frequency carrier, and T is the transmitted pulse duration. The matched filter has an impulse response, $h(t)$, which is the time inverse of the signal at the receiver input as

given below

$$H(t) = \sqrt{\frac{2\mu}{\pi}}\, cos\,(\omega_o\, t\, -\, \frac{1}{2}\mu t^2),\ -T/2 \leq\ t\ \leq T/2 \qquad (2.18)$$

where the $\sqrt{2\mu/\pi}$ is a factor that results in unity gain[42]. By translation to the frequency domain via the Fourier transform, simplifying, and passing back to the time domain, as in Appendix A experiment assuming the Doppler is zero, one can show that the output $\psi_1(t)$ resulting from passing $s(t)$ through $h(t)$ is given by

$$\psi_1(t) = \sqrt{\frac{\mu T^2}{2\pi}}\, \frac{sin\,(\mu Tt/2)}{(\mu Tt/2)}\, \exp[j\,(\omega_o\, t\, -\, \frac{1}{2}\mu t^2 + \pi/4)] \qquad (2.19)$$

the resulting response envelope form unweighted chirped pulse is shown in Fig. 2.7.

In communication systems the receiver signal processing is similar to that used in chirp radar. The main difference is that in the communication system, both upward and downward frequency sweeps have to be detected, whereas in radar application only sweeps in one direction are used. Also, in communication SS systems Mark and Space data signals are defined by chirp signals having ascending and descending frequency sweeps, respectively, and are transmitted in the same frequency band. At the receiver, two matched filters are used, one matched to the mark chirp signal and the other to the space chirp signal, where mark and space are used to represent "ones and zeros" in digital communication. Conventional interfering signal such as white noise and carrier do not contain the frequency pattern required for time compression and pass through the matched filters essentially unchanged in amplitude. The mark signal input to the mark dispersive network (signal matched to the filter) the output is as given in equation (2.19) and

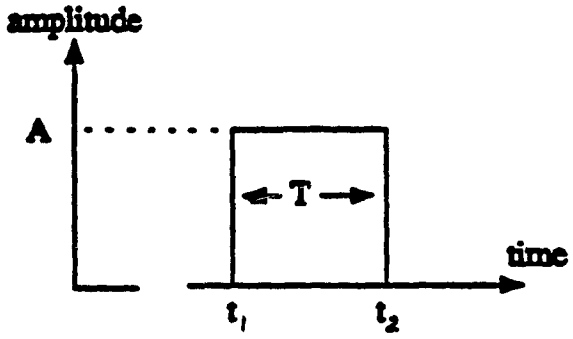

a, Transmitted pulse of amplitude A and duration T.

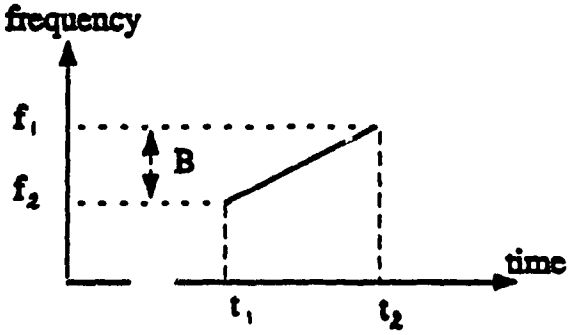

b, linear frequency variation over bandwidth B and transmitted pulse.

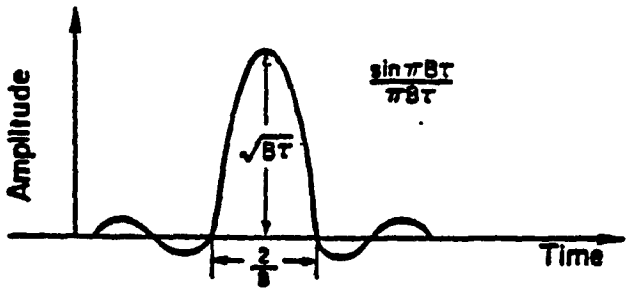

c,output of the receiver filter.

Fig.(2. 7):- Linear FM spectrum signals, (a) transmitted pulse, (b) variation of transmitted pulse, (c) output of the receiver filter.

the output $\psi_2(t)$ from the same network for space input signal (signal not matched to the filter) is

$$\psi_2(t) = \begin{cases} \frac{1}{\sqrt{2}} \exp j\left[\omega_o t - \frac{\mu t^2}{4} + \frac{\pi}{4}\right], & -T < t < T \\ 0 & , \textit{elsewhere} \end{cases} \tag{2.20}$$

where unity network gain and zero mean time delay are assumed. The mark signal is increased in amplitude to peak value of $\sqrt{\frac{\mu T^2}{2}\pi}$ and compressed in time to a signal with $\frac{sin(x)}{x}$ envelope form. The space signal is reduced in amplitude by a factor $1/\sqrt{2}$. These two signals are shown in Fig. 2.7.

Chirp SS Systems advantages

- Significant power reduction is possible
- Coding is not normally used

2.5 Hybrid Spread-Spectrum Systems

Hybrid spread spectrum systems made up by combining two two or more of, direct-sequence, frequency-hopping, time-hopping, chirp, modulation technique, to offer certain advantage of a particular (method/technique) while avoiding the disadvantages, or to offer very wide-band and/or very high process gain, or to combine some of the advantages of two or three types of systems in a single system, and minimize the disadvantages of those types. Many different hybrid combination are possible. Some of these are :

DS/FH

DS/TH

DS/Chirp Signals

FH/TH

DS/FH/TH

Hybrid systems are widely used in military spread spectrum systems and they are now being employed in most of the newest systems at this time, as mobile communication services, indoor communication, ... , etc. Use of hybrid systems meets two basic needs : First, high performance which requires wide spectrum expansions; by combining more techniques, wide spectrum expansion is achieved without stressing too much each single one. Second, the high flexibility that actual operational scenario, a hybrid system allows to adjust the mix of (evasion) and (resistance) to optimize the (protection) against any defined (threat) and, in perspective, to keep pace with the evolution of the threat. Implementation in hybrid systems is not necessarily increased in difficulty by the same factor, however; that is, a combined frequency hopping and direct sequence (DS/FH) transmitter might be built up of readily constructed code sequence generators and frequency synthesizers whereas a straightforward direct sequence modulator or frequency hopper could not be constructed to do the same job.

2.5.1. FH/DS Hybrid Systems

The analysis and results of this section are from the above references. the same as an example of hybrid system that have been dealt with in the given section are applied to the new system in chapter 4.

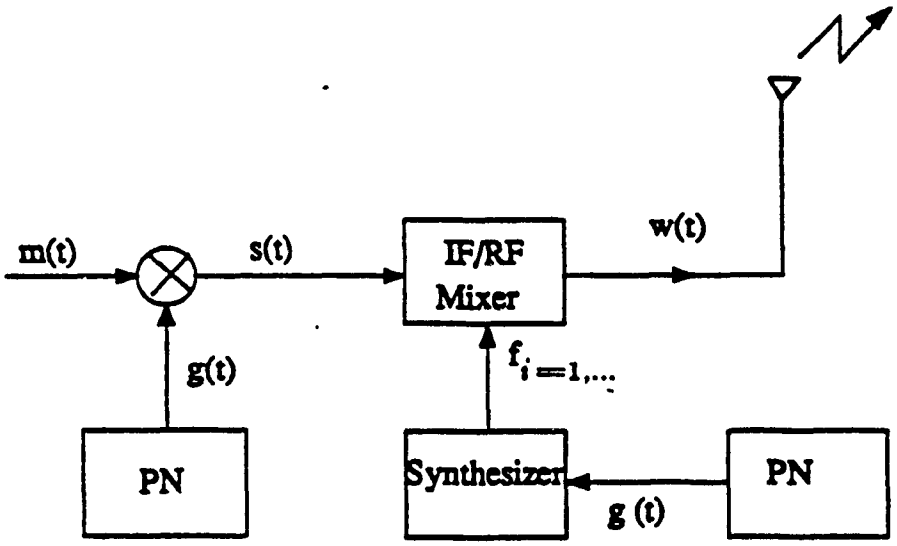

Fig.(2. 8):- FH/DS hybrid transmitter

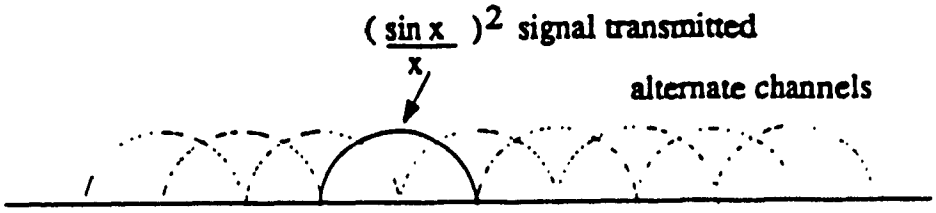

Fig.(2. 9):- Frequency spectrum of hybrid FH/DS system

Many methods of combining direct sequence and frequency hopping are possible, depending on the goal to achieve [22], [23]. The basic block diagram of an FH/DS transmitter is shown in Fig. 2.8. In this system PN code is used to spread the signal to an extent limited by either code generator acquisition time or speed, and the frequency hopping would be used to increase the frequency spread. The DS code rate is normally much faster than the rate of frequency hopping, and the number of frequency channels available is usually much smaller than the number of code chips. The difference between the frequencies in the frequency-hopping portion of the system would normally be equal to the bandwidth of the PN code modulation. The hybrid FH/DS modulation differs from a single direct sequence modulator mainly in that the carrier frequency is varying (hopping) rather than being at a constant frequency, as far simple as modulation. In this system the synchronization between the frequency-hopping and the direct sequence patterns means that whenever a given sector of the direct sequence code pattern is transmitted the frequency channel will be the same. The frequency system of the FH/DS output is shown in Fig. 2.9.

Fig. 2.10 illustrates a typical FH/DS receiver, the received hopping signal first converted to a fixed frequency and then de-spread into its original band, while any other uncorrelated signals is spread. The spread spectrum demodulation is achieved by using locally generated replicas of the PN codewords used at the transmitter for frequency hopping and direct sequence modulation. The code must be synchronized with the received signal before the signal can be properly demodulated.

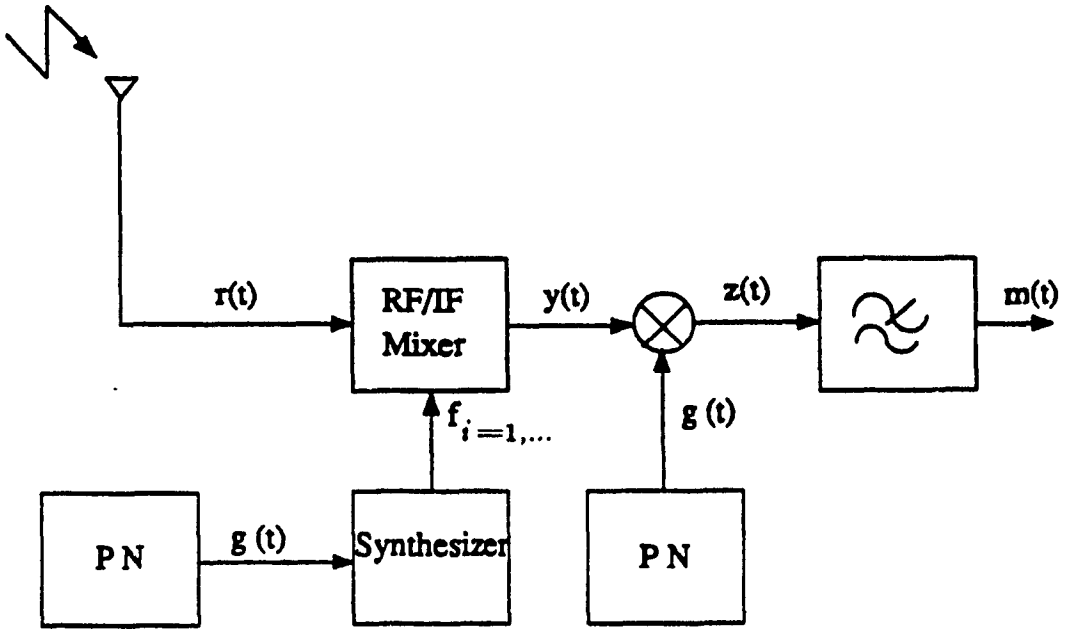

Fig.(2. 10):- FH/DS hybrid system receiver

The hybrid FD/DS process gain is a function of

$$BW_{RF} / R_{info} \tag{2.21}$$

where BW_{RF} is the RF bandwidth of the transmitted signal and R_{info} is the bit rate of the information [18]. A well dimensional hybrid system offers to the communication a very good and sophisticated protection. A high process gain is easily achieved by the FH technique, and signal keeps all the great advantages of the direct sequence modulation as the resistance to narrow-band interference, and the multipath rejection.

As an example of DS/FH hybrid communication system [22], [23] was presented a Coherent and a Noncoherent direct-sequence/Slow Frequence-Hopping Multi-Access Spread Spectrum (DS/SFH MA) Communication system. The performance of synchronous and asynchronous of each one over additive white Gaussian noise channels is examined. In coherent DS/SFH multi-access communication, the performance of the system was examined employing binary or quaternary Phase-Shift-Keying (PSK) data modulation with arbitrary chip waveforms. The signature sequences are concerned in both cases, deterministic and random, as well as Reed-Solomon periodic frequency-hopping patterns. The proposed transmitter and receiver of this system, and the system models are given in [22]. The probabilities of error were calculated, and one of the results, as shown in Fig. 2.11, it shows the average error probability versus the signal to noise ratio E_b / N_O for synchronous and asynchronous binary hybrid spread spectrum multiple - access systems with different values of number of active users K. Notice that hybrid SSMA systems employing random signature sequences the asynchronous systems perform better than the corresponding synchronous systems (due to the extra averaging with respect to the time delays which takes place in the

former case), whereas for deterministic signature sequences, the synchronous system outperform the corresponding asynchronous systems. Fig. 2.12 show the average probability of error versus the signal to noise ratio E_b/N_o for synchronous and asynchronous quaternary SSMA systems compare favorably to the DS-SSMA, SFH-SSMA systems using the same modulation and demodulation schemes and have the same bandwidth spread. It was concluded that hybrid spread spectrum systems with quaternary PSK modulation can support fewer users than the corresponding systems which employ binary PSK modulation [22]. Also it was found that synchronous hybrid spread spectrum systems can support fewer users than asynchronous hybrid spread spectrum systems when hopping patterns and signature sequences are employed.

In the noncoherent hybrid direct sequence slow frequency hopped spread spectrum multiple-access (DS/SFH SSMA) system [23], deal with the situation in which the receiver can acquire time synchronization with the desired signal but it can not acquire a phase reference Also here the hopping rates are slightly smaller than or even equal to the data rate. The modulation schemes used are differential phase shift keyed DPSK and frequency shift keying FSK. Fig. 2.13 show the proposed transmitter . Where the $b_k(t)$ is the kth data signal $c_k(t)$ is the output of the kth DS/SS modulation it is different for DPSK modulation schemes. For the binary FSK modulation $c_k(t)$ of the K^{th} user is given by

$$c_k(t) = 2\sqrt{2P}\,\psi(t)a_k(t)\cos[2\pi(f_c + b_k(t)W)t + \theta_k(t)] \qquad (2.22)$$

Where P is the common power of the transmitted signal, $\psi(t)$ and the hop duration T_c are normalized so that $T_c^{-1}\int_0^{T_c}\psi^2(\lambda)\,d\lambda = 1$, where $\psi(s) = \psi(t)$ for $s = t \pmod{T_c}$. $a_k(t)$ is the code wave form which is periodic which is a

periodic sequence of unit amplitude positive and negative rectangular pulses of duration T_c , f_c is the carrier frequency $b_k(t)$ is the kth data signal, W is the spacing frequencies and $\theta_k(t)$ is the phase introduced by the kth frequency shift keying modulator . If the lth pulse of the information sequence $b_l^{(k)} = m$ for $m = +1$ or -1 then $\theta_k(t) = \theta_k$, where θ_k is the phase angle which corresponds to the frequency tone $f_c + mW$ $(m = 1, -1)$, and the spacing between the two frequency tone is $2W$).

For the Differential Phase shift Keying (DPSK) modulation the output of the kth (user) DS/SS modulator $c_k(t)$ is given by.

$$c_k(t) = 2\sqrt{2P}\ b_{(k)}\,\psi(t)\,a_k(t)\cos(2\pi f_c\,t + \theta_k) \tag{2.23}$$

Where θ_k is the phase angle introduced by the kth DPSK modulator. $c_k(t)$ the DS/SS signal as shown in the transmitter system is frequency-hopping according to the kth hopping pattern $f_k(t)$ it is derived from a sequence of frequencies $f_i^{(K)}$ from a set $S = [v_1, v_2, \cdots, v_q]$ of q. By assuming $W >> 2T^{-1} = 2(NT_c)^{-1}$ so there is no overlapping of the DS/SS signals when hopped to adjacent frequencies. Let $f_j^{(k)}$ denote the frequency used by the kth signals during the jth dwell time and T_h the duration of a single hopping interval. The number of data bits transmitted per hop is $N_b = T_h/T$ is a positive integer. At the end of the transmitter, the transmitted signal for FSK DS/SFH SS signal is given by .

$$\begin{aligned} S_k(t) &= \sqrt{2P}\ \psi(t)\,a_k(t) \\ &\quad .\cos\left[2\pi(f_c + b_k(t)W + f_k(t))t + \theta_k(t) + \alpha_k(t)\right] \end{aligned} \tag{2.24}$$

In case of DPSK DS/SFH SS signal the transmitted signal is given by

$$S_k(t) = \sqrt{2P}\ b_k(t)\,\psi(t)\,a_k(t) \cos\left[2\pi(f_c + f_k(t))t + \theta_k + \alpha_k(t)\right] \tag{2.25}$$

where $\alpha_k(t)$ in both of the above equations represent the phase waveform introduced by the kth frequency hopper. This waveform takes on the constant value $\alpha_j^{(k)}$ during the jth dwell time.

At a particular receiver the received signal has the form

$$r(t) = \sum_{k=1}^{K} S_k(t - \tau_k) + n(t) \tag{2.26}$$

where $n(t)$ is an Additive White Gaussian Noise AWGN process of two-sided spectral density $\frac{1}{2}N_o$, and τ_k for $1 \le k \le K$ is the time delays along the communication links between the K transmitters and the particular receiver. The receiver for hybrid DS/ SFH SSMA system employing DPSK modulation is shown in [23]. The receiver is assumed to be capable of acquiring frequency-hopping pattern, time synchronization with ith signal, and signature sequence. The received signal pass through band pass-filter, which is followed by the de hopper. The de-hopper introduces a phase waveform $\beta_k(t)$ analogous to that introduced by the frequency hopper ($\beta_j^{(k)}$ which is now a constant phase introduced during the jth hopping interval). To remove the high frequency components, the de-hopper is followed by a band-pass filter. The output of this filter is $r_d(t)$ where $r_d(t)$ for the DPSK signals is given by

$$r_d(t) = \sum_{k=1}^{K} \sqrt{\frac{1}{2}P}\,E\{f_k(t-\tau_k)\,f_i(t)\,b_k(t-\tau_k)\,\psi(t-\tau_k)\,a_k(t-\tau_k)\cos[2\pi f_i t + \Phi_k(t) + \sigma_i] \tag{2.27}$$

where $\hat{n}(t)$ is a band limited version of $n(t)$, and it can be treated as white Gaussian noise WGN with spectral density $N_o/8$, $\Phi_k(t)$ is the phase waveform and it is defined as

$$\Phi_k(t) = \theta_k - 2\pi[f_k(t-\tau_k)]\tau_k + \alpha(t-\tau_k)-\beta_i(t) \tag{2.28}$$

and δ is defined by $\delta(u,v) = 0$ for $u \neq v$ and $\delta(u,v) = 1$ for all real u and v . The de-spreader demodulator part of the receiver shown in [23] use differentially coherent matched filter. It is required that $f_c T = 2\pi L$ is a positive integer. The output during the reception of the λth data bit (where $\lambda = j_i N_b + n_i$, i.e. for $n_i\ th$ data bit of the $j_i\ th$ hop), for in phase components it is given by

$$Z_c = \int_{\lambda T}^{(\lambda+1)T} r_d(t)\,\psi(t)\,a_i(t)\,\cos(2\pi f_c t)\,dt \tag{2.29}$$

and

$$Z_{c,d} = \int_{\lambda T}^{(\lambda+1)T} r_d(t-T)\,\psi(t)\,a_i(t)\,\cos(2\pi f_c t)\,dt \tag{2.30}$$

for the quadrature components it is given by

$$Z_s = \int_{\lambda T}^{(\lambda+1)T} r_d(t)\,\psi(t)\,a_i(t)\,\sin(2\pi f_c t)\,dt \tag{2.31}$$

and

$$Z_{s,d} = \int_{\lambda T}^{(\lambda+1)T} r_d(t-T)\,\psi(t)\,a_i(t)\,\sin(2\pi f_c t)\,dt \tag{2.32}$$

The receiver forms the statistic $Z_c Z_{c,d} + Z_s Z_{s,d}$ for the DPSK and compares it with a zero threshold. The estimate $b_\lambda(i)$ should then be differentially decoded in the DPSK, and as in the usual spread spectrum multiple-access communication systems, and time synchronization is acquired. Therefore $\tau_1 = 0$ can be set and time delays relative to the delay of the $1th$ signal can be considered. It is also required that the phase θ_1 does not change over the duration of two adjacent data bits. Also it is assumed that the number of data bits transmitted during each dwell (frequency hop) time is larger than 1 i.e. $N_b > 1$.

For DS-FSK SSMA system the receiver is shown in [23]. The first part of this receiver (the frequency de-hoppers part) is the same as for the DS-DPSK system. For this receiver the signal $r_d(t)$ is given by

$$r_d(t) = \sum_{k=1}^{K} \sqrt{\frac{1}{2}P}\ \delta[f_k(t-\tau_k), f_1(t)]\ \psi(t-\tau_k)\ a_k(t-\tau_k) \cos[2\pi(f_c + b_k(t-\tau_k)W)t + \Phi(t)] + n(t) \tag{2.33}$$

where

$$\Phi_k(t) = \theta_k(t-\tau_k) - 2\pi[f_k + b_k(t-\tau_k)W + f_k(t-\tau_k)]\tau_k + a_k(t-\tau_k) - \beta_1(t) \tag{2.34}$$

In the second part of the receiver shown in [23], for the case of binary FSK hybrid systems, during the reception of the λth data bit ($\lambda = j, N_b + n_1$) the output of the in-phase components is given by

$$Z_{c,1} = \int_{jT}^{(j+1)T} r_d(t)\,\psi(t)\,a_1(t)\cos[2\pi f_1 + \beta_1]t\ dt \tag{2.35}$$

and

$$Z_{c,-1} = \int_{\lambda T}^{(\lambda+1)T} r_d(t)\,\psi(t)\,a_i(t)\cos[2\pi(f_c-\delta)t]\,dt \qquad (2.36)$$

$$Z_{s,1} = \int_{\lambda T}^{(\lambda+1)T} r_d(t)\,\psi(t)\,a_i(t)\sin[2\pi(f_c+\delta)t]\,dt \qquad (2.37)$$

and

$$Z_{s,-1} = \int_{\lambda T}^{(\lambda+1)T} r_d(t)\,\psi(t)\,a_i(t)\sin[2\pi(f_c-\delta)t]\,dt \qquad (2.38)$$

The receiver forms the statistics

$$\tilde{R}_1^{\,2} = Z_{c,1}^{\,2} + Z_{s,1}^{\,2} \qquad (2.39)$$

and

$$\tilde{R}_{-1}^{\,2} = Z_{c,-1}^{\,2} + Z_{s,-1}^{\,2} \qquad (2.40)$$

the estimate $\hat{\beta}_\lambda^{(i)} = m'$ if $\hat{R}_{m'}^{\,2} = Max[\hat{R}_1^{\,2},\hat{R}_{-1}^{\,2}]$ where $m = 1,-1$. It is also assumed here that the receiver is time synchronous with the *ith* signal, but there is no any restriction on the phases $\theta_{i,1}$, $\theta_{i,-1}$, and here the number of data bits per hop $N_b \leq 1$.

Next is the evaluation of the average error average error probability for asynchronous hybrid DS/SFH SSMA systems. First for the DS/SFH hybrid system employing DSPSK modulation, in this case by use of equations (2.27), (2.29), (2.30), and the fact that $f_c >> T^{-1}$ in the practical spread spectrum communication systems to express the output of the in-phase component equations (2.29),

(2.30), Z_c as

$$Z_c = D_c + N_c + \sqrt{P/8}\, T \sum_{k \neq 1} I_c^{(k,1)} \tag{2.41}$$

where N_c is a zero-mean Gaussian random variable with variance $N_0 T/16$ and the desired signal component D_c is given by

$$D_c = \sqrt{P/8}\, T b_\lambda^{(1)} \cos[\theta_1 + \alpha_{j_1}^{(1)} - \beta_{j_1}^{(1)}] \tag{2.42}$$

$I_c^{(k,i)}$ is the multiple-access interference due to the kth signal, corresponds to a possible full hit during the $(j_i - j_k)$th dwell time of the kth signal. It is given by

$$I_c^{(k,1)} = d(j_k)\,[e(j_k, n_k)]\cos(\psi(j_k)] \tag{2.43}$$

for $o \leq n_k \leq n_1$

where $j_k = [\tau_k / T_h]$ and $n_k = [(\tau_k - j_k T_h)/T]$. $d(j_k) = 1$, then during the $(j_i - j_k)$th dwell time of the kth dwell time of the kth signal and the jth dwell time of the ith signal, the same frequency is occupied. If $d(j_k) = 0$, then there is no interference during the j_1th dwell time of the ith signal caused from the $(j_i - j_k)$th dwell time of the kth signal. corresponds to possible partial hits during either the $(j_i - j_k - 1)$th or the $(j_i - j_k)$th dwell time of the kth signal. $I_c^{(k,1)}$ for $n_k = n_1$ is given by

$$\begin{aligned} I_c^{(k,1)} = {} & d(j_k + 1)\, e(j_k, n_k)\cos[\psi(j_k + 1)] \\ & + d(j_k)\, e(j_k, n_k)\cos(\psi(j_k)) \end{aligned} \tag{2.44}$$

During the $(j_i - j_k - 1)$th dwell time of the kth signal and corresponding to a possible full hit, $I_c^{(k,1)}$ is for $n_1 < n_k < N_1$ given by

$$I_c^{(k,i)} = d(j_k + 1)\,[e(j_k, n_k) + \hat{e}(j_k, n_k)]\,\cos[\tilde{\psi}(j_k + 1)] \tag{2.45}$$

which corresponds to a possible full hit during the $(j_i - j_K - 1)$th dwell time of the Kth signal. In (2.43), (2.45) the the quantities e, $\hat{e}$, and $\tilde{\psi}$ are defined as

$$e(j,n) = b_{l(j,n+1)}^{(k)} R_{k,i}(\tau_k - jT_h - nT)/T \tag{2.46}$$

$$\hat{e}(j,n) = b_{l(j,n)}^{(k)} \hat{R}_{k,i}(\tau_k - jT_h - nT)/T \tag{2.47}$$

and

$$\tilde{\psi}(j) = \theta_k - 2\pi[f_c + f_{ji-j}^{(k)}]\tau_k + \alpha_{ji-j}^{(k)} - \beta_{(ji)}^{(i)} \tag{2.48}$$

where $R_{k,i}$ and $\hat{R}_{k,i}$ are the continuous partial cross-correlation function of the DS codes of users (i, K).

In case of binary FSK modulation the outputs of the in-phase components $Z_{c,1}$ and $Z_{c,-1}$ are given by

$$Z_{c,1} = D_{c,1} + N_{c,1} + \sqrt{P/8}\; T\sum_{k\neq i} I_{c,1}^{(k,i)} \tag{2.49}$$

$$Z_{c,-1} = D_{c,-1} + N_{c,-1} + \sqrt{P/8}\; T\sum_{k\neq i} I_{c,-1}^{(k,i)} \tag{2.50}$$

the desired signal component is given by

$$D_{c,1} = \sqrt{P/8}\; T\,\delta(b_\lambda, 1^{(i)})\,\cos[\theta_{i,1} + \alpha_{ji}^{(i)} - \beta_{j_i}^{(i)}] \tag{2.51}$$

The analysis of the multiple-access interference was shown in [23].

For the evaluation of the average error probability of the hybrid spread spectrum multiple-access system $\bar{P}_e$ in the systems employing random signature sequences and hopping patterns which is independent of i is defined as

$$\bar{P}_e = \sum_{k_f=0}^{K-1} \sum_{k_p=0}^{K-1-k_f} P_h(k_f, k_p)\, \bar{P}_e(k_f, k_p) \tag{2.52}$$

where $P_e(k_f, k_p)$ is the probability of the occurrence of the k_f full hits, k_p partial hits from the other $K-1$ users, and $\bar{P}_e(k_f, k_p)$ is the conditional error probability of the system, given that k_f full hits and k' partial hits occurred. The joint probability of k and k' partial bits for independent hopping patterns is given by

$$P_h(k, k') = \binom{K-1}{k} \binom{K-1-k}{k'} P_f^{\,k} P_f^{\,k'} (1-P_f-P_p)^{K-1-k-k'} \tag{2.53}$$

where $0 \le k < K$, $0 \le k' < K-k$ and P_f, P_p are the probability of a full and partial hit from other users respectively.

$$P_f = (1-N^{-1})q^{-1} \tag{2.54}$$

and

$$P_p = 2N^{-1}q^{-1} \tag{2.55}$$

this is for asynchronous system, first order Markov random hopping patterns, and additive white Gaussian noise channels

The probability of error at the output of the receiver matched to the ith signal

for asynchronous DS/SSMA system with K users, which employs binary FSK modulation and noncoherent demodulation with an AWGN channel, it is given by

$$\bar{P}_{e,i} = v_{i,-1}(v_{i,1} + v_{i,-1})^{-1} \exp[-\frac{1}{2}(v_{i,1} + v_{i,-1})^{-1}] \tag{2.56}$$

where the normalized variances $v_{i,1}$ and $v_{i,-1}$ of $Z_{c,1}$, $Z_{c,-1}$, are given by

$$v_i = (2E_b/N_o)^{-1} + \sum_{k \neq i} \sigma_{k,i;m}^2 \tag{2.57}$$

where $m = 1, -1$, $E_b = PT$ is the average energy per bit in the absence of multiple-access interference and $\sigma_{k,i;m}{}^2 = Var\left\{ I_{c,m}{}^{(k,i)} \right\}$ is given by

$$\sigma_{k,i;m}{}^2 = \frac{1}{4} T^{-3} \int_0^T [R_{k,i}{}^2(\tau) + R_{k,i} \hat{R}_{k,i}(\tau)] \, d\tau \tag{2.58}$$

when the *kth* users causes a partial bit

$$\sigma_{k,i;m}{}^2 = \frac{1}{8} T^{-3} \int_0^T [R_{k,i}{}^2(\tau) + \hat{R}_{k,i}{}^2(\tau)] \, d\tau \tag{2.59}$$

Suppose that the signal sequences are random, and they are assigned to different users and are naturally independent. Averaging the variance $\sigma_{k,i,m}{}^2$ over the ensemble of random signature sequences of length N, and for the case of full hit

$$\bar{\sigma}_f{}^2 = \bar{E}\left\{ \sigma_{k,i,m}{}^2 \right\} = m_\psi / 2N \tag{2.60}$$

and for the case of partial hit

$$\bar{\sigma}_p^{\,2} = \bar{E}\left\{\sigma_{k,i,m}^{\,2}\right\} = m_\psi/4N \tag{2.61}$$

where $\bar{E}$ is the expectation with respect to the ensemble of random signature sequences of length N and $m_\psi = T_c^{-3}\int_0^{T_c} R_\psi^{\,2}(\tau)\,d\tau = T_c^{-3}\int_0^{T_c} \bar{R}_\psi^{\,2}(\tau)\,d\tau$, for the rectangular chip waveform $m_\psi = 1/3$; for a sine chip waveform $m_\psi = (15 + 2\pi^2)/12\pi^2$. The final result of the average probability of error assuming that k_f users cause full hits and k_p users cause partial hits is given by

$$\bar{P}_e(k_f, k_p) = \frac{1}{2}\exp\left\{-\frac{1}{4}\left[\left(\frac{2E_b}{N_o}\right)^{-1} + (k_f + \frac{1}{2}k_p)\frac{m_\psi}{2N}\right]^{-1}\right\} \tag{2.62}$$

and for the DPSK modulation it is given by

$$\bar{P}_e(k_f, k_p) = \frac{1}{2}\exp\left\{-\frac{1}{2}\left[\left(\frac{2E_b}{N_o}\right)^{-1} + (k_f + \frac{1}{2}k_p)\frac{m_\psi}{2N}\right]^{-1}\right\} \tag{2.63}$$

The average probability of error for synchronous hybrid DS/SFH SSMA for binary FSK modulation is given by

$$\bar{P}_e(k) = \frac{1}{2}\exp\left\{-\frac{1}{4}\left[\left(\frac{2E_b}{N_o}\right)^{-1} + \frac{k}{4N}\right]^{-1}\right\} \tag{2.64}$$

and for DPSK modulation it is given by

$$\bar{P}_e(k) = \frac{1}{2}\exp\left\{-\frac{1}{2}\left[\left(\frac{2E_b}{N_o}\right)^{-1} + \frac{k}{4N}\right]^{-1}\right\} \tag{2.65}$$

Same numerical results are obtained for the average probability of error for the above system are shown in Fig. 2.14 where $\overline{P}_e$ is obtained for different number of users K employing FSK modulation and noncoherent demodulation, here the error probability of error is larger than the case of DPSK modulation with the same parameters [23].

Fig.2. 15 shows the comparisons for the error probability for PSK, DPSK, and binary FSK modulation schemes with coherent, differentially coherent, and noncoherent demodulation respectively. For asynchronous hybrid SSMA system with error probability of 10^{-4} The system employing DPSK modulation requires almost 2 dB more signal-to-noise ratio to achieve the same error probability as the system employing PSK modulation. Similarly, FSK requires 3 dB more than DPSK. In Fig.2. 16 the probability of error employ 16-ary FSK modulation with noncoherent demodulation, we notes here for $K \geq 200$ the synchronous systems perform better than the asynchronous ones. This is a contract to the results of Fig.2. 14, this is justified by the fact that now one ($N_s = 1$) 16-ary symbol per hop is transmitted instead of $N_b = 10$ bits/hop; therefor for asynchronous systems only partial hits occur with probability $2/q$, which is twice the probability of a full hit for the synchronous systems. For a small number of users (see the effect of partial hits is not dominant and, as in the cases described in Fig.2. 14, the asynchronous systems perform slightly better than the synchronous systems, although the bandwidth expansion required for this system is identical to that of the system of Fig.2. 14, the 16-ary FSK modulation provides considerably higher multiple access capability.

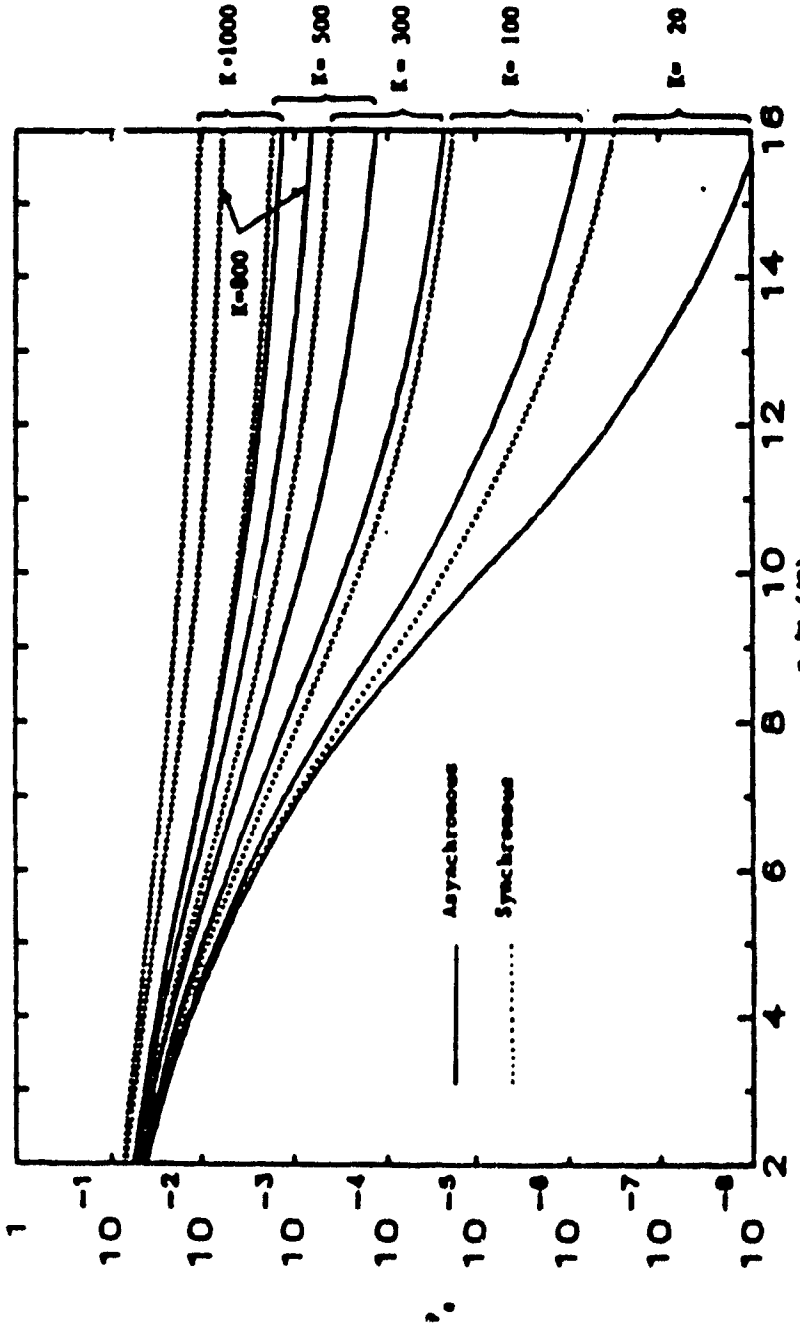

Fig(2. 11):- Probability of error for binary DS-SFH/SSMA systems employing random signature sequence ($N = 31$, $q = 100$, $N_h = 100$) [22].

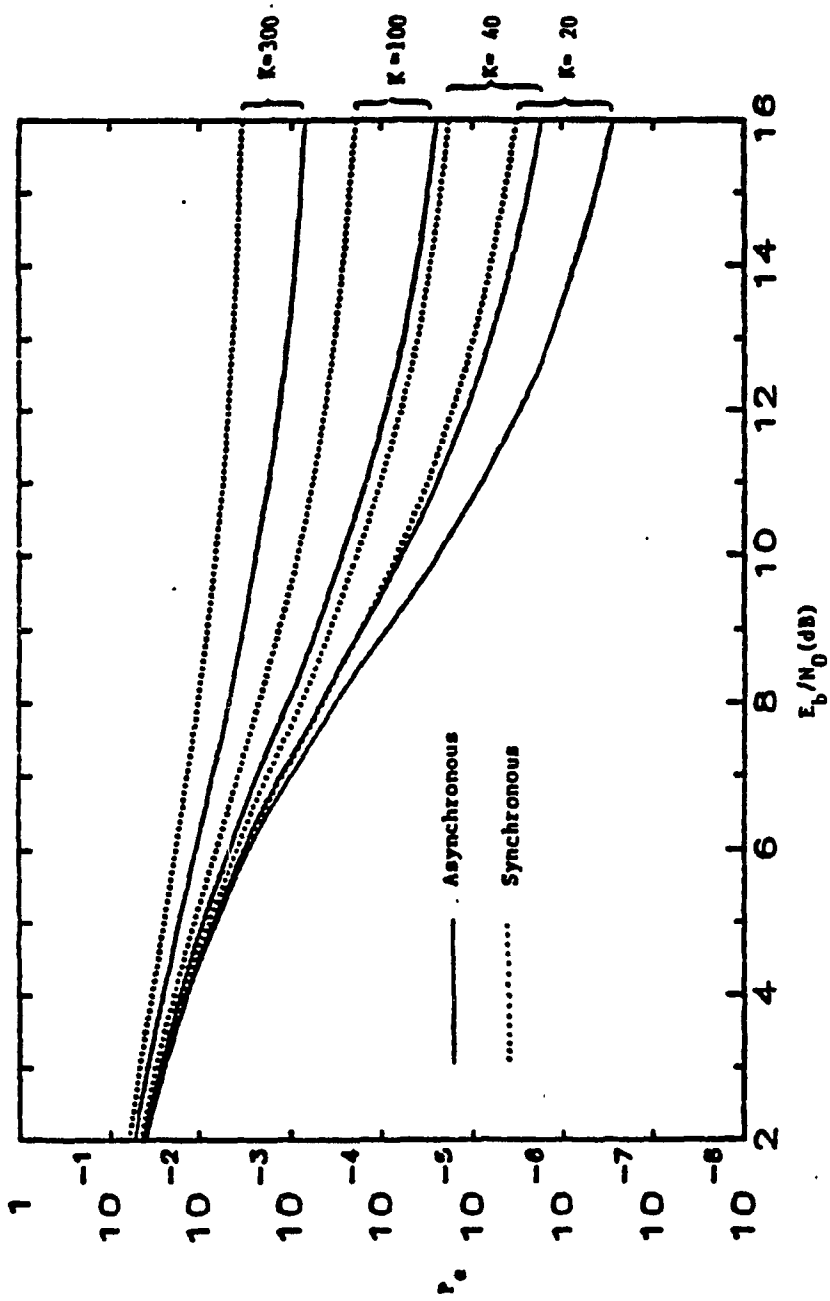

Fig(2. 12):- Probability of error for quaternary DS-SFH/SSMA systems employing random signature sequences ($N = 31$, $q = 100$, $N_b = 100$) [22].

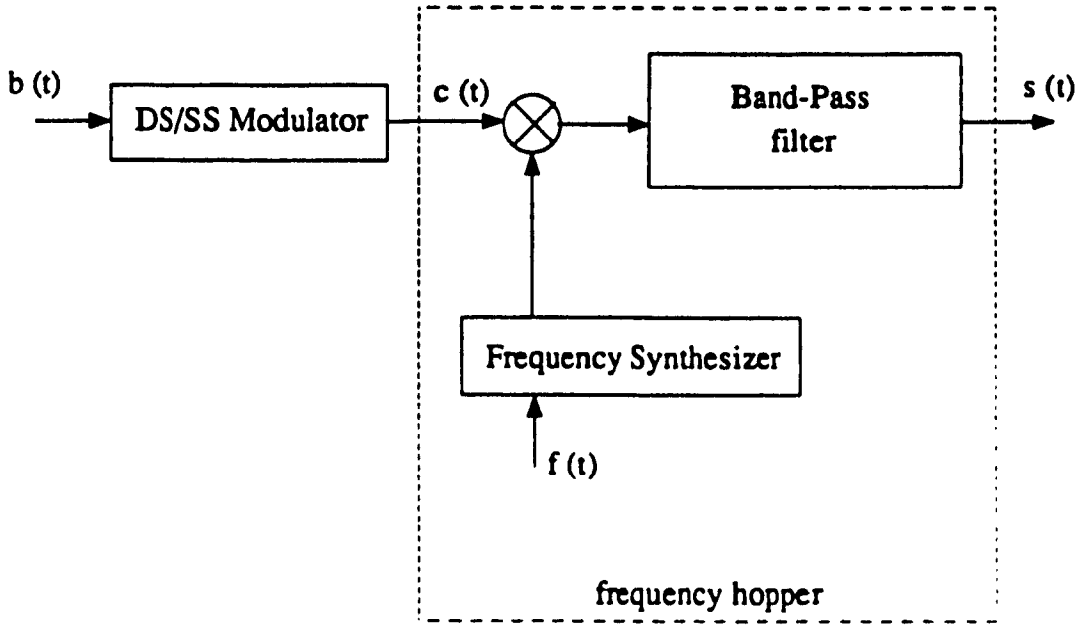

Fig (2. 13):- Hybrid DS-SFH/SSMA system transmitter [23].

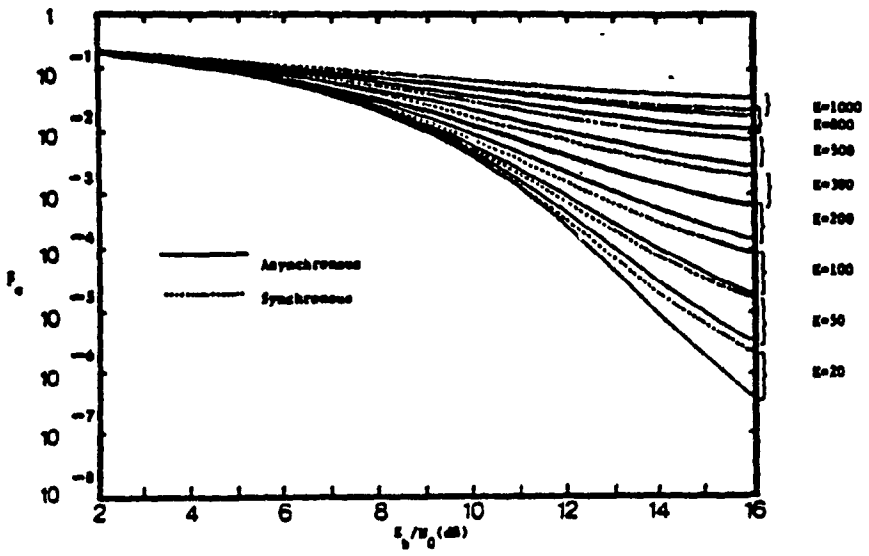

Fig(2. 14):- Probability of error for DS-SFH/SSMA systems employing binary FSK modulation ($N = 31$, $q = 100$, $N_b = 10$) [23].

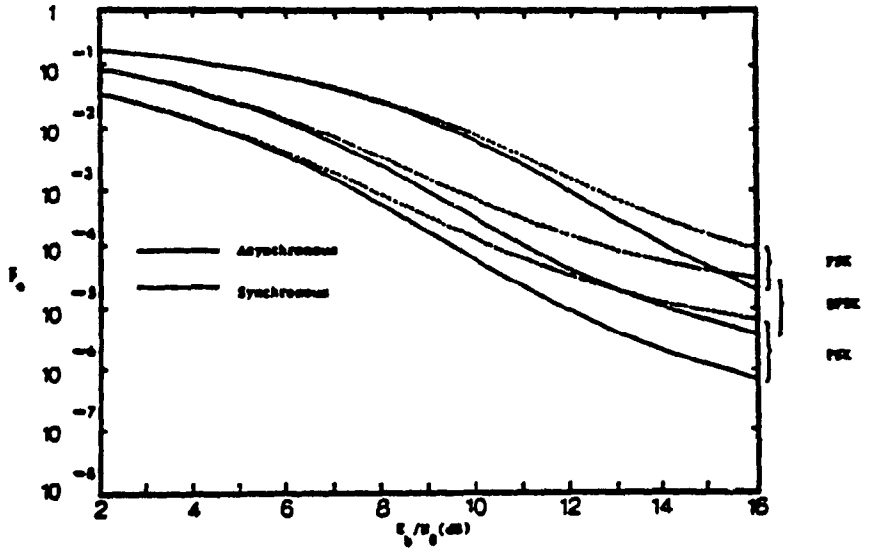

Fig(2. 15):- Probability of error for DS-SFH/SSMA systems with different modulation schemes ($K = 100$, $N = 31$, $q = 100$, $N_b = 10$) [23].

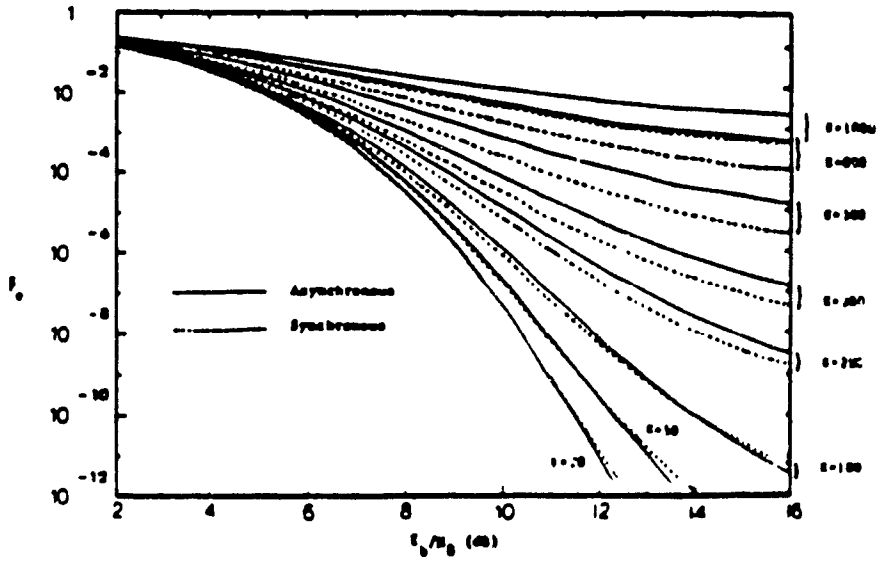

Fig(2. 16):- Probability of error for DS-SFH/SSMA systems employing 16-ary FSK modulation ($N' = 31$, $q = 50$, $N_0 = 1$) [23]

2.5.2. TH/DS Hybrid Systems

Fig. 2.17 illustrates a time-hopping direct sequence transmitter. Time-hopping has proved to be a useful way of adding TDM (Time division Multiplexing) to aid in traffic control, where the use of direct sequence transmission and code divisor multiplexing does not permit sufficient access to the link. The on and off for time-hopping can be derived from the same code sequence generator which used to derive the spectrum spreading code. An implemented keying control would be an n-input gate which senses previously chosen shift register state.

The TH/DS systems receive is shown in Fig. 2.18 where the control signal be used to enable the receiver front and synchronously with the expected transmit signal. Shift register state can be chosen after selecting the code state for time control, and this shift register state occurs repeatedly and detect the occurrence of that state.

2.5.3. TH/FH Time-Hopping/Frequency-Hopping Hybrid Systems

A basic frequency hopping/time hopping hybrid transmitter and receiver are shown in Fig. 2.19. At the transmitter the PN code generator and the state of the input binary message are used to select one of the M-frequencies to transmit a message bit. A new frequency determined by the PN code generator and the message bit is chosen for the next message bit. The transmitted signal is a sequence of carrier pulses which are hopped pseudo-randomly over a frequencies band. At the receiver and the received signal is mixed with a local oscillator, and that is hopped in synchronism with the transmitter. The signal resulted from that at the difference frequency is free from the pseudo-band frequency hops. This

FH/TH demodulator detects incoherently the signal power in one of two frequencies. It was shown in Fig. 2.20 the curve of probability of error as a function of E_b/N_o with the curve for a coherent PN system for comparison. The FH/TH hybrid modulation has found its greatest application in those systems in which a large number of users with widely variable distances or transmitted power are to operate simultaneously in a single link, as satellite communication systems. The FH/TH hybrid systems are also used to offer a solution to the near-far problem for some communication systems.

It is necessary in a practical system to incorporate some filtering at the transmitter to reduce the interference created by sidebands of the $(\frac{\sin(x)}{x})^2$ shaped spectrum. It will no be possible usually to introduce similar filtering of the PN code generated in the receiver that is because of the multipliers require a constant amplitude drive.

2.5.4. Direct sequence/Chirp Hybrid Systems

The combination of chirp modulation with pseudo-noise (PN) code (phase shift keying PSK) offers a significant advantage in its lower Doppler sensitively compared to purely PN-PSK. This technique also increases the intercept and antijam protection of a transmission system compared to a conventional chirp pulse compression system. The PN-chirp modulation offers an advantage of a lower code rate compared to the overall bandwidth is the easier code synchronization.

Fig. 2.21a. illustrates transmission system of PN chirp modulation, where a bi-phase double balanced mixer modulates a linear chirp according to logic 1 or 0 at the output of a PN-code generator with the bit rate R_c. The transmitted signal is given by

$$s_c(t) = c(t).s(t) \tag{2.66}$$

where $c(t)$ is a PN sequence generated by a binary feedback shift register of length 4 , with period $N = 2^n - 1$, $s(t)$ is a chirp linear pulse, which defined in terms of the center frequency f_o , and the dispersive slop μ

$$s(t) = \begin{cases} cos\,(2\pi(f_o t + \mu t^2/2) & -T/2 \leq t \leq T/2 \\ 0 & elsewhere \end{cases} \tag{2.67}$$

where $\mu = B_s/T$, B_s is the bandwidth and T the duration of the chirp signal. The transmitted signal of the PN-Chip signal then is given by

$$S_c(t) = \begin{cases} \sum_{i=0}^{N-1} C_i\ P_i(t)\ cos\,[2\pi(f_o t + \mu\frac{t^2}{2})] & -T/2 < t < T/2 \\ 0 & elsewhere \end{cases} \tag{2.68}$$

$$P_i(t) = \begin{cases} P\,[t - (-\frac{N}{2} + i)T_c = 1 & (-N/2 + i)T_c < t < (-N/2 + i + 1)T_c \\ 0 & elsewhere \end{cases} \tag{2.69}$$

The up-chirp and the down-chirp are described by choosing $\mu_1 = B_s/T$ for the up-chirp and $\mu_2 = -B_s/T$ for the down-chirp , these are used to represent a binary data (1 or 0). The envelop of the noiselike modulator output shape for a particular code rate R_c depends on B_s the chirp bandwidth, and it has a chap of $\frac{sin\,(x)}{x}$.

At the receiver end Fig. 2.21b. the code-related phase transitions are removed by modulation with a synchronous local replica of the PN-code (which was generated by the generator) before the chirp signal is compressed. The remaining chirp is applied to matched filters (pulse compression filters) for noncoherent data detection. If the synchronization take place at the receiver, the output signal of the MF for a single chirp input (neglecting the effect of bandpass filtering) is given by

$$g(t) = \begin{cases} \sqrt{TB_s}\,\dfrac{\sin[\pi B_s t(1 - \frac{|t|}{T})]}{\pi B_s t}\cos(2\pi f_c t) & -T < t < T \\ 0 & elsewhere \end{cases} \tag{2.70}$$

The peak amplitude of $g(t)$ is increased over the chirp amplitude by $\sqrt{TB_s}$, and this improve the peak signal-to-noise ratio to the matched filter, which called compression gain G_c , and it is given by

$$G_c = 10\log(TB_s) \qquad (dB) \tag{2.71}$$

[2] proposed PN-Chirp system use search/lock strategy (S/L S) for synchronization, which varies relative code position in discrete steps of $T_c/4$. This is implemented by digital controlling the receiver clock in a way that in each code period, one chip shorter by $T_c/4$, until the synch detector declares acquisition of synchronization . Fig. 2.22 illustrates the search/lock strategy (S/L S)

A tau-dither loop is employed for code tracking, where the loop operates with a time-continuous input waveform. This waveform is obtained by means of a sample-and-hold circuit. The loop error signal is only a very weak spectral com

ponent, it will be more difficult to process if the sample-and-hold circuit is not there.

The mean acquisition time, mean hold-in-time, probability of detection, probability of false alarm and the probability of error are calculated for the transmission system under additive white Gaussian noise [2]. Fig. 2.23 illustrate the bit error probability P_e in synchronized operation, where tracking jitter has been neglected in the calculation. The results were obtained by transmitting random data, with receiver externally synchronized and comparing the demodulated message to the properly delayed original data stream.

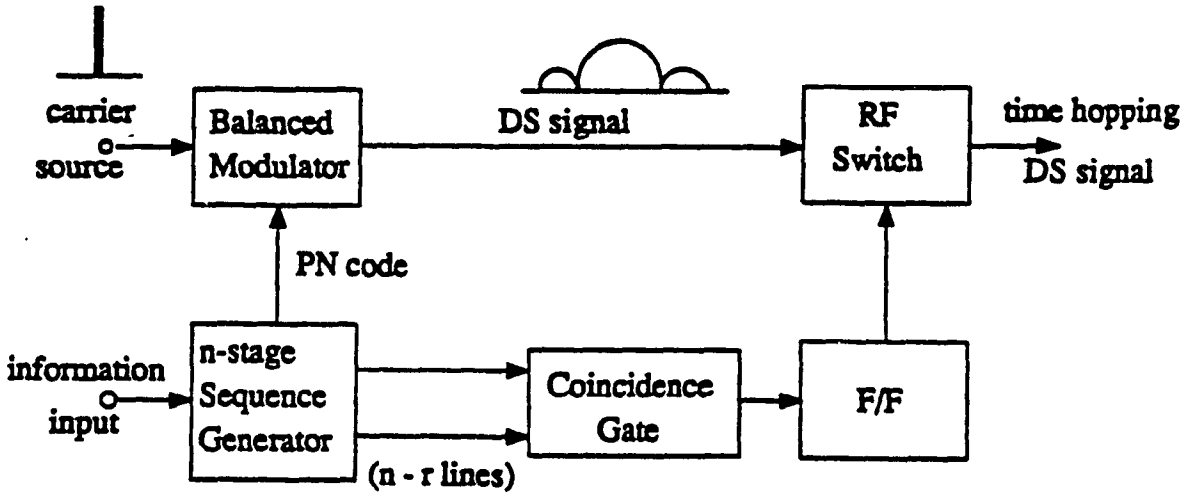

Fig.(2. 17):-TH/DS time hopping/direct sequence transmitter.

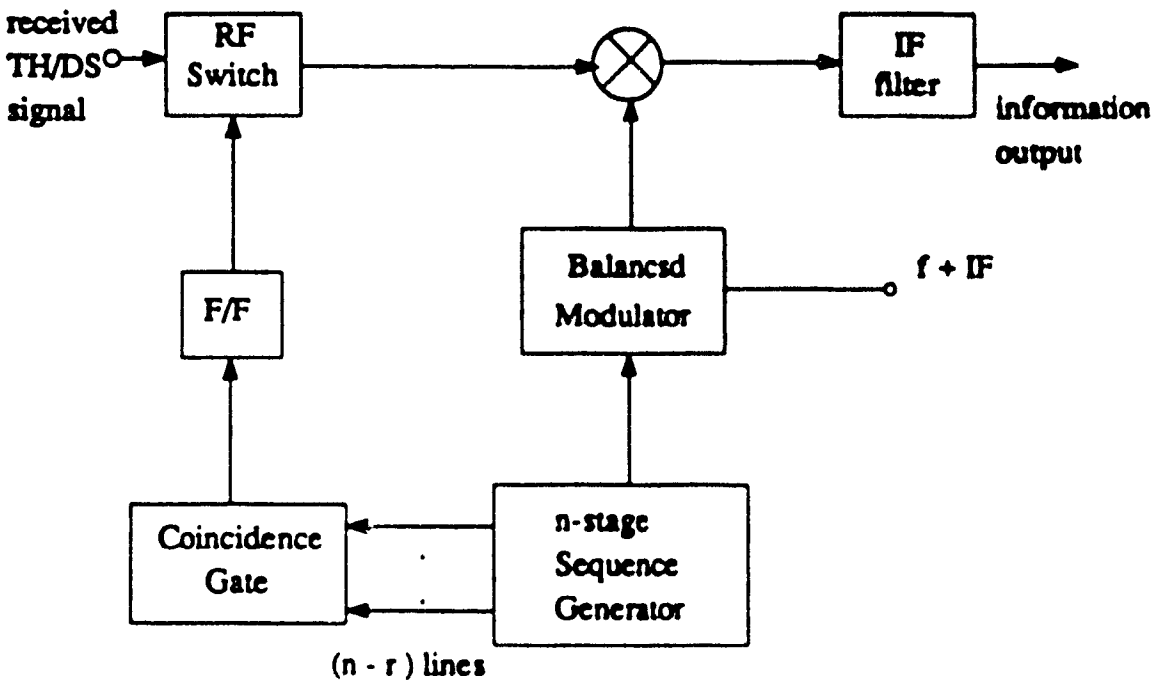

Fig (2 18) - TH DS hybrid receiver

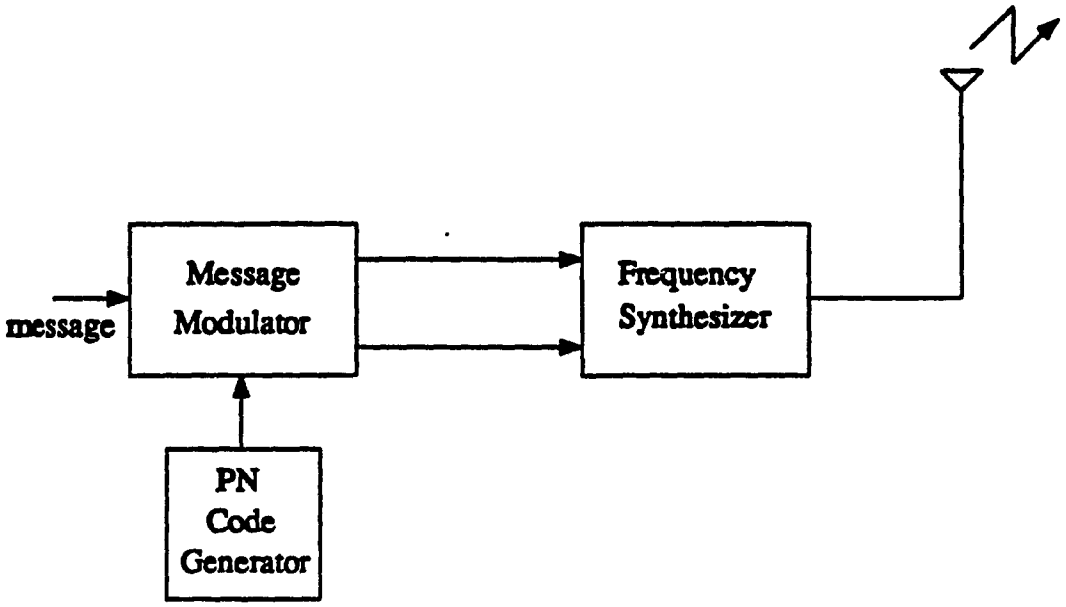

a, FH/TH transmitter

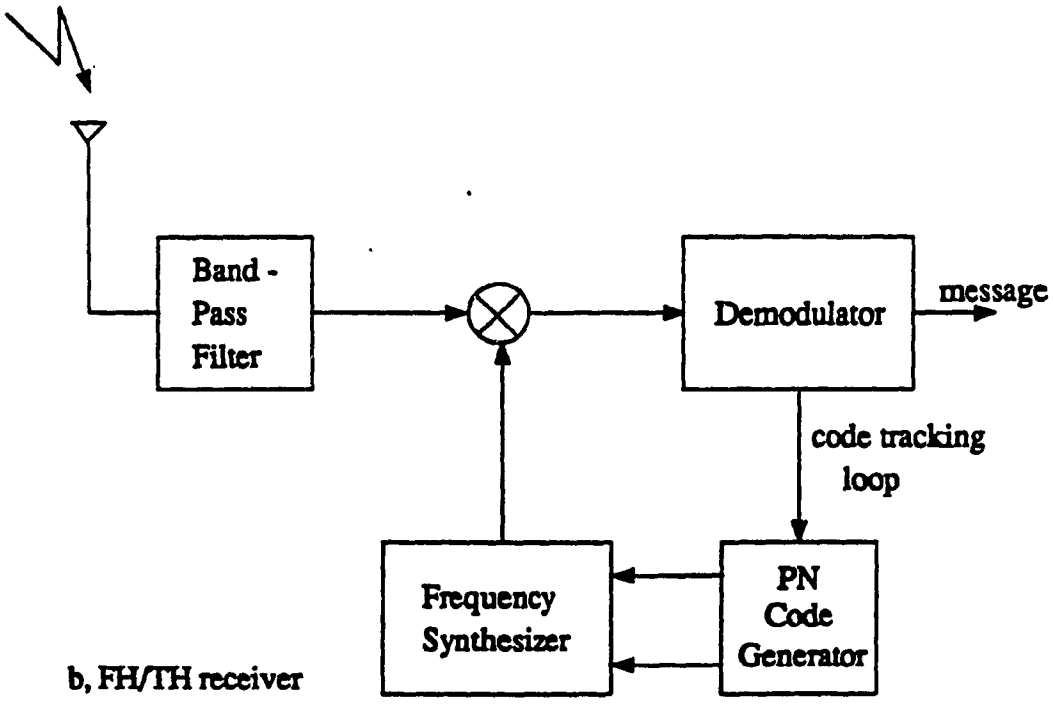

b, FH/TH receiver

Fig.(2. 19):- The FH/TH hybrid system block digram, (a) transmitter, (b) receiver

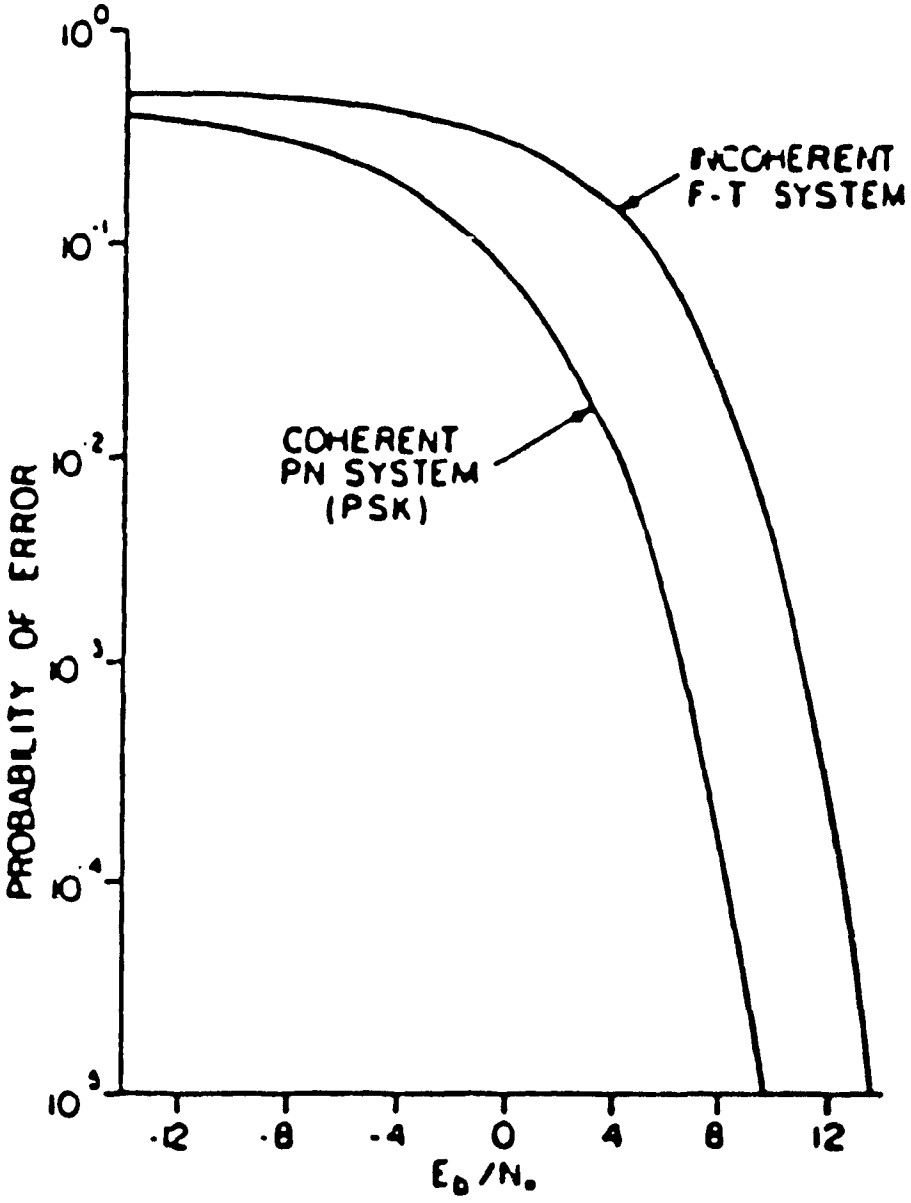

Fig(2. 20):- Comparison of PN and F-T systems [43].

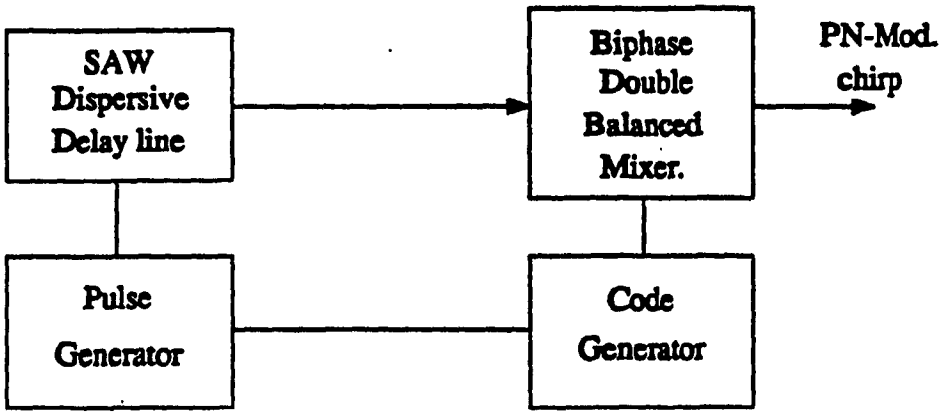

a, transmitter

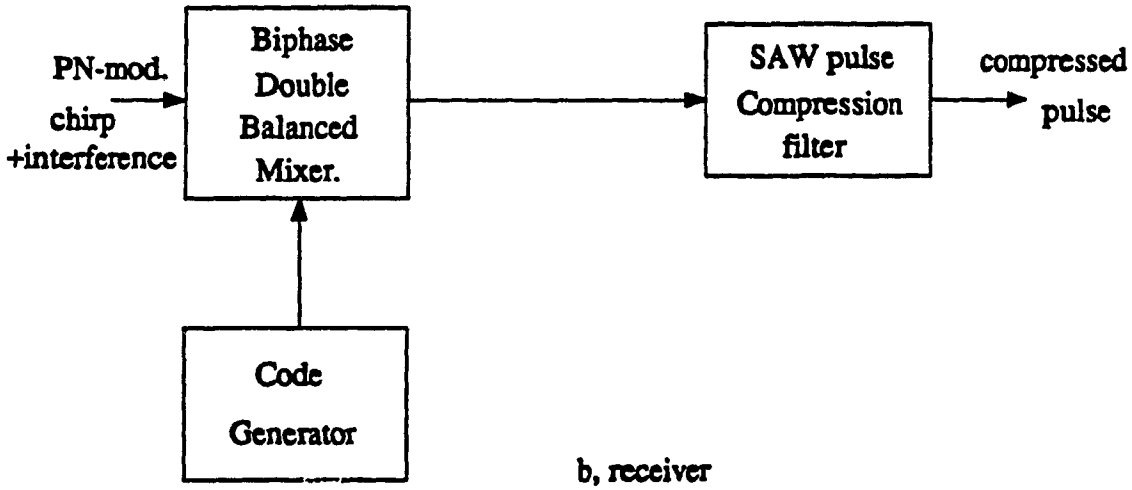

b, receiver

Fig.(2. 21):- PN-chirp system, (a) transmitter, (b) receiver.

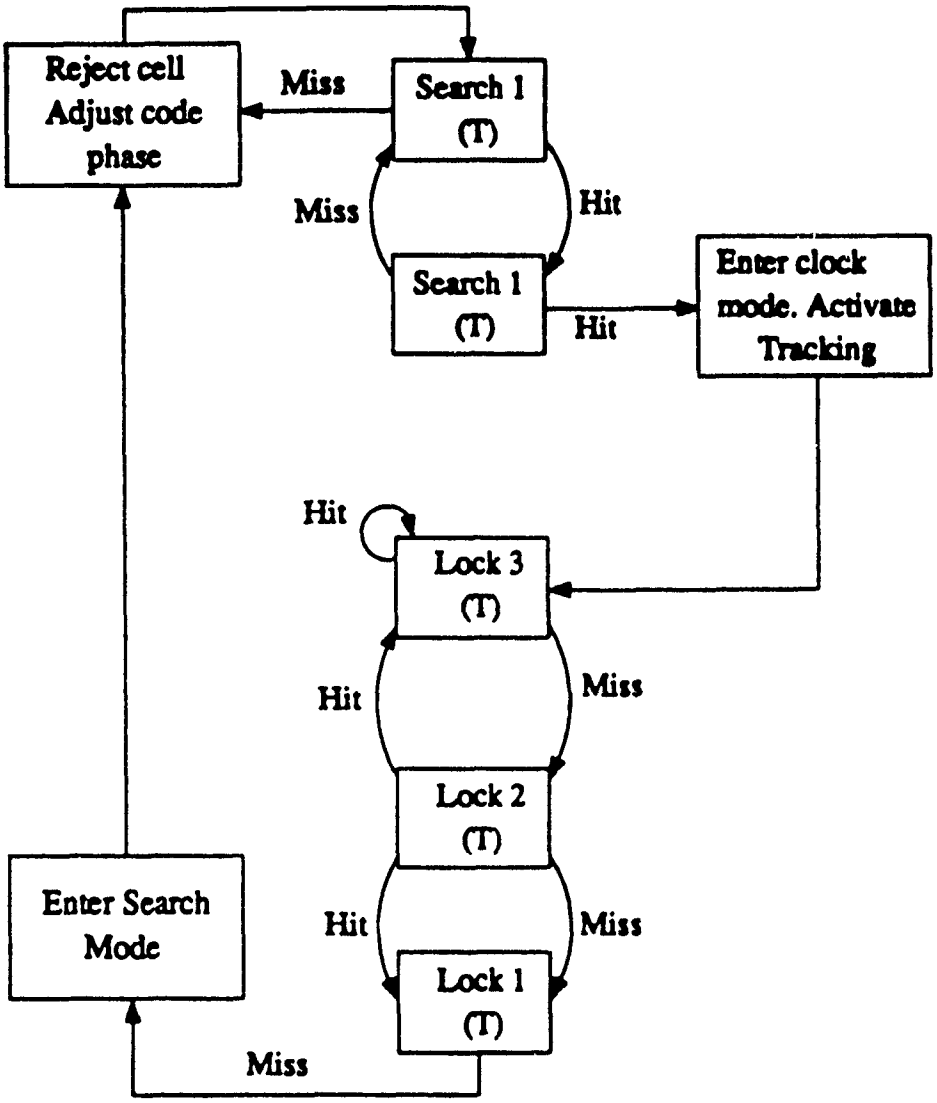

Fig.(2. 22):- Search/lock strategy (SLC)

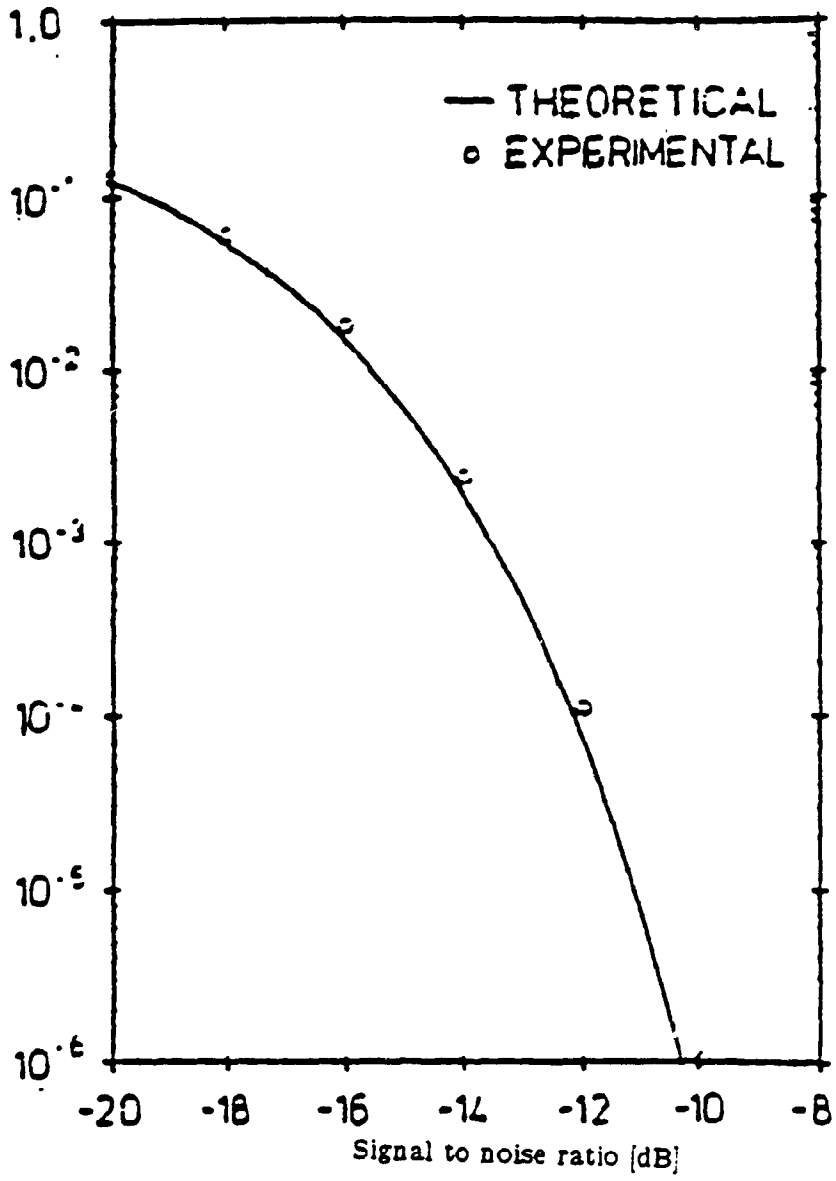

Fig(2. 23):- Probability of error P_e ($S_n = 0.91$, $\beta = 0.8$) [2].

CHAPTER 3

PERFORMANCE OF HYBRID CHIRP/DS SIGNALS UNDER DOPPLER AND PULSED JAMMING

3.1. Introduction

Chirp signaling schemes have been used for quite some time in radar applications. The spectra and time function of a particular class of pulse compression signals were analyzed and the basis for compression filter design were also derived [1]. Investigation of the relative utility of linear FM show that signals with a linear frequency variation have good cross-correlation properties at $FT > 50$ [5]. The representation of binary data by chirp signals was proposed by [40]. The theory of pulse compression and data transmission by using chirp signal in a system operating at high frequency band was investigated in [6]. The error rate of coherent binary continuous phase chirp waveform in respect of its signal form and spectrum shape was investigated in [41].

The interaction among the frequency modulation, and cross-talk interference parameters that determine the number of different linear FM signals which can be used within the constraints of a bounded time frequency region has been shown in [3], which also described several techniques for the expansion of the signal capability in both synchronous and nonsynchronous operation. The combination of chirp modulation and pseudonoise PSK for spread spectrum transmission of digital data was recently investigated in [2].

In this chapter the envelope of the output of the chirp matched filter is

derived under frequency Doppler Δ and DS code delay τ in the proposed DS/chirp system (Fig.3. 1 and Fig.3. 2). These outputs are obtained for different values of FT_b (i.e. the time bandwidth product of the chirp signal). This is followed by evaluating the probability of error under Doppler Δ, delay τ, and pulse jamming is analyzed and the results are obtained for different values of F, T_b, Δ, σ^2, R_c, B_{RF}, J_J and α. It is shown that certain values of F, R_c allow the minimization of both the effects of jamming and frequency Doppler.

3.2. The Chirp/DS System Description

The proposed chirp/DS system is shown in Fig. 3.1, the impulse generator is used to generate the pulse, the chirp signals are generated by the up and down chirp signal generators, the up chirp signal with dispersive slope μ_1 and the down-chirp with μ_2 where $\mu_1 = -\mu_2$ to represent binary data [1]. The partial band jammer is used to transmit all the available power in a limited bandwidth.

One of the up and down chirp signals is selected by the binary data and the output of the analog multiplexer is spread by the DS code (G_i) with a chip duration T_c. This is generated by means of a (LFSR) linear feedback shift register.

Fig. 3.2 shows the receiver of the hybrid DS/chirp system. The received signal is modulated with a synchronous code replica prior to matched filtering of the chirp pulses. Finally, the detected information bits are found by a max of decision on the two chirp filters.

3.3. Bit Error Analysis Under Doppler, Code Delay and Partial Band Jamming in The Chirp/DS System

The received signal r(t) under Doppler Δ, independent code time delay and partial band jamming can be expressed as,

$$r(t) = \sum_{i=-N/2}^{N/2} C_i D_i(t+\tau) \cos(2\pi(f_o+\Delta)(t+\tau) \pm \frac{\mu}{2}(t+\tau)^2) + J(t+\tau) + n(t+\tau) \tag{3.1}$$

where $C_i = \pm 1$ is the identity of the DS code chip whose rate is, $R_c = \frac{1}{T_c}$, and period $N = 2^n - 1$, $n =$ number of stages in the LFSR, $D_i(t)$ is the unit pulse defined as,

$$D_i(t) = \begin{cases} U((t-i)T_c) & iT_c < t < (i+1)T_c \\ 0 & elsewhere \end{cases} \tag{3.2}$$

where $U(t)$ is the unit step function. f_o is the center frequency, Δ is the frequency Doppler, the time delay is τ, $n(t)$ is the noise of two side power spectral density equal to $\eta/2$, $J(t)$ is the partial band noise jamming of power J_J and duty factor α_J. The factor μ called dispersive slope where

$$\mu = \frac{2\pi F}{T_b} \tag{3.3}$$

where F is the maximum frequency sweep and FT_b is the chirp signal dispersion. Figure(3.3) shows a typical hybrid DS/Chirp signal.

Following dispreading (multiplication by the local code) we obtain,

$$\lambda(t) = r(t) \sum_{i=-N/2}^{N/2} C_i D_i(t)$$

$$= \cos(2\pi(f_o + \Delta)(t + \tau) \pm \frac{1}{2}\mu (t + \tau)^2) \tag{3.4}$$

$$\cdot (1 - 2 \sum_{i=-N/2}^{N/2} C_i G_i(t)) + n'(t) + J'(t)$$

where $G_i(t)$ is the unit pulse defined as

$$G_i(t) = \begin{cases} 1 & i\tau < t < (i+1)\tau \\ 0 & \textit{otherwise} \end{cases} \tag{3.5}$$

where $|\eta| \leq T_c$ is the delay between the arriving and local codes.

$$J'(t) = J(t)\, c(t) = J(t) \sum_{i=-N/2}^{N/2} C_i D_i(t) \tag{3.6}$$

and

$$n'(t) = n(t) \sum_{i=-N/2}^{N/2} C_i D_i(t) \tag{3.7}$$

The two equations above, (3.6) and (3.7), show that both the receiver noise and jammer are spread by SS correlation. However, as is well known, the bandwidth of $n(t)$ is usually large enough compared to the SS bandwidth, (R_c) ignored consider that the level of AWGN density $\eta/2$ to become $\frac{K_o \eta}{2}$ where $K_o \approx 1$ [4].

The pulsed spread jammer $J'(t)$ should have two states depending on whether

the jammer is present or absent. When the jammer is on we assume for all practical purposes that $J'(t)$ is like a flat noise in the applicable bandwidth (i.e. the chirp bandwidth F). This is justified if $F \leq R_c$.

As a matter of fact, $J(t)$ and $C(t)$ of equation (3.6) are uncorrelated leading to multiplication of the autocorrelations and the $J(t)$ will be the convolution of the p.s.d. of $J(t)$ and the DS code $C(t)$, and the bandwidth of $J'(t)$ will equal the summation of the bandwidths i.e. $B'_J = B_{RF} + R_c$. So based on $F \leq R_c$, $J'(t)$ will have a flat density over the chirp band. Finally, the p.s.d., height when the jammer is on, becomes,

$$N'_J = \frac{K_o N_J}{\alpha B_{RF}} \tag{3.8}$$

where B_{RF} is the total spread spectrum BW of the signal.

For the remaining terms of (3.4) we note that $v(t) = -2 \sum_{i=-N/2}^{N/2} C_i G_i(t)$ This is a random binary waveform of pulse width τ as in Fig. 4. The autocorrelation of such a signal has been shown to be [4],

$$R_V(\xi) = \begin{cases} \frac{4|\eta|}{T_c}(1 - |\eta|) & \tau \leq \xi \leq \tau,\ 0 \leq |\eta| \leq T_c/2 \\ 0 & otherwise,\ 0 \leq |\eta| \leq T_c/2 \end{cases} \tag{3.9}$$

where we assume that the semirandom code is approximately random (if $2^n - 1$ is large). The power spectral density of $v(t) = -2 \sum_{i=-N/2}^{N/2} C_i G_i(t)$ is,

$$G_V(f) = \frac{4|\eta|^2}{T_c} \left(\frac{\sin(\pi f \tau)^2}{(\pi f \tau)^2}\right) \tag{3.10}$$

It follows that for small values of any single delay τ, the p.s.d. of the flat noise of $v(t)$ at the MF

$$N_V = \frac{P_V}{B_V} = \frac{4|\eta|/T_c}{2/|\eta|} = \frac{2|\eta|^2}{T_c} \qquad 0 < \tau \leq T_c/2 \tag{3.11}$$

Up until now, we have modeled all $n'(t)$, $J'(t)$ and $v(t)$ as flat noise in the chirp band (for all practical purposes). Next we evaluate the output of the up and down chirp filters in the receiver due to the signal term of equation (3.4). Appendix A shows that the outputs of the up and down chirp filter due to an up chirp signal (assumed transmitted without losing generality) are given by,

$$\begin{aligned} y_1(t) &= \sqrt{FT_b}\ sinc\,(\pi F(t+\tau) + \frac{\Delta T_b}{2}) \\ &\quad .\ cos\,(2\pi f_o t - \frac{\mu t^2}{2} + \frac{\pi}{4}) \end{aligned} \tag{3.12}$$

and

$$\begin{aligned} y_2(t) &= \frac{1}{2}\sqrt{(C(x_1)+C(x_2))^2 + (S(x_1)+S(x_2))^2} \\ &\quad .\ cos\,(2\pi f_o t - \frac{\mu t^2}{2} + \phi(\Delta,\tau)) \\ &= \sigma(\tau,\Delta)\ cos\,(2\pi f_o t - \frac{\mu t^2}{2} + \phi(\Delta,\tau)) \end{aligned} \tag{3.13}$$

where

$$x_1 = \sqrt{FT_b} + \frac{\Delta}{2\pi}\sqrt{\frac{T_b}{F}} + \tau\sqrt{\frac{F}{T_b}} \tag{3.14}$$

$$x_2 = -\sqrt{FT_b} + \frac{\Delta}{2\pi}\sqrt{\frac{T_b}{F}} + \tau\sqrt{\frac{F}{T_b}} \tag{3.15}$$

$$C(x) = \int_0^x \cos\left(\frac{\pi}{2} y^2\right) dy \tag{3.16}$$

and

$$C(x) = \int_0^x \sin\left(\frac{\pi}{2} y^2\right) dy \tag{3.17}$$

Equations (3.16) and (3.17) are the Fresnel cosine and sine integrals. The power spectral density of the flat noise at the output of up or down chirp filters is given by

$$N_o \quad \left(\frac{\eta}{2} + N_V + \frac{J_J}{2\alpha B_{RF}}\right) \qquad 0 \le |\tau| \le \frac{T_c}{2} \tag{3.18}$$

where N_V is given in equation (3.11). It follows that the total noise power at the output of the up or down chirp filters is given by

$$\sigma_1^2 = 2FN_o = 2F\left(\frac{\sigma^2}{2B_{RF}} + \frac{2|\tau|^2}{T_c} + \frac{J_J}{2\alpha B_{RF}}\right) \quad 0 \le |\tau| \le \frac{T_c}{2} \tag{3.19}$$

Equation (19) applies only when the pulsed jammer is on, if it is off we obtain,

$$\sigma_2^2 = 2FN_o = 2F\left(\frac{\sigma^2}{2B_{RF}} + \frac{2|\tau|^2}{T_c}\right) \quad 0 \le |\tau| \le \frac{T_c}{2} \tag{3.20}$$

Now the distribution of the envelope of the signal appearing at the output of the up chirp (assumed to have the transmitted signal) is well known to be Rician, i.e.

$$P(r/\tau,\Delta,\alpha) = \frac{r}{\bar{\sigma}^2}\, e^{-(r^2+A^2)/2\bar{\sigma}^2} I_o\left(\frac{Ar}{\bar{\sigma}^2}\right) \tag{3.21}$$

where

$$A = y_1(0) = \sqrt{FT_b}\ sinc\ (\pi F \tau + \frac{\Delta T_b}{2}) \tag{3.22}$$

and $\bar{\sigma}^2$ take one of the values of σ_1^2 and $\bar{\sigma}_2^2$ in equations (3.19) and (3.20), depending on the value of $|\eta|$ and presence or absence of pulsed jammer as will follow shortly. Similarly the envelope corresponding to the down chirp (not being the transmitted signal) is given by,

$$P(z/\tau,\Delta,\alpha) = \frac{z}{\bar{\sigma}^2}\ e^{-(z^2+B^2)/2\bar{\sigma}^2}\ I_o\left(\frac{Bz}{\bar{\sigma}^2}\right) \tag{3.23}$$

where

$$B = y_2 = \frac{1}{2}\sqrt{(C(x_1) + C(x_2))^2 + (S(x_1) + S(x_2))^2} \tag{3.24}$$

x_1 and x_2 are given in equations (3.14) and (3.15).

The next step is to evaluate the probability of error at the chirp device i.e. the probability that envelope output of the down chirp filter exceeds that of the up filter, which is given by,

$$P(e/\Delta,\tau,\alpha) = \int_0^\infty \frac{x}{\bar{\sigma}^2}\ e^{-(x^2 + A^2)/2\bar{\sigma}^2}\ I_o\left(\frac{Ax}{\bar{\sigma}^2}\right) \cdot \int_x^\infty \frac{z}{\bar{\sigma}^2}\ e^{-(z^2 + B^2)/2\bar{\sigma}^2}\ I_o\left(\frac{Bz}{\bar{\sigma}^2}\right) dz\ dx \tag{3.25}$$

We note that A and B are functions of F, T_b, τ, Δ according to equations (3.12)

and (3.13), while $\overline{\sigma}^2$ can take one of the values ${\sigma_1}^2$ or ${\sigma_2}^2$ given in equations (3.19) and (3.20). These values are also functions F, T_b, B_{RF}, T_c, τ and the input noise power σ^2 at the receiver. The following step is a two step averaging (3.25) over the condition of jamming (due to factor of jammer α) and over the random delay τ assumed uniformly distributed in the range $(-\frac{T_c}{2} < \tau < \frac{T_c}{2})$ .This gives the final bit error probability as,

$$
\begin{aligned}
P_e = \frac{\alpha}{T_c} \int_{-T_c/2}^{T_c/2} \int_{0}^{\infty} \frac{x}{\sigma^1} e^{-(x^2 + A^2)/2{\sigma_1}^2} I_o \left\{ \frac{Ax}{{\sigma_1}^2} \right\} \\
\cdot \int_{x}^{\infty} \frac{z}{{\sigma_1}^2} e^{-(z^2 + B^2)/2{\sigma_1}^2} I_o \left\{ \frac{Bz}{{\sigma_1}^2} \right\} dz \; dx \; d\tau \\
+ \frac{(1-\alpha)}{T_c} \int_{-T_c/2}^{T_c/2} \int_{0}^{\infty} \frac{x}{{\sigma_2}^2} e^{-(x^2 + A^2)/2{\sigma_2}^2} I_o \left\{ \frac{Ax}{{\sigma_2}^2} \right\} \\
\cdot \int_{x}^{\infty} \frac{z}{{\sigma_2}^2} e^{-(z^2 + B^2)/2{\sigma_2}^2} I_o \left\{ \frac{Bz}{{\sigma_2}^2} \right\} dz \; dx \; d\tau
\end{aligned}
\tag{3.26}
$$

where α is the duty factor of the jammer, $I_o \left\{ \frac{Ax}{{\sigma_1}^2} \right\}$, $I_o \left\{ \frac{AZ}{{\sigma_2}^2} \right\}$ are first kind Bessel function of zero order.

3.4. RESULTS

We compute first the envelope of the output of the chirp MFs, in the presence and absence of the corresponding signal. As given by equations (3.22), (3.24) respectively. This is followed by computing the probability of errors of equation (3.26), by numerical integration. Figures (3.5-3.18) show samples of the results obtained with F, T_b, Δ, σ^2, R_c, B_{RF}, J_J and α being the input parameters. Figs. (3.5) and (3.6) reveal the fact that the compressed chirp pulse at the output of the filter matched to the received signal and under no noise, no jamming, becomes sharper with increasing F under constant frequency Doppler Δ, constant chirp duration T and varying delay τ.

For the output of the chirp filter not matched to the received signal, under the same conditions mentioned, we see from Figs. (3.7) and (3.8) that under Doppler Δ and delay τ the output becomes more like a constant with an increasing FT. This latter effect becomes more pronounced in the case of small frequency Doppler. This comes in agreement with known classic result [5].

For the bit error performance in noise, without Doppler no jamming, no delay, Fig. (3.9) shows a sample of obtained results at different time bandwidth product FT, and noncoherent detection. Fig. (3.10) shows the same probability of error at nonzero Doppler value comparing Figs. (3.9) and (3.10) at $FT = 50$, say we see a difference of about 3dB of received S/N ratio.

In all of our results so far, the spread spectrum processing gain (i.e. $\frac{T_b}{T_c}$, and the total RF bandwidth B_{RF} did not come into the picture because our AWGN bandwidth is greater than the direct sequence bandwidth R_c. Next the pulsed jamming effects are investigated under both Doppler and Jamming (Figs. 3.11 -

3.17). From Fig. (3.11), we can see that increasing F improves the error performance by about $5dB$ at $F = 4 \cdot 10^4$ relative to $F = 3 \cdot 10^4$. However, for negligible Δ values as in Fig. (3.12), it will be more cost effective to increase R_c and hence decrease F (keeping B_{RF} constant), even when the pulsed jammer has a smaller value in Fig. (3.12) as compared to Fig. (3.11). Comparing Fig. (3.13) and Fig. (3.10) reveals the fact that the Doppler effect is multiplied by the effect of the jammer. Figs. (3.14) and (3.15) show the effect of the duty factor of the pulsed jammer α the classic result favouring, smaller values of α also prevails here (under Doppler and code delay). Fig. (3.14) shows that it is advantageous to decrease F (i.e. increase R_c) to improve the error performance under heavy jamming. The same figure also shows that increasing R_c makes further increases in the level of S/N ratio more cost effective in the sense of decreasing the resulting probability of error.

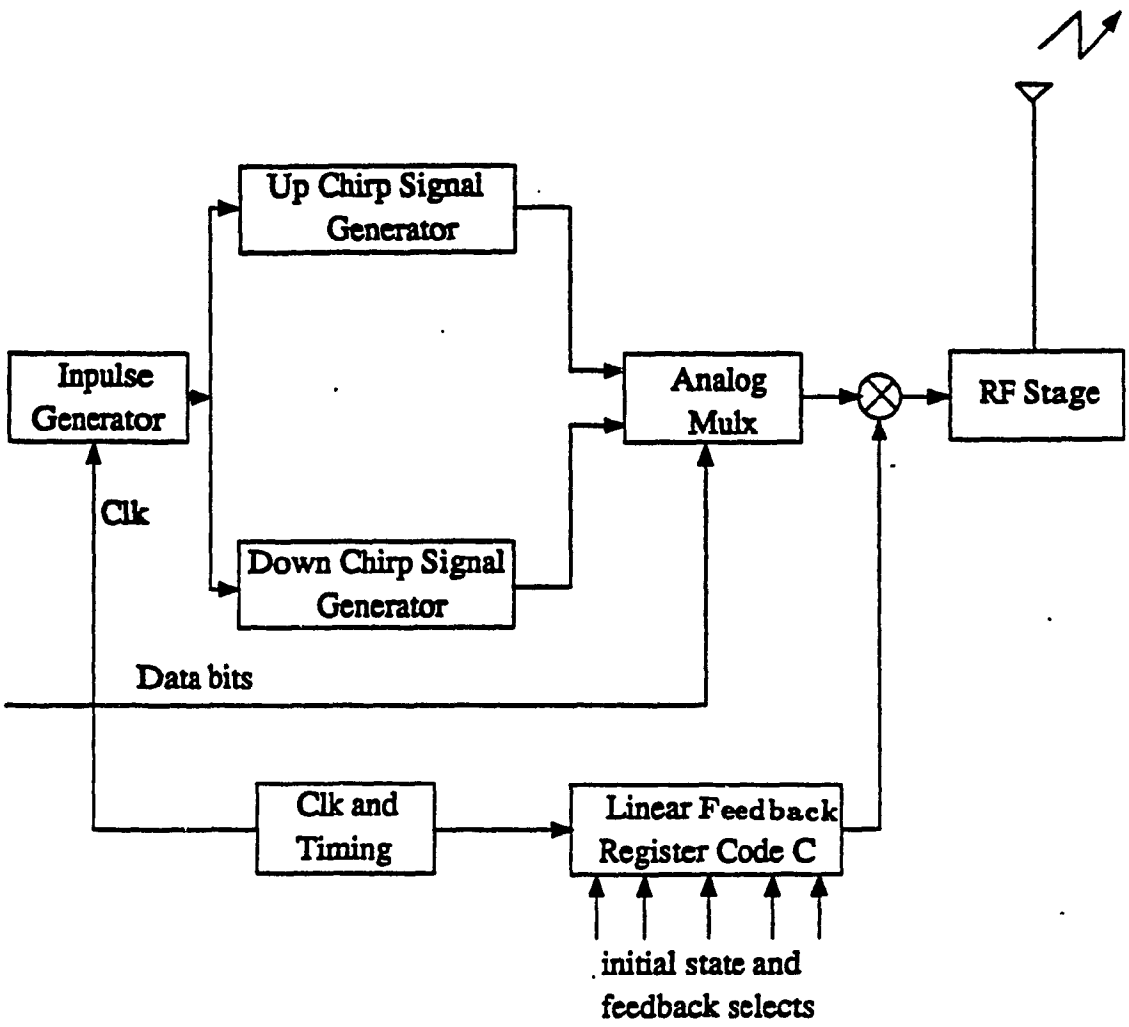

Fig.(3. 1):- Transmitter of the hybrid chirp/DS spread spectrum system.

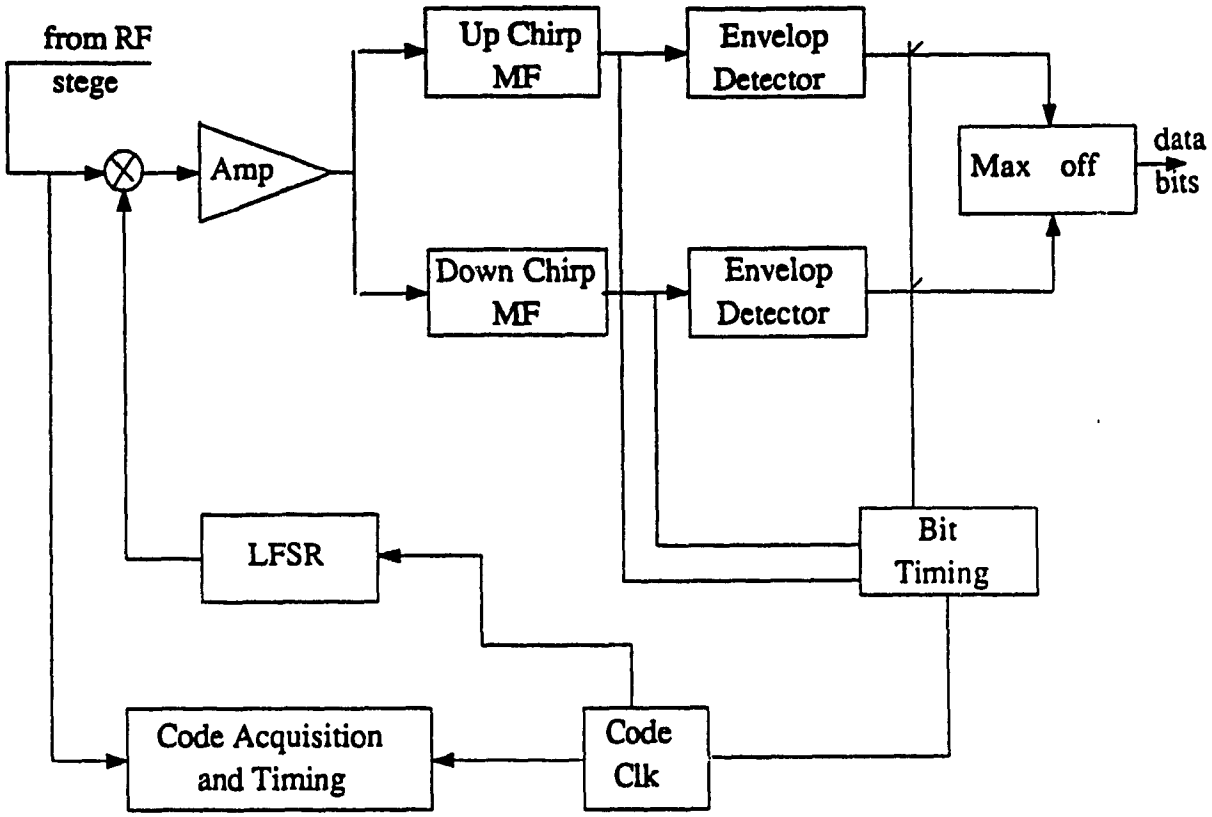

Fig.(3. 2):- Receiver of the hybrid chirp/DS spread spectrum system.

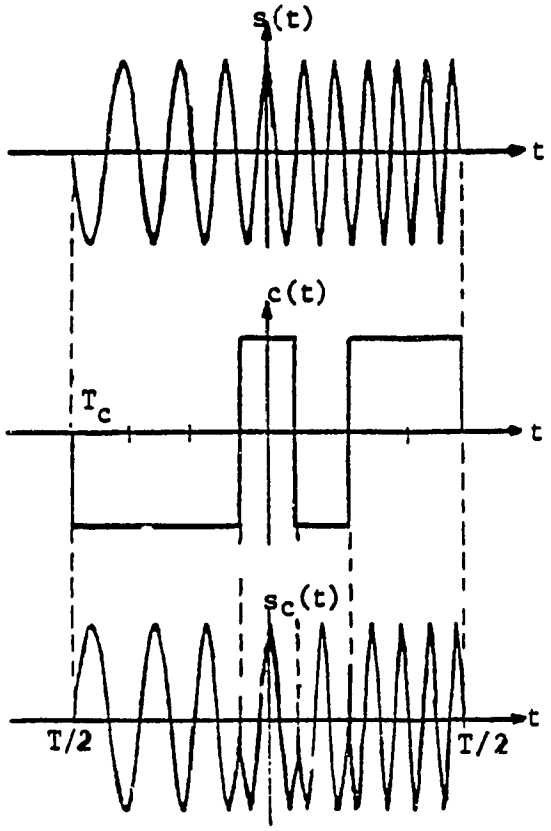

Fig(3. 3):- Basic waveform of chirp pulse, PN code and DS/chirp signal.

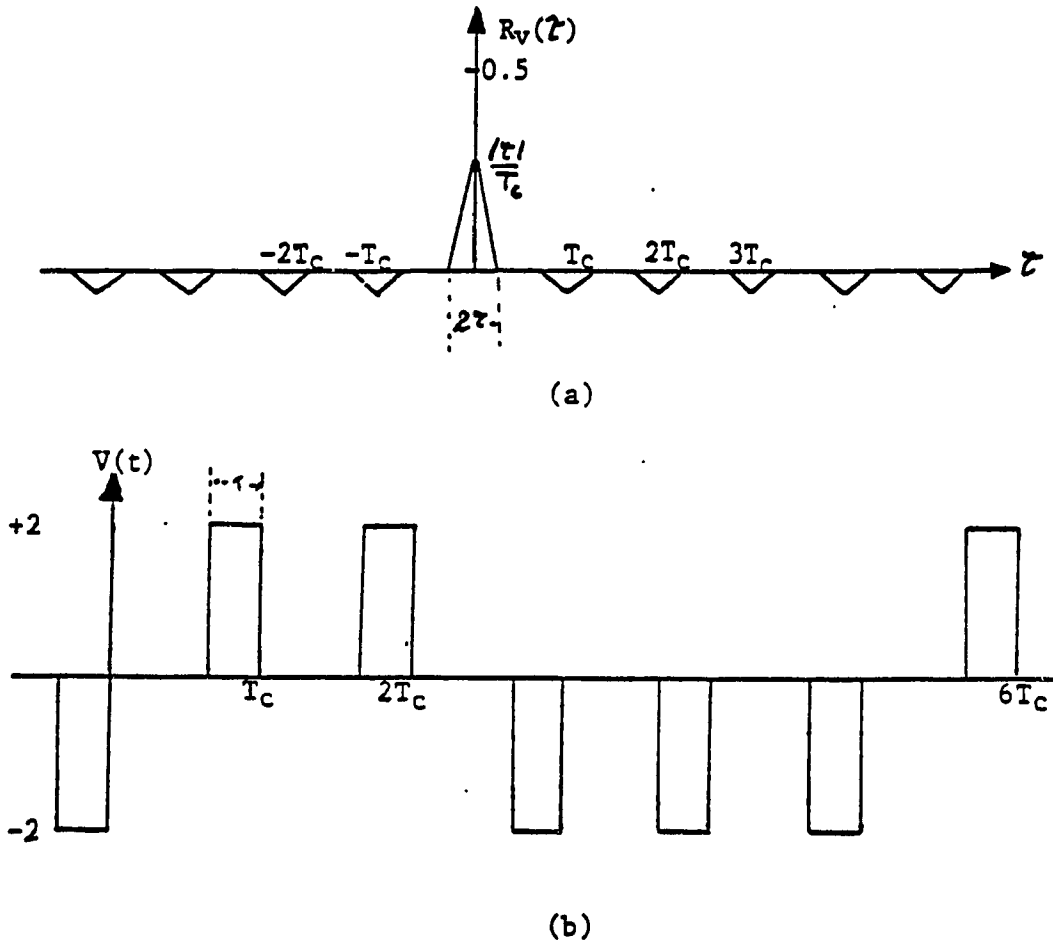

Fig(3. 4):- Waveform and autoccorrelation of the DS/self noise of equation (3.9).

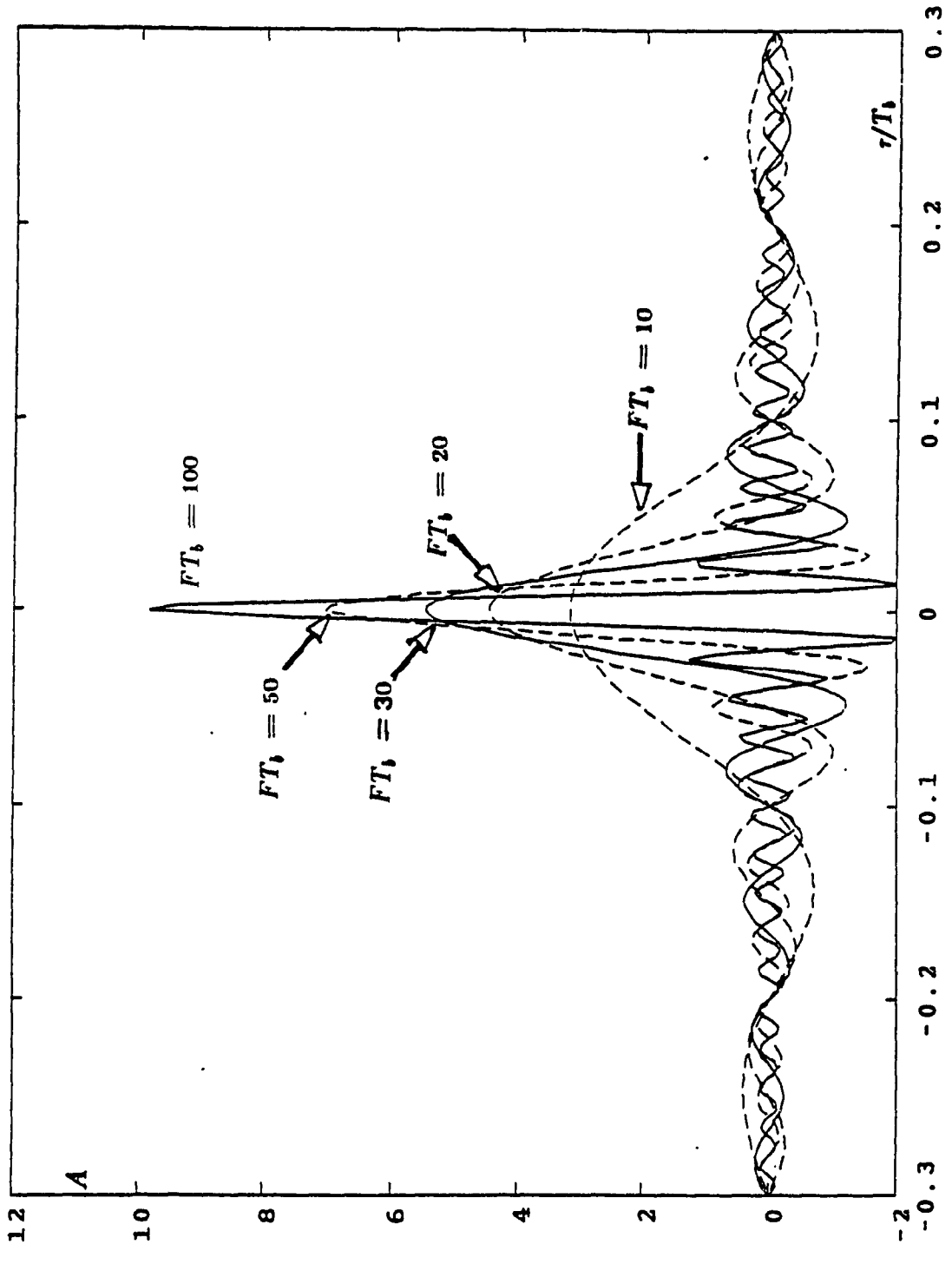

Fig(3. 5):- The compressed chirp pulse at the output of the filter matched to the received signal pulse under no noise no jamming for $\Delta = 0$.

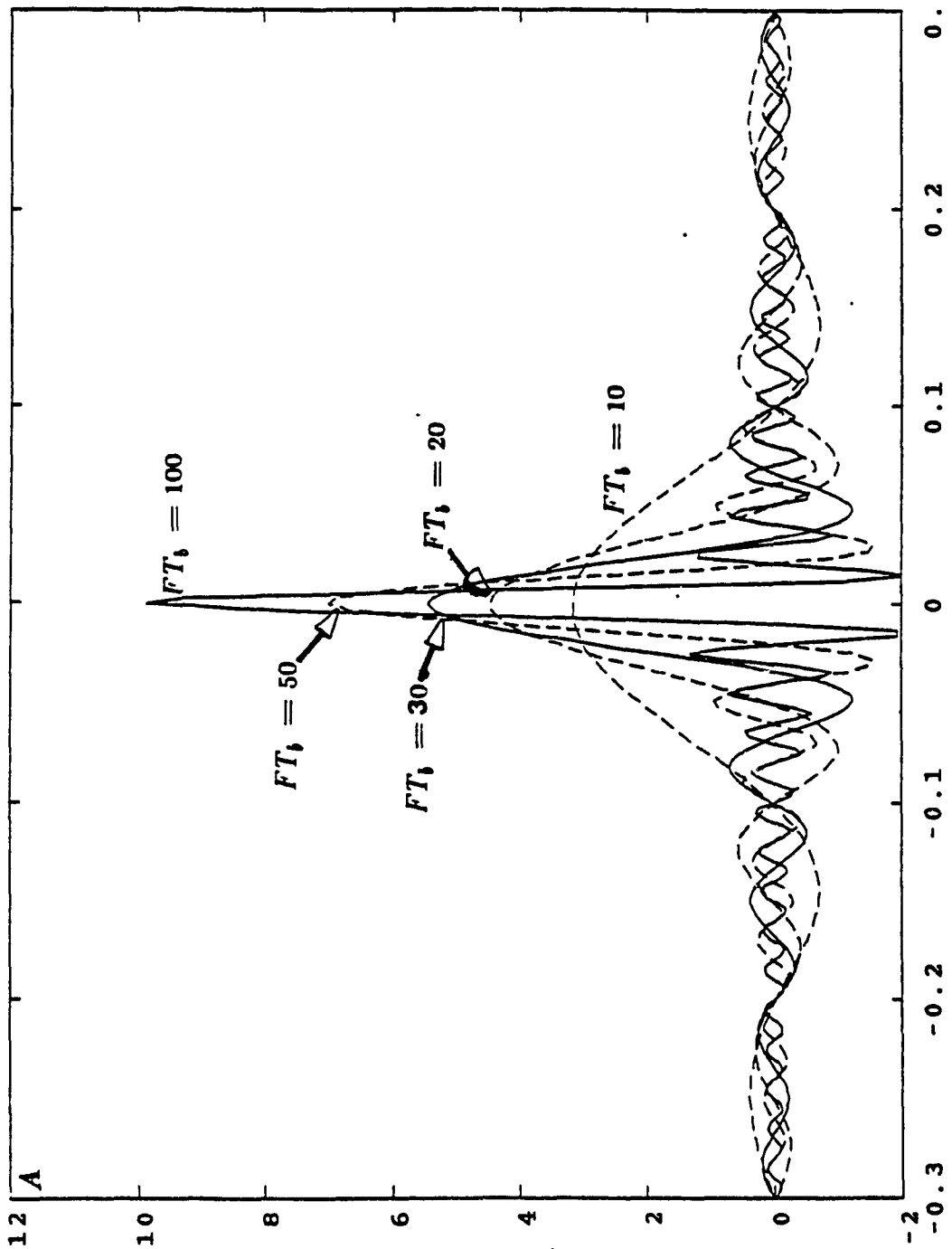

Fig(3. 0):- The compressed chirp pulse at the output of the filter matched to the received signal pulse under no noise no jamming for $\Delta = 0.1$.

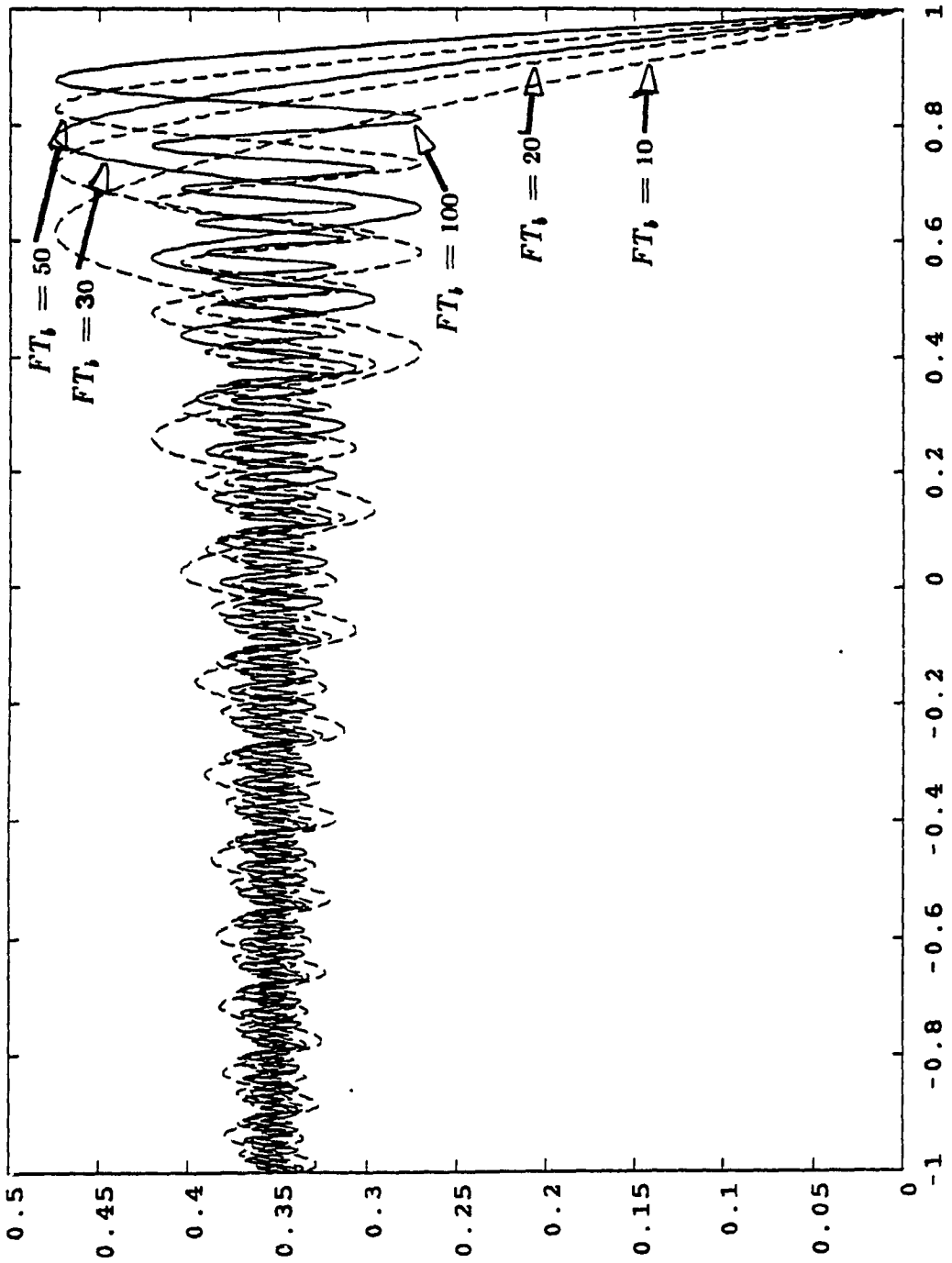

Fig(3. 7):- The compressed chirp pulse at the output of the filter not matched to the received signal pulse under no noise no jamming for $\Delta = 0$.

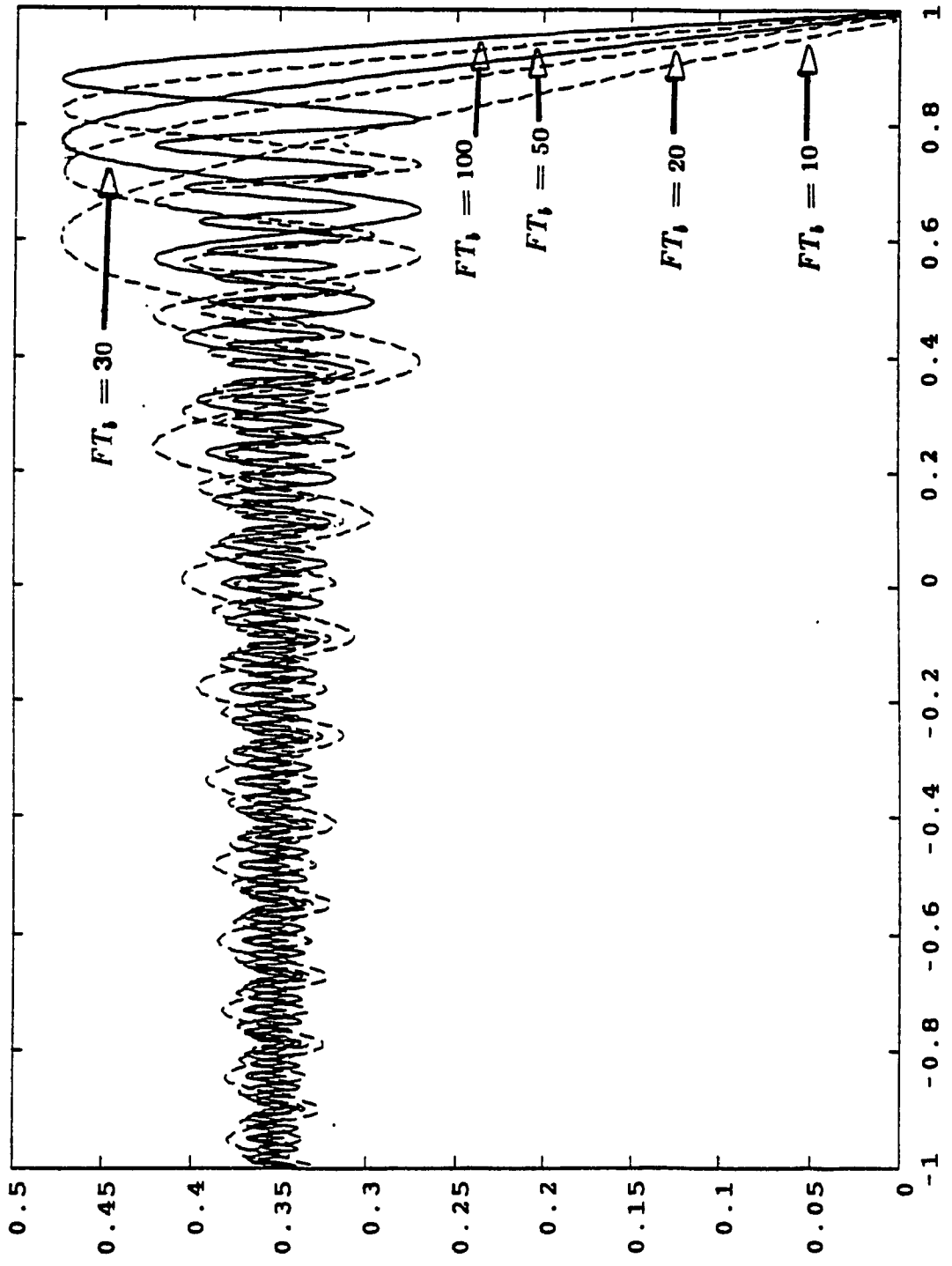

Fig(3. 8):- The compressed chirp pulse at the output of the filter not matched to the received signal pulse under no noise no jamming for $\Delta = 0.1$.

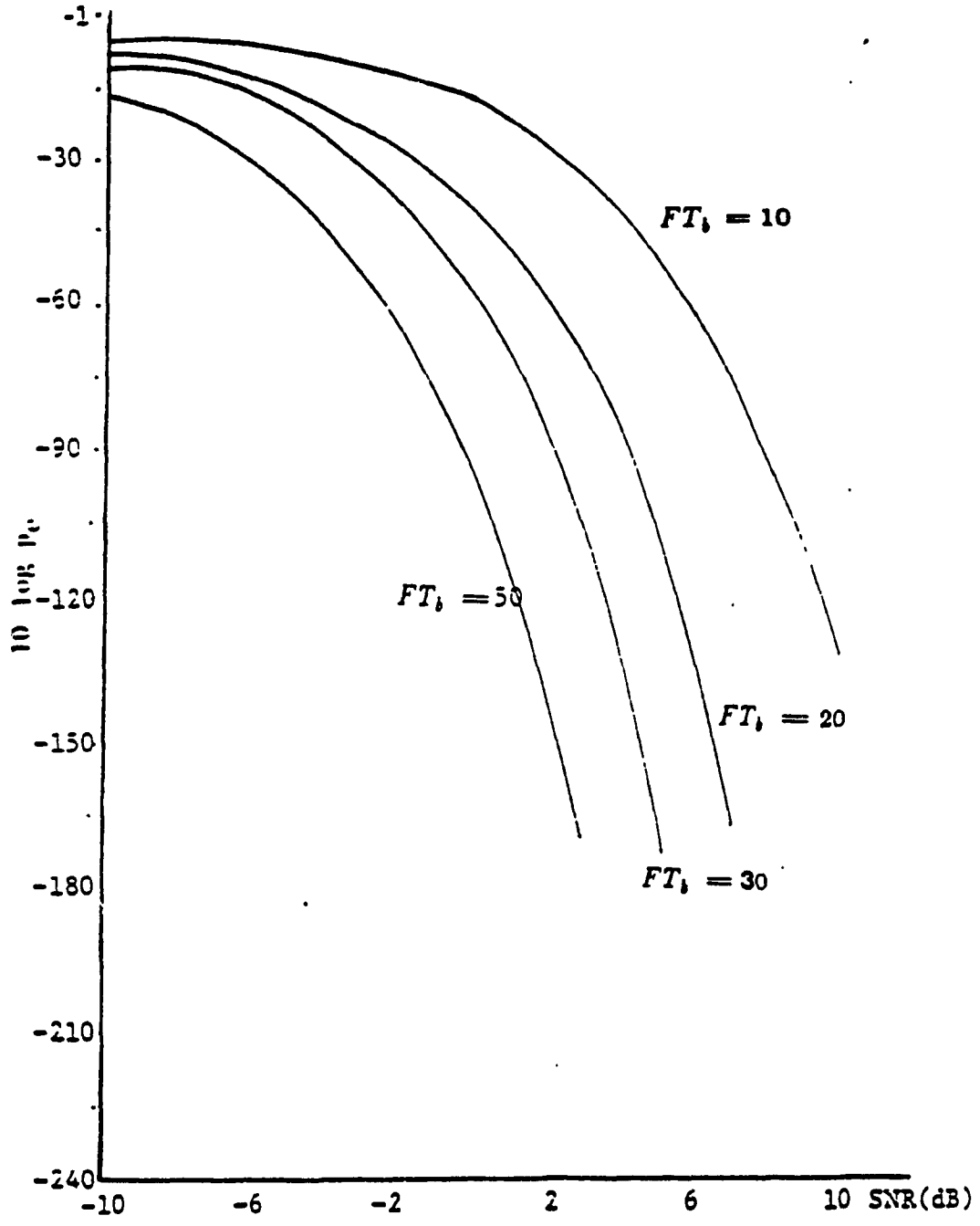

Fig(3. 9):- Probability of error vs. signal to noise ratio for $\Delta = 0$, $\tau = 0$ and $T_b = 1m$.

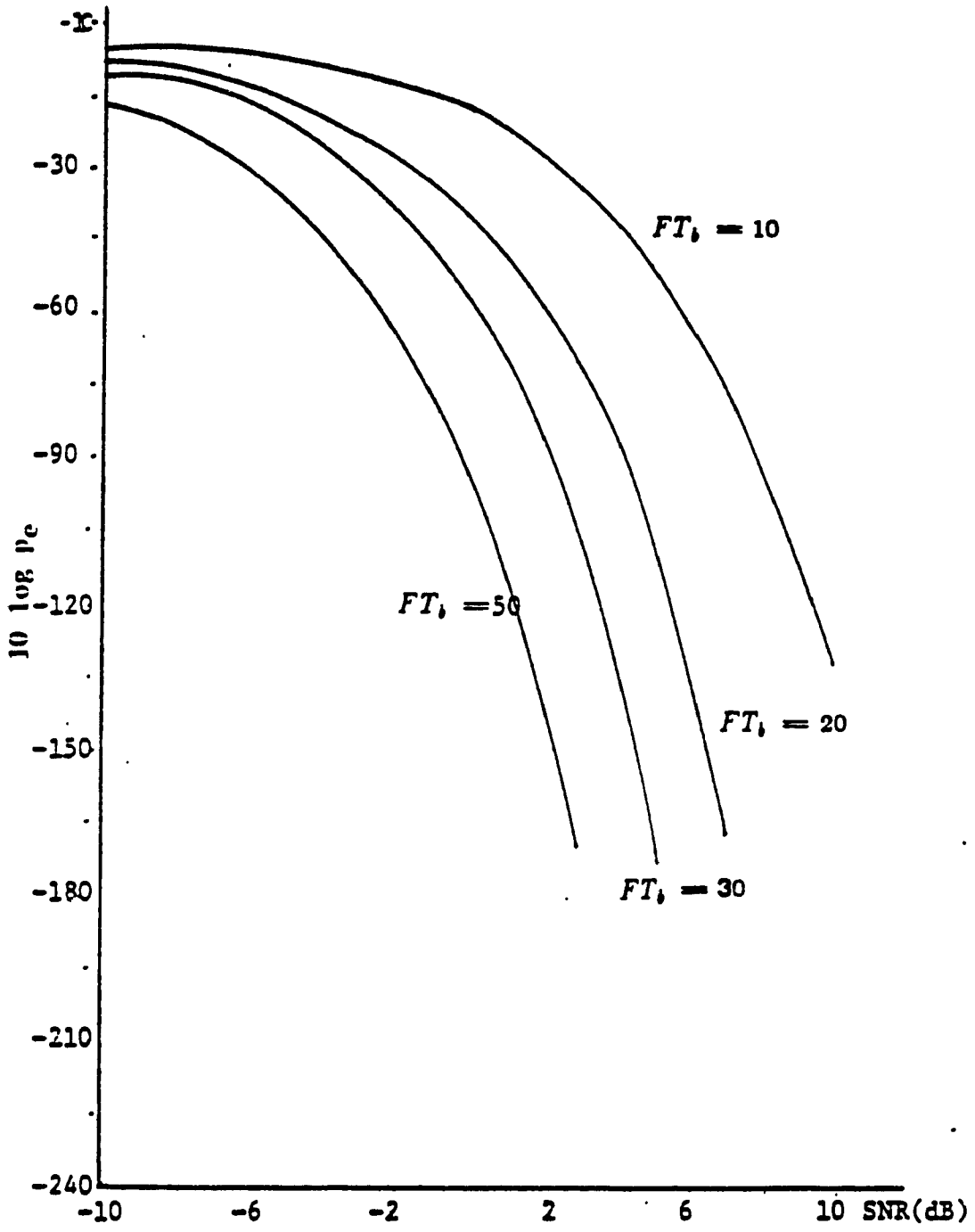

Fig(3. 10):- Probability of error vs. signal to noise ratio for $\Delta = 2K$, $\tau = 0$ and $T_b = 1m$.

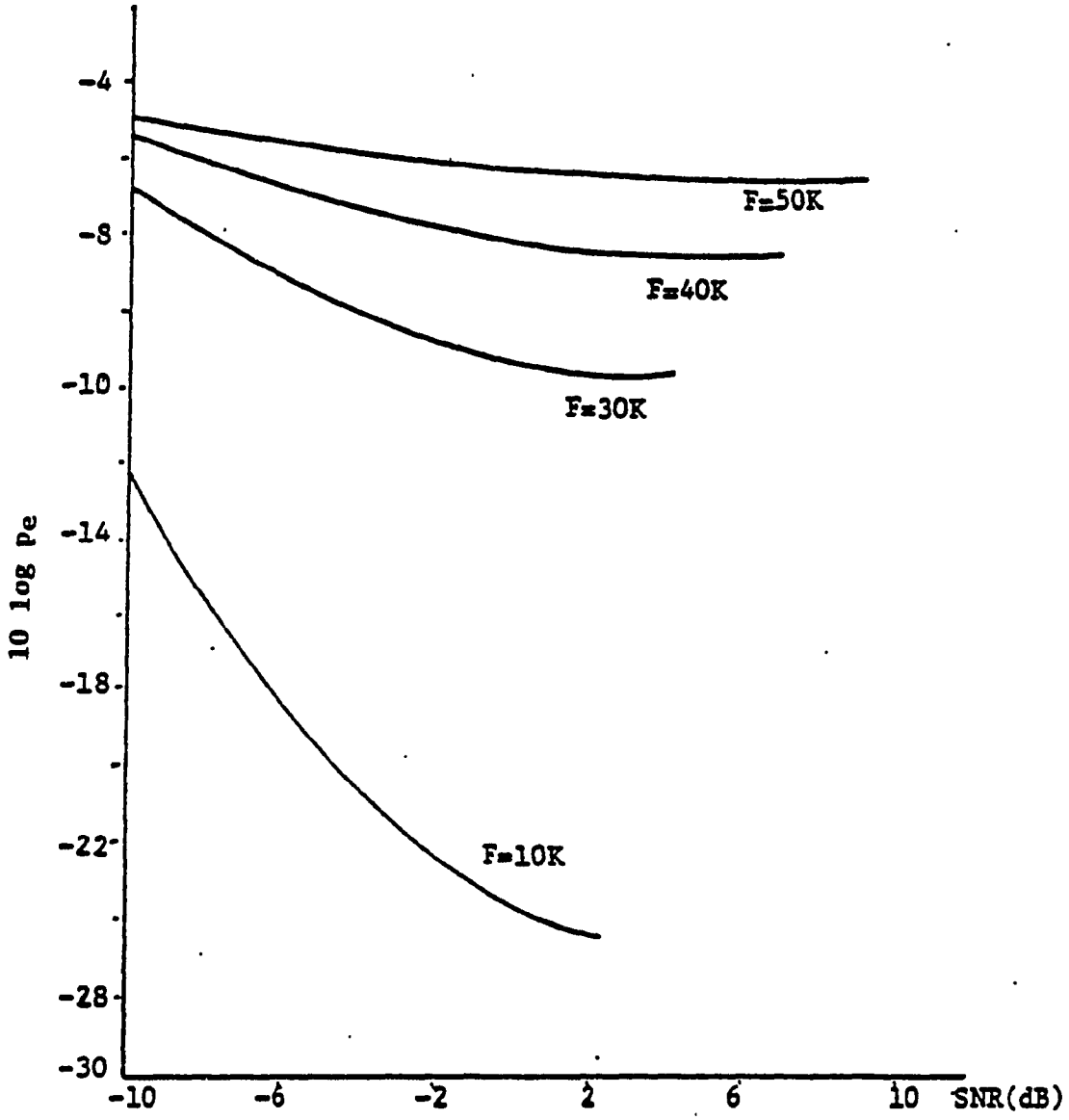

Fig(3. 11):- Probability of error for $\Delta = 1K, J_J = 100$, $B_{RF} = 0.1M$, $\alpha = 0.01$ and $FT_b = 10$.

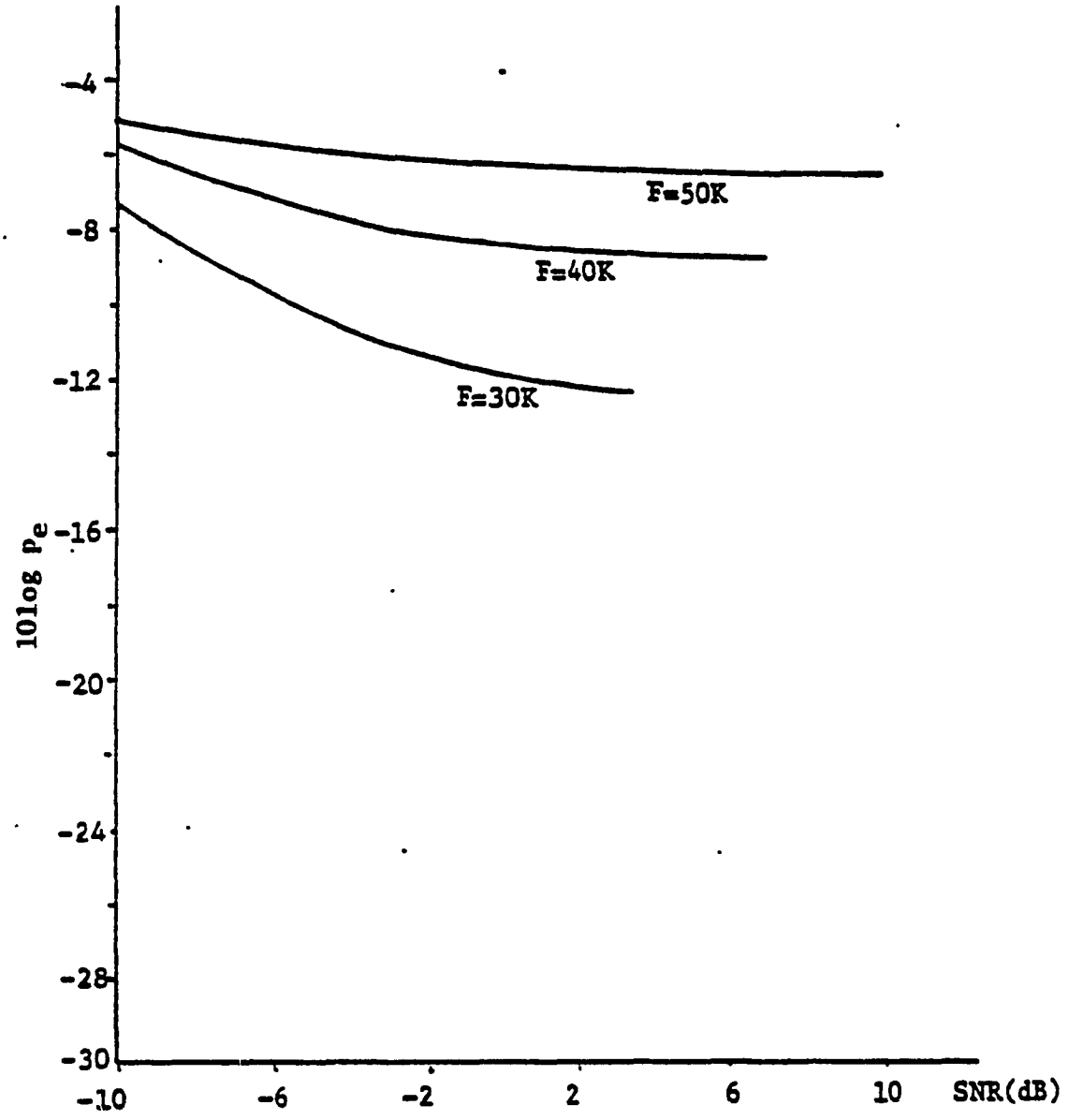

Fig(3. 12):- Probability of error under doppler, time delay and pulse jamming for $\Delta = 100$, $J_J = 20$, $B_{RF} = 0.1M$, $\alpha = 0.01$ and $FT_b = 10$.

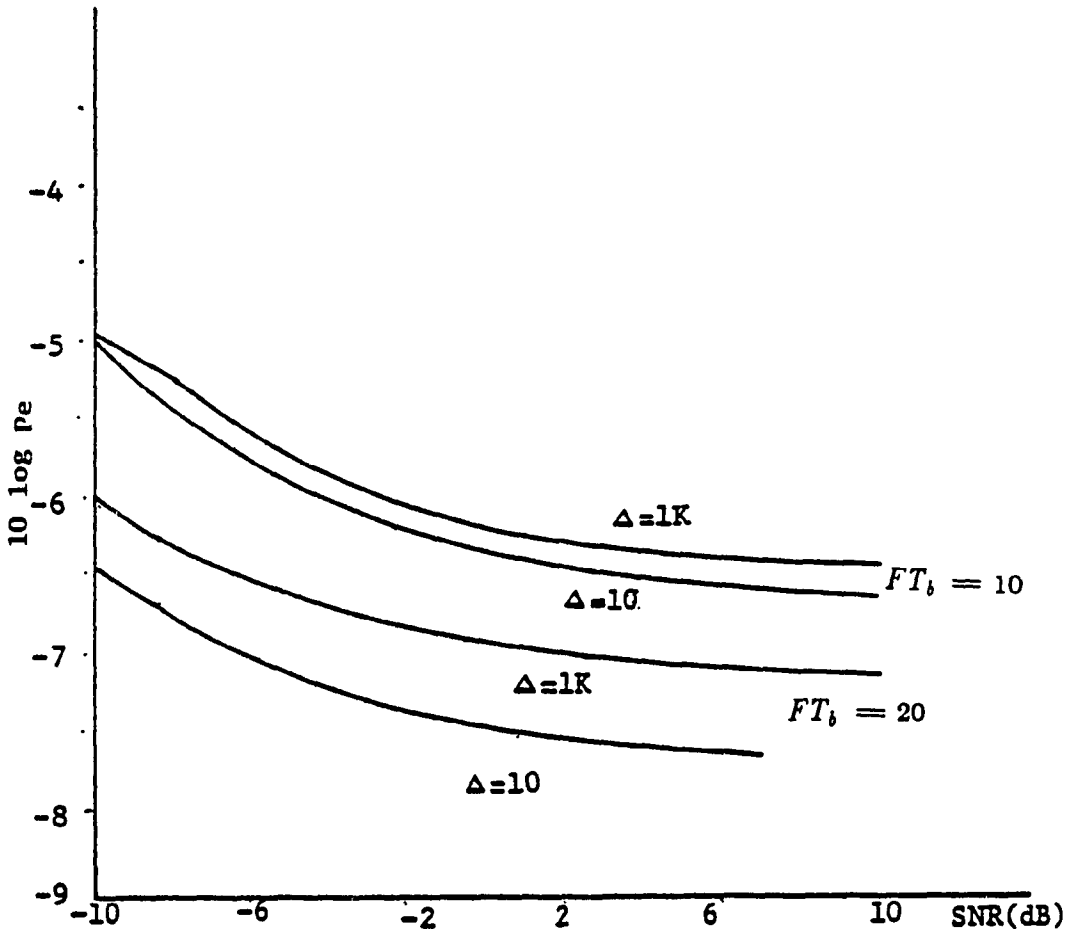

Fig.(3. 13):- Probability of error for the effect Doppler and jamming for $\Delta = 0.1$, $J_J = 100$, $B_{RF} = 0.1M$, and $\alpha = 0.01$.

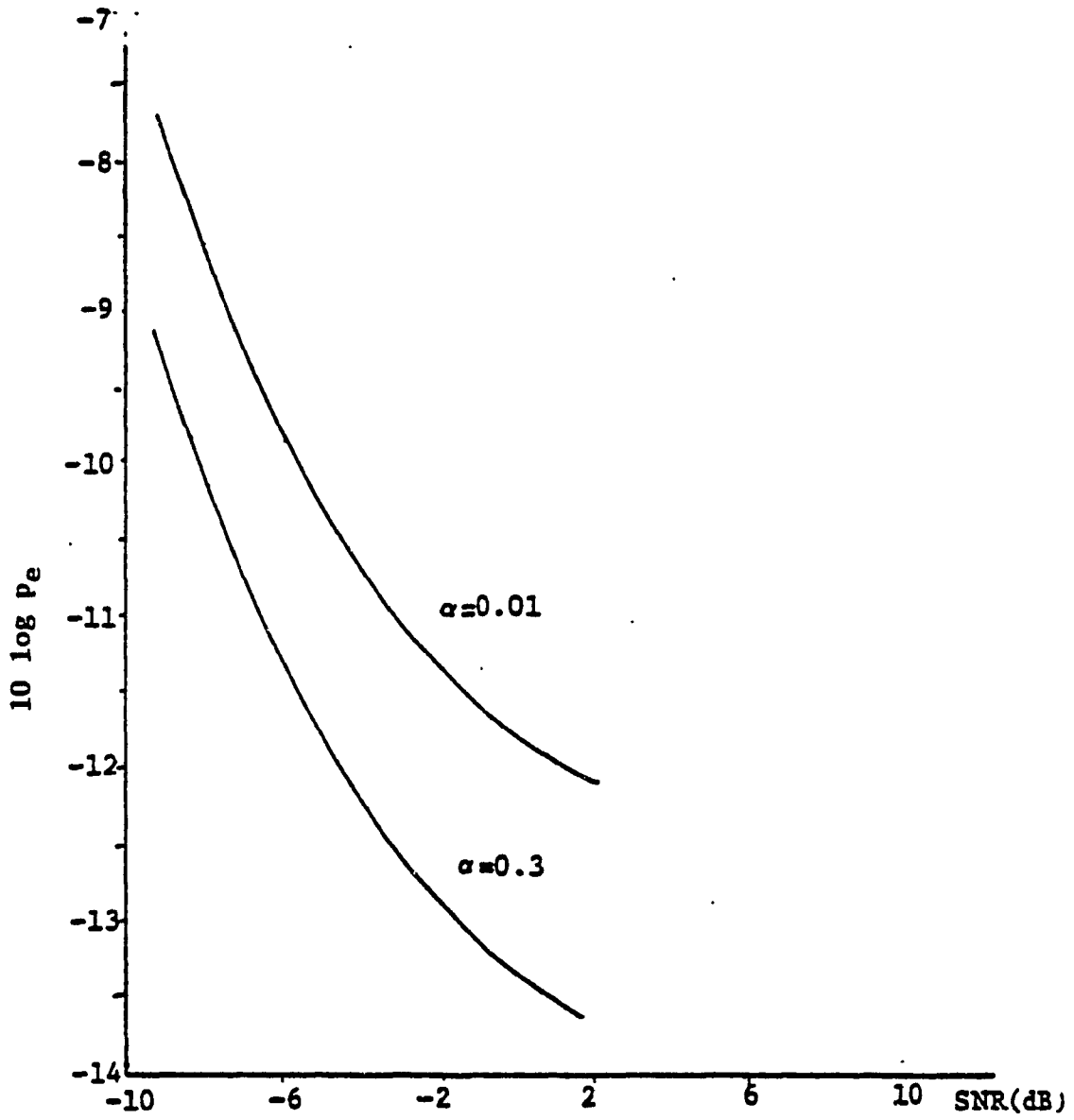

Fig(3. 14):- Probability of error and the effect duly factor with $\Delta = 100$, $J_J = 1K$, $B_{RF} = 0.1M$, and $FT_b = 10.$,

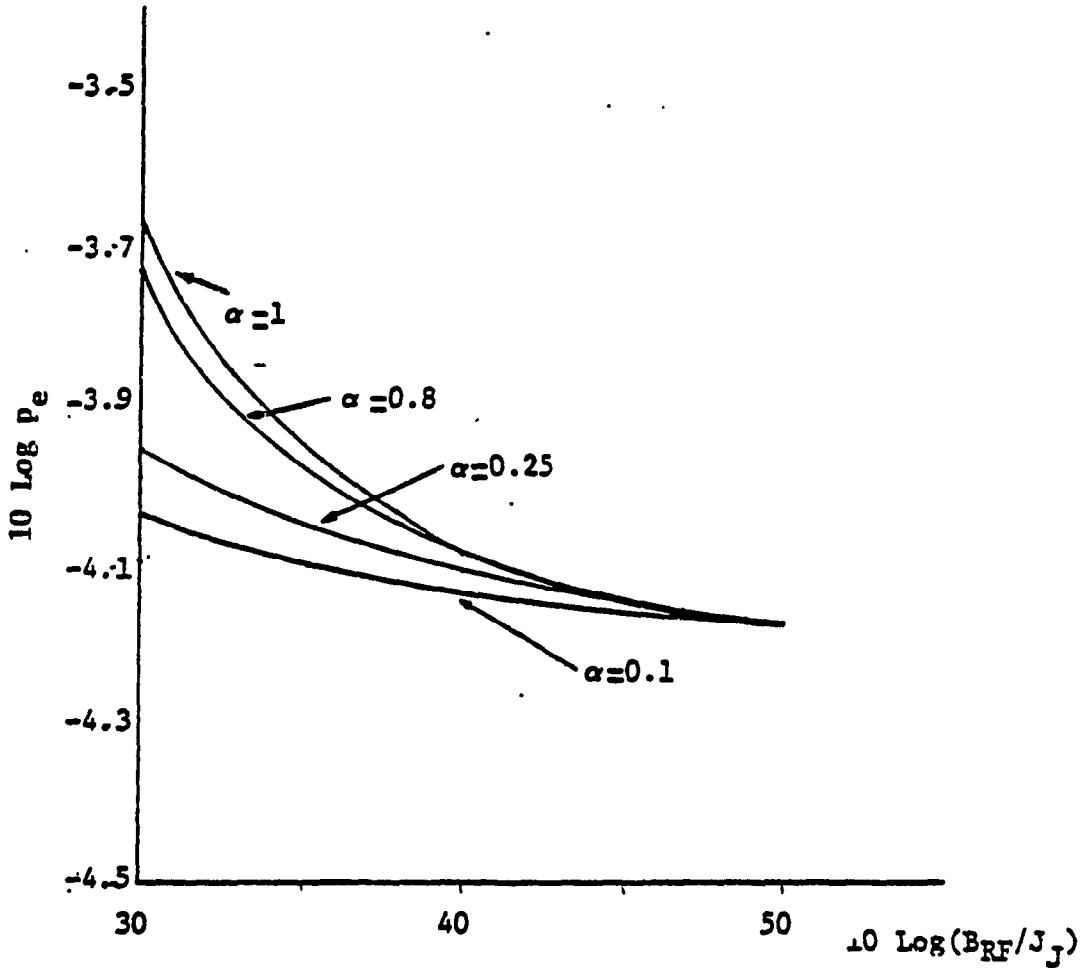

Fig(3. 15):- Probability of error vs. Jamming for $\Delta = 0$, $B_{RF} = 0.1M$, $F = 10K$ and $FT_b = 10$.

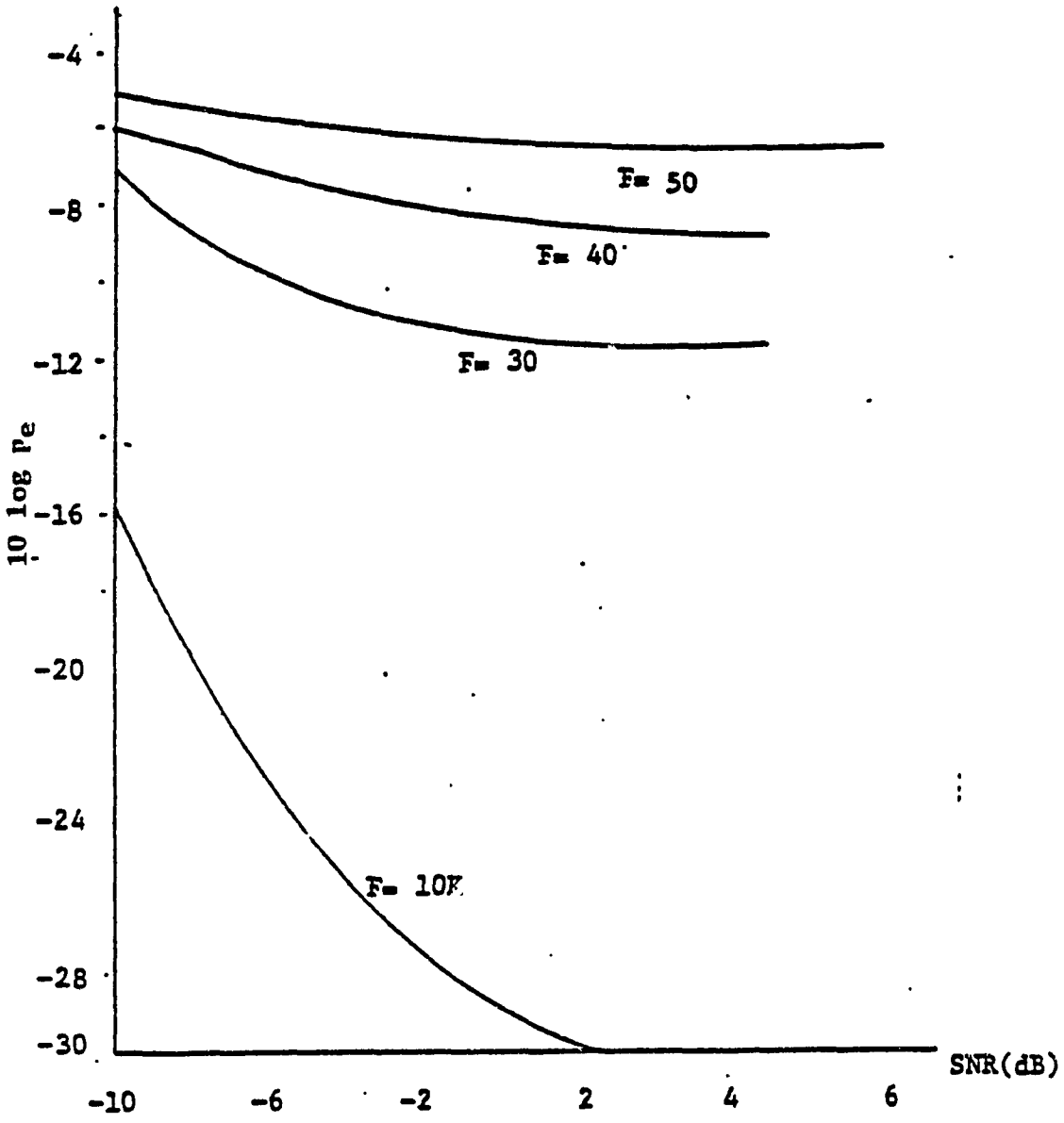

Fig(3. 16):- Probability of error vs. signal to noise ratio for $\Delta = 100$, $B_{RF} = 0.1M$, $J_J = 100$, $\alpha = 0.01$ and $FT_b = 10$.

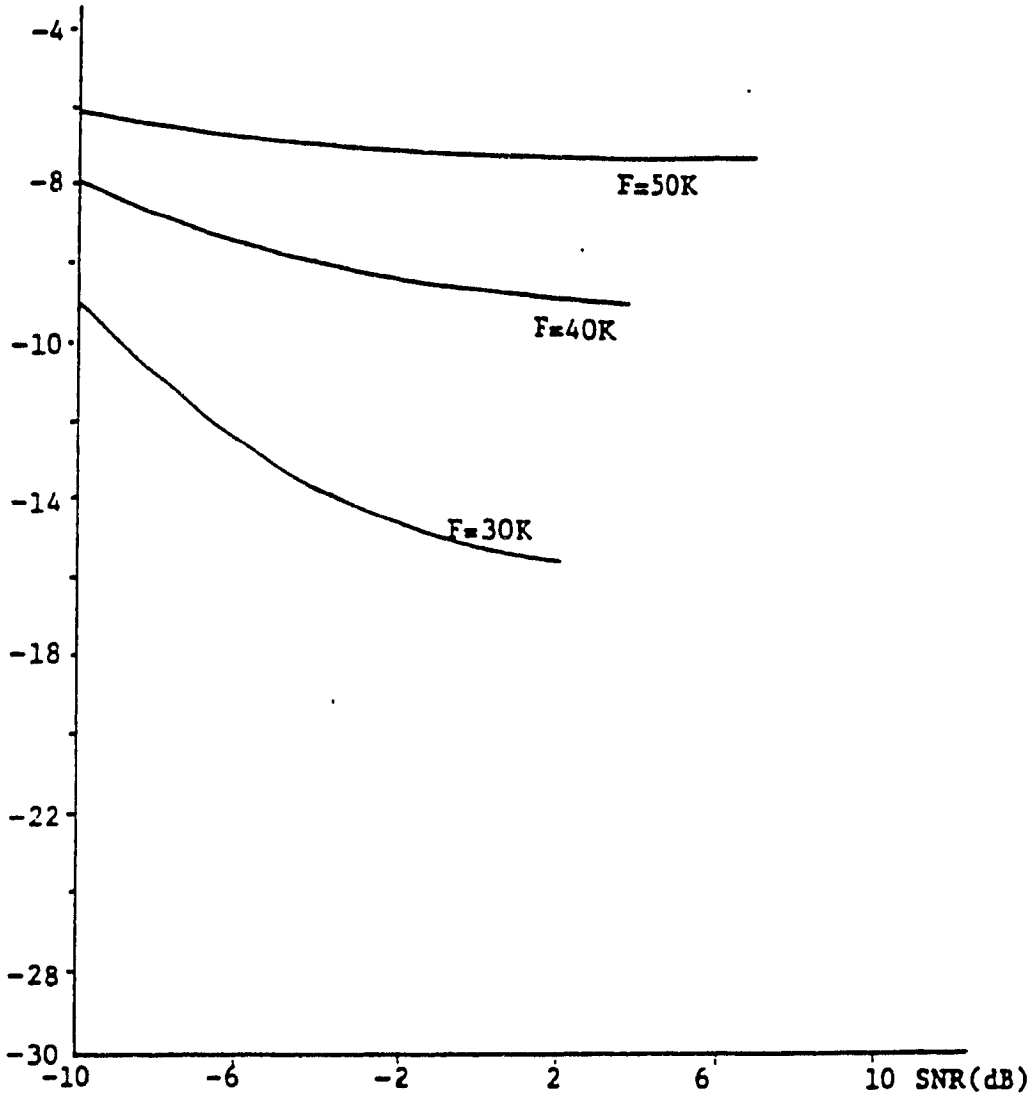

Fig(3. 17):- Probability of error for $\Delta = 100$, $B_{RF} = 0.1M$, $J_J = 20$, $\alpha = 0.01$ and $FT_b = 20$.

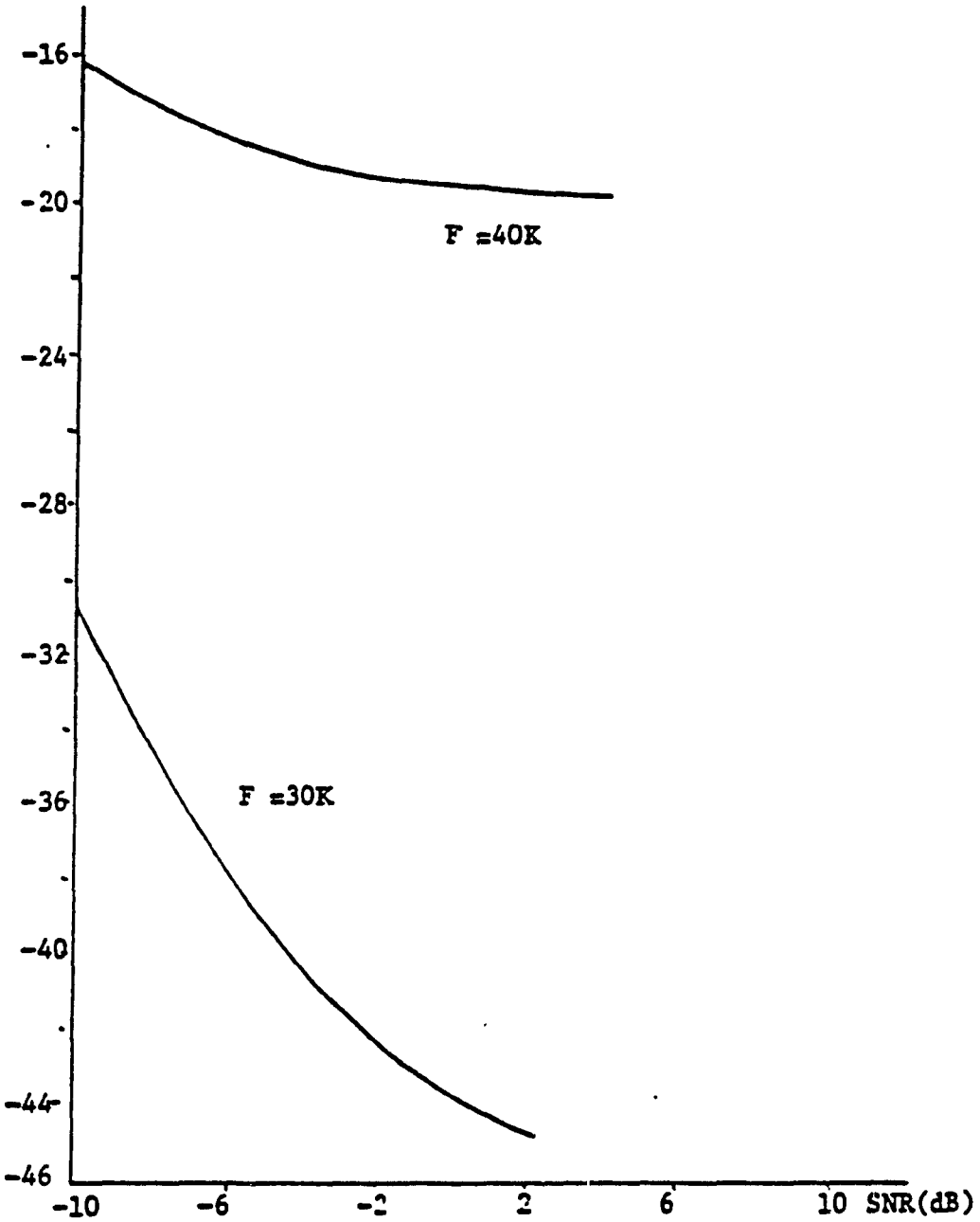

Fig(3. 18):- Probability of error for $\Delta = 100$, $B_{RF} = 0.1M$, $J_J = 20$, $\alpha = 0.01$ and $FT_b = 100$.

CHAPTER 4

ERROR AND THROUGHPUT PERFORMANCE OF MULTI-DECODED, ERASURE-BASED DIRECT SEQUENCE/TIME HOPPING SELECTION DIVERSITY MULTIACCESS SYSTEMS

4.1. Introduction

Minimizing the bit error rate of spread spectrum by use of forward error correction has been the subject of greater interest. This has been motivated by the need of the user to protect his signal against elaborate jamming techniques [9],[10],[38], and for friendly like user signals in a multiaccess environment. Predecoding diversity techniques have been tried [10],[38]. Also, parallel erasure based decoding has resulted in minimizing the final bit errors at the receiver. In all the efforts of [10],[38],[12], different cases of partial band jamming nonselective Rician fading were assumed but cost of diversity was not considered. In this chapter we consider a hybrid Time Hopping (TH)/Direct Sequence (DS) Multiaccess system where Gold codes are used for both DS spreading and TH. In addition to the inherent time diversity in TH, each user transmits the same message in two slots in each frame. At the receiver, the two replicas are used to advantage in involved modulation-acquisition-multidecoding algorithm which effectively resembles a post decoding diversity combining. The environment is a multiaccess network, the data modulation is noncoherent Frequency Shift Keying (FSK). BCH codes form the basic codes in this chapter and the side information in the

preamble of each slot is used to insert or eliminate erasures. An erasure modification logic is also used to eliminate bit erasures of one TH slot according to demodulated bit values in the other slot.

The worst case analysis in the chapter will demonstrate the superior error and throughput characteristic of the proposed hybrid TH/DS network due to the dynamic erasure threshold rule, erasure modification and multidecoding majority voting rule.

The outline of the chapter is as follows. In Section 4.2 we describe the DS/TH/FSK Multiaccess System. Section 4.3 contains the combined acquisition demodulation multi-decoding algorithm, where the proposed algorithm is described. The bit error and network throughput analysis are described in detail in Section 4.4. In Section 4.5, we have summarized the results of the chapter. Finally, the conclusions are drawn in chapter 5.

4.2. Description of the DS/TH/FSK Multi-Access System

We take a population of U users, having different codes $d_i(t)$, $i = 1, 2, \ldots, U$ but same carrier w_c and two FSK frequencies (f_1, f_2). Pseudorandom codes and accurate code epoch are assumed. A user may use his code to both spread the signal and time hop, however, he may in a different scheme use two independent codes for (DS) and (TH) (depending on the availability of codes) (Fig. 4.1). In this chapter we assume the first case and that each user transmits the same data in two time hopping TH slots of each frame, thus providing time diversity. At the beginning of each TH slot (the preamble period) (Fig. 4.1), each user transmits anall Mark (1) signal mixed with the DS code for a fraction $\left(\frac{M_p}{M_p + N_b}\right)\frac{T_F}{N_F}$ of the duration of the TH slot whose duration equals

(T_F/N_F) where T_F is frame length and N_F is the number of TH slots. M_p is the number of data bits equivalent of the preamble, N_b is the number of data bits in the remainder of the TH slot. In the remaining time of the slot $\left(\frac{N_b}{M_p + N_b} \cdot \frac{T_F}{N_F}\right)$, the transmitter sends the (1,0) information on an FSK signal. Fig. 4.2 shows a typical transmitter in the proposed system. To communicate with destination 1, the user selects the code (out of U codes) for transmission. The figure shows also that the data is forward error encoded (FEC) using BCH codes

The frequency synthesizer in Fig. 4.2 is intended to extend the capability of our system by changing the two FSK tones (f_1, f_2) over a certain range on a slow basis. (However, for the analysis purposes, we do not pursue further in this chapter the effects of this extra feature).

In the receiver (Fig. 4.3), we see the carrier recovery, code acquisition, tracking circuits, and bit timing circuits typical with any spread spectrum receiver. The DS preamble matched filter is used to provide for both code synchronization (code epoch) in light traffic conditions, and the threshold adjustment for erasure decoding in all conditions.

The comparator, decoder, and multiplexer (MUX) combination serve the purposes of identifying the range within which the output of the MF lies and finally selects one of the erasure thresholds (TH_j) (see Fig. 4.3 and the first loop of the flow chart of Fig. 4.4).

The two BPF, envelope detectors and Max of comparison yield a (1 or 0) data demodulated bit. However, this demodulated bit may change to an erasure depending on the dynamic threshold comparison with TH_j . In case the like-user interference level in the applicable TH slot rises, the output of the preamble MF

lies outside a certain range and j is a higher value (Equ. 4.35) and the resulting range $(TH_{1,j}, TH_{2,j})$ is used for erasure consideration of all N_b bits of this TH slot, (Fig. 4.3, 4.4).

To detect a bit erasure, the output of the two BPF are squared and added, the threshold comparison with the current TH slot threshold $(TH_{1,j}, TH_{2,j})$, as was detected from the previous stage, thus determines if we should insert an erasure in place of the demodulated bit.

At the end of each of the two TH slots (i.e., II = 2 in Fig. 4.4), the erasure count will be stored in (CCC(1), CCC(2)) and the demodulated bits will be stored in $(D_1(u), D_2(u); u = 1, 2, \ldots, N_b)$. These two vectors, together with the corresponding vectors $G_1(u)$, $G_2(u)$, containing no erasures, will feed the sophisticated multidecoder scheme of Fig. 4.6.

This decoder, together with the remaining bottom blocks of Fig. 4.3 (i.e., the erasure modification logic and the final modified voting algorithm), will be the subject of the next section.

4.3. The Combined Acquisition-Demodulation-Multidecoding Algorithm

This is the combination of the erasure modification logic (Fig. 4.5), the multidecoding scheme (Fig. 4.6), and the modified majority voter (Fig. 4.7). It is amenable to fast software implementation, however, for higher data rates, hardware implementation is possible with of shelf ECL technology for data rates up to 20Mb/sec.

The use of the word 'acquisition' here should not be very misleading since we actually use the output of the DS preamble MF for demodulation purposes as stated previously. Moreover, this output can be used in an evident way for initial code acquisition (epoch) without needing to elaborate search techniques such

as [9].

The erasure modification logic (Fig. 4.5) works on the two vectors $D_1(u)$, $D_2(u)$ (the output demodulated bits from the first TH slot and the erasure bits of the second TH slots), and finally provide corresponding vectors $DD_1(u)$, $DD_2(u)$ (Fig. 4.5, 4.6). The logic simply replaces the erasure bits from one TH slot by the corresponding demodulated (1,0) bit from the other TH slot. If both bit locations in the two TH slots contain erasures, we simply retain the erasure in both bit locations in the two TH slots. Finally, Fig. 4. 5 gives the new vectors $DD_1(u)$, $DD_2(u)$, and the new erasure count $CCC(3)$, $CCC(4)$ of the first and second TH slots respectively.

The 6 vectors $D_1(u)$, $DD_1(u)$, $DD_2(u)$, $D_2(u)$, $G_1(u)$, $G_2(u)$ now feed the multidecoders of Fig. 4.6. Two of those decoders (those fed by $(D_1(u), G_1(u))$ and $(D_2(u), G_2(u))$ are of the parallel erasure-error type discussed in [10], [38]. The other two decoders are of the ordinary erasure error correcting decoder [12].

As a matter of fact, our multidecoding approach shares in common with [38] the fact that a better channel bit error can be obtained by diversity (TH in our case), and the subsequent parallel FEC will work on a better bit channel error and a superior performance result.

In our multidecoding scheme, we employ the inherent time diversity in TH and the erasure modification logic is one way to improve this diversity. Actually this rings like selection diversity known to Mobile Communication experts [13]. This should improve the starting effective channel bit errors and the subsequent multidecoding should improve these errors to a greater extent.

Another point worth mentioning is that diversity is never without a price, either cost or throughput, or both, whether it is time or frequency or antenna diversity, etc. This factor was ignored in [10], [38]. In our chapter we have a

nonoptimistic analysis mechanism that doubles the effective number of users since each user transmits the same signal in two TH slots.

The details of the parallel erasure-error decoder can be found in [10], [38], while an ordinary erasure-error FEC can be found in [12], and their reflections on our analysis is clear in Section 4.5, and Appendix B. The final block (voter) is shown in Fig. 4.7. Here, similar 4- or 3-bits from any 3 or 4 decoder outputs will be accepted. If we have a tie, (i.e., two of the decoders output (1) and the other active output (0)), we vote in favor of the decoders having a smaller erasure count $CCC(.)$ as was mentioned earlier. If however, the two decoders providing the same output bit (1 or 0) are fed by bits belonging to different TH slots, again we have a tie and with probability $\frac{1}{2}$ we select (1) or (0).

Actually, it is this event that lower bound the final bit error decoding as will follow shortly.

4.4. Bit Error and Network Throughput Analysis

The received signal at the ith receiver is given by (following the DS preamble) and after, carrier recovery, mixing and assuming l interfering users with our intended i^{th} receiver at this slot,

$$r_{i,l}(t) = Ac_i(t)\cos((w_c t + f_i)t + \phi_i) + \sum_{j=0}^{l} Ac_j(t)\cos((w_c t + f_j)t + \phi_j) + n(t) \qquad (4.1)$$

All users are assumed to have the same power $= A^2/2$, slotted TH operation is assumed, $c_i(t)$, $c_j(t) = \pm 1$ are the DS chips of users i, j as generated by Gold codes of rate $= 1/T_c$.

f_i, f_j takes one of two values (Mark and Space frequencies)

w_c is the IF of the FSK modulation

ϕ_i, ϕ_j, are the random uniformly distributed phases of i^{th} and j^{th} signals

$n(t)$ is the AWGN of double sided density $(N_0/2)$

Approximating the pseudorandom codes by completely random code, the probability of any one user selecting a specific TH slot for transmission is given by,

$$P_h = (1/N_F) \tag{4.2}$$

and the probability of l users selecting the same TH slot used by the i^{th} user is given by,

$$S_l = \binom{2U' - 1}{l} (P_h)^l (1 - P_h)^{2U' - l - 1} \tag{4.3}$$
$$, l = 0, 1, \quad , 2U' - 1$$

We note $2U'$ rather than U', which is due to the fact that each user transmits the same message in 2 TH slots of each frame thus doubling the effective number of users on each frame. Following despreading by the local i^{th} code at the i^{th} receiver of $r_i'(t)$, we obtain,

$$y_{i,l}(t) = A \cos((w_c t + f_i)t + \phi_i) + \sum_{j=0}^{l} A c_i(t) c_j(t) \cos(w_c t + f_j)t + \phi_j) + n(t) c_i(t) \tag{4.4}$$

Now by analysis, we replace the instantaneous value $c_i(t)$ and $c_j(t)$ by the upper bound on Gold codes cross correlation based on one information bit period T_b (i.e., C_b).

To evaluate C for the whole code length, we take a family of Gold codes [6] where the cross correlation C is upper bounded by

$$C \leq \left(2^{(L'+1)/2}+1\right) \qquad (L' \quad odd) \tag{4.5}$$
$$C \leq \left(2^{(L'+2)/2}+1\right) \qquad (L' \quad even)$$

where L' is the length of the feedback shift registers used to generate the code. Moreover, if we divide C above by the code self correlation peak we obtain

$$C \leq \frac{2^{\frac{L'+1}{2}}+1}{2^{L'}-1} \leq 2^{-L'/2} \tag{4.6}$$

for *large* L'

Moreover, it is known that the number of users that can be supported by this L' is given by,

$$U = 2^{L'}+1 \tag{4.7}$$

and the code length of each member of the family is given by,

$$LL = 2^{L'}+1 \tag{4.8}$$

For large enough L', we see that,

$$LL = U \approx 2^{L'} \tag{4.9}$$

We assume that M_p encoded data bits constitute the preamble length, N_b encoder data bits constitute the remainder of the TH slot whose length $= (T_F/N_F)$, T_c is the DS chip period, frame length T_F and number of TH slots

per frame $= N_F$, the data bit length on the channel following the forward error encoding (FEC) at the transmitter is given by T_b^c. The intrinsic source data rate is given by R'_b bits/sec and the FEC rate is $\frac{k}{n}$. To preserve the same R'_b under (TH) and coding and the overhead, T_b^c on the channel has to be much smaller than $(1/R'_b)$, i.e.,

$$T_b^c = \frac{1}{R'_b} \quad \frac{1}{N_F} \quad \frac{N_b}{M_p + N_b} \quad \frac{k}{n} \tag{4.10}$$

while the (DS) bit processing gain is defined as,

$$PG = \frac{T_b^c}{T_c} \tag{4.11}$$

Recalling that the cross correlation C in (6) is based on a whole code length while C_t should be based on only one coded bit period T_b^c, and assuming that the cross correlation relation prevails over shorter code periods, we obtain,

$$C_t \leq 2^{L \quad 2} = 2^{1\ 2\log(PG)} = \frac{1}{\sqrt{PG}} \tag{4.12}$$

Evaluating C_t, i.e., Gold codes cross correlation taking the preamble length of M_p encoded data bits based on the same assumption as above leads to

$$C_p \leq 2^{L \quad 2} = 2^{1\ 2\log(M_p \quad PG)} = \frac{1}{\sqrt{PG \quad M_p}} \tag{4.13}$$

The design of our TH/DS multiaccess network starts with assuming a certain available spread spectrum bandwidth W_{ss} and hence $T_c = \frac{2}{W_{ss}}$, a certain

intrinsic source data rate R'_b. a certain slot preamble overhead R == ratio $= M_p/(N_b + M_p)$, from which T_b^c and PG can be calculated as per (10), (11). The choice of the user Gold code length (same for all users) is next. This is related to the maximum possible number of users in the network as per (9) and to allow for load variations a certain worst case is assumed such that

$$U_{\max} = r \cdot PG \cdot N_F = 2^{L'} + 1 \tag{4.14}$$

where r is a certain integer. The Gold code length of each user $(2^{L'} - 1) \equiv U_{\max}$ and is spanned in each TH slot such that,

$$(N_p + M_p)\, T_b^c = (2^{L'} - 1) T_c \tag{4.15}$$

from which one obtains

$$\begin{aligned}(N_p + M_p) &= (2^{L'} - 1)/PG \\ &\approx U_{\max}/PG \approx r \quad N_F\end{aligned} \tag{4.16}$$

and the TH frame length is given by

$$T_F = T_c \cdot (2^{L'} - 1) N_F \tag{4.17}$$

The tradeoff in the parameter design of the network are now clear higher values of r allow for more users to be accommodated and more code lengths (4.14) (of course as probability of error on the channel permits). However, this also means larger $(M_p + N_p)$ and frame size T_F for the same (R'_b, T_c) longer T_F times means more delay which might be prohibitive for some voice applications. Also the frame length T_F has its implications on the retransmission delay in case Automatic Repeat Request is used for acknowledgement. Finally, the number of

encoded date bits equivalent of the preamble period is given by,

$$M_p = R'_b (\quad_p + M_p) = R'_b \ . r \ . N_F \tag{4.18}$$

and the network throughput is given by

$$\Delta = \frac{U(1 - P_b)R'_b}{(2/T_c)} \tag{4.19}$$

where P_b is the probability of bit errors, as will follow shortly.

To evaluate the bit and packet error probability, we go back to equation (4.4) where it is readily seen that the term $c_i(t)\, n(t)$ is essentially an AWGN with p.s.d. height $= \frac{N_o}{2} K_o$, [4] where $K_o \approx 1$. The cross correlation of two Gold codes in the same family is an irregular function which we model as noise of average zero and variance equal to the maximum given by (4.12), (4.13). The bandwidth of the FSK signal is neglected compared to the much wider term $c_i(t)\, c_j(t)$ and so the term $cos(w_c + f_j t + \phi_j)$ vanishes from under the summation of (4.1), finally we obtain

$$y_{i,l}(t) = A \ cos((w_c t + f_i)t + \phi_i) + (l \quad 1) A c_{ij}(t) + n'(t) \tag{4.20}$$

$$\cdot A \ cos((w_c t + f_i)t + \phi_i) + n''(t) \tag{4.21}$$

where $c_{ij}(t)$ is an AWGN of zero mean and variance given by C_i of equation (12), $n''(t)$ is an equivalent BP noise process.

The subsequent BPF and envelope detection in the receiver (see Fig. 4.3) yields the following envelope distributions at the output of each bit interval

$$P'_{r,s}(r) = \frac{r}{\sigma_i^2} e^{-(r^2 + A^2)/2\sigma_i^2} I_o\left[\frac{rA}{\sigma_i^2}\right] \tag{4.22}$$

$$P_n^l(r) = \frac{r}{{\sigma_l}^2}\, e^{-(r^2 + A^2)/2{\sigma_l}^2} \tag{4.23}$$

where

$P_{s+n}{}^l(r)$ is the envelope of the branch having the signal (assumed Mark for example) given l interfering users

$P_n(r)$ is the envelope of the branch not containing the signal

$I_o(.)$ is the Bessel function of first kind and order zero

σ_l^2 is the equivalent noise variance

This is the total of AWGN power $\frac{N_o}{2}(2R'_b) = N_o / T_b^c$ and the equivalent cross interference noise ($l\ A\ c_{ij}(t)$) (whose power is $\frac{1}{2} \cdot \frac{2}{3}\ l\ A^2 \frac{k}{n} C_b$) of the l users multiaccess interference

$$\begin{aligned} \sigma_{l,b}^2 &= \frac{k}{n} \cdot \frac{1}{2} \cdot \frac{2}{3} \cdot \frac{A^2}{2} \cdot l \cdot C_b + N_o\ R'_b \\ &= \frac{1}{3}\ \frac{k}{n} A^2\ l\ C_b + \sigma_n^2 \end{aligned} \tag{4.24a}$$

we also define for the preamble period

$$\sigma_{l,p}^2 = \frac{1}{3}\ \frac{k}{n} A^2\ l\ C_b + \sigma_n^2 \tag{4.24b}$$

The factor $\frac{k}{n}$ accounts for the fact that the energy of the FEC encoded bit is less by $\frac{k}{n}$ than that of the original data bit. The term $\frac{A^2}{2}$ is the transmitted power of each interfering user at the intended user with $\frac{1}{2}$ due to differential location of different users. The factor $\frac{2}{3}$ is an averaging term stemming from the fact that

each Gold code cross correlation function is a three valued signal with the maximum (C_b) given by (4.6) and a negative and an appropriate equal second line and a third negligible minimum value so averaging over all possibilities and assuming equally likely probability of encountering each level yields the term (2/3). Under AWGN only, (no multiaccess) we would only have increased the user i^{th} power to $\left(\frac{A^2}{2} \cdot N_F\right)$ to have the same average power in the two systems (with and without TH). However, this increases σ_l^2 correspondingly if the l interferers have the same received power at the intended receiver). If topology and the user's location are considered, the above increase in power might prove to be useful. However, in this chapter we choose to keep the same source power $A^2/2$ in our case of TH and for noncoherent detection of FSK signals the probability of error (given l) is given by,

$$\mu_l = \frac{1}{2} e^{-(A^2 \frac{k}{n})/2\sigma_l^2} \tag{4.25}$$

with the factor $\frac{k}{n}$ again accounting for the decrease in bit energy due to use of FEC.

The final bit error decoding probability will depend on μ_l, as well as the bit erasure error probability $\gamma_{j,l}$. To evaluate $\gamma_{j,l}$ which is defined as (see the erasure channel of Fig. 4.8) the probability that the sum of the squares of the outputs of the Mark and Space filters lies outside a certain range ($TH_{1,j}$, $TH_{2,j}$) as dumped by the preceding preamble detection. Assuming that the erasure variable (to be tested against $TH_{1,j}$, $TH_{2,j}$ for each bit) is $z = (a^2 + b^2)$. If a,b are approximately Gaussian random variables with means $A^2 \frac{k}{n}$, 0 and variance

σ_l^2 for both of them (obtained by sampling the Mark and Space at the end of each received bit), the pdf of z is known to be a non- central Chi-Square with 2 degrees of fraction, i.e.,

$$P_{z,l}(z) = \frac{1}{2\sigma_l^2} e^{-(A^2 \frac{k}{n} + z)/2\sigma_l^2} I_o \left(\frac{A\sqrt{z\ k/n}}{\sigma_l^2} \right) \tag{4.26}$$

where the noncentrality parameter $= s_2 = m_1^2 + m_2^2 = A^2 \frac{k}{n} + 0 = A^2 \frac{k}{n}$. Recall either the Mark or the Space signal is transmitted. $I_0(.)$ is the Bessel function of zero order of the first kind. The mean and variance of z are given by

$$\mu_{z,l} = 2\ \sigma_{l,b}^2 + A^2 \frac{k}{n} \tag{4.27}$$

$$\sigma_{z,l}^2 = 4\ \sigma_{l,b}^4 + 4\ \sigma_{l,b}^4\ A^2 \frac{k}{n} \tag{4.28}$$

Approximating $p_{z,l}(z)$ of (4.26) by a Gaussian distribution, we obtain the erasure probability as

$$\gamma_{j,l} = 1 - \int_{TH_{2,j}}^{TH_{1,j}} \frac{1}{\sqrt{2\pi}\sigma_{z,l}} e^{-(z-\mu_{z,l})^2/2\sigma_{z,l}^2}\, dz \tag{4.29}$$

$$= 1 - \frac{1}{2} Erf_c \left(TH_{1,JJ-j+1} - \mu_{z,l} \right) \tag{4.30}$$

$$+ \frac{1}{2} Erf_c \left(TH_{2,JJ-j+1} - \mu_{z,l} \right)$$

$$j = 1, 2, \ldots, JJ$$

where JJ is the number of allowable thresholds ($TH_{1,j}$, $TH_{2,j}$) as a parameter

$$TH_{1,j} = A^2 \frac{k}{n} / (\nabla j + 1) \tag{4.31}$$

$$TH_{2,j} = A^2 \frac{k}{n} \cdot (\nabla j + 1) \tag{4.32}$$

Both JJ and ∇ are treated as performance improvement parameters in our computation. The inverse relation between signal level (4.27) and erasure is noted here. Smaller values of $\mu_{z,l}$ (around the mean) implies smaller value of j and TH_j and by replacing j by $JJ - j + 1$ in (4.30) we guarantee a smaller erasure value in this case. On the other hand, high multiaccess interference means higher $\mu_{z,l}$ and higher j and TH_j and high erasure probability from (4.30).

The determination of an erasure bit (and hence $\gamma_{l,j}$) depends on the threshold dumped from the preamble stage, i.e., the outcome of the comparator stage of Fig. 4.3 which is fed by the signal from the preamble MF, i.e., $c(t)$ sampled at the end of the preamble of every TH slot, we obtain again a noncentral chi-square distribution for $z' = y^2$ (i.e., a distribution given by (4.26) except that the means and variances are given by

$$\mu_{z',l} = \sigma_{l,p}^2 + A^2 \frac{k}{n} \tag{4.33}$$

$$\sigma_{z',l}^2 = 2\sigma_{l,p}^4 + 4\sigma_{l,p}^2 A^2 \frac{k}{n} \tag{4.34}$$

The variable z' (distributed as in (4.26), which is again approximated by a Gaussian density), is tested by preamble comparator (Fig. 4.3) and the comparison result is dumped as a threshold TH_j to the bit erasure decision circuit according to the following rule,

Threshold range $= (TH_{1,j}, TH_{2,j})$ if

$$V_{1,j} < z' < V_{2,j} \text{ or } V_{3,j} < z' < V_{4,j} \tag{4.35}$$

where the preamble thresholds are given by:

$$
\begin{aligned}
V_{1,j} &= A^2 \frac{k}{n} \frac{1}{j} \\
V_{2,j} &= A^2 \frac{k}{n} \frac{1}{(j+1)} \\
V_{3,j} &= A^2 \frac{k}{n} j \\
V_{4,j} &= A^2 \frac{k}{n} (j+1)
\end{aligned}
\qquad (4.36)
$$

$$Where \quad j = 1, 2, \ldots, JJ$$

The probability of dumping slice j (i.e., $TH_{1,j}$, $TH_{2,j}$) from the preamble to the bit erasure decision circuit is then given by (in light of (4.36)

$$
\begin{aligned}
\lambda_{j,l} &= \int_{V_{1,j}}^{V_{2,j}} \frac{1}{\sqrt{2\pi}\sigma_{z',l}} e^{-(\xi - \mu_{z',l})^2/2\sigma_{z',l}^2} d\xi \\
&\quad + \int_{V_{3,j}}^{V_{4,j}} \frac{1}{\sqrt{2\pi}\sigma_{z',l}} e^{-(\xi - \mu_{z',l})^2/2\sigma_{z',l}^2} d\xi \qquad (4.37) \\
&= \frac{1}{2} Erf_c \left(\frac{V_{1,j} - \mu_{z',l}}{\sqrt{2}\sigma_{z',l}} \right) - \frac{1}{2} Erf_c \left(\frac{V_{2,j} - \mu_{z',l}}{\sqrt{2}\sigma_{z',l}} \right) \\
&\quad + \frac{1}{2} Erf_c \left(\frac{V_{3,j} - \mu_{z',l}}{\sqrt{2}\sigma_{z',l}} \right) - \frac{1}{2} Erf_c \left(\frac{V_{4,j} - \mu_{z',l}}{\sqrt{2}\sigma_{z',l}} \right) \qquad (4.38)
\end{aligned}
$$

The probability of having K erasures in a record of N_b demodulated bits in a certain TH slot is binomially distributed (assuming independence of bits in the TH slot), as,

$$\xi_{K,l} = \binom{N_b}{K} \gamma_{j,l}^K \left(1 - \gamma_{j,l}\right)^{N_b - K} \qquad (4.39)$$

where K is to be assigned values according to (4.45). Averaging this over all pos-

sible thresholds TH_j as given by the preamble stage (equation 4.25), we obtain

$$\xi_l = \sum_{j=1}^{JJ} \lambda_{j,l} \begin{pmatrix} N_b \\ K \end{pmatrix} \gamma_{j,l}^{K} \left(1 - \gamma_{j,l}\right)^{N_b - K} \tag{4.40}$$

where JJ is the number of possible thresholds. On the other hand, the single bit erasure probability averaged over all thresholds (TH_j) is given by

$$\theta_l = \sum_{j=1}^{JJ} \lambda_{j,l}\, \gamma_{j,l} \tag{4.41}$$

The bit error probability on the channel is given from equation 25, i.e.,

$$q_l = (1 - \theta_l)\, \mu_l \tag{4.42}$$

θ_l, μ_l, q_l will enter into the derivation of the decoding error probability of the four decoders of Fig. 4.6 as shown in the Appendix B. From this we arrive with,

$P_{1,l}$ the probability of decoding bit error from the first decoder (fed by $DD_1(u)$)

$P_{2,l}$ the probability of decoding bit error from the second decoder (fed by $DD_2(u)$)

$P_{3,l}$ the probability of decoding bit error from the third decoder (fed by $D_1(u)$, $G_1(u)$)

$P_{4,l}$ the probability of decoding bit error from the fourth decoder (fed by $D_2(u)$, $G_2(u)$)

It follows from the modified majority voting rule of Fig. 4.7 that the final probability of decoding error is given by

$$
\begin{aligned}
P_{e,l} = {} & P_{1,l}P_{2,l}P_{3,l}P_{4,l} + (1-P_{1,l})P_{2,l}P_{3,l}P_{4,l} \\
& + (1-P_{2,l})P_{1,l}P_{3,l}P_{4,l} + (1-P_{3,l})P_{1,l}P_{2,l}P_{4,l} \\
& + (1-P_{4,l})P_{1,l}P_{2,l}P_{3,l} + \frac{1}{2}(1-P_{1,l})(1-P_{2,l})P_{3,l}P_{4,l} \\
& + \frac{1}{2}(1-P_{1,l})(1-P_{3,l})P_{2,l}P_{4,l} + \frac{1}{2}(1-P_{1,l})(1-P_{4,l})P_{2,l}P_{3,l} \\
& + \frac{1}{2}(1-P_{2,l})(1-P_{3,l})P_{1,l}P_{4,l} + \frac{1}{2}(1-P_{2,l})(1-P_{4,l})P_{1,l}P_{3,l} \\
& + \frac{1}{2}(1-P_{3,l})(1-P_{4,l})P_{1,l}P_{2,l}
\end{aligned}
\tag{4.43}
$$

The one half in the above represents the tie breaker when two bits are 1 and the other two bits are 0 from the four FEC decoders. The above expression actually does not utilize fully the extra information inherent in the erasure count of the two TH slots and so represents a lower bound on decoded bits. The probability of the error event corresponding only to this event (i.e., one of the cases in equation 29),

$$
\rho\,(1-P_{1,l})\,(1-P_{3,l})\,P_{2,l}\;P_{4,l} \tag{4.44}
$$

where ρ is the probability that these decoded bits coming from a TH slot with lower erasure count actually yields higher probability of decoding error (i.e., opposite to our selection rule and one's expectations).

While the exact evaluation of ρ proved to be a difficult task, we can still approximate it by (depending on the erasure correction capability of the code)

$$
\rho = \sum_{K_2=1}^{N_t} \sum_{K_1=1}^{N_t} \xi_{K_1/l}\;\xi_{K_2/l}\;\frac{\mu_{K_1}}{(\mu_{K_1}+\mu_{K_2})} \tag{4.45}
$$

$$
K_1 > 2,\; K_1 > K_2
$$

where μ_{K_1} is obtained by inserting $l = K_1$ in equation 25.

For the decision rule implied in the flow chart of Fig. 4.7, the probability of final error conditional on (l) the interference level is given by ($P_{e,l}$) of (43) is an upper bound on $P_{e,l}$ of (46),

$$\begin{aligned} P_{e,l} = {} & P_{1,l}P_{2,l}P_{3,l}P_{4,l} + (1-P_{1,l})P_{2,l}P_{3,l}P_{4,l} \\ & + (1-P_{2,l})P_{1,l}P_{3,l}P_{4,l} + (1-P_{3,l})P_{1,l}P_{2,l}P_{4,l} \\ & + (1-P_{4,l})P_{1,l}P_{2,l}P_{3,l} + \frac{1}{2}(1-P_{1,l})(1-P_{2,l})P_{3,l}P_{4,l} \\ & + \rho(1-P_{1,l})(1-P_{3,l})P_{2,l}P_{4,l} + \frac{1}{2}(1-P_{1,l})(1-P_{4,l})P_{2,l}P_{3,l} \\ & + \frac{1}{2}(1-P_{2,l})(1-P_{3,l})P_{1,l}P_{4,l} + \rho(1-P_{2,l})(1-P_{4,l})P_{1,l}P_{3,l} \\ & + \frac{1}{2}(1-P_{3,l})(1-P_{4,l})P_{1,l}P_{2,l} \end{aligned} \tag{4.46}$$

where we still notice the tie breaking term $\frac{1}{2}$ in some of the terms (similar to equation 4.43). These terms are due to the fact that in some situations (Fig. 4.8) the two similar decoded bits may have come from TH slots with different erasure counts, in which case a tie breaker is inevitable leading to $\frac{1}{2}$, rather than ρ in equation 4.32.

The decoded bit error probability $P_{1,l}$, $P_{2,l}$, $P_{3,l}$, $P_{4,l}$ are derived in the Appendix B. We note that $P_{1,l}$, $P_{2,l}$ are pure error correcting codes (no handling of erasures). However, they are not conventional FEC since (Fig.4.5,4.6) the erasures are deleted from the input vectors $D_1(u)$, $D_2(u)$ according to the bit from the other TH slot (Fig. 4.6), and so we have to alter the input error statistics $D_1(u)$ and $D_2(u)$ before computing the known decoding error bounds (for different code types as in the Appendix B). Recall that we transmit same bit in two TH slots to achieve diversity.

Averaging overall conditions of multiaccess interference l (from equations (4.3), (4.46), (4.43), we obtain the average bit error probability as,

$$P_b = \sum_{l=1}^{2U} S_l \; P_{e,l} \tag{4.47}$$

The probability of packet success then becomes (in terms o fFEC word error probability P_b''),

$$P_{ps} = (1 - P_b'' \;)^{N_B} \tag{4.48}$$

assuming that the packet length equals N_B code words and the independence of all bits in the TH slot (packet) in which case the throughput can be defined as

$$\Delta_s = \frac{U \; P_{ps} \; R'_b}{2/T_b} \tag{4.49}$$

P_b'' of (4.48) is the same as that of (4.47), except that in the process of evaluating equation (B-1), (B-3) of the Appendix B the factors $\frac{\alpha + \beta}{n}$ and $\frac{\gamma + \beta}{n}$ is set to 1 to reflect the fact that we are dealing with word errors rather than bit errors in this case.

It is also possible to easily extend the results of this chapter to the case where each user transmits the same message over three or more TH slots in each frame, in which case voting among the outputs of six or more decoders (extension of Fig. 4.6,4.7) is expected to lower P_b even further. In the case of three TH slots per frame we have the following $P_{e,l}$ replacing (4.43)

$$\begin{aligned} P_{e,l} = {} & P_{1,l} P_{2,l} P_{3,l} P_{4,l} P_{5,l} P_{6,l} + \sum_{i=1}^{6} (1 - P_{i,l}) \prod_{j=1}^{6} P_{j,l} \\ & + \sum_{i=1}^{6} \sum_{j=1}^{6} (1 - P_i)(1 - P_j) \cdot \prod_{\substack{k=1 \\ i \neq j \neq}} P_{k,l} \\ & \cdot \frac{1}{2} \sum_{i=1}^{6} \sum_{j=1}^{6} \sum_{k=1}^{6} (1 - P_{i,l})(1 - P_{j,l}) \cdot (1 - P_{k,l}) \cdot \prod_{\substack{m=1 \\ m \neq i \neq j \neq t}} P_{m,l} \end{aligned} \tag{4.50}$$

and the inequality stems from the fact that some of the terms inside the multisummation of (4.50) is actually multiplied by ρ, similar to that of (4.43), and ρ is always $\leq \frac{1}{2}$.

All the equations in this chapter finally leading to the evaluations of the error probabilities and network efficiency still apply in the latter case, except for replacing 3U by 2U only in (4.3), (4.47) (not (4.19), (4.49), or the remaining equations).

In this chapter we have also considered the following nine different cases pertaining to the process of modifying the erasure, (all other considerations, e.g., 2 TH slots versus 3 TH slots transmissions, or packet versus bit errors, or replacing ρ by 0.5 (i.e. neglecting ρ computation acording to (4.39), (4.45)) remaining the same as previously discussed. (The reader is cautioned that these nine trial cases have their immediate and evident implication on the receiver structure)

Case 1: Replace $\overline{q}_l$, $\overline{\theta}_l$, by q_l, θ_l in the appendix, i.e., ignore the erasure modification logic in computing $P_{1,l} = P_{2,l}$ of Appendix B in Equs. (B-1). Moreover in (B-3), (B-4) set $\theta_l \rightarrow \theta_1 = \alpha_{1,l}$, $q_l \rightarrow q_1 = \mu_l(1 - \theta_1)$ for all l. This means ignore the threshold adaptation and the preamble stage.

Case 2: Replace q_l, θ_l in (B-3), (B-4) by $\overline{q}_l$, $\overline{\theta}_l$, i.e. apply the threshold modification rule to both the modified erasure decoders (1,2), and the combined parallel-error erasure decoders (3,4), and keep $\overline{q}_l$, $\overline{\theta}_l$ of Equ. (B-1).

Case 3: Change $\overline{q}_l$, $\overline{\theta}_l$ to q_1, θ_1 in Equ. (B-1) and replace q_l, θ_l by q_1, θ_1 in Equs. (B-3), (B-4).

Case 4: Replace $\overline{q}_l$, $\overline{\theta}_l$ in (B-1) and replace q_l and θ_l by $\overline{q}_l$, $\overline{\theta}_l$ in Eques. (B-3), (B-4).

Case 5: Replace $\overline{q}_l$ and $\overline{\theta}_l$ in (B-1) by q_l and θ_l and keep q_l and θ_l in Eques. (B-3), (B-4).

Note: In all the cases above, and actually in all parts of this chapter, we had two similar decoders (1,2) giving rise to $P_{1,l} = P_{2,l}$ and another (3,4) $P_{3,l}$, $P_{4,l}$, it may be interesting to try to make $P_{1,l} \neq P_{2,l}$ and $P_{3,l} = P_{4,l}$. It may be interesting to try to mak $P_{1,l} \neq P_{2,l}$ and $P_{3,l} \neq P_{4,l}$. Again, this means changing the decoding rule and the receiver structure accord'ngly in an evident manner, as in the following cases.

Case 6: For decoder 1 keep $\overline{q}_l$, $\overline{\theta}_l$ in (B-1) For decoder 2 change $\overline{q}_l$, $\overline{\theta}_l$ to q_l, θ_l in (B-1) For decoder 3 keep q_l, θ_l in (B-3), (B-4) For decoder 4 change q_l, θ_l to $\overline{q}_l$, $\overline{\theta}_l$ in (B-3), (B-4)

Case 7: For decoder 1 keep $\overline{q}_l$, $\overline{\theta}_l$ in (B-1) For decoder 2 change $\overline{q}_l$, $\overline{\theta}_l$ to q_1, θ_1 in (B-1) For decoder 3 change q_l, θ_l to $\overline{q}_l$, $\overline{\theta}_l$ in (B-3), (B-4). For decoder 4 change q_l, θ_l to q_1, θ_1 in (B-3), (B-4)

Case 8: For decoder 1 change $\overline{q}_l$, $\overline{\theta}_l$ in (B-1) to q_l, θ_l For decoder 2 change $\overline{q}_l$, $\overline{\theta}_l$ in (B-1) to q_1, θ_1 For decoder 3 change q_l, θ_l to $\overline{q}_l$, $\overline{\theta}_l$ in (B-3), (B-4) For decoder 4 change q_l, θ_l to q_1, θ_1 in (B-3), (B-4)

It seems that there is a large number of possible combinations. The results of this chapter will show the merit of each case.

4.5. Results

We have taken the case of a TH/DS network with a varying number of users U, used a basic (127, 71) BCH code(see Appendix F), assumed thermal noise (20db SNR), fixed $\nabla = 1$ (to start with), $T_c = 8.75X10^{-7}$, $R_b' = 8K$, $N_F = 8$. We then computed the various decoding probability P_1' , P_2' , P_3' , P_4' of the various codes used in this chapter, as well as word and packet successes and the network throughput.

In the following we summarize the results of the different cases. (In all cases P_1' , P_2' , P_3' , P_4' are computed as a function of number of users U. Also, the final decoding word error, packet success, and efficiency are based on the combination of P_1' , P_2' , P_3' , P_4' as in the chapter).

Case A: The word error performance of the parallel decoders P_1' , P_2' , is better than that of modified erasure coding P_3' , P_4' . For a probability of word error equal to 0.05, four users can be accommodated in the network in the case of codes P_1' , P_2' , . For codes P_3' , P_4' , we can accommodate up to 110 users. Fig. 4.9 shows too that P_3' , P_4' decrease for an increasing number of users in the range (50-100). This is due to the erasure threshold adaptation rule followed, and the parallel decoding selection rule.

As a matter of fact, as the number of users rise, more erasures are declared and one of the two parallel decoder output is selected. Once the threshold on the number of erasures is exceeded we select the second decoder of the parallel core, thus improving the performance. This leads to the oscillatory behaviors noticed in the probability of packet success (Fig. 4. 11) and is more pronounced at higher values of B (number of FEC words in a packet).

The probability of packet success peaks at a number of users of 100 and $B = 3$, however the throughput in Case A equals 0.3 at $B = 1$. It is easily seen

In Case A and all cases too that increasing B leads to deteriorating η performance.

In Case 1, we kept the same erasure modification coding P_1' , P_2' , . For parallel decoders P_3' , P_4' , we replaced q_l , θ_l , $\overline{q}$, $\overline{\theta}$, respectively (see text). Over the range ($U = 2$ to 100), Case A P_3' , P_4' , outperform those of case 1 (compare Figs. 4.9, 4.13). At higher multiaccess load ($U >>$), the performances are comparable.

Comparing Figs. 4.14, 4.10 reveals too that the network efficiency η h remains essentially the same in higher loads, while Case 1's efficiency is better for low end medium loads.

Figs. 4.15, 4.16 reveal that for high values of B (number of FEC words per packet) the packet success and the corresponding efficiency η can become very low at medium loads ($2 < U < 100$).

The results of cases (2,4) came close to those of Case A, especially the efficiency η, while the results of Case 3 came very close to those of Case 1. Compare Figs. 4.21-4.24) to Figs. 4.13-4.16 respectively. From all these comparisons one can realize that using the modified erasure logic (i.e., inserting $\overline{q}_l$, $\overline{\theta}_l$ in the error bounds of certain code can outperform the same code performance when using $\overline{q}_1$, $\overline{\theta}_1$ for a certain load range, especially for codes P_1' , P_2' , , (e.g., compare Fig. 4.9 to Fig. 4.21, or Fig. 4.9 to Fig. 4.13.

However, for codes replacing $\overline{q}_l$, $\overline{\theta}_l$ by q_l , θ_l (compare Fig. 4.9 to Fig. 4.13), or replacing $\overline{q}_l$, $\overline{\theta}_l$ by q_1, θ_1 (compare Fig. 4.9 to Fig. 4.21), P_1' , P_2' , did not yield much improvement.

The results in Cases 4,5,6, i.e., Figs. 4.25-4.34, came close to those in Fig. 4. A, however, when we compare P_3' , P_4' , of Fig. 4.31, we see that at low loads and very high loads $P_4' < P_3'$, while for average loads $P_3' < P_4'$, . This means that the erasure modification logic is effective only for average load ranges. The results of Cases 7, 8 support the above facts.

So far we did not change ∇ Equs. (4.31), (4.32)). In Figs. 4.41-4.45 we show the noticeable effects of this change.

Fig. 4.41 shows that increasing ∇ from 1 to 2 results in improving ∇ and word error for the overall scheme (at high loads), while for low leads $\nabla = 1$ yields a better performance. Going to the specific codes yielding this performance and comparing $P_3' = P_4'$, Figs. 4.21, 4.22 emphasizes the fact that higher values of ∇ are adequate for high loads and vice versa.

Increasing both ∇ and using erasure modification logic $(\overline{q}_l , \overline{\theta}_l)$ results in better improvement at high loads. Increasing ∇ beyond 4 has resulted in deteriorating error performance of all code types ($P_1' = P_2'$, $P_3' = P_4'$). This statement is supported by Fig. 4.43 which also shows that using $(\overline{q}_l , \overline{\theta}_l)$ rather than q_l , θ_l results in performance improvement at high loads.

The best efficiency obtained was $\eta = 0.48$ at $\nabla = 2$ (Fig. 4.41) comparing Figs. 4.45, 4.44 emphasizes the facts above. We see that decreasing ∇ from 4 to 3 for code P_3' using (q_1, θ_1) results in a relatively better performance at medium loads, but going all the way to $\nabla = 1$ results in a deteriorating oscillatory performance in Fig. 4.37 that was mentioned before.

This shows the dangers in using parallel decoding [3] with poor erasure and threshold values which were shown to be bad by independent.

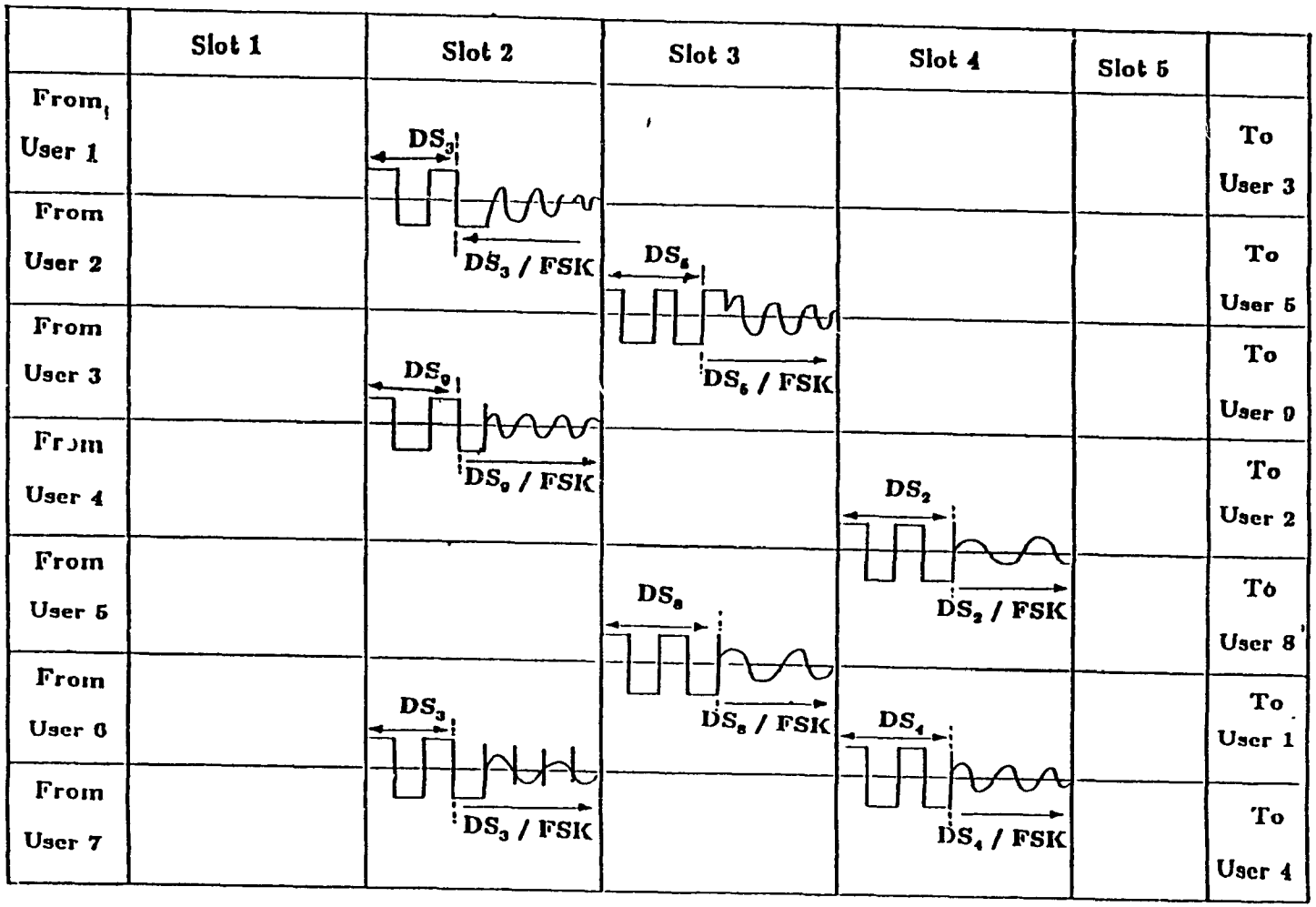

Fig(4. 1):- Typical Transmission timing diagram in the proposed DS/TH/FSK Network.

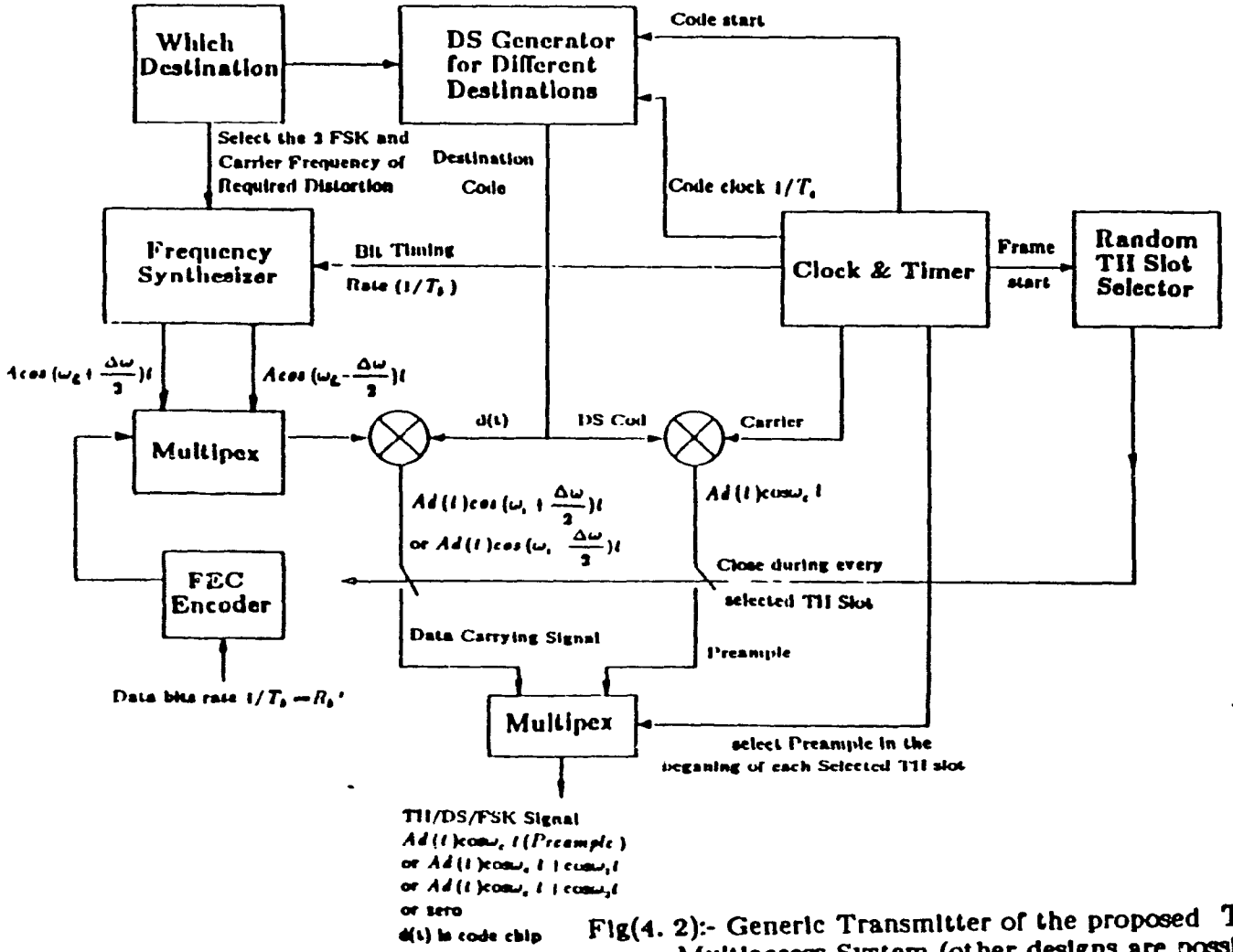

Fig(4. 2):- Generic Transmitter of the proposed **TH/DS/FSK** Multiaccess System (other designs are possible depending on the Spread Spectrum bandwidth ...etc)

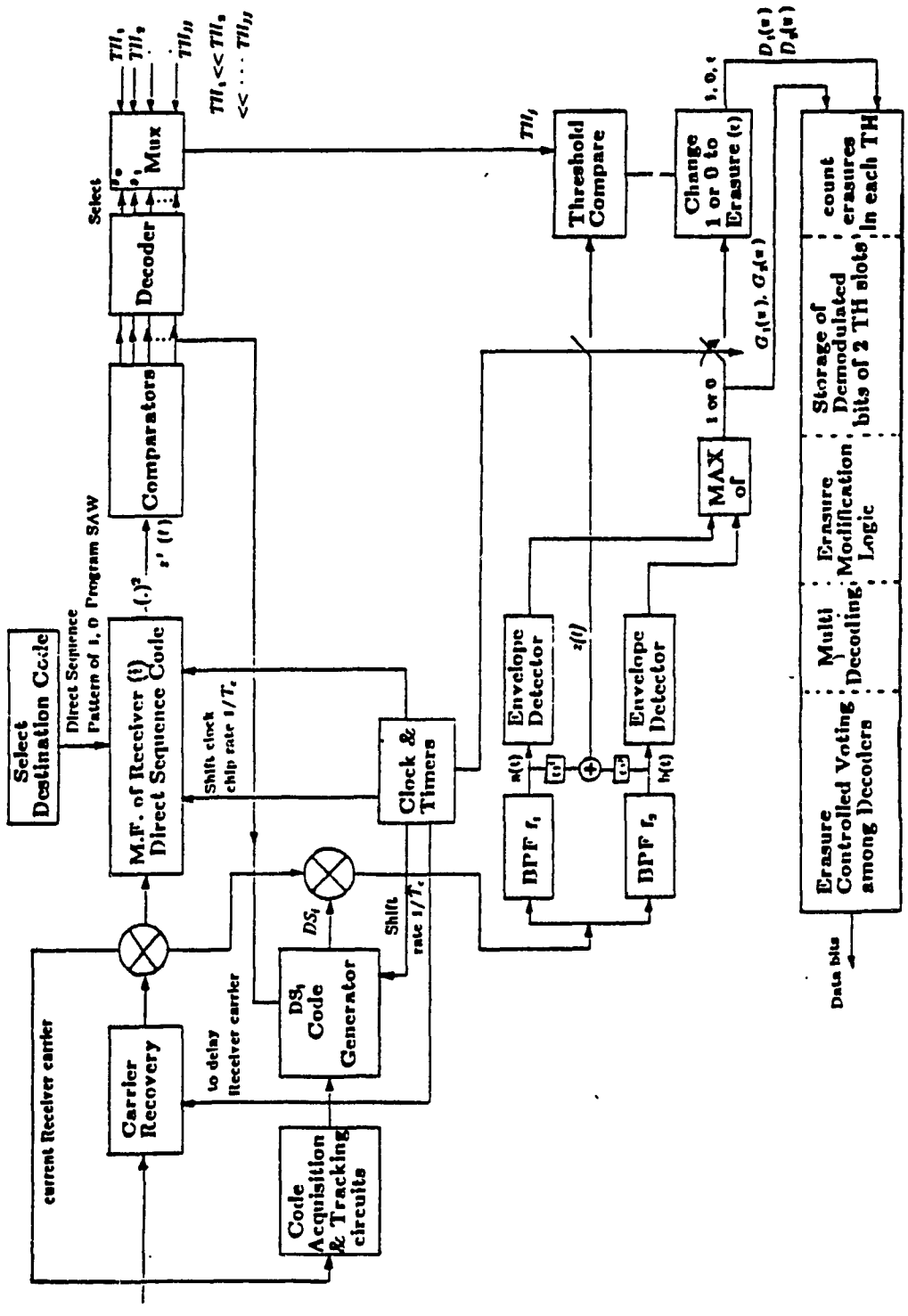

Fig(4. 3):- Generic Receiver (Synchronous mode) of the TH/DS/FSK Multiaccess System.

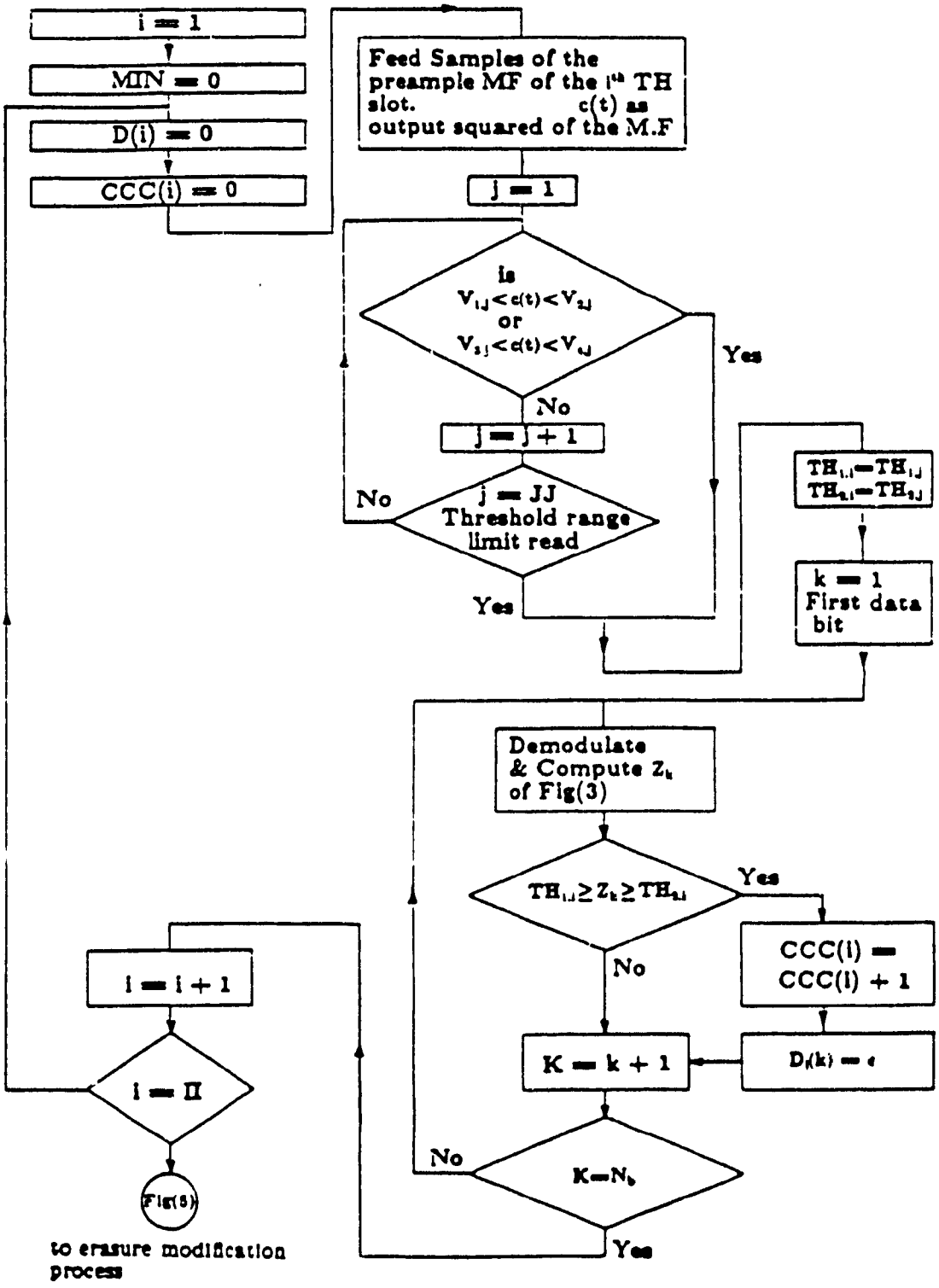

Fig(4. 4):- Represents the logic by withch all the equipments of Fig(4 3) works best Erasure error detection algorithm, here the receiver detects the best detection out of all transmitted TH slots based on error count

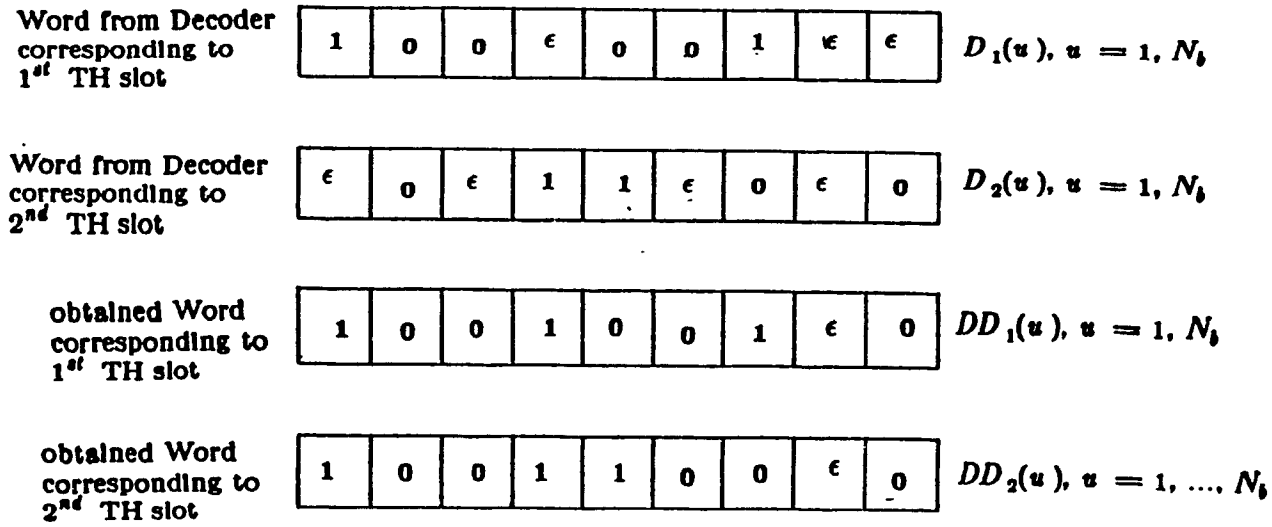

Fig(4. 5):- Example on Erasure modification logic (part of Algorithmic detection pertaining to the process of modifying the erasure of one TH slot according to the detected value (0, 1) from the other TH slot. Finally the FEC decoders outputs are handled according to Figs (4. 7), (4. 6).

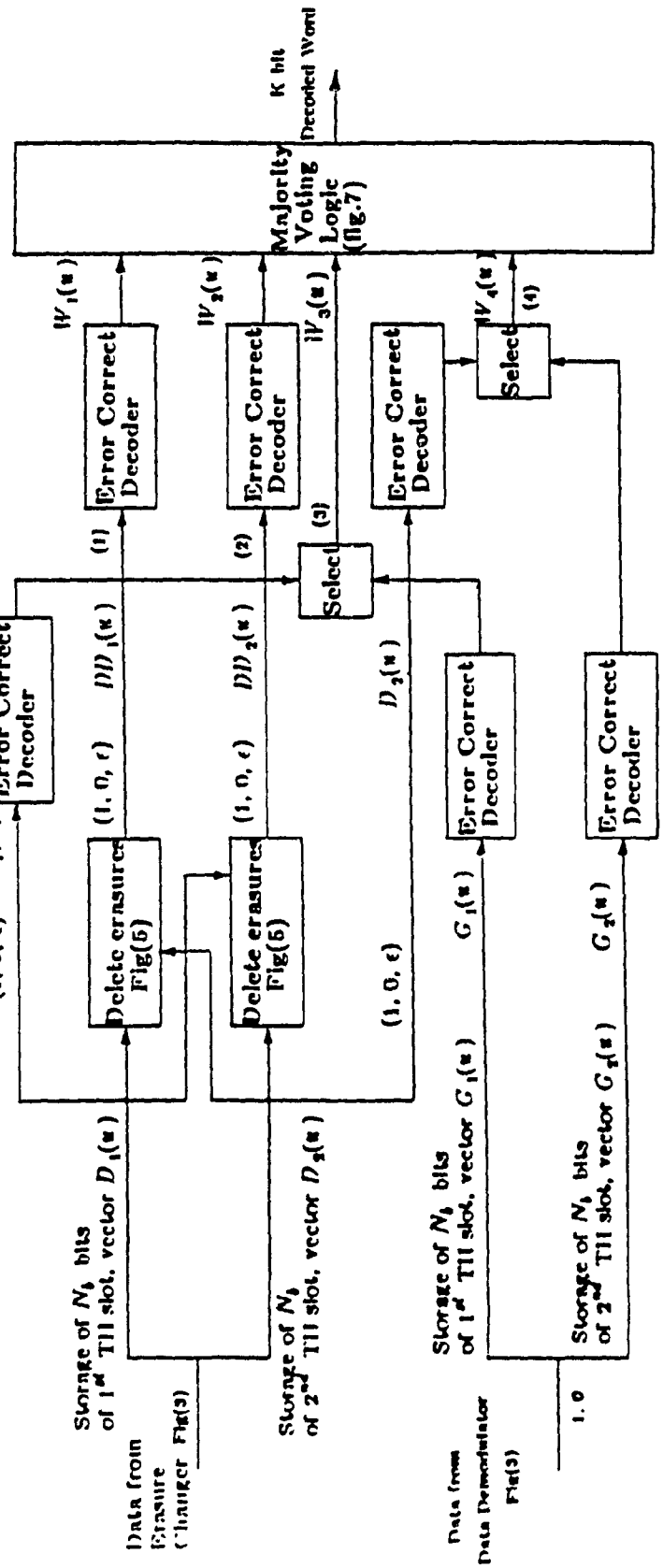

Fig(4. 6):- Erasure Modification, Error Decoding, Majority Voting Block
(details of lower block of Fig(4. 3)).

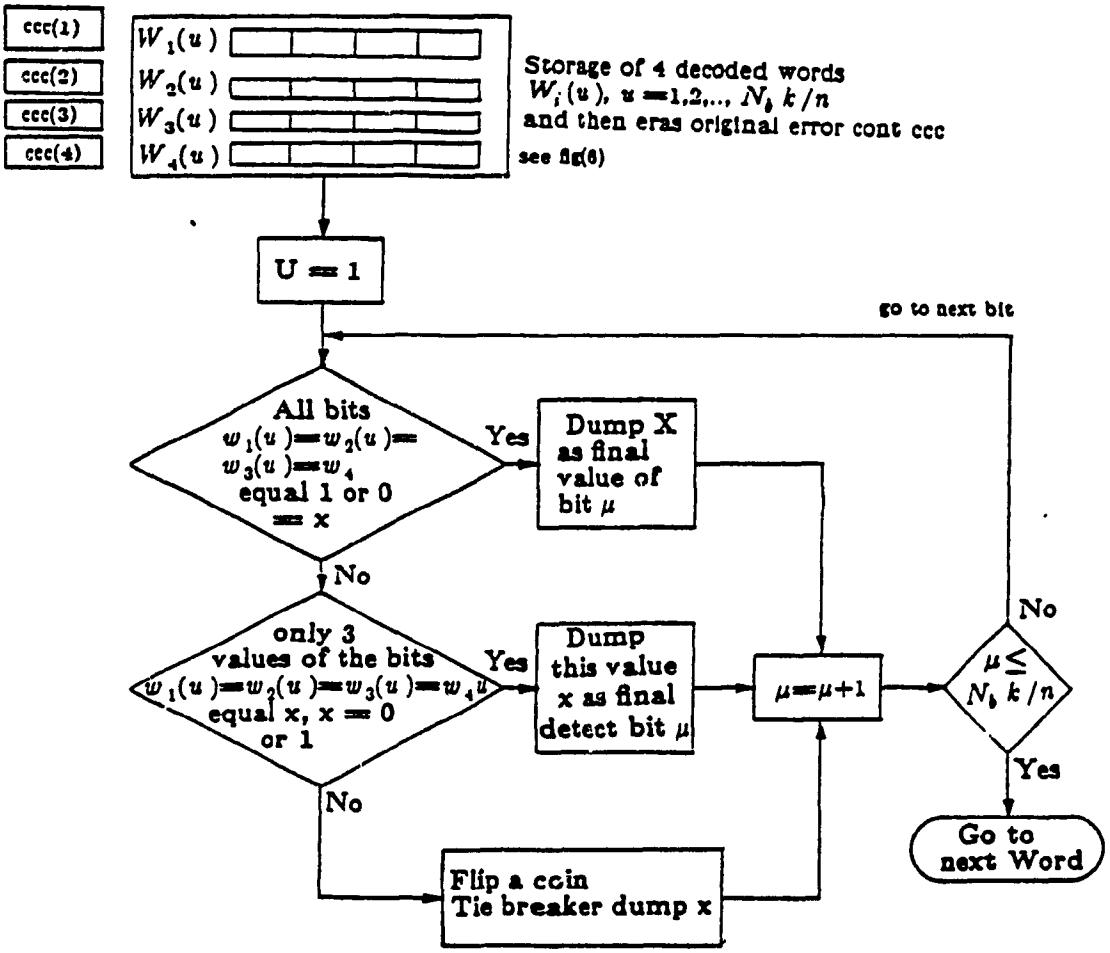

Fig(4. 7):- Modified majority vote among 4 resulting decoded Words according to values of the erasure count of each TH slot where the Word cames from (see Fig(4. 6)). (e.g. $W_1(u)$ comes as a result of decoding $DD_1(u)$.

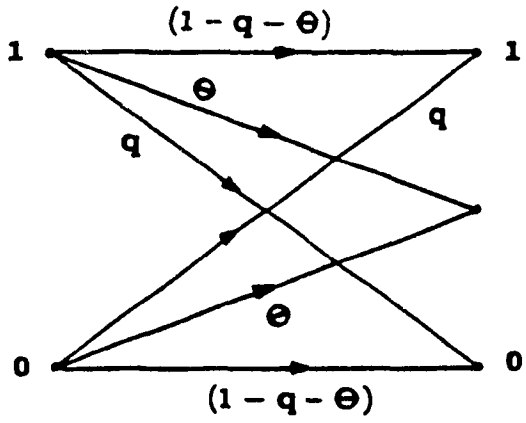

Fig(4. 8):- Binary - erasure error channel
values of q, Θ depend on the case

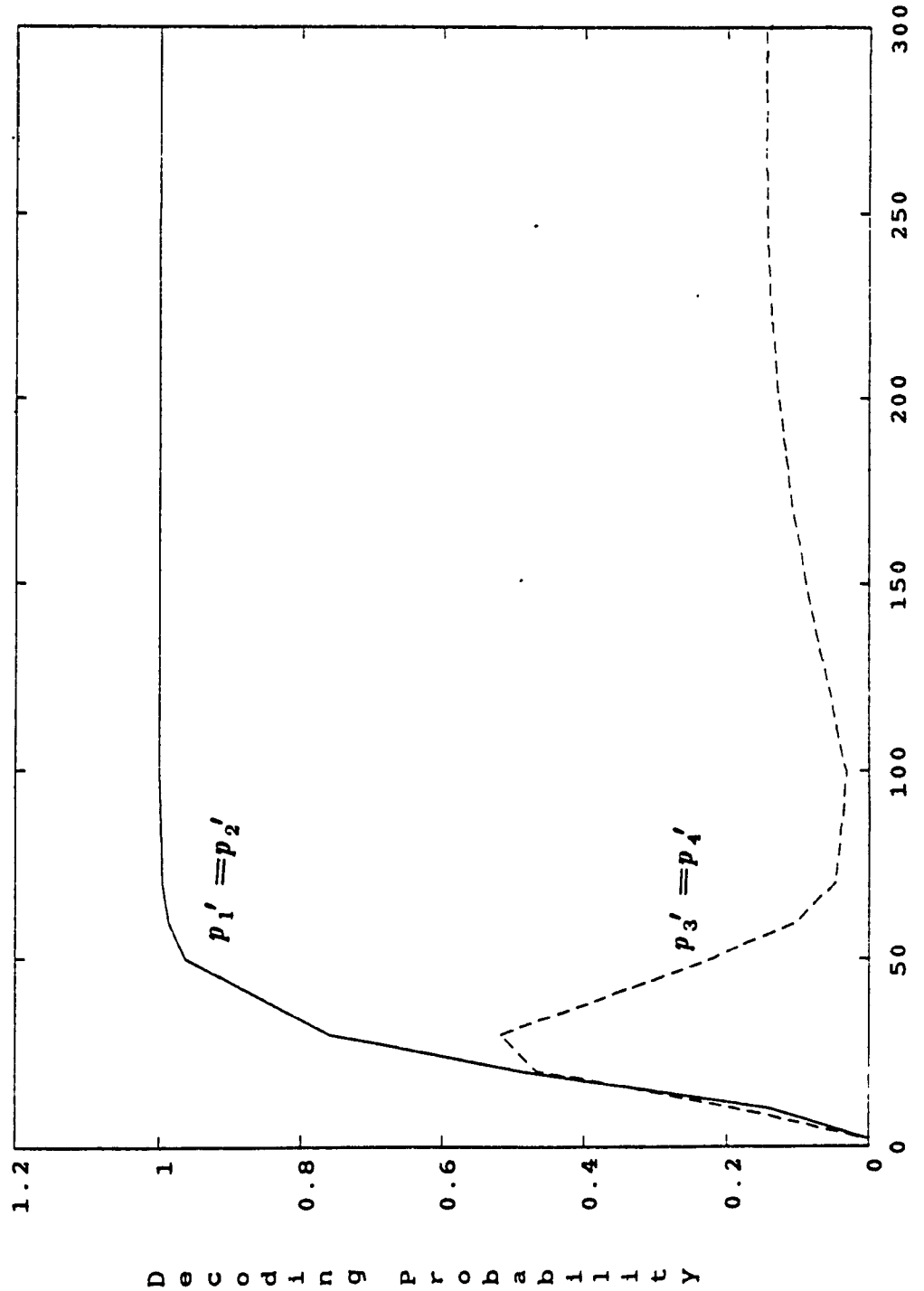

Fig(4. 9):- Probability of BCH word error at the decoder, and the total error probability at the output of the BCH decoder varying the number of users (case a).

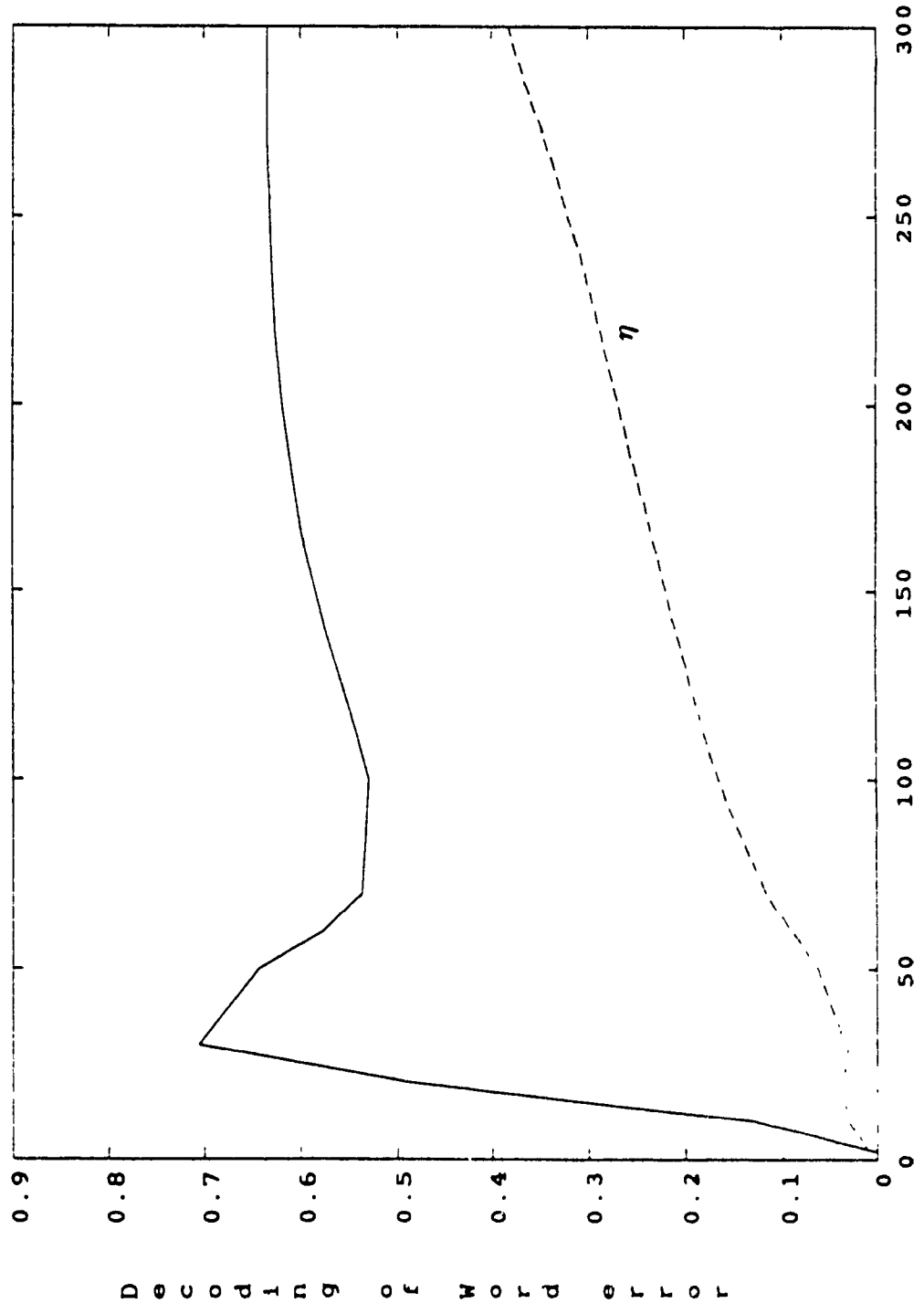

Fig(4. 10):- Probability of word error and the efficiency η for varying number of users (case a).

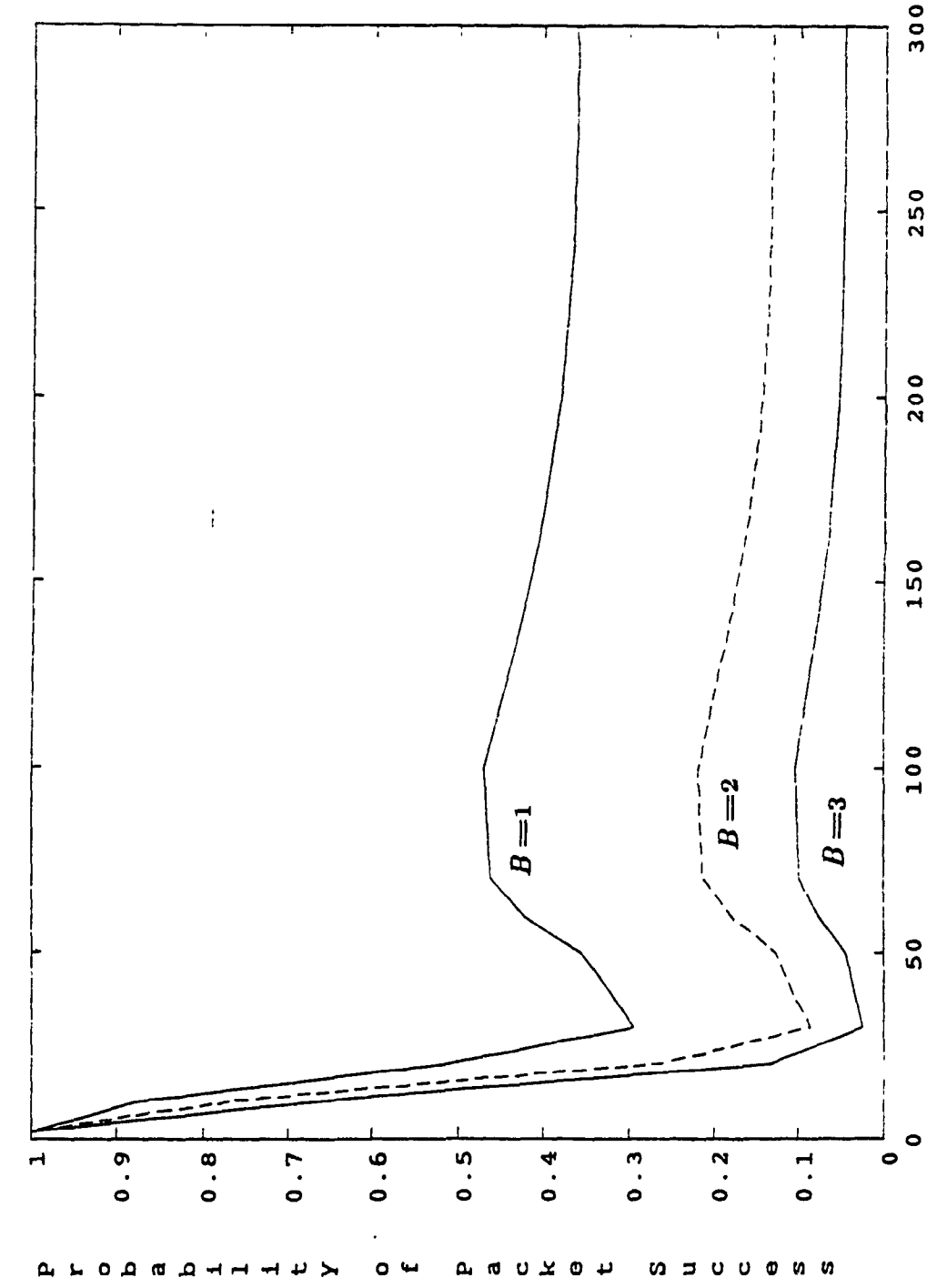

Fig(4. 11):- Probability of packet success verying number of users and different packet size, (case a)

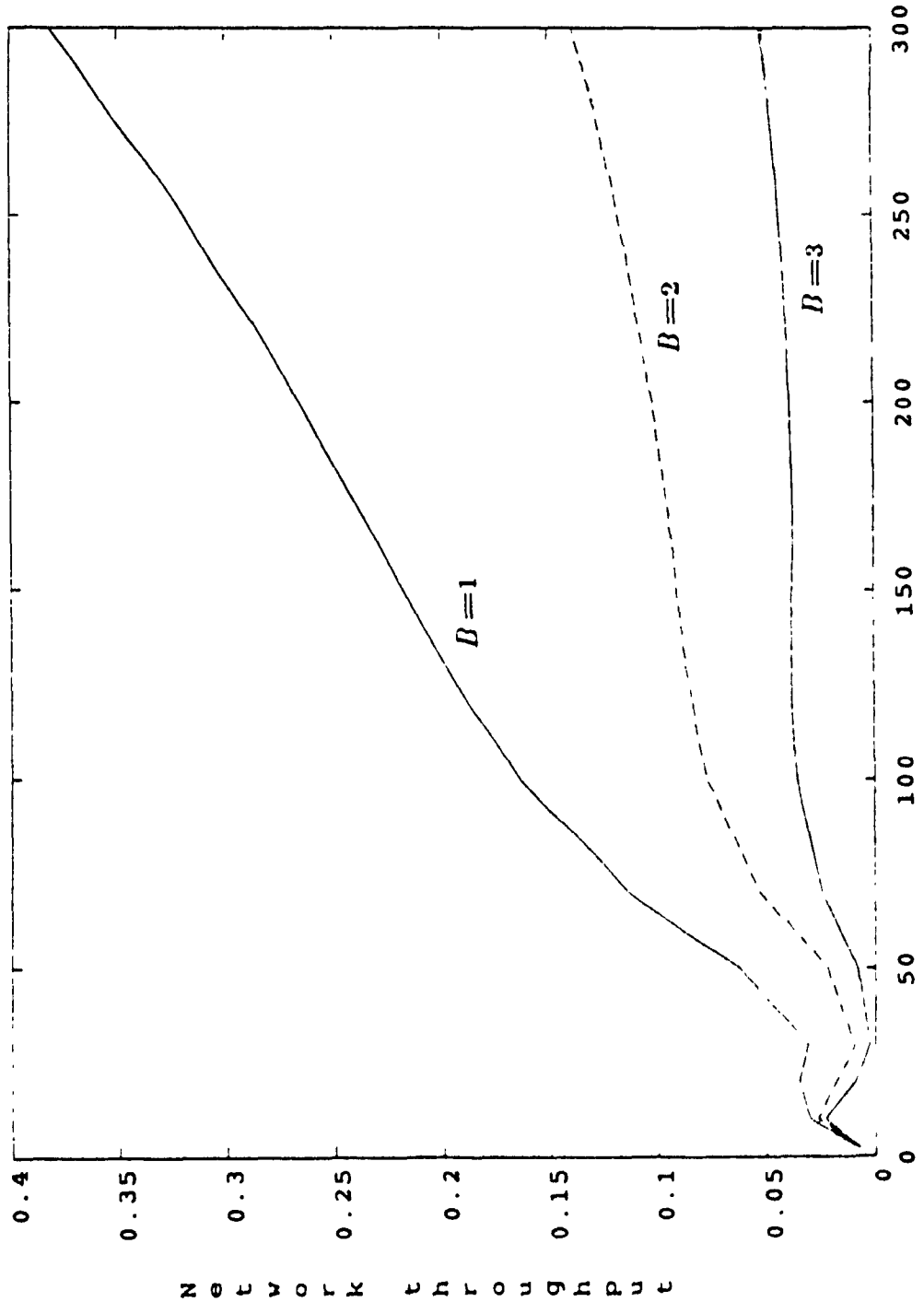

Fig(4. 12).- The throughput for different packet size and varying number of users, (case a).

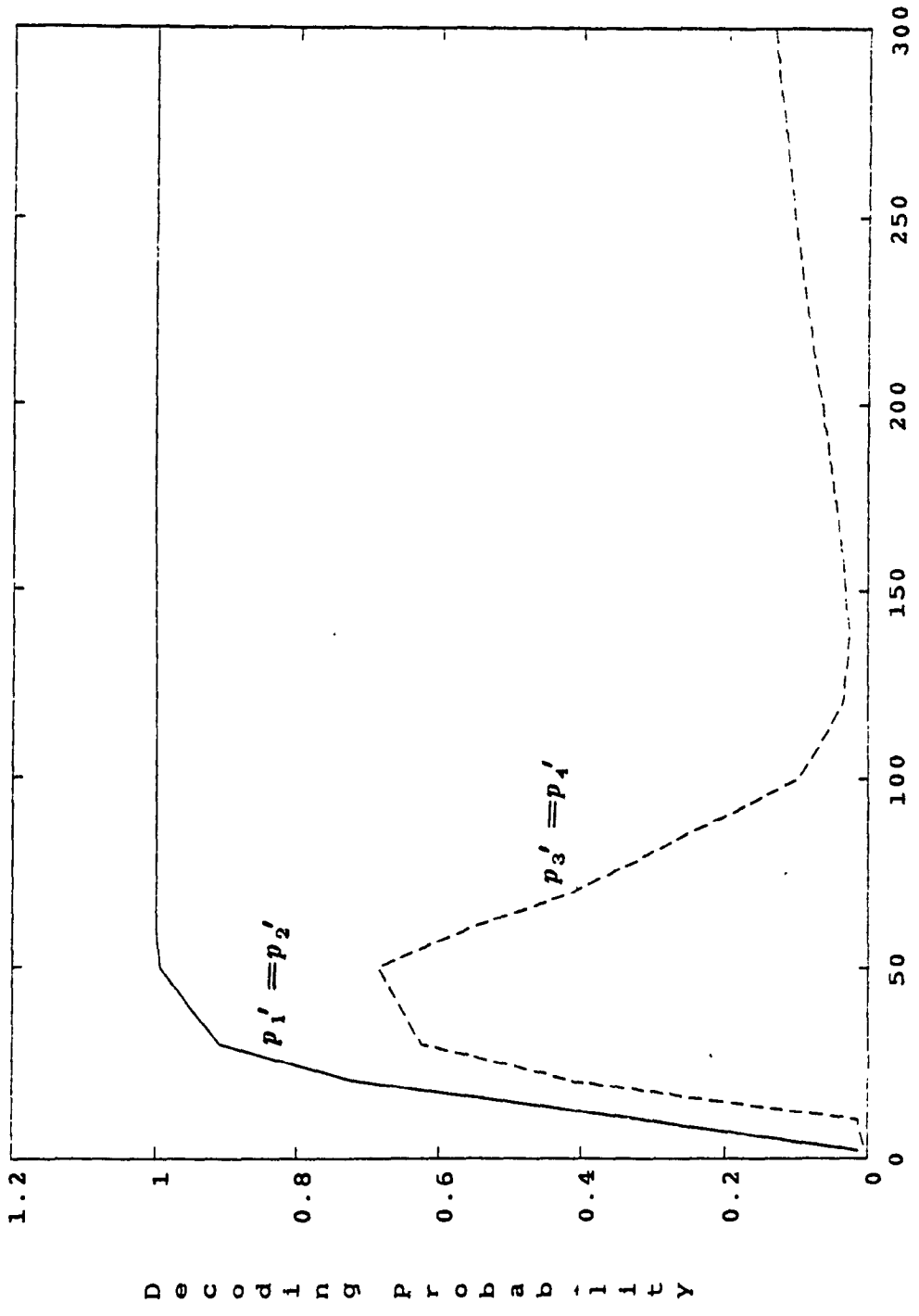

Fig(4. 13):- Probability of BCH word error at the decoder, and the total error probability at the output of the BCH decoder varying the number of users (case 1).

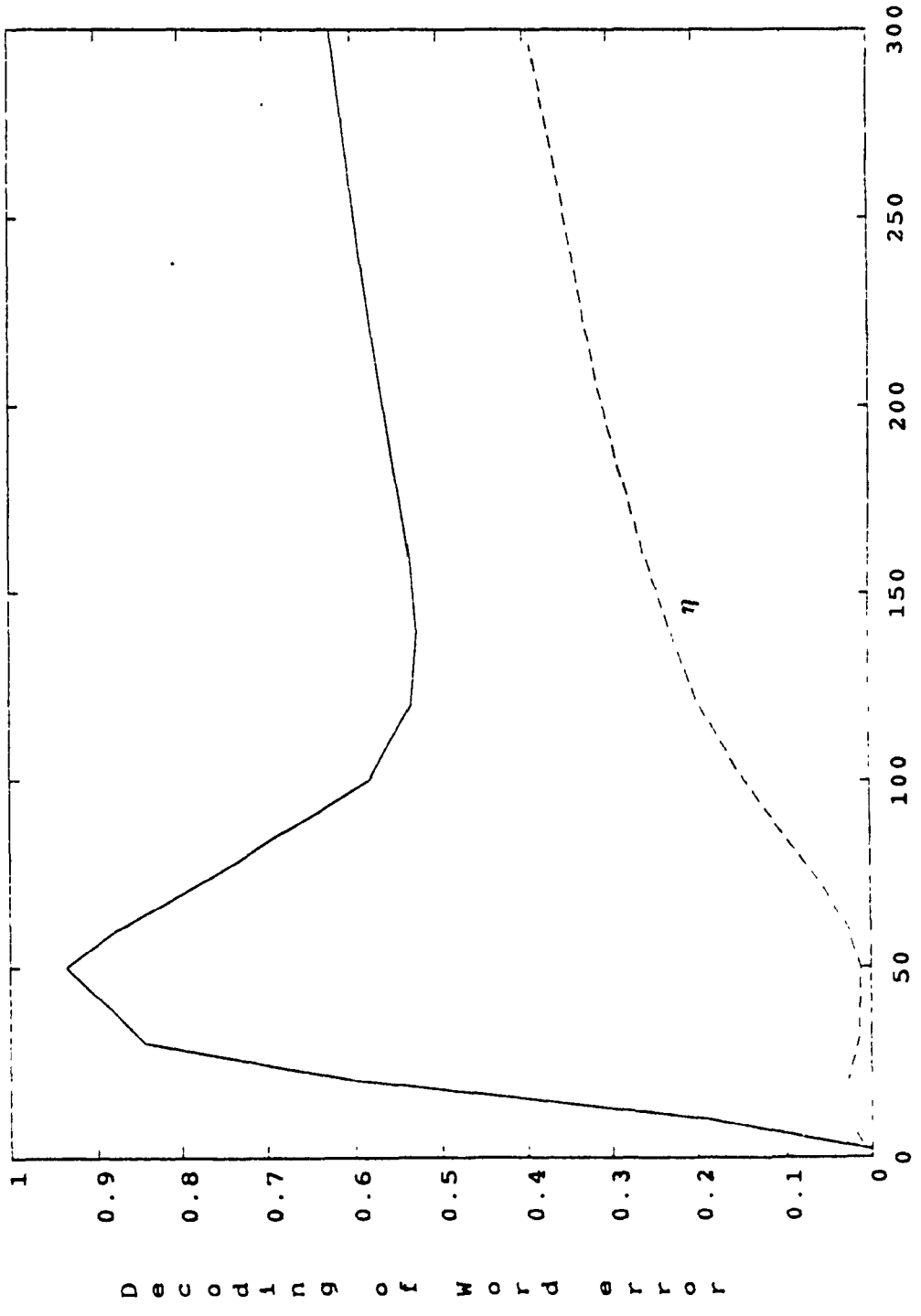

Fig(4. 14):- Probability of word error and the efficiency η for varying number of users (case 1).

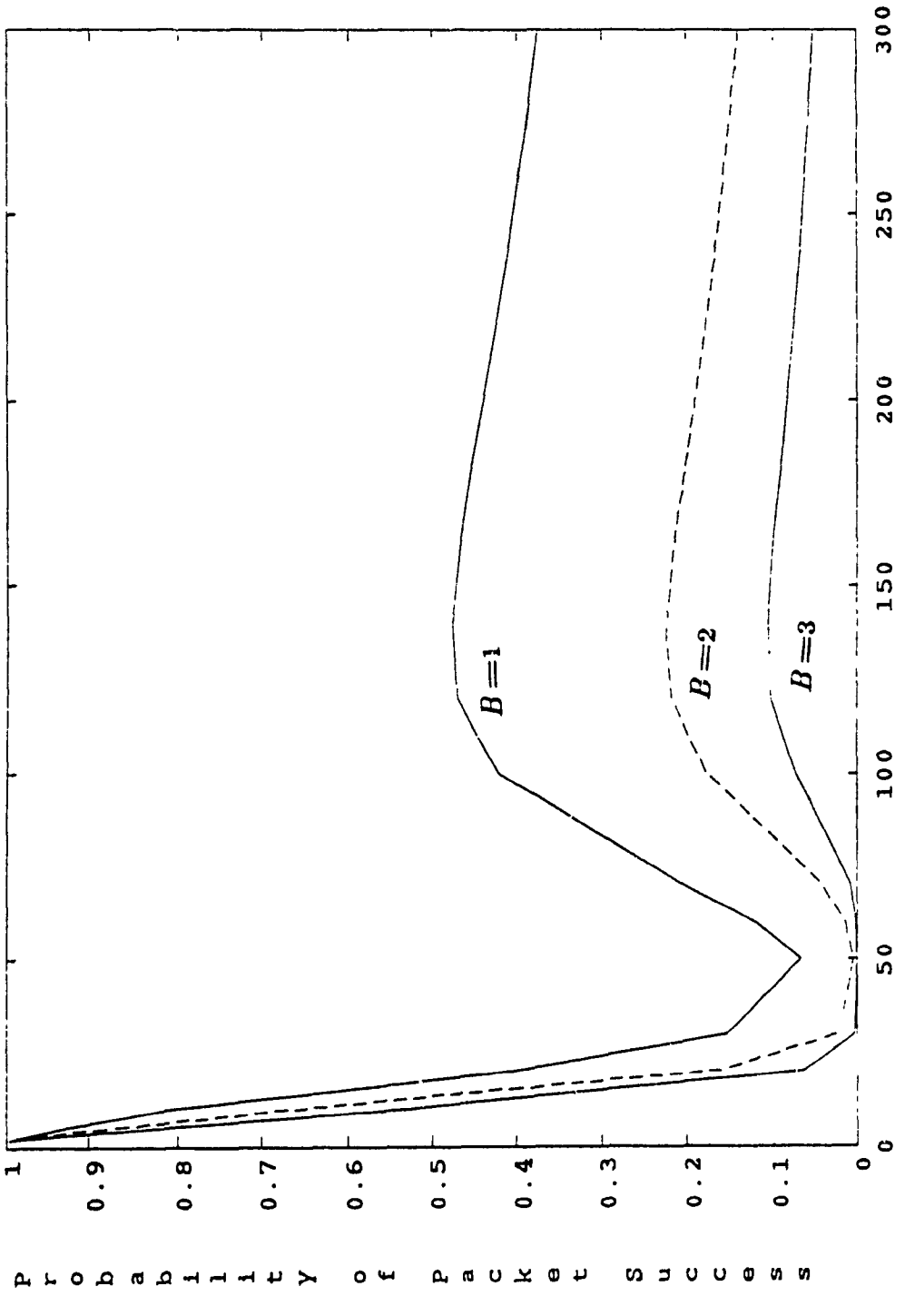

Fig(4. 15):- Probability of packet success verying number of users and different packet size, (case 1)

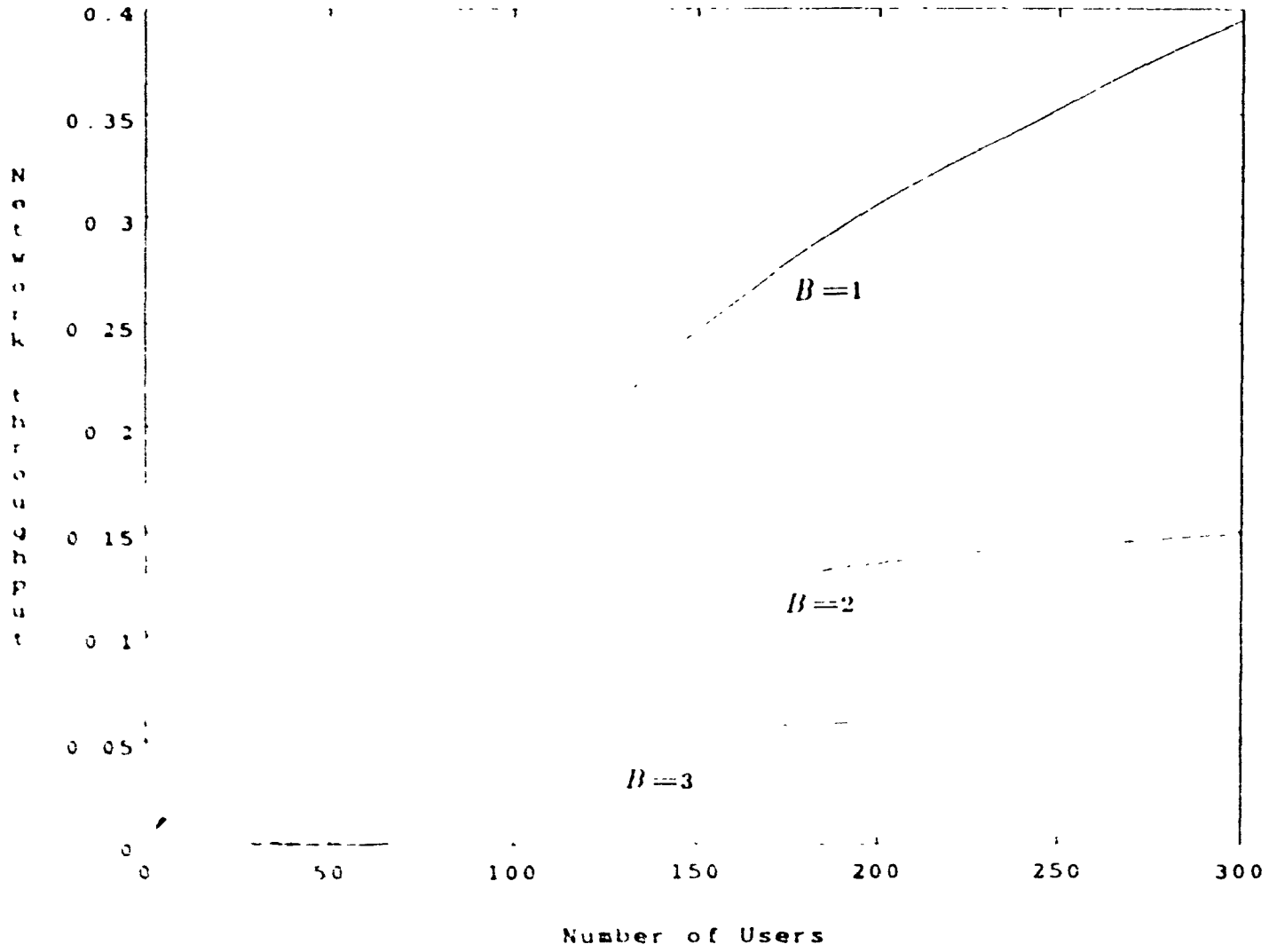

Fig. 4.16 - The throughput for different packet size and varying number of users (case 1)

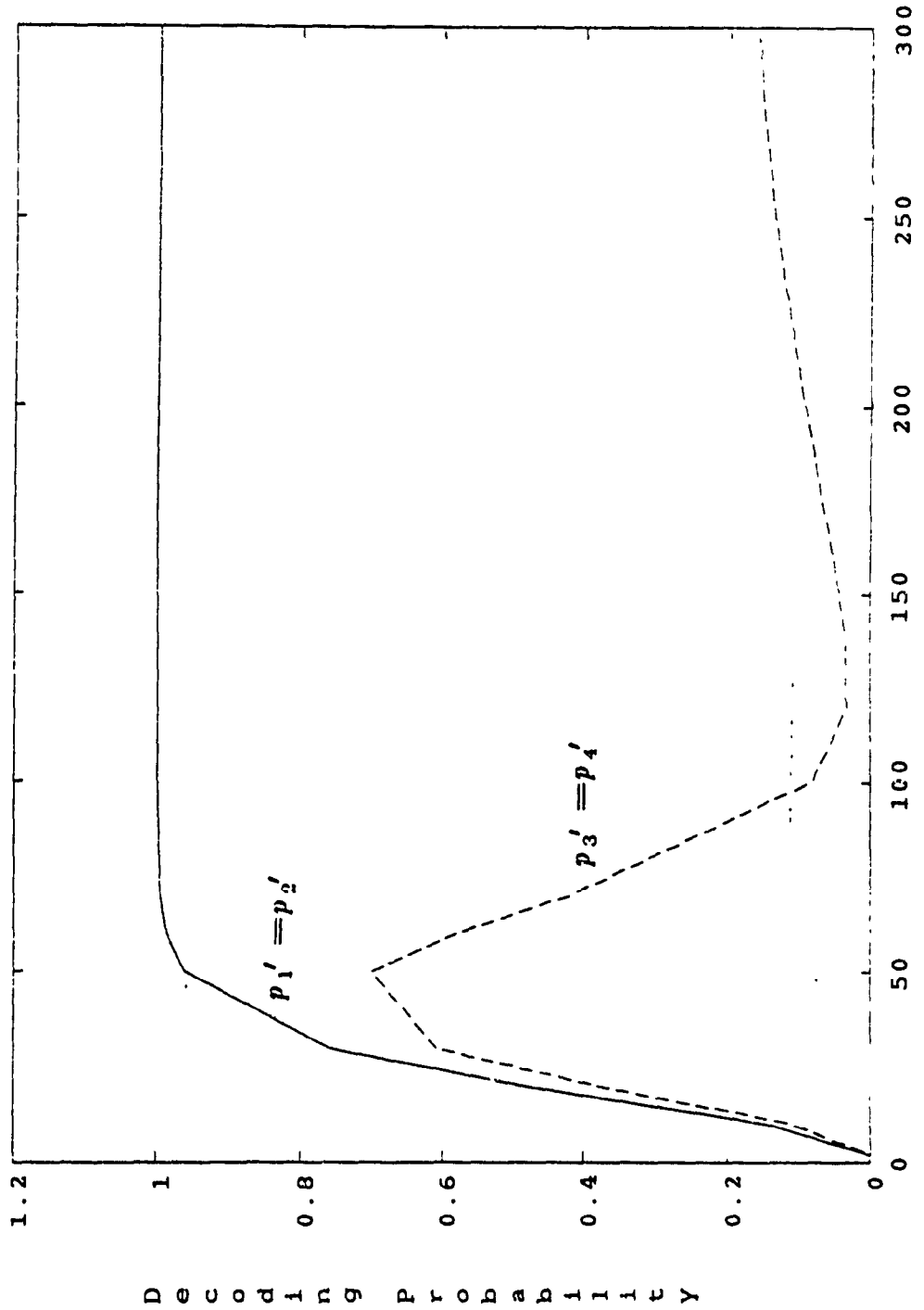

Fig(4. 17):- Probability of BCH word error at the decoder, and the total error probability at the output of the BCH decoder varying the number of users (case 2).

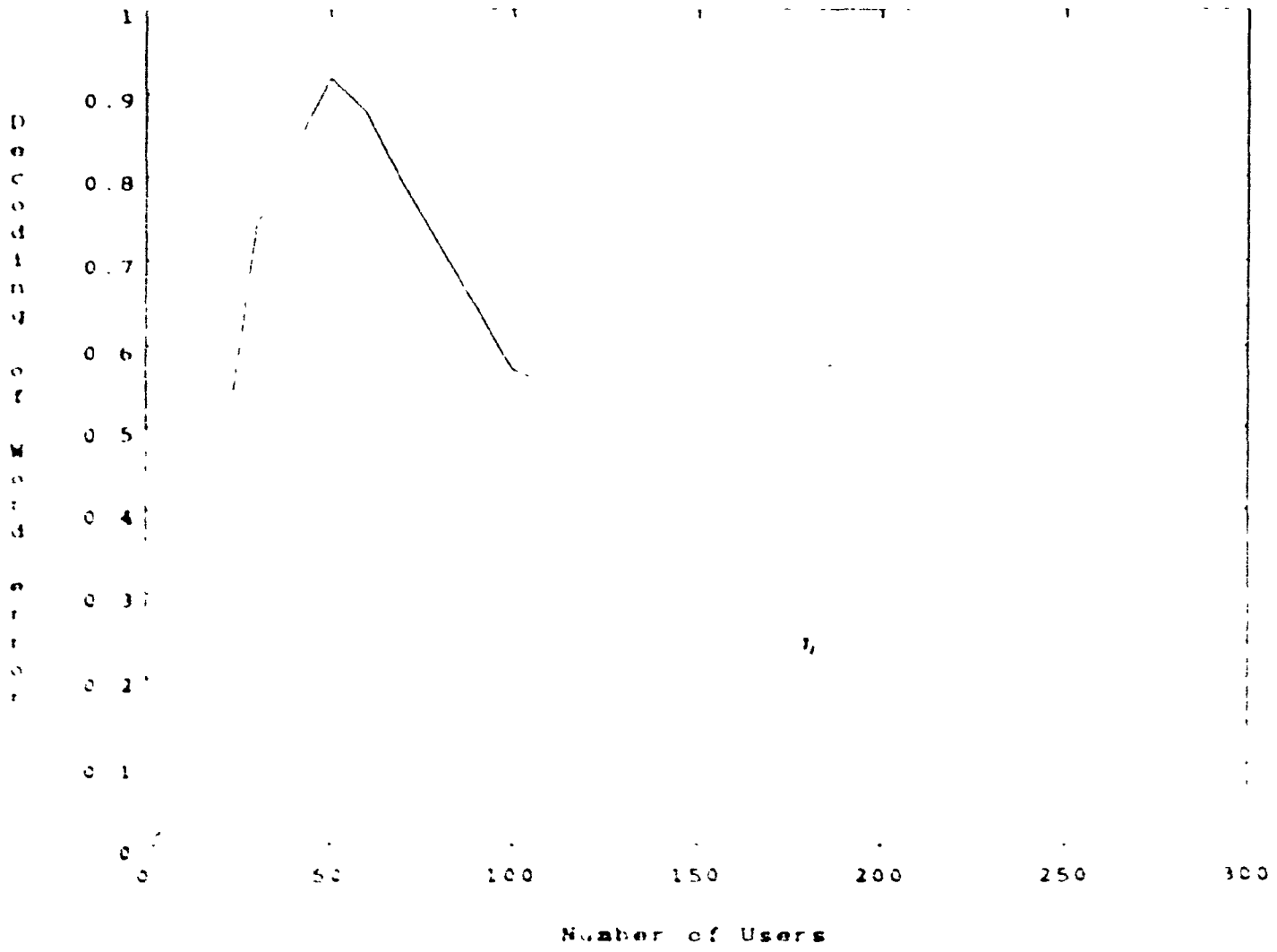

Fig. 4 (a) - Probability of word error and the efficiency η for varying number of users (case 2)

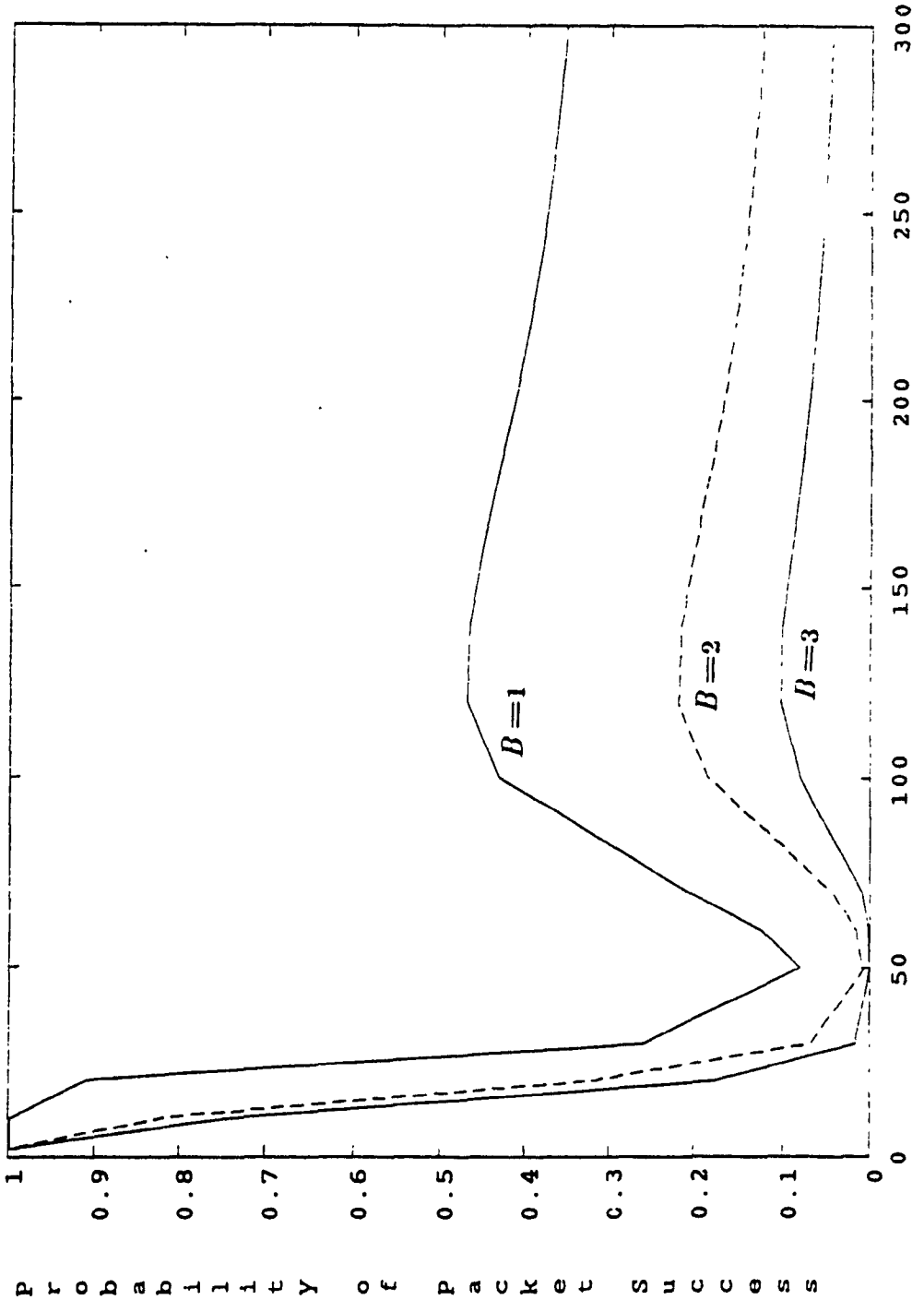

Fig(4. 19):- Probability of packet success verying number of users and different packet size, (case 2)

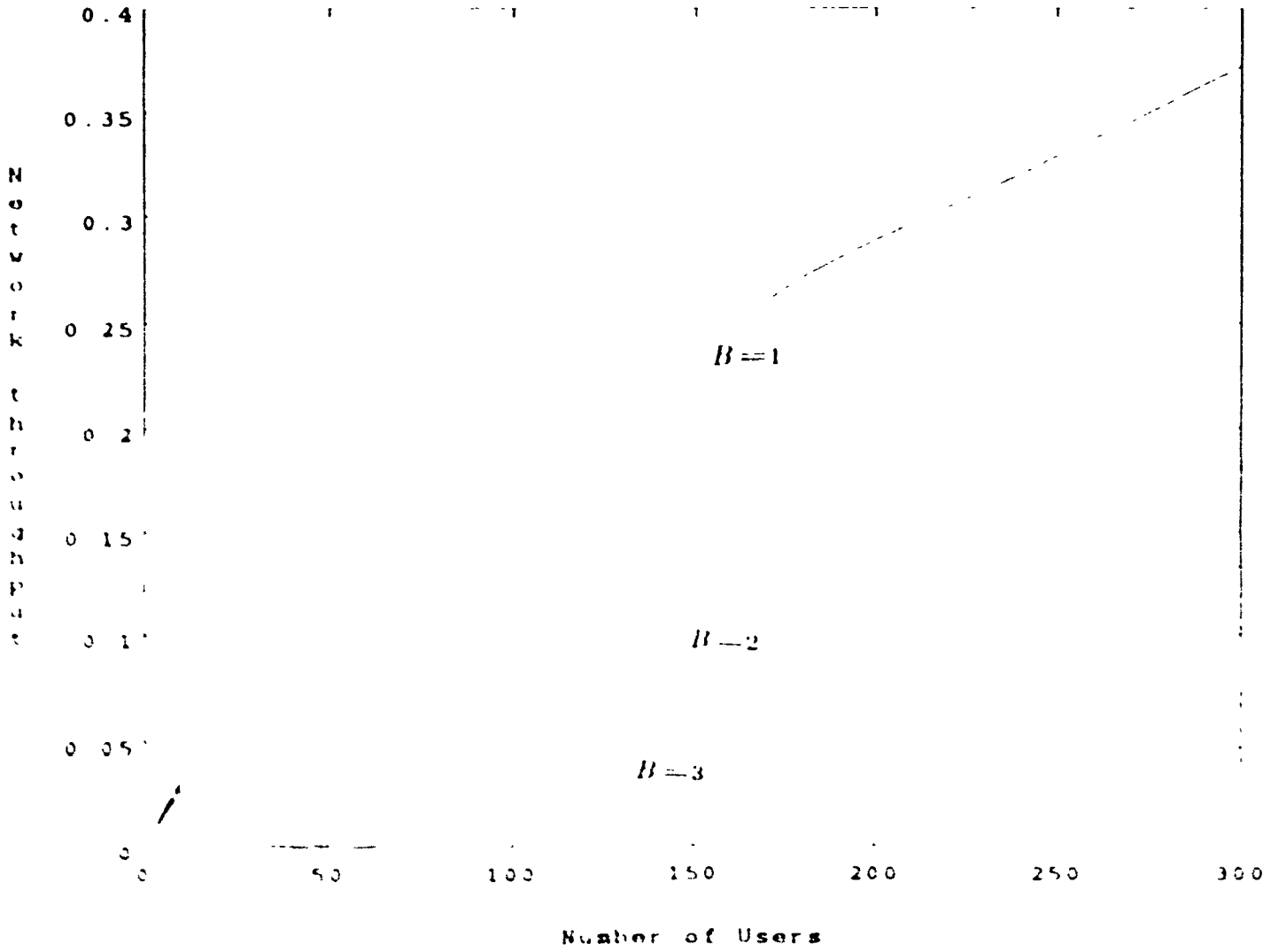

Fig. 4 (b) - The throughput for different packet size and varying number of users (case 2)

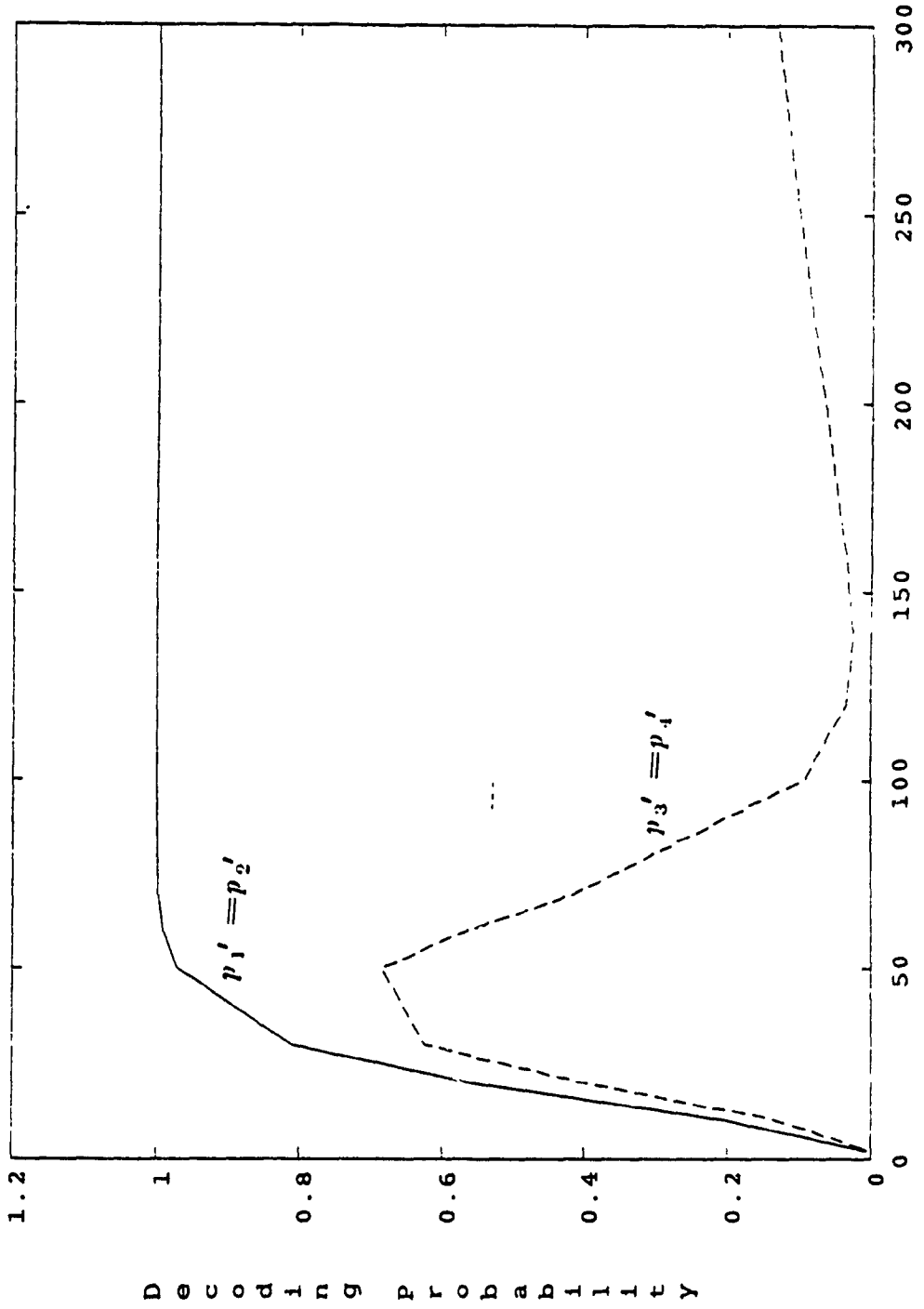

Fig(4. 21):- Probability of BCH word error at the decoder, and the total error probability at the output of the BCH decoder varying the number of users (case 3).

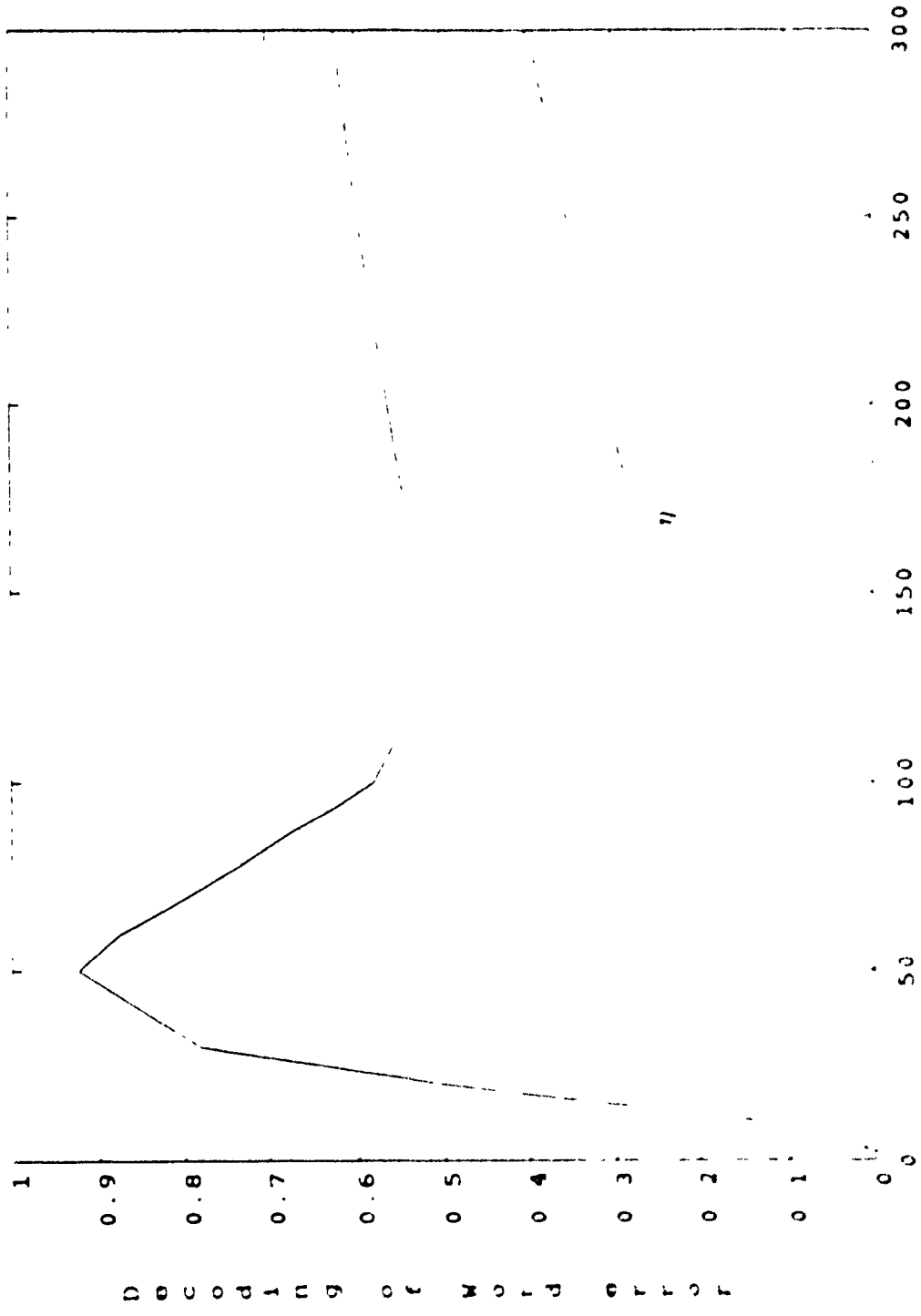

Fig 4.22 - Probability of word error and the efficiency η for varying number of users (case 3)

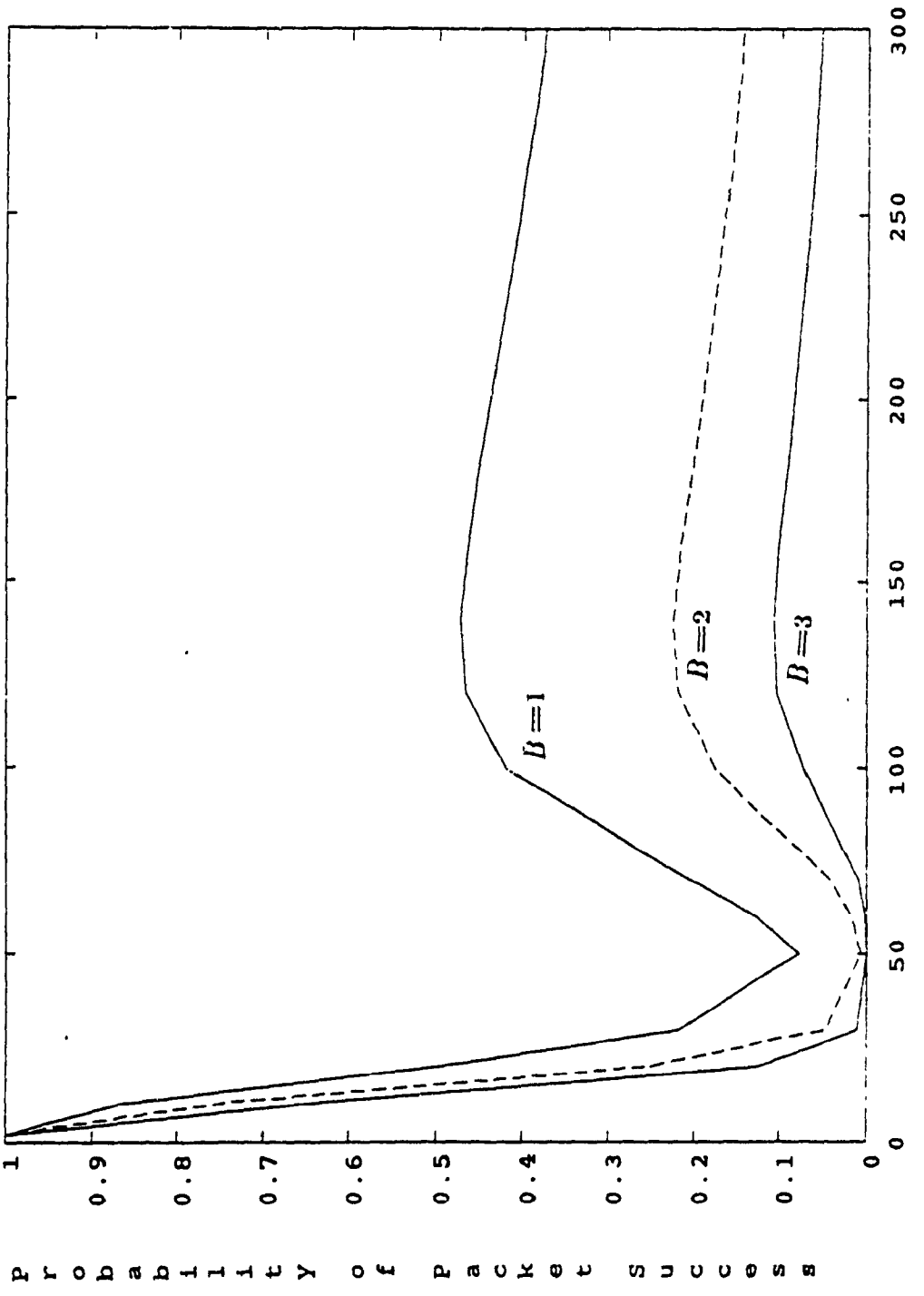

Fig(4. 23):- Probability of packet success verying number of users and different packet size, (case 3)

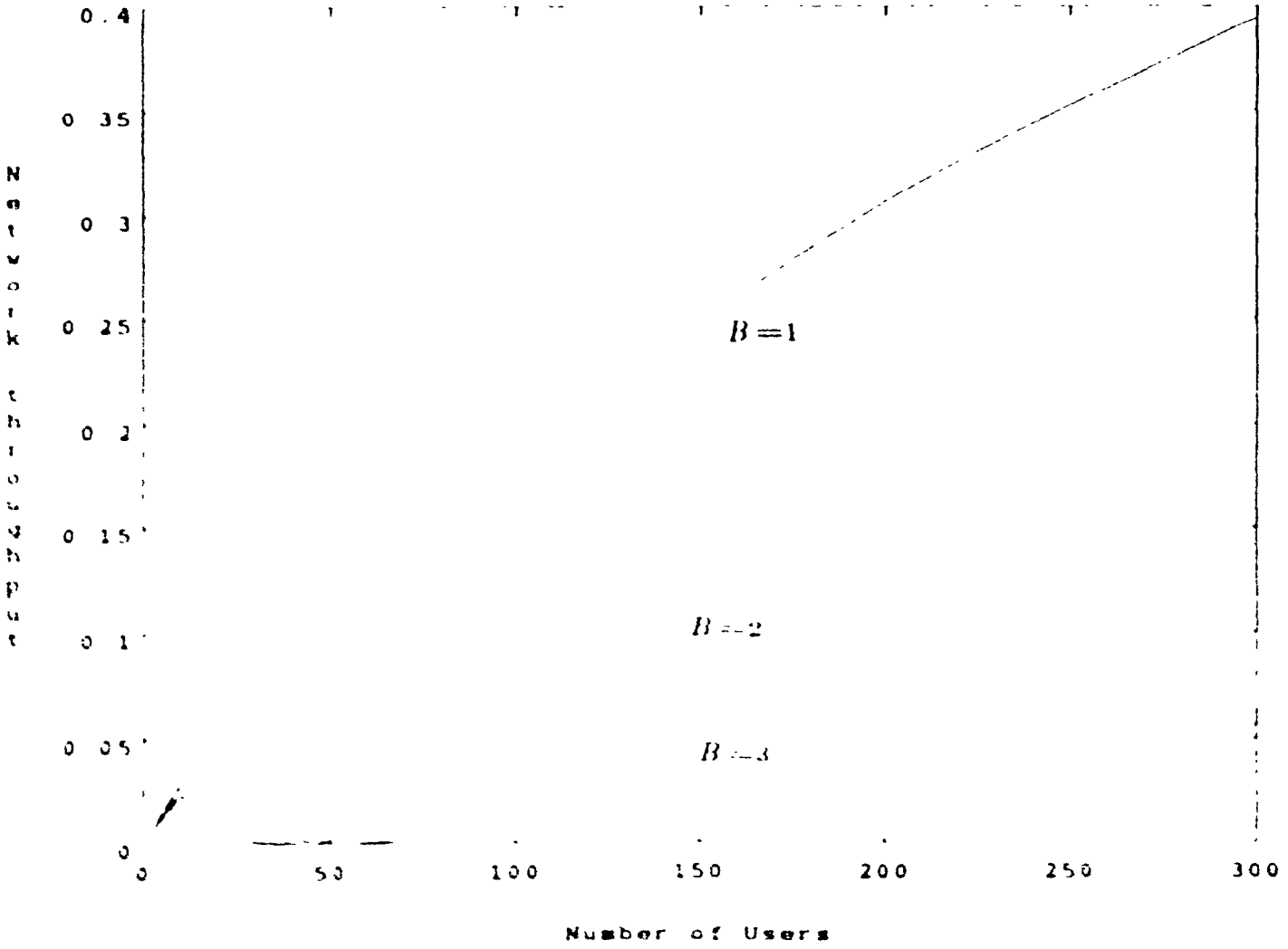

Fig. 4 24 - The throughput for different packet size and varying number of users (case 3)

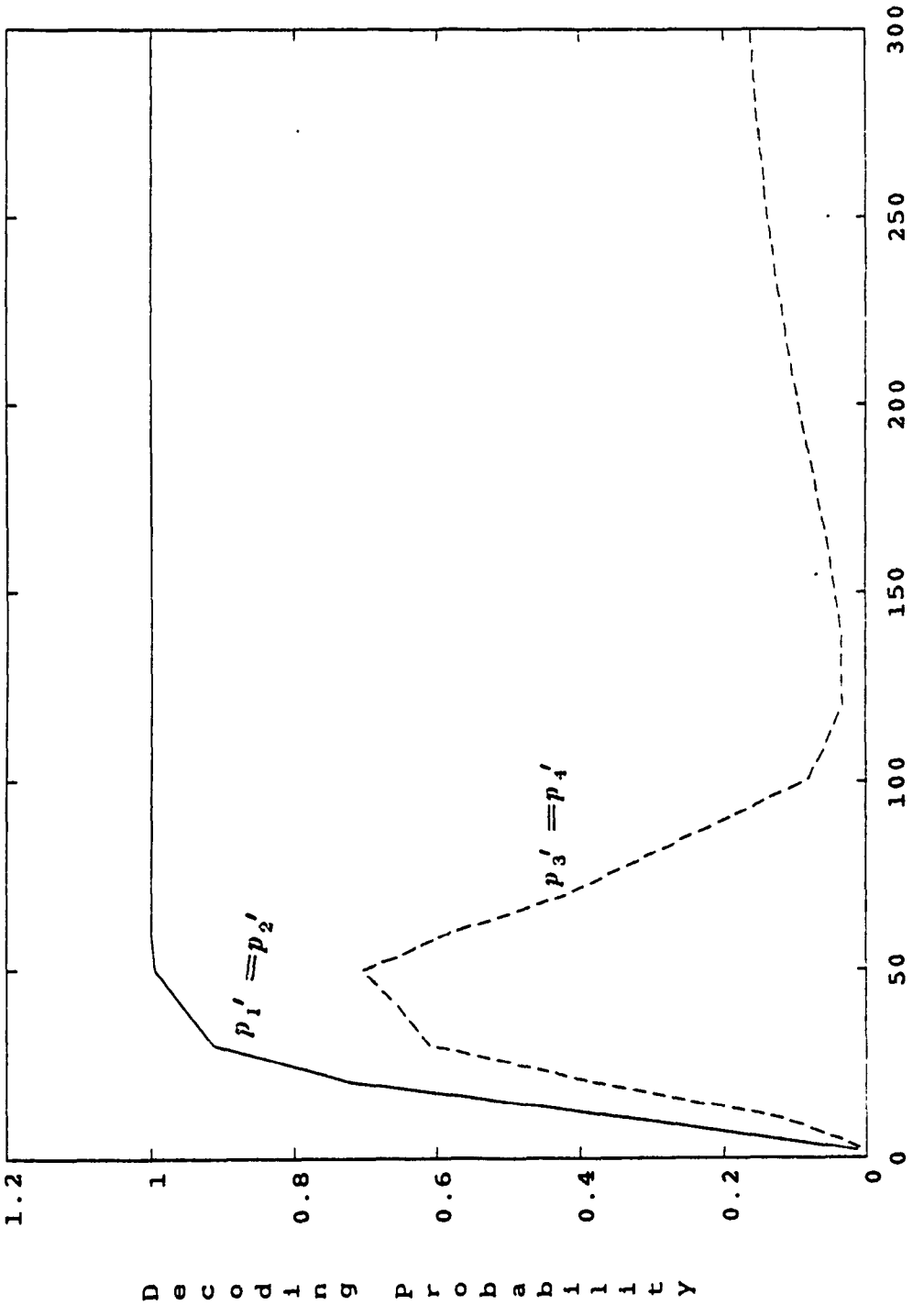

Fig(4. 25):- Probability of BCH word error at the decoder, and the total error probability at the output of the BCH decoder varying the number of users (case 4).

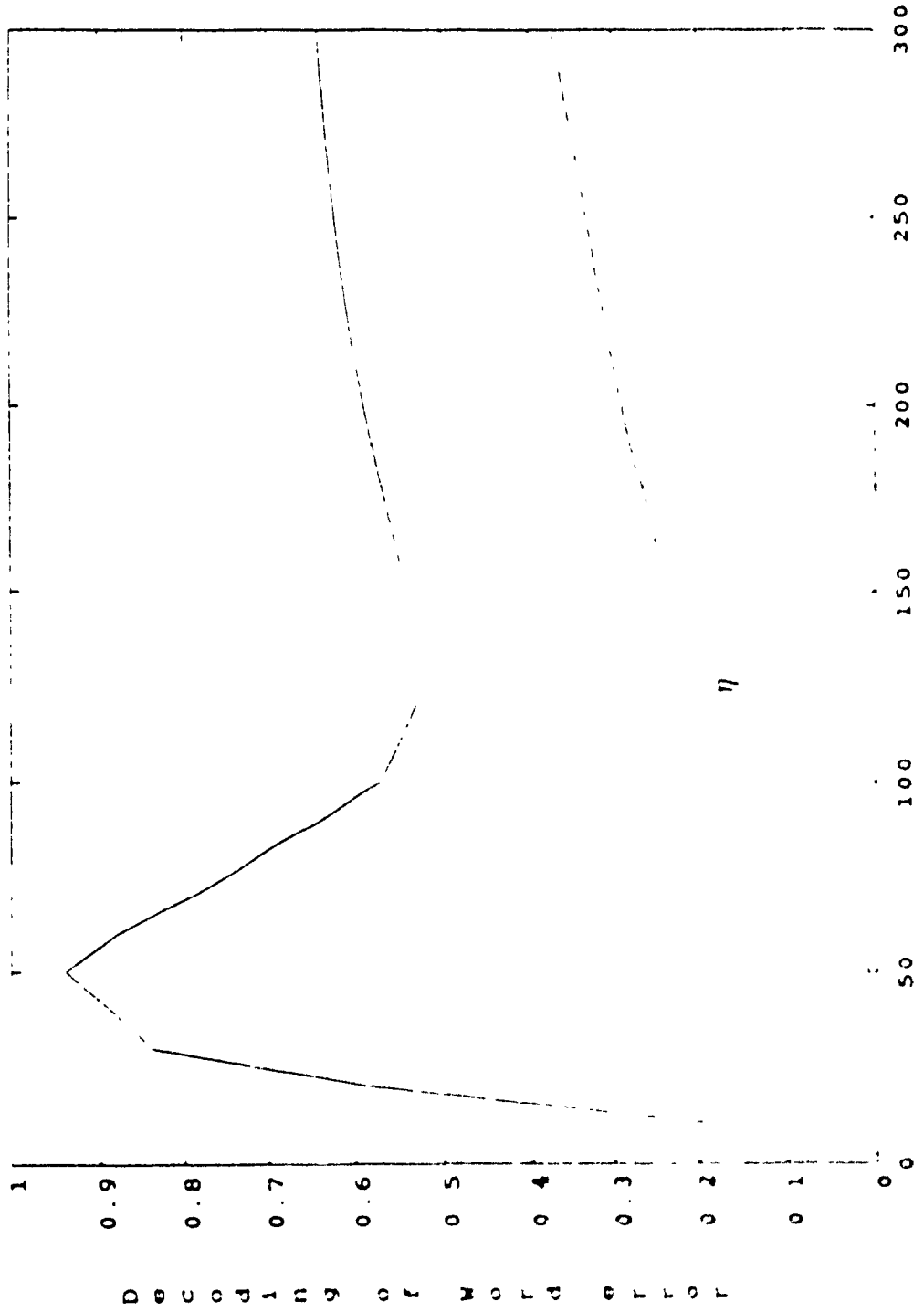

Fig. 4 26) - Probability of word error and the efficiency η for varying number of users (case 1)

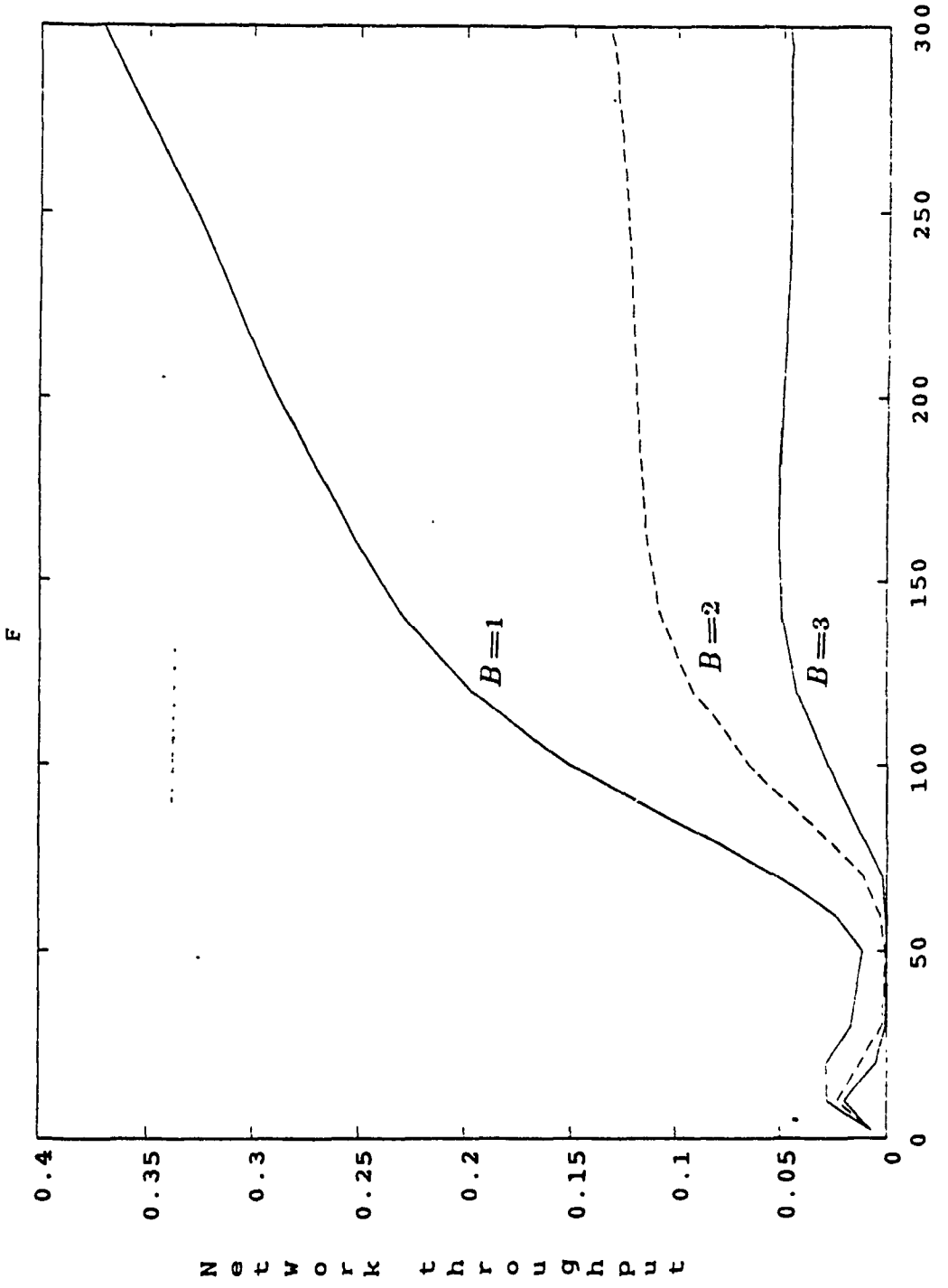

Fig(4. 27):- The throughput for different packet size and varying number of users, (case 4).

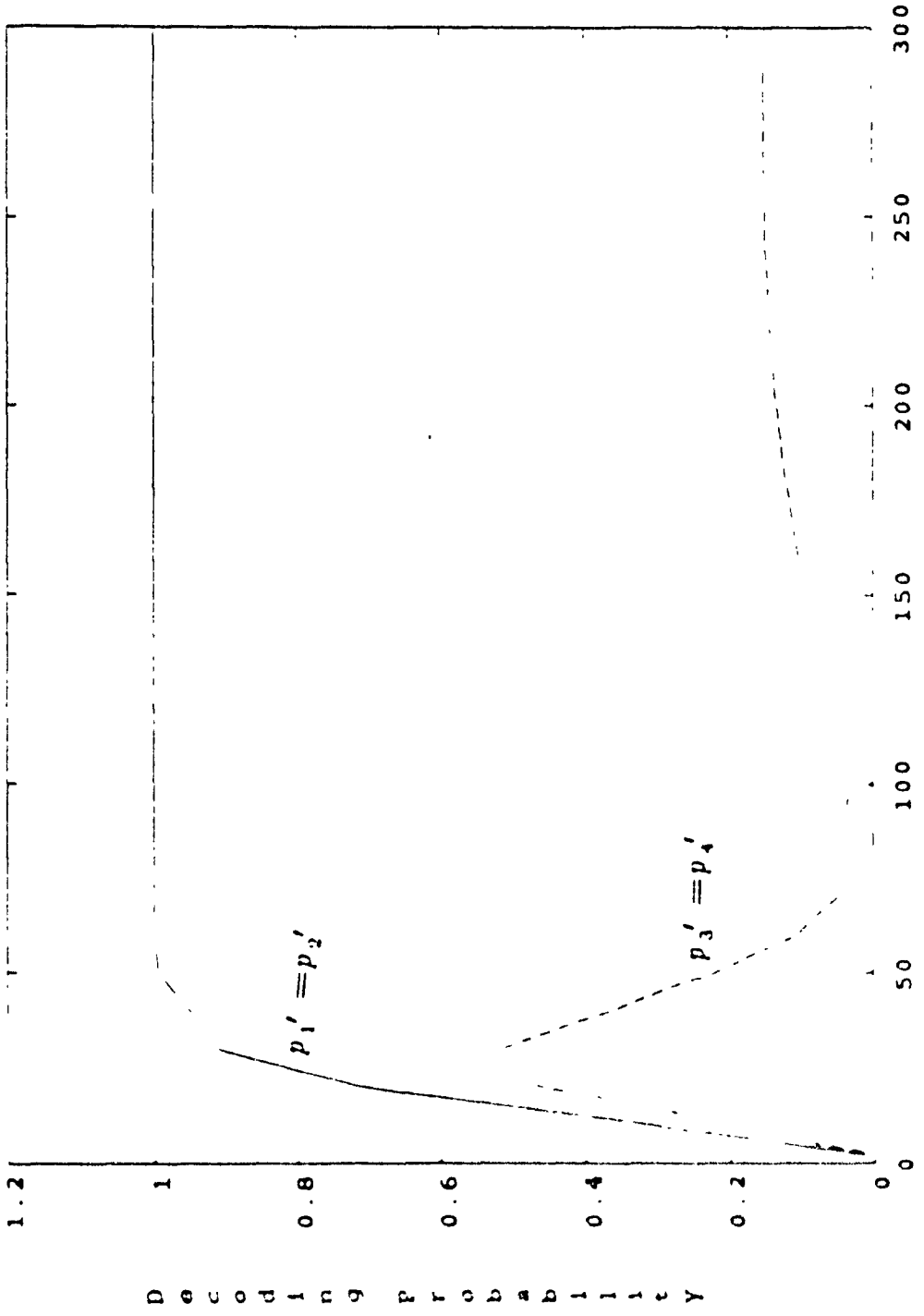

Fig(4.28) - Probability of BCH word error at the decoder, and the total error probability at the output of the BCH decoder varying the number of users (case 5)

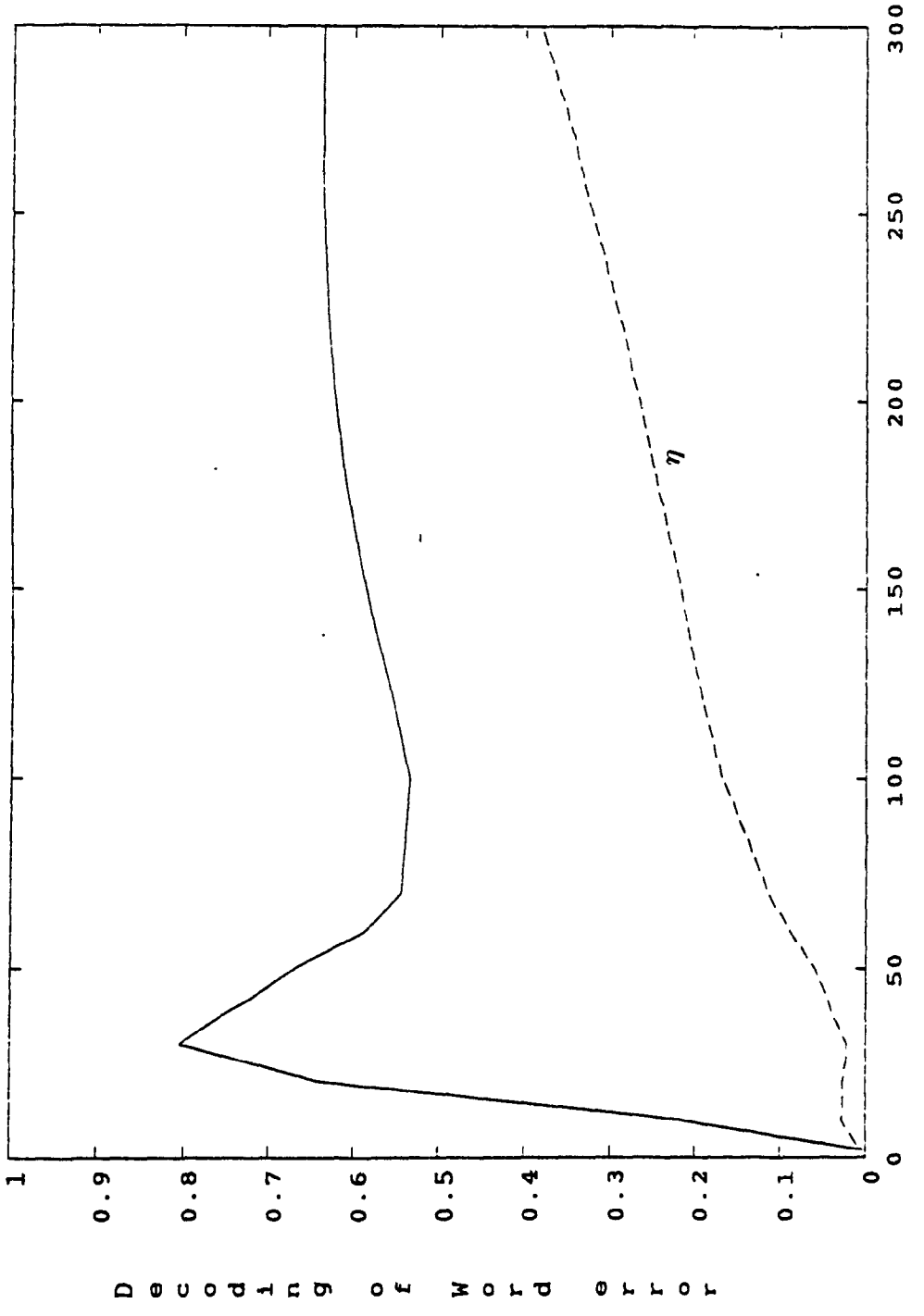

Fig(4. 29):- Probability of word error and the efficiency η for varying number of users (case 5).

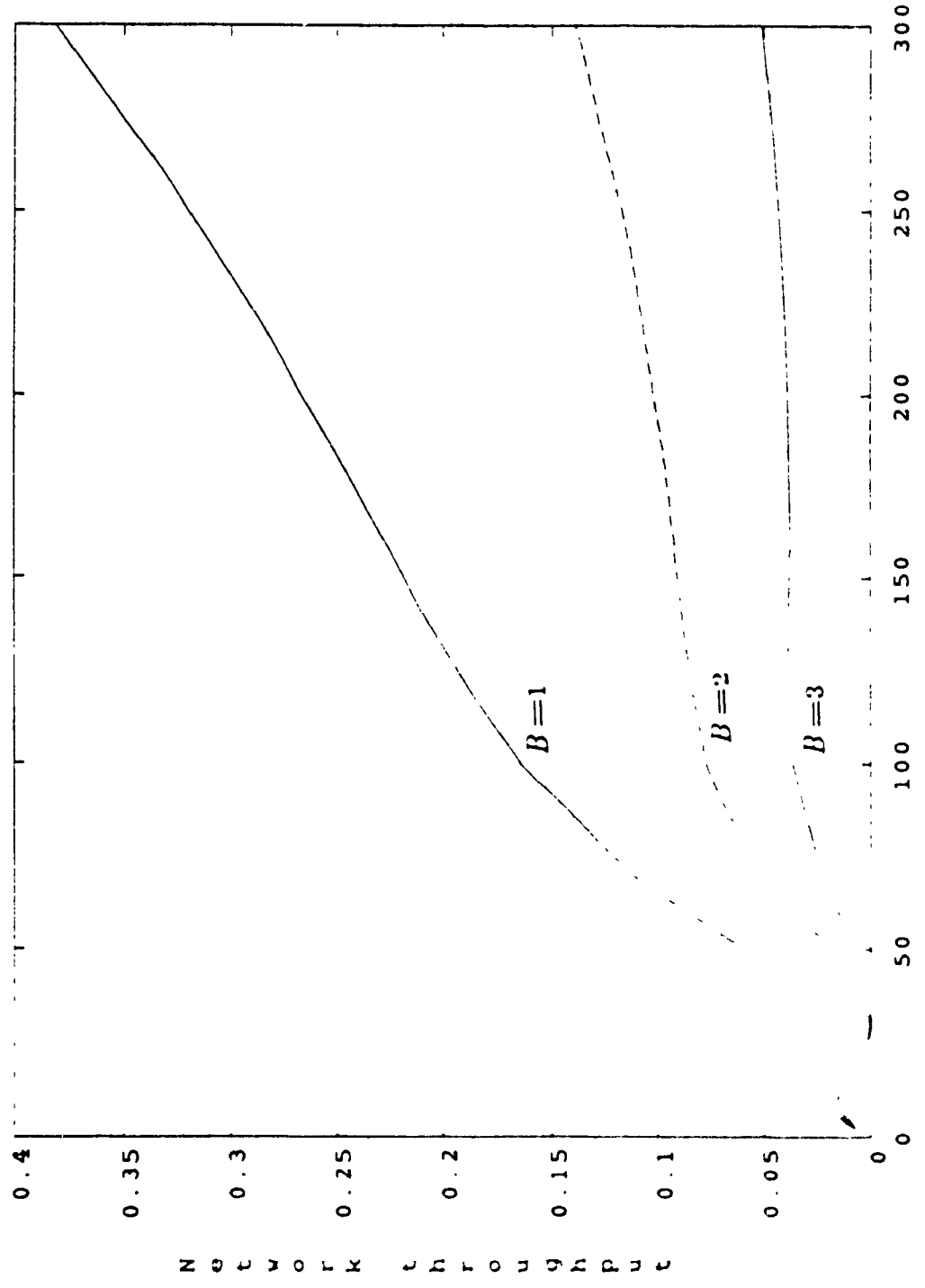

Fig(4.30) - The throughput for different packet size and varying number of users, (case 5)

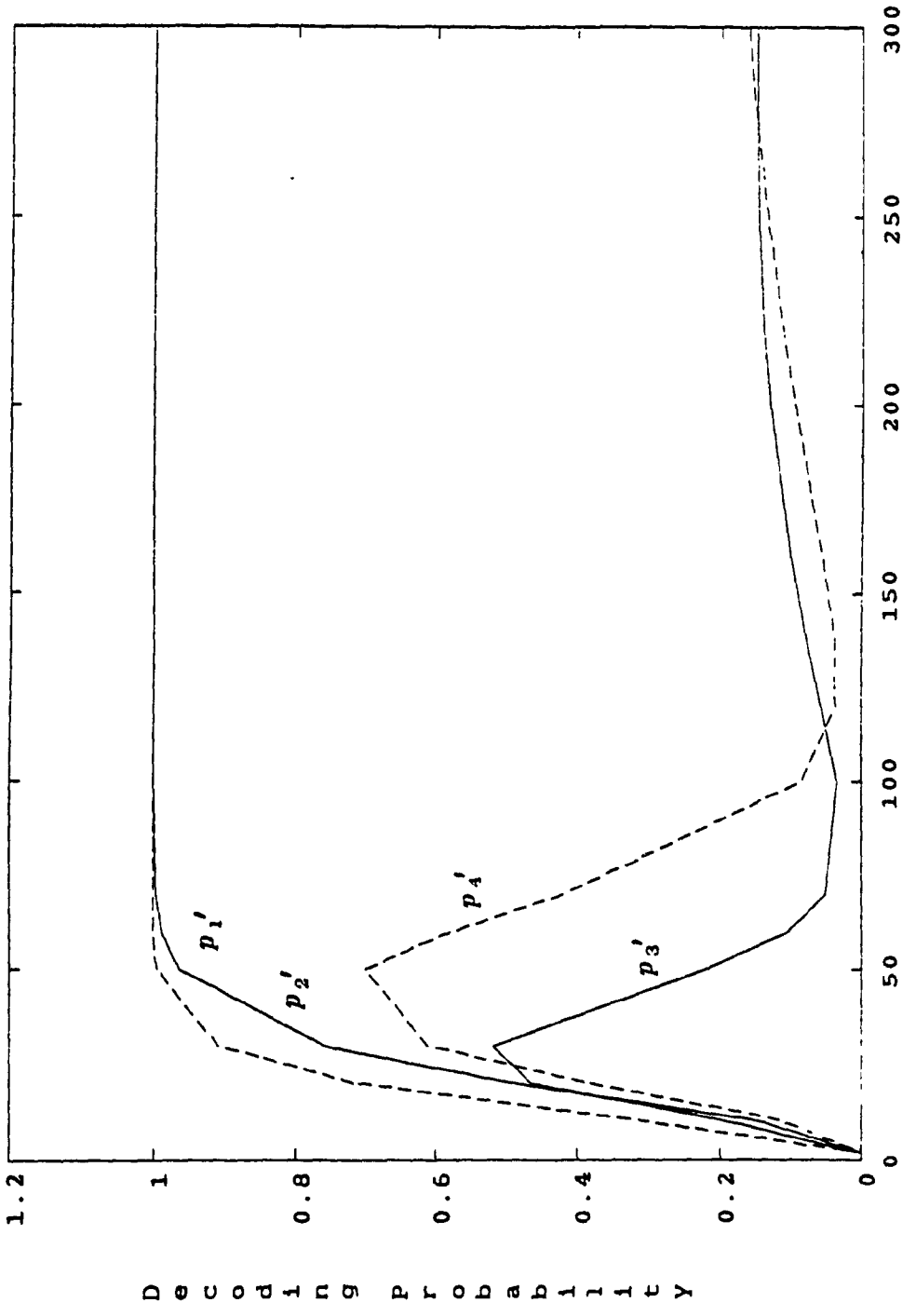

Fig(4. 31):- Probability of BCH word error at the decoder, and the total error probability at the output of the BCH decoder varying the number of users (case 6).

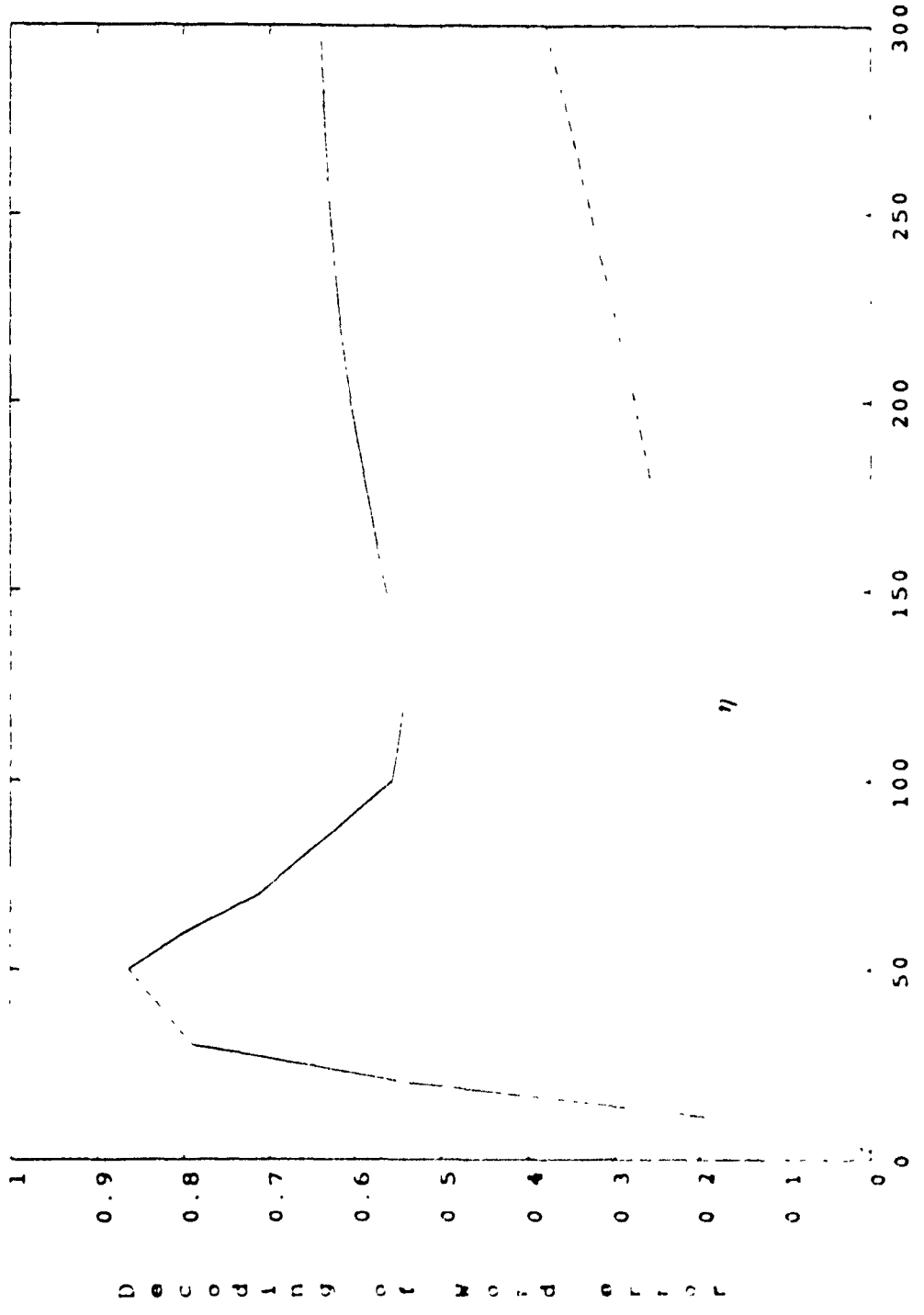

Fig 4.32 - Probability of word error and the efficiency η for varying number of users (case 6)

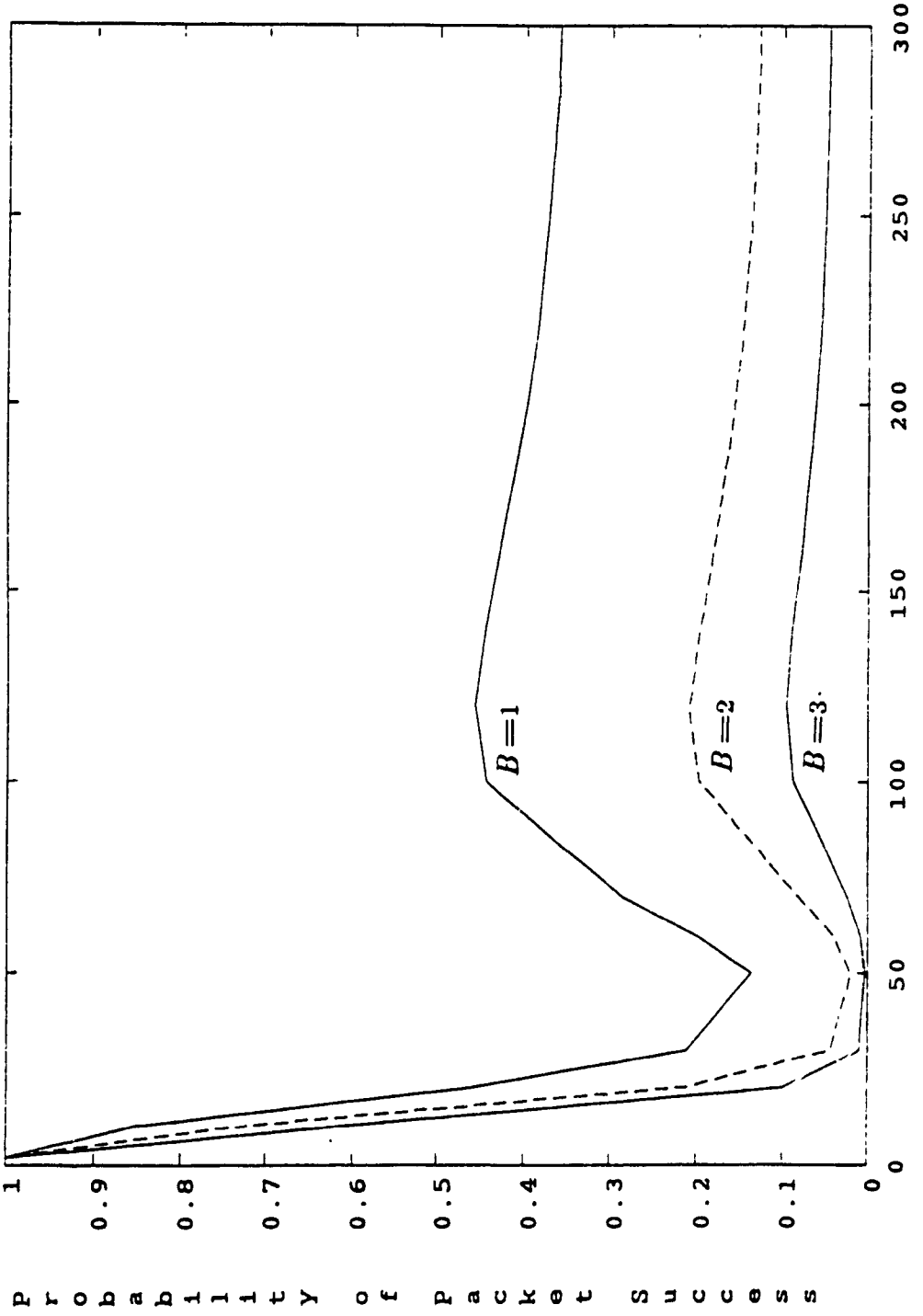

Fig(4. 33):- Probability of packet success verying number of users and different packet size, (case 6)

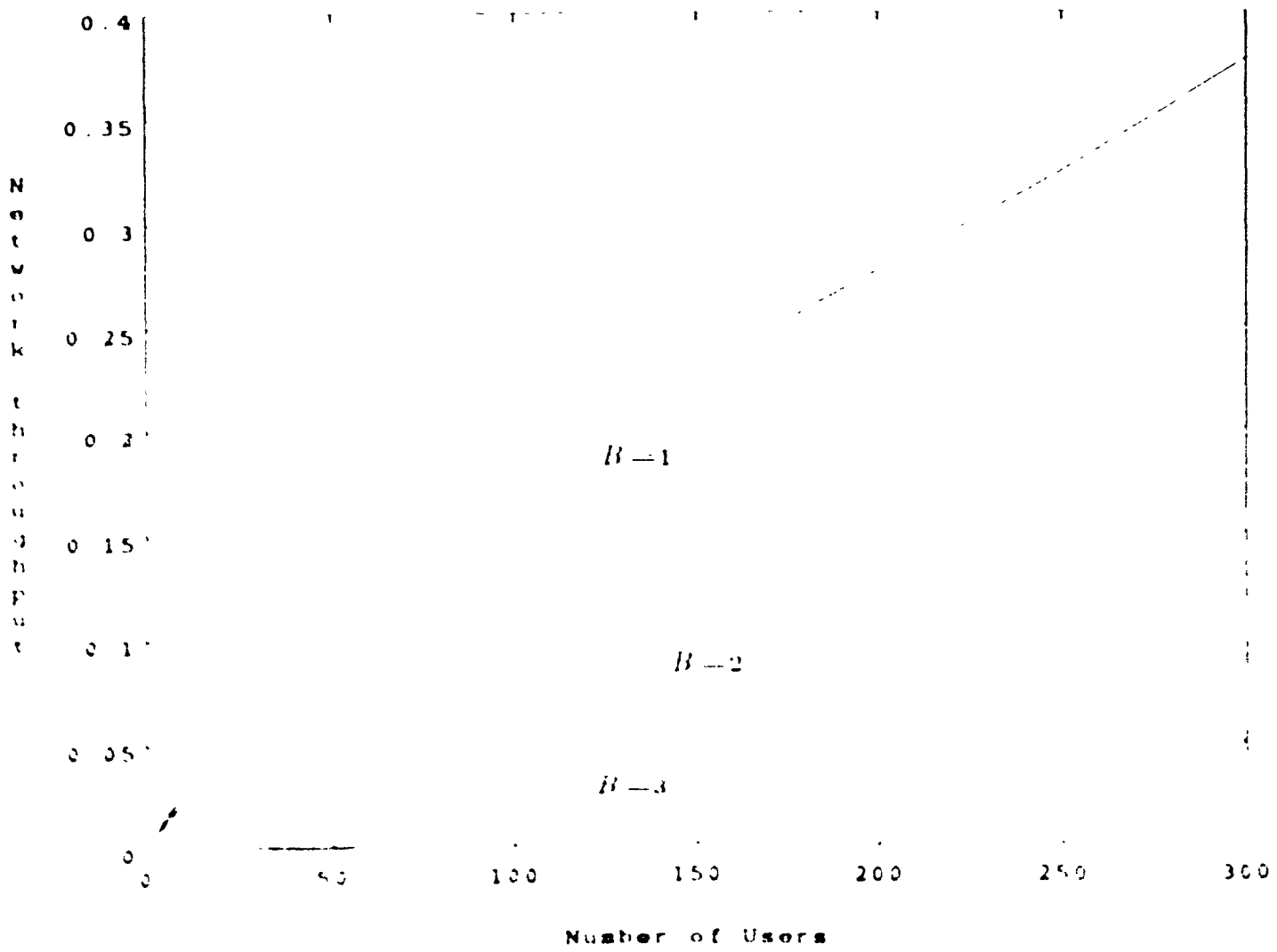

Fig. 3.4 The throughput for different packet size and various number of users in case 6

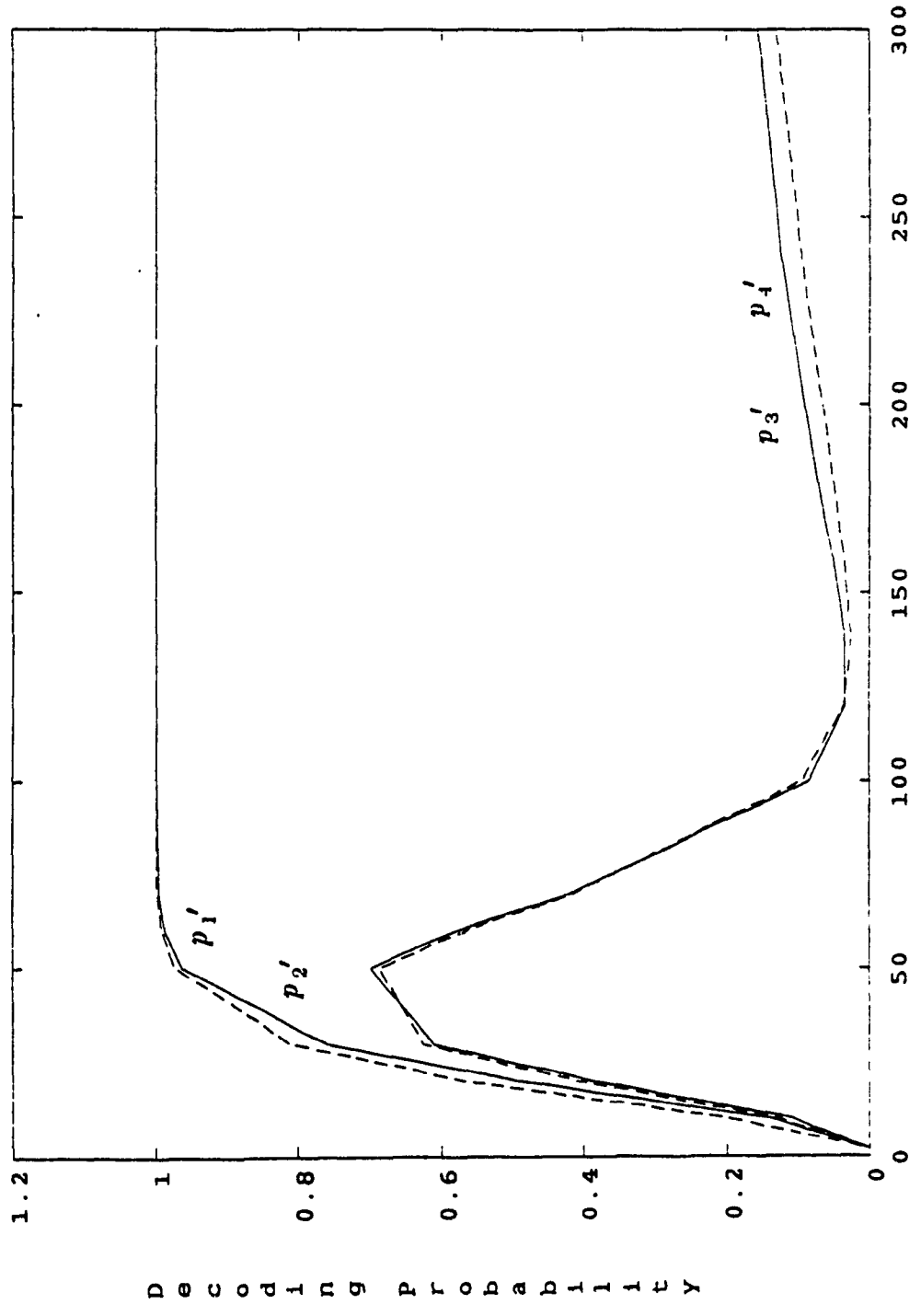

Fig(4. 35):- Probability of BCH word error at the decoder, and the total error probability at the output of the BCH decoder varying the number of users (case 7).

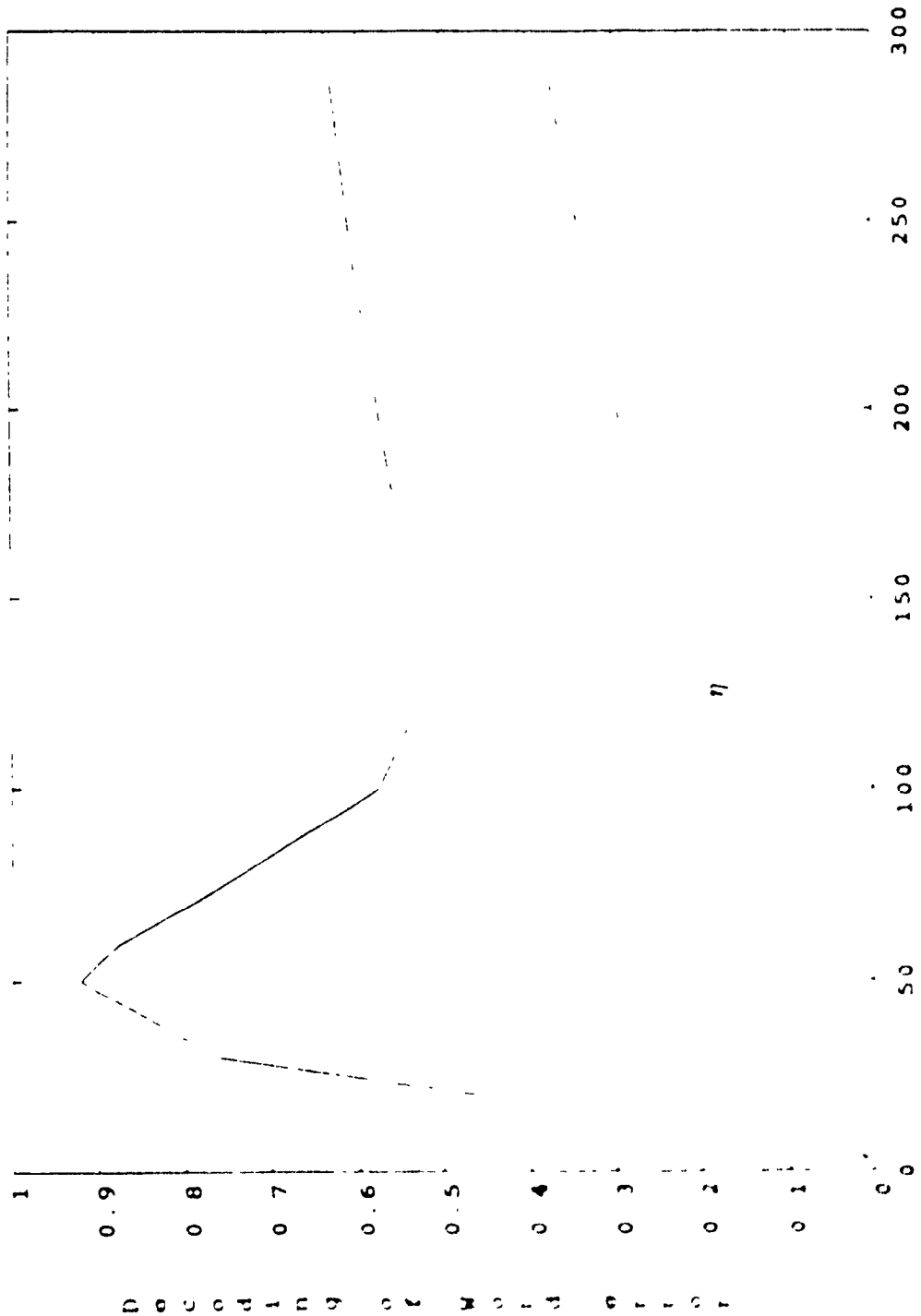

Fig. 4.38 - Probability of word error and the efficiency η for varying number of users (case 7)

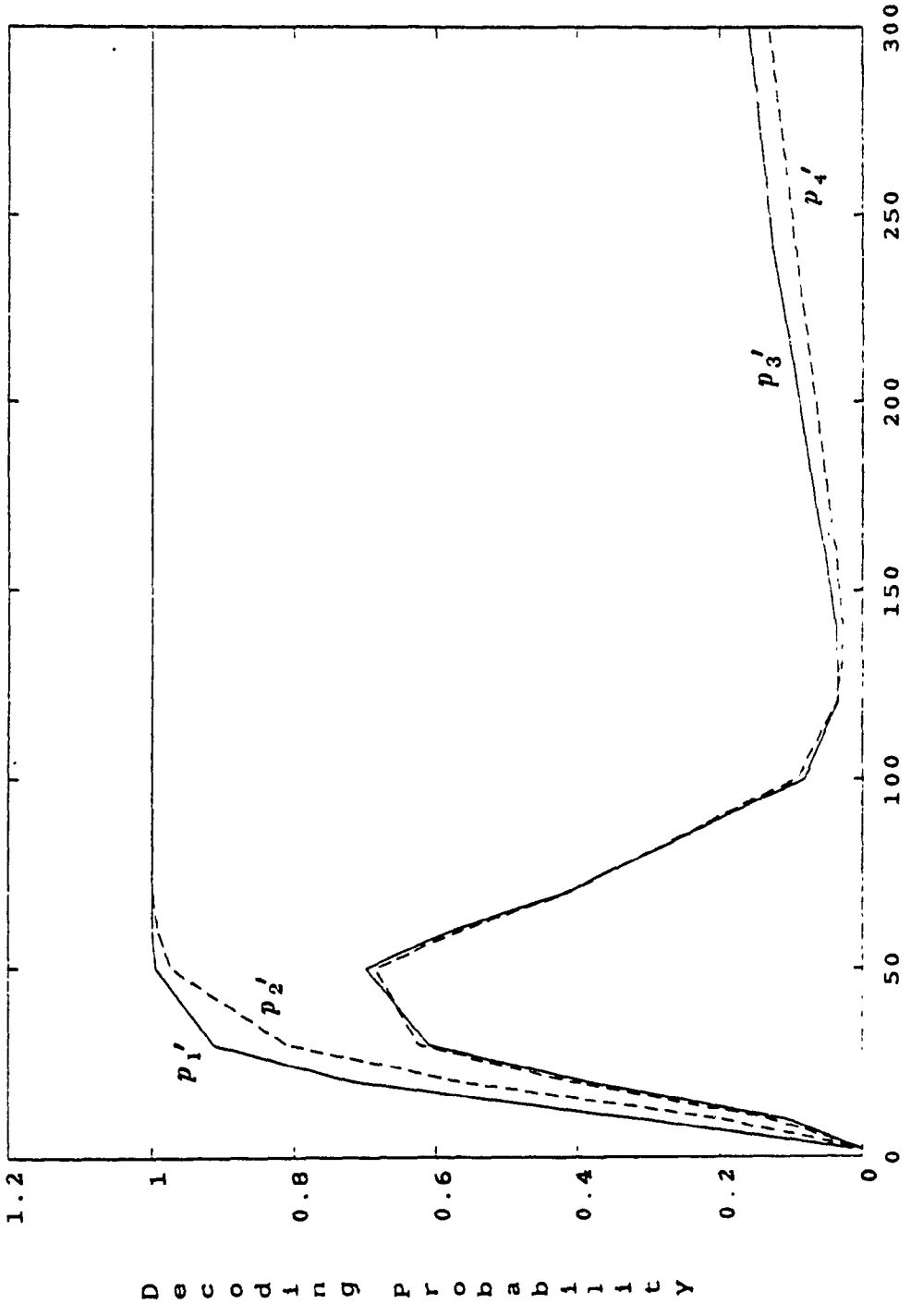

Fig(4. 37):- Probability of BCH word error at the decoder, and the total error probability at the output of the BCH decoder varying the number of users (case 8).

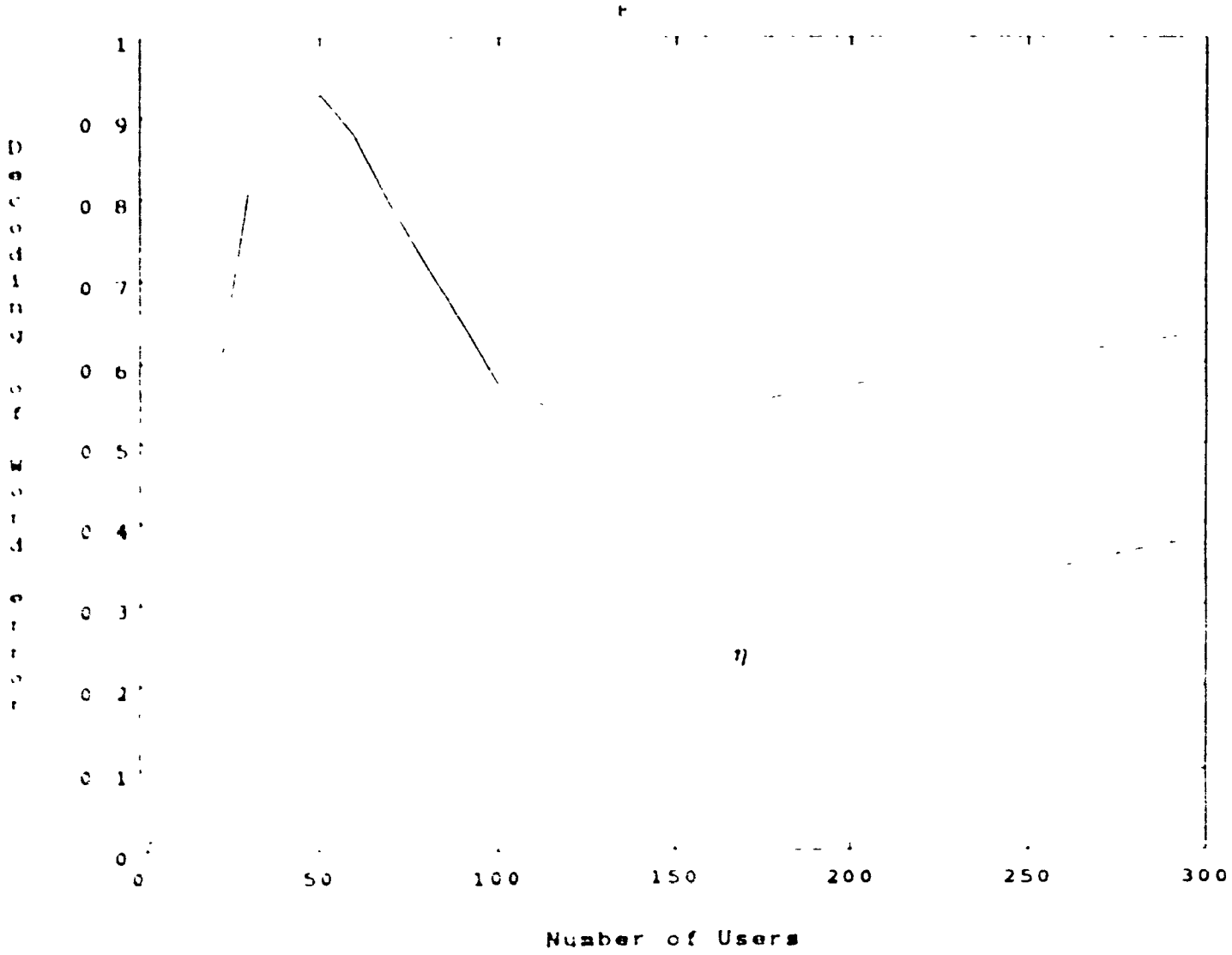

Fig. 4 3a) - Probability of word error and the efficiency η for varying number of users (case a)

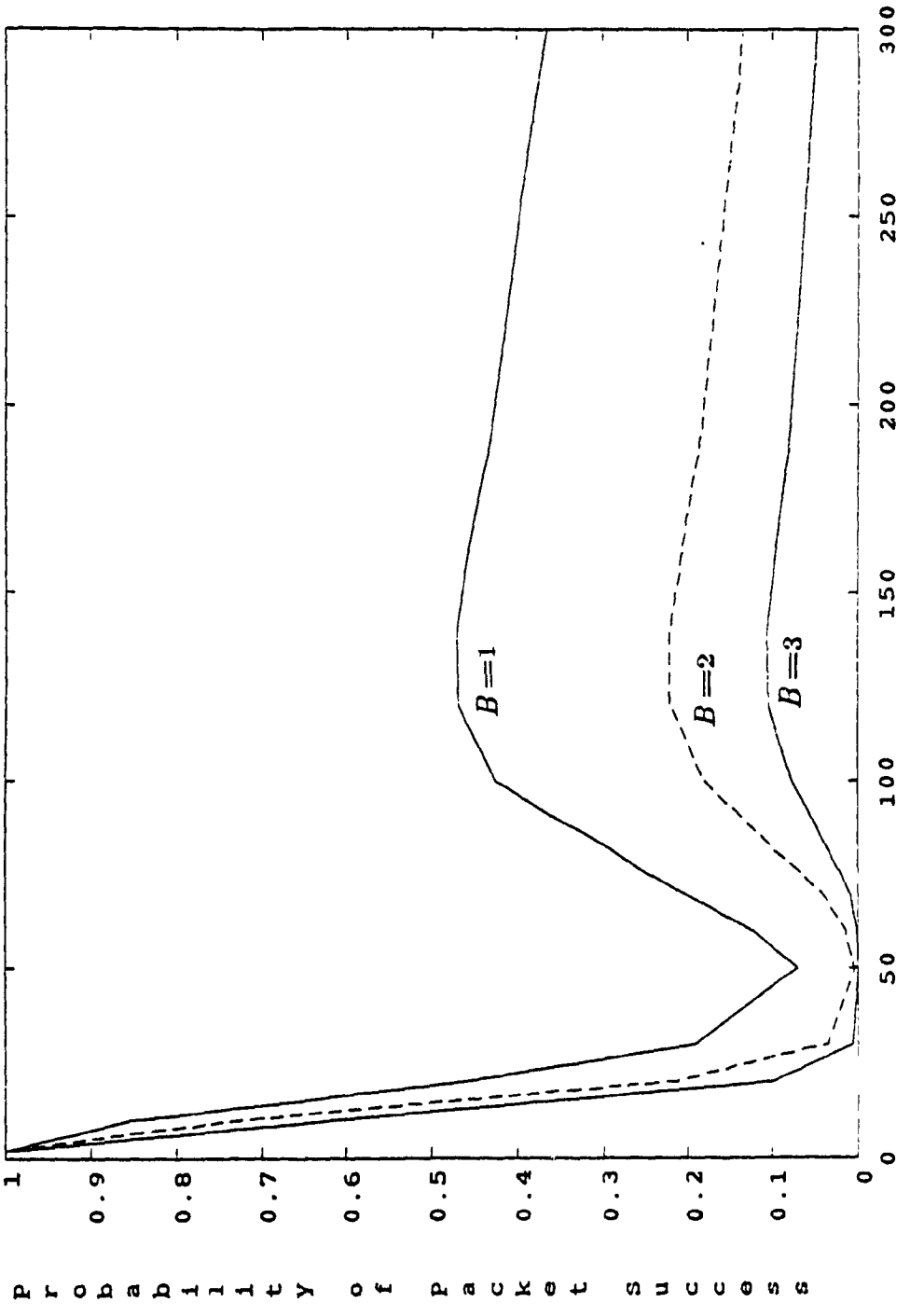

Fig(4. 39):- Probability of packet success verying number of users and different packet size, (case 8)

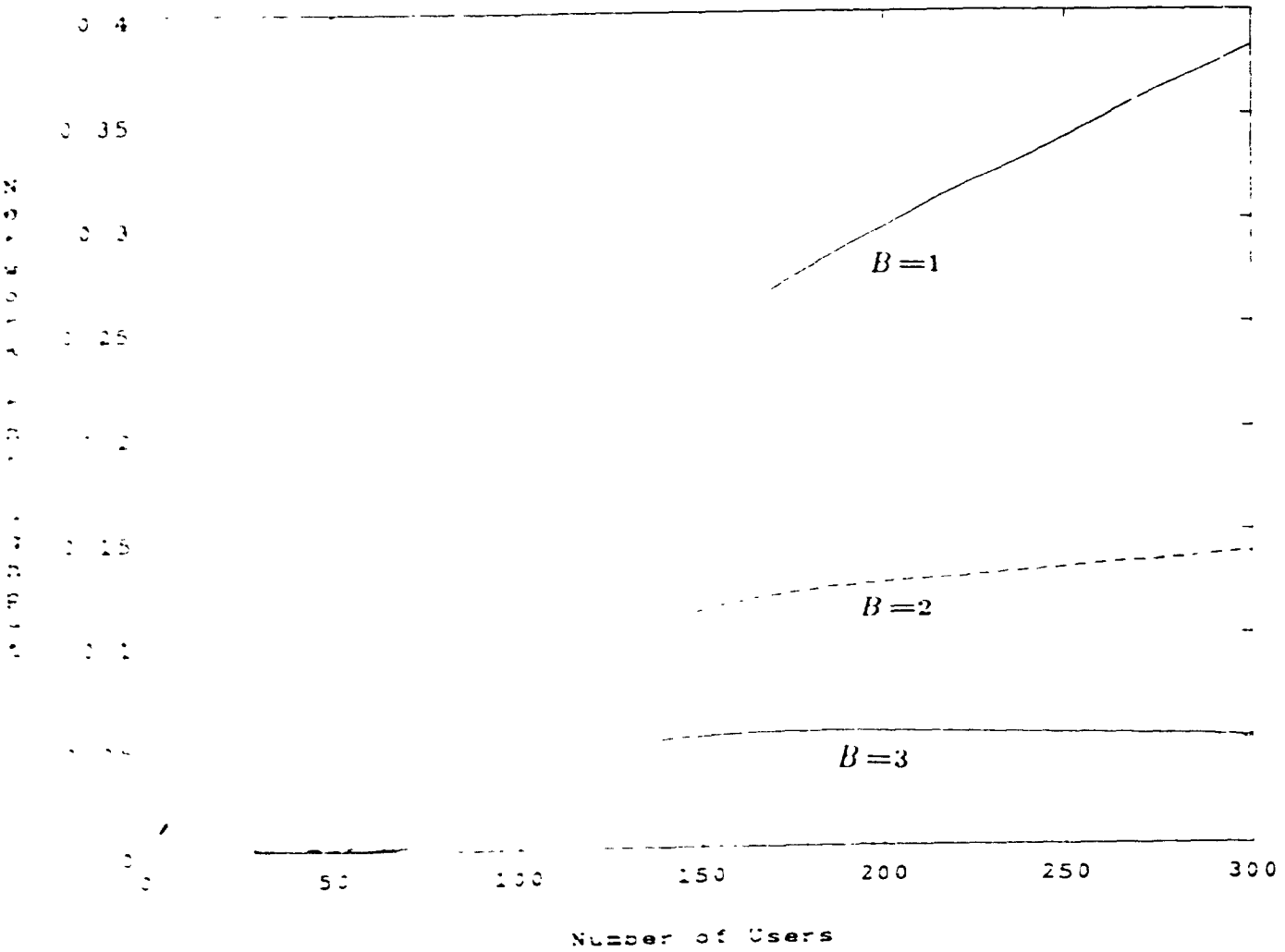

Fig. 4.40 - The throughput for different packet size and varying number of users (case 8)

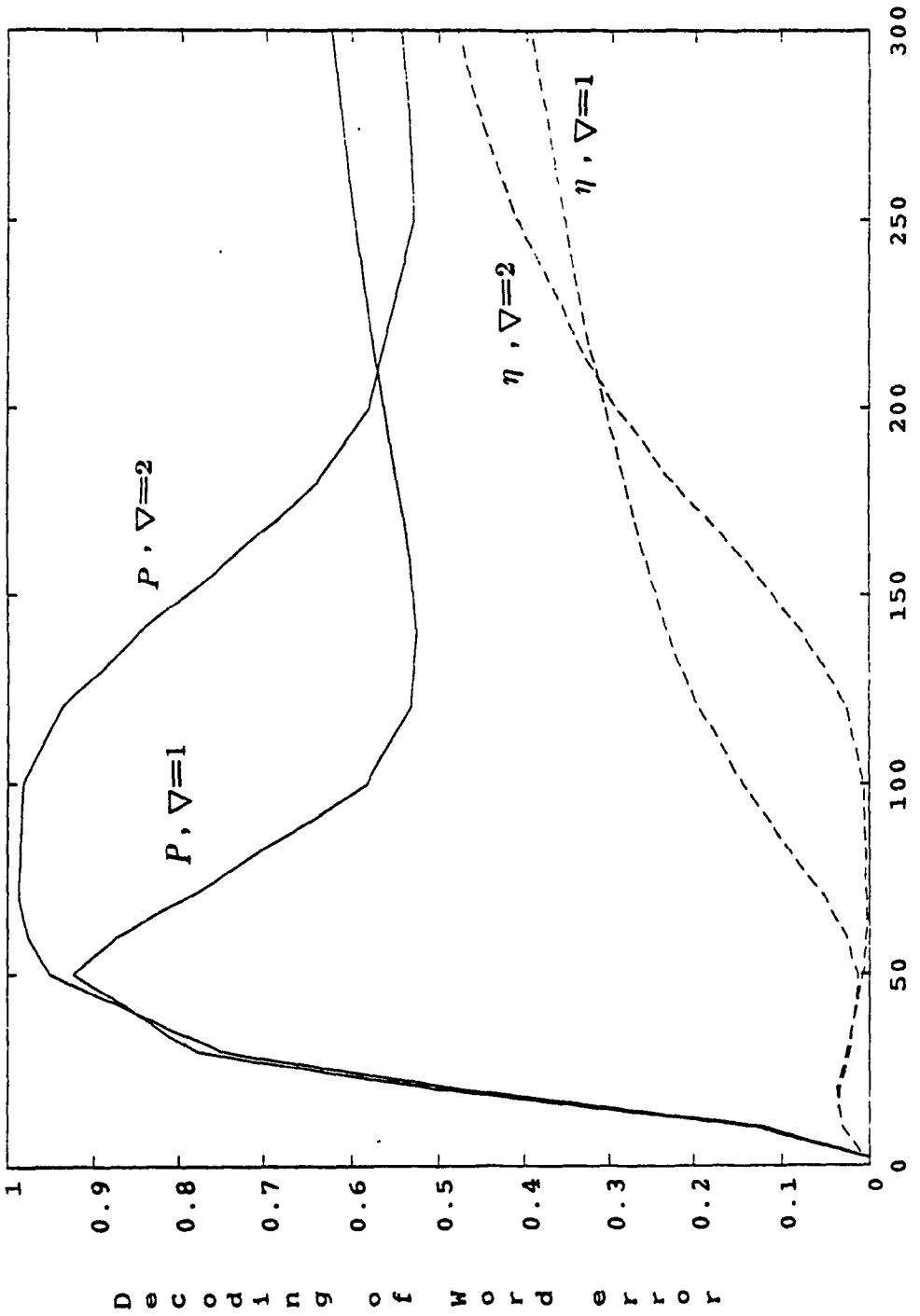

Fig(4. 41):- Probability of word error and the efficiency η for varying number of users and Δ (case 3).

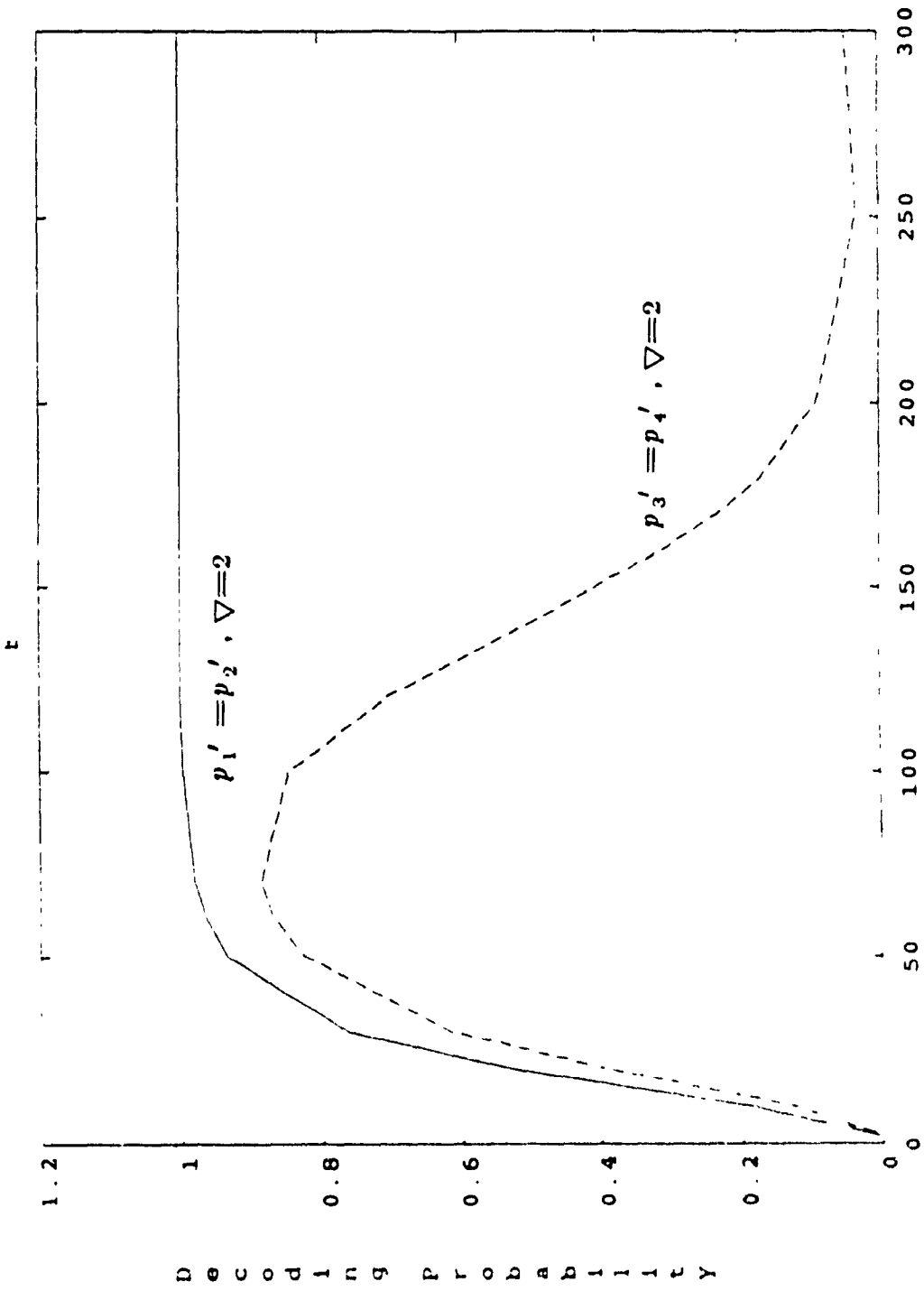

Fig(4.42) - Probability of BCH word error at the decoder, and the total error probability at the output of the BCH decoder varying the number of users and Δ (case 3).

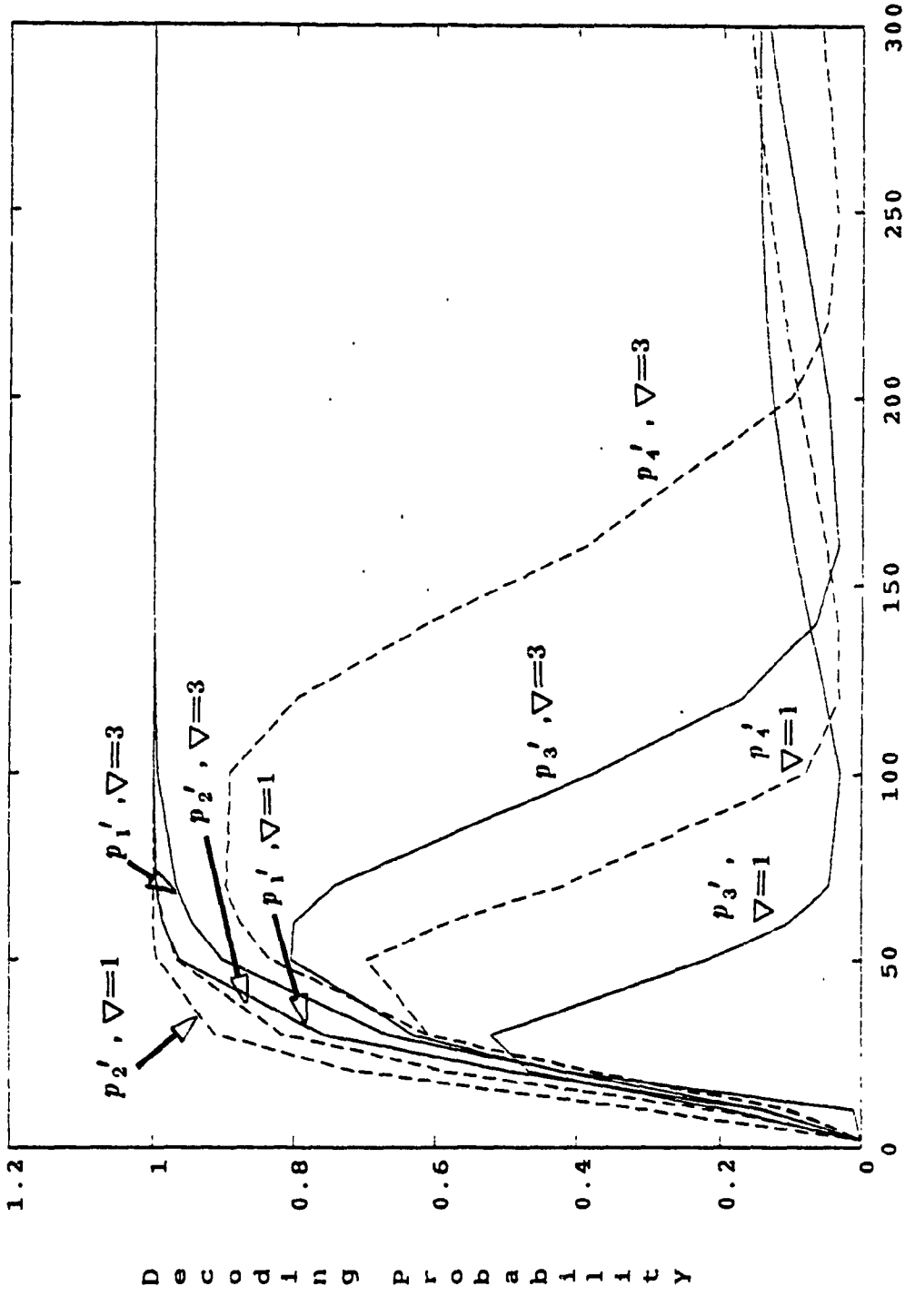

Fig(4. 43):- Probability of BCH word error at the decoder, and the total error probability at the output of the BCH decoder varying the number of users and Δ (case 6).

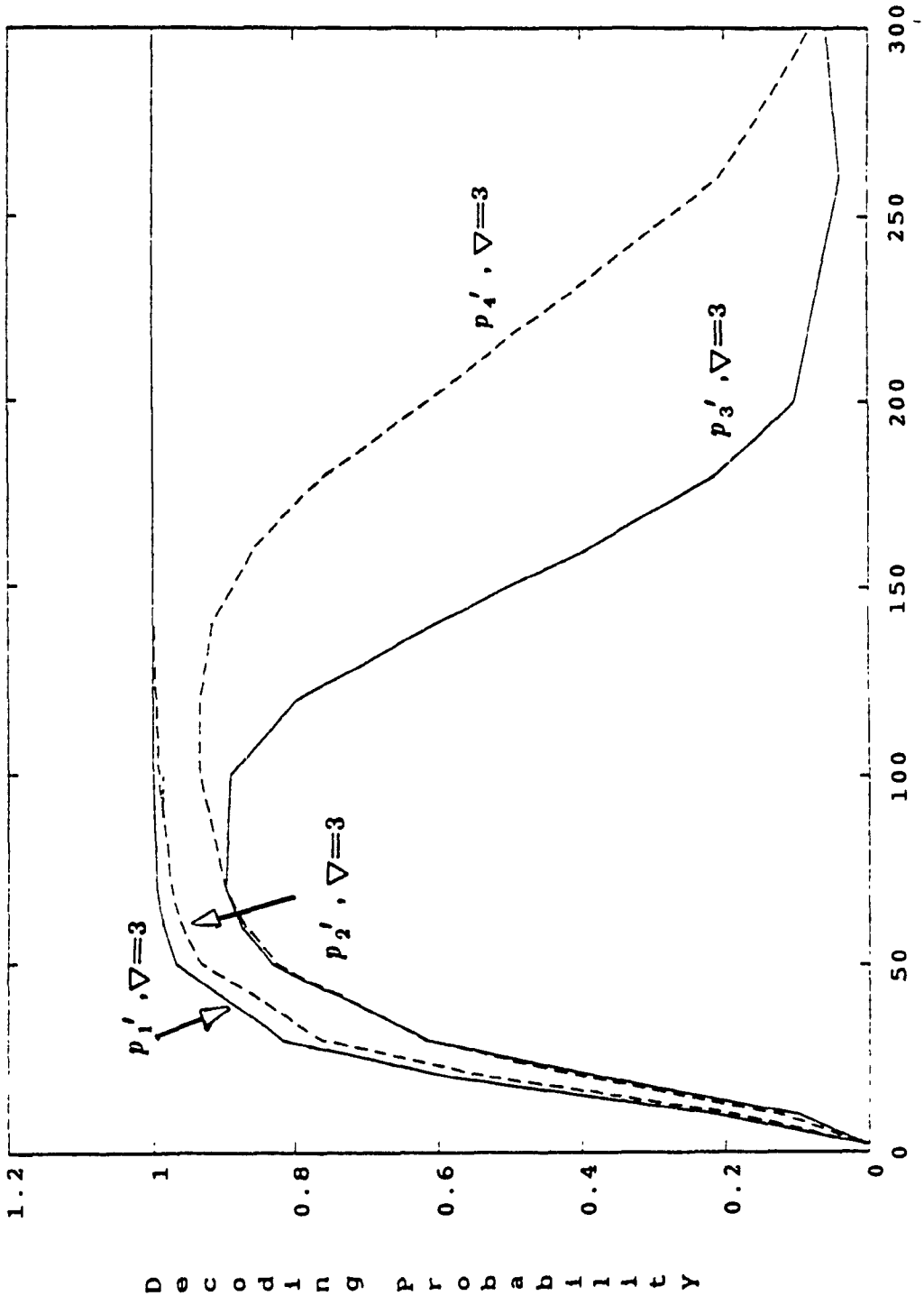

Fig(4. 44):- Probability of BCH word error at the decoder, and the total error probability at the output of the BCH decoder varying the number of users and Δ (case 8).

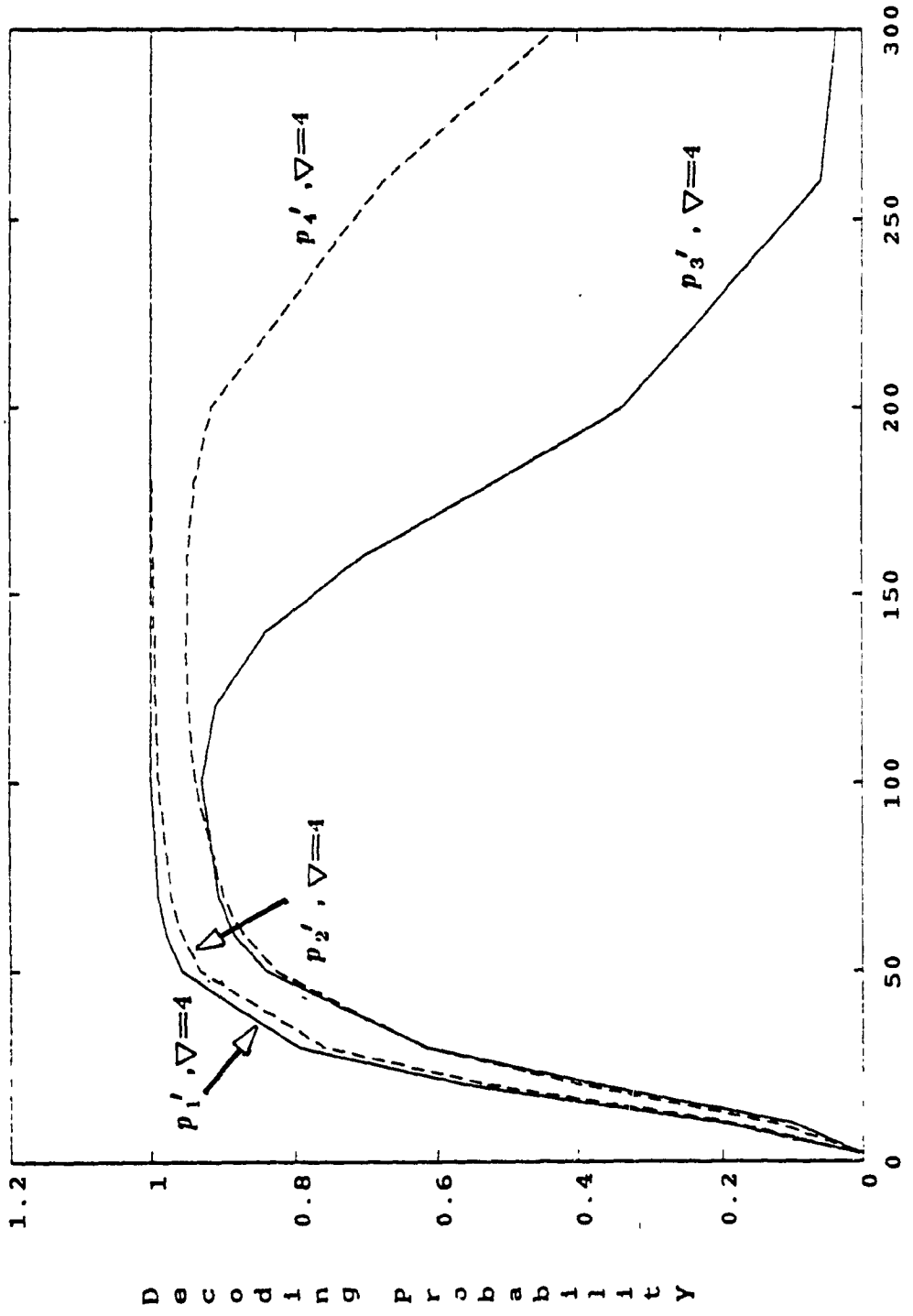

Fig(4. 45):- Probability of BCII word error at the decoder, and the total error probability at the output of the BCII decoder varying the number of users and Δ (case 8).

CHAPTER 5

CONCLUSION

In chapter 3 the envelope of the output of the chirp matched filter is derived under frequency Doppler Δ and DS code delay τ in the proposed DS/chirp system (Fig.3. 1 and Fig.3. 2). These outputs are obtained for different values of FT_b (i.e. the time bandwidth product of the chirp signal). This is followed by evaluating the probability of error under Doppler Δ, delay τ, and pulse jamming is analyzed and the results are obtained for different values of F, T_b, Δ, σ^2, R_c, B_{RF}, J_J and α. It is shown that certain values of F, R_c allow the minimization of both the effects of jamming and frequency Doppler. It was found that the output of the matched filter with the signal matched to the received signal, the maximum amplitude increasis by increasing FT. Increasing F improves the performance of the system. This is also the case , under the effects of Doppler and jamming. But under the effects of Doppler and jamming there is a choice to increase F or R_c to improve the probability of error. The classical results of the effect of the duty factor α are also seen in the results of chapter three. Increasing the SNR does not improuve the performance of the system in the case of Δ the adjustment of Doppler, and loss of DS correlation (τ) and pulsed jamming. A careful design should involve increasing F, R_c and for sure using an error correcting code to combat these threats. One might also try to use parallel matched filters each tuned to a certain delay and choosing the maximum. These issues are currently under investigation.

In chapter 4 we have introduced the concept of multidecoding, applied to hybrid TH/PS networks which is equivalent to post decoding selective diversity

combining obtained by voting among the outputs of few FEC decoder. Recent literature [10] was concerned with the problem of diversity combining following demodulation and before Forword Error Control FEC. It is expected in this regard that a combination of preceding diversity and post decoding diversity will yield best error and throughput performance. This will be the subject of future research. The second concept introduced here was the erasure modification process in one TH slot according to demodulation outputs in other TH slots. It was found that the FEC decoding performance obtained in this case, as well as recent FEC decoders of [10], have performed differently depending on the multiaccess load with each code giving its best performance at a certain load range. It is expected that an adaptive load measurement policy, which selects only one decoding result out of a few decoders, will enable the receiver to pick the output of the best FEC decoder at each load. This will be the subject of future research. The extra side information in the DS preample of each TH slot should help not only for code acquisition acceleration, but also to break this possible between the outputs of the multidecoders. Our realistic throughput analysis (considering rate loss due to FEC, TH, DS, noise, multiaccess, etc.), have resulted in a maximum throughput of 0.48 bits/Hz, a reasonable figure for the subject TH/DS network. However, the maximum throughputs obtained in chapter 4 were obtained at high packet and FEC word error probability, for voice applications those values may become prohibitive and for data, retransmission upon failure using the appropriate ARQ technique which cuts down our throughputs obtained. The results of the paper are extendible to concatenated convolutional codes and other hybrid formats such as FH/TH, FH/DS systems.

The results have shown that too, it is much advantageous to work with the shortest possible packet size (subject to packet overhead control constraint naturally) at low multiaccess loads, the best decoder was the (P_1', P_2') decoder with

low values of the threshold ∇. At medium loads (P_3' , P_4') decoders based on q_l , θ_l and still low values of $\nabla = 1$ performed better than other codes.

Finally, at high loads higher values ∇ and use of the erasure modification rule have resulted in a superior error and throughput performance. Based on this result, the modification of our proposed post decoding diversity scheme (based on Equ. (4.43)) to an overall adaptive decoding scheme is straightforward.

The receiver will switch itself in between decoders, and samples only one of them, depending on the load range, thus achieving the best error and throughput results. It is to be finally noted all of the complex decoding schemes in chapter 4 implicates only the receiver structure. There is no complicated handshaking required between transmitter and receiver as in recent combined ARQ/FEC techniques [15].

REFERENCES

[1] C. E. Cook, " Pulse compression-key to more efficient radar transmission", *Procceding of the IRE*, vol. 48 , March 1960, pp 310-316.

[2] M. Kowatsch and J. T. Lafferl, "A spread spectrum concept combining charp modulation and pseudonoise coding", *IEEE trans. on commun.* , vol. COM-31, No. 10 (1983).

[3] C. E. Cook, "Linear FM signal formats for beacon and communication systems", *IEEE trans. on aerosp. electron. syst* , vol. AES-10, July 1974, pp 471-478.

[4] R. E. Ziemer and R. L. Peterson, *Digital communications and spread spectrum systems* , New York, Macmillan, 1985.

[5] D. L. Zaytsev and V. I. Zhuravlev, " Noise immunity of digital data transmission system using linear frequency modulated signals", *telecommunication* , vol. 22, No. 4, 1968.

[6] G. F. Gott and J. P. Newsome, "Data transmission using chirp signals", *Proc. IEEE* , vol. 118, Sept 1971, No. 9, pp. 1162-1166.

[7] A. K. Elhakeem and Ali Targi, "Performance of hybrid chirp/DS signals under Doppler and pulsed jamming", *GLOBCOM' 89 IEEE Communication society* , paper 45.5.1, pp. 1618-1623, 1989.

[8] Ali Targi, A. K. Elhakeem, T. Le-Ngoc and Anisur Rahman, "Error and thoughput performane of multidecoded erasure-bassed direct sequence/time hopping selection diversity multi-access Systems", *ICC SUPERCOM' 90 IEEE Commnunication Society* , paper 289, session: 340.5, April 1990.

[9] M.K. Simon, J.K. Omura, R.A. Scholtz, and B.K. Levitt, *Spread spectrum communications* , computer science press, 1985.

[10] E. Geraniotis and Jeffrey W. Gluck, "Coded FH/SS communications in the presence of combined partial band noise jamming, rician nonselective fading and multiuser interference", *IEEE journal of selected areas in communication* , vol. SAC-5, No. 2, pp. 194-213, February 1987.

[11] Clark and Cain, *Error-correction coding for digital communications* , New York, Plenum Press 1981.

[12] M.B. Pursley and W.E. Stark, "Performance of Reed-Solomon coded frequency hop spread spectrum communications in partial-band interference", *IEEE trans. on commun.* , vol. COM-33, No. 8, pp. 767-774, August 1985.

[13] W.G. Lee, *Mobile communications engineering* , New York, McGraw-Hill Company, 1982.

[14] D.V. Sarmete and M.B. Pursley, "Crosscorrelation properties of pseudorandom and related sequences", *Proceedings IEEE* , vol. 68, pp. 593-619, May 1980.

[15] S. Lin and Daniel J. Costello, *Error control coding fundamentals and application* , New Jersey, Prentice-Hall, 1983.

[16] R. C. Dixon, *Spread spectrum techniques* , IEEE Press, 1976.

[17] George R. Cooper and clare D. Mc Gillen, *Modern communications and spread spectrum* , USA, Mc Graw-Hill, 1986.

[18] R. C. Dixon, *Spread spectrum systems* , New York, Wiley & sons, 1985.

[19] Claudio Conticello, " Spread spectrum communication: an overview ", FI ALTA FREQUENZA , vol. LVI-N. 6, AUG. 1987.

[20] Michael A. Komar and Carl F. Andren, " Digital chirp modulation ", *IEEE trans commun* , vol. Com , 1985, pp. 30 - 34.

[21] Hhamles M. El-shennawy, Onsy Abdel Alim and M. A. Ezz-El-Arab, " Linear FM chirp filters in pulse compression radars ", *IEEE trans*

instrumentation and measurement , vol. IM-36, No. 3, Sep. 1987, pp. 783-788.

[22] Evaggelos A. Geraniotis, " Coherent hybrid DS-SFH spread spectrum multiple-access communications ", *IEEE journal on selected areas in commun.* , vol. SAC-3, No. 5, Sep. 1985, pp. 695-705.

[23] Evaggelos A. Geraniotis, " Non coherent hybrid DS-SFH spread spectrum multiple-access communications ", *IEEE trans. on commun.* , vol. COM-34, No. 9, Sep. 1986, pp. 862-872.

[24] Roger Allon, " Spread spectrum rf schemes keep military signals safe ", *electronic design* , Apr. 3, 1986, pp. 11-122

[25] M. Kavehrad and P. J. Mc lane, " Spread spectrum for indoor digital radio ", *IEEE communications magazine* , 1987, pp. 32-40.

[26] J. E. Mazo, " Some theoretical observations on spread-spectrum communications " , *The bell system technical journal* , Nov. 1979, pp. 2013-2023.

[27] Robert A. Scholtz, " The spread spectrum concept " , *IEEE trans. on commun.* , vol. COM-25, No. 8, AUG. 1977, pp. 748-755.

[28] Gaylord K. Huth, " Optimization of coded spread spectrum system perfornance " , *IEEE trans. on commun.* , vol. COM-25, No. 8, AUG. 1977

[29] R. C. Dixon, " Why spread spectrum ? ", *IEEE commu. society magazine* , July 1975, pp. 21-25.

[30] William F Utlout, " Spread spectrum: principles and possible application to spectrum utilization and allocation ", *IEEE commun. society magazine* , Sep. 1978, vol. 16, No. 5, pp. 21-31.

[31] Marlin P. Ristenbatt and James L. Daws, " Performance criteria for Spread Spectrum Communications ", *IEEE trans. commun.* , vol. COM-25, No. 8, AUG. 1977, pp. 756-762.

[32] A. K. El-hakeem, G. S. Takhar and S. C. Gupta, " Acquisition of spread spectrum codes in hybrid systems ", *IEEE intern. conference on Commu.*, paper 35.5.1, 1978.

[33] Tzannes, *Communication and radar systems* , U.S.A., Prentice-Hall, 1985.

[34] G. P. Kefalas, " Combination of digital phase shift keying and chirp modulation", *IEEE trasn. on aerospace and electronic systems*, vol. AES-17, No. 2, March 1981, pp. 300- 303.

[35] David L. Nicholson, *Low probability of exploitation and anti-jam spread spectrum communications* , Virginia, Nov. 1987.

[36] Albert J. Berni and William D. Gregg, " On the utility of chirp modulation for digital signaling", *IEEE trans. on commu., June 1978, pp. 748-751.*

[37] W. Hirt and S. Pasupathy, " Continous phase chirp (CPC) signals for binary data communication - part I: Coherent detection", *IEEE trans. on commu. vol. COM-29, No. 6, June 1981, pp. 836-847.*

[38] Wayne E. Stark, " Coding for frequency-hopped spread spectrum communication with partial-band interference - part II: Coded performance", *IEEE trans. on commun. vol. COM-33, No. 10, OCT 1985, pp. 1045-1057.*

[39] J. E. Wieselthier and A. Ephremides, "Discrimination against partially overlopping interference - its effect on throughut in frequency-hopped multiple access channels", *IEEE trans. on commun., vol. COM-34, No. 2, Feb. 1986, pp. 136-142.*

[40] M. R. Winkler, "Chirp signals for communications", *IEEE WESCON conv. Rec.* , 1962.

[41] M. Kowatsch, F. J. Selfert and J. Lafferl, "Comments on transmission system using pseudonoise modulation of linear chirp", *IEEE trans on aerospace and electronic systems* , vol. AES-17 March 1981, No. 2, pp 300-

303.

[42] Jerry L. Eaves and Edward K. Reedy, " Principles of modern radar ", New York, Van nostrand Reinhold, 1986.

[43] R. L. Harris, "Introduction to spread spectrum techniques ", U.K., Christchuh Hampchire, 1973.

APPENDIX A

Evaluation of the Signals envelop at the Chirp Matched Filters

In this appendix we derive the envelopes of the inputs of the mark and space chirp matched filters of the receiver under Doppler and code delay (only the signal part we derive here, the noise and jammer is treated separately by the quasistatic averaging analysis explained in page 57,63).

Equation (3.4) gives the input signal to the MF containing the mark signal $(+\mu)$

$$f(t) = \cos((\omega_o + \Delta + \mu\tau)t + \frac{1}{2}\mu t^2 + \phi'_k) \tag{A-1}$$

where

$$\phi'_k = \phi_k + \frac{\mu\tau^2}{2} + \Delta\tau + \mu\tau \tag{A-2}$$

and $\omega_o = 2\pi f_o$.

ϕ_k is a uniformly random variable in the interval $(-\pi, \pi)$, and τ is also a uniformly distributed random variable in the range of $0 \leq |\tau| \leq T_c/2$.

$$S_1(\omega) = \int_{-T_1/2}^{T_1/2} \cos(\omega_o + \mu_1\tau + \Delta)t + \frac{1}{2}\mu_1 t^2 + \phi'_k)e^{-j\omega t}\, dt$$

$$= \int e^{j[(\omega_o - \omega + \mu_1\tau + \Delta)t + \frac{1}{2}\mu_1 t^2 + \phi'_k]}\, dt \tag{A-3}$$

$$+ \int e^{-j[(\omega_o + \omega + \mu_1\tau + \Delta)t + \frac{1}{2}\mu_1 t^2 + \phi'_k]} dt$$

Following the reduction in [1], where $\mu_1 = 2\pi F / T_b$, we obtain

$$S_1(\omega) = \frac{1}{2}\sqrt{\frac{\pi}{\mu_1}}\, e^{-j[(\omega_o - \omega + \mu_1\tau + \Delta)^2 \frac{1}{2\mu_1} - \phi'_k]} \cdot [C(U_1) + jS(U_1) + C(U_2) + jS(U_2)] \tag{A-4}$$

where

$$C(x) = \int_0^x \cos\left(\frac{\pi}{2}y^2\right) dy$$

$$S(x) = \int_0^x \sin\left(\frac{\pi}{2}y^2\right) dy$$

$$U_1 = \sqrt{\frac{1}{\pi\mu}}\left[\mu_1\frac{T}{2} + (\omega_o - \omega + \mu_1\tau + \Delta)\right]$$

and

$$U_2 = \sqrt{\frac{1}{\pi\mu_1}}\left[\mu_1\frac{T}{2} + (\omega_o - \omega + \mu_1\tau + \Delta)\right]$$

Realizing that the term in the square bracket in (A-4) is almost a constant, we obtain the generalized compression filter function of the first MF, i.e

$$H_1(\omega) = e^{j((\omega_o - \omega)^2/2\mu_2)} \tag{A-5}$$

Similarly, the transfer function of the second filter is given by

$$G_1(\omega) = e^{j((\omega_o - \omega)^2/2\mu_2)} \tag{A-6}$$

where $\mu_2 = -\mu_1$, the first MF output spectrum is given by

$$G_1(\omega) = S_1(\omega)\, H_1(\omega) \tag{A-7}$$

and the output time function is given by

$$\begin{aligned} y_1(t) &= \frac{1}{2}\int_{-\infty}^{\infty} G_1(\omega)\, e^{j\omega t}\, d\omega \\ &= \frac{1}{2\pi}\int_{-\infty}^{\infty} S_1(\omega)\, e^{j\omega t}\, d\omega \\ &= \frac{1}{2\pi}\int_{-\infty}^{\infty} e^{j(\omega_o - \omega)^2/2\mu_1} \\ &\quad \cdot \int_{-T_b/2}^{T_b/2} e^{j\left[(\omega_o + \mu_1\tau + \Delta - \omega)\tau' + \phi'_k + \frac{1}{2}\mu_1\tau'^2\right]} d\tau'\; e^{j\omega t}\, d\omega \end{aligned} \tag{A-8}$$

following a suitable change of variables, we obtain,

$$\begin{aligned} y_1(t) &= \sqrt{\frac{2\mu_1}{2\pi}}\int_{-T_b/2}^{T_b/2} \\ &\quad \cdot e^{j\left[\frac{\omega_o^2}{2\mu_1} + \mu_1\tau'\tau + \omega_o t + \frac{1}{2}\mu_1\tau'^2 - \frac{1}{2\mu_1}(\omega_o + \mu_1\tau' - t)^2 + \phi'_k\right]} \int_{-\infty}^{\infty} e^{jx^2} dx\, d\tau' \end{aligned} \tag{A-9}$$

where $$x = \frac{(\omega - (\omega_o + \mu_1\tau' - \mu_1 t}{\sqrt{2\mu_1}}$$

but

$$\int_{-\infty}^{\infty} e^{jx^2}\, dx = \int_{-\infty}^{\infty} (\cos x^2 + j \sin x^2) dx = \sqrt{\pi} e^{j\pi/4}$$

so

$$y_1(t) = \sqrt{\frac{\mu_1}{2\pi}} e^{j(\omega_o t - \frac{\mu_1}{2}t^2 + \frac{\pi}{4} + \phi'_i)} \cdot \int_{-T_b/2}^{} e^{j(\mu_1\tau + \Delta + \mu_1 t)\tau'} d\tau' \tag{A-10}$$

$$= \sqrt{\frac{2\mu_1 T_o^2}{\pi}} e^{j(\omega_o t - \frac{\mu_1 t^2}{2} + \frac{\pi}{4} + \phi'_i)} sinc\,(\mu_1\tau + \Delta + \mu_1 t)T_o$$

defining μ_1 in terms of the frequency sweep F and duration T_b, $\mu_1 = \frac{2\pi F}{T_b}$, the output becomes

$$y_1(t) = \sqrt{FT}\, e^{j(\omega_o t - \frac{\pi F T_b}{T} + \frac{\pi}{4} + \phi'_i)} sinc\,(\pi F\tau + \frac{\Delta T_b}{2} + \pi F t) \tag{A-11}$$

where $-\frac{T_b}{2} < t < \frac{T_b}{2}$. for the mark signal passing through the space matched filter (2 sup nd filter), we obtain,

$$y_2(t) = \frac{1}{2\pi} \int_{-T_b/2}^{T_b/2} e^{j(\omega_o - \omega)^2/2\mu_2} \cdot \int_{-T_b/2}^{T_b/2} e^{j[(\omega_o + \mu_1\tau' + \Delta - \omega)\tau' + \phi'_i + \frac{1}{2}\mu_1\tau'^2]} d\tau'\, e^{j\omega t}\, d\omega \tag{A-12}$$

Following the same earlier steps we get,

$$y_2(t) = \sqrt{\frac{\mu_2}{2(\mu_1 - \mu_2)}}\, e^{j(\omega_o t - \frac{\mu_2 t^2}{2} + \frac{\pi}{4} + \phi'_i - \frac{(\mu_1\tau + \Delta + \mu_2 t)^2}{2(\mu_1 - \mu_2)})} \cdot \int_{x_1}^{x_2} e^{j\frac{\pi}{2}x^2}\, dx \tag{A-13}$$

where

$$x_1 = \sqrt{FT_b} + \sqrt{\frac{F}{T_b}}\left(\tau + \frac{\Delta T_b}{2\pi F} - t\right) \tag{A-14}$$

$$x_2 = -\sqrt{FT_b} + \sqrt{\frac{F}{T_b}}\left(\tau + \frac{\Delta T_b}{2\pi F} - t\right) \tag{A-15}$$

reducing, we obtain,

$$y_2(t) = \sqrt{\frac{\mu_2}{2(\mu_1 - \mu_2)}}\, e^{j\left(\omega_0 t - \frac{\mu_2 t^2}{2} + \frac{\pi}{2} + \phi' t - \frac{(\mu_1\tau + \Delta + \mu_2 t)^2}{2(\mu_1 - \mu_2)}\right)} \cdot [C(x_1) + jS(x_1) + C(X_2) + jS(x_2)] \tag{A-16}$$

magnitude of $y_2(t)$ is given by,

$$\sigma(\tau, \Delta) = \frac{1}{2}\sqrt{(C(x_1) + C(x_2))^2 + (S(x_1) + S(x_2))^2} \tag{A-17}$$

where $C(.)$, $S(.)$ are the predefined Fresnel integrals.

APPENDIX B

Evaluation of the Probabilities $P_{1,l}$, $P_{2,l}$, $P_{3,l}$, $P_{4,l}$

We follow an approach similar to [10], [11] to evaluate the probability of $P_{1,l}$, $P_{2,l}$, $P_{3,l}$, $P_{4,l}$ of equations (38), (41). We start with the modified erasure-error $P_{3,l}$ (a similar one yields $P_{4,l}$ and the procedures will be similar). For evaluating $P_{3,l}$ we first take an (n, k) BCH code of word length n and message left of k bits. The number of erasures that can be corrected is $e = (n - k)$ and the number of errors that can be corrected is $t \geq \left\lfloor \frac{n-k}{m} \right\rfloor$. For details on correcting erasures the reader is referred to [11] and Appendix E. For the first and second decoders in Fig. 4. 6, many erasures are modified according to Fig. 4.5. and all errors and erasures are corrected straightforwardly as in [10]. The probability of an BCH bit symbol error at the decoder is given by

$$P_{1,l} = P_{2,l} \sum_{\alpha}^{n} \sum_{\substack{\alpha+\beta \leq n \\ (t+1) \leq 2\beta+\alpha}} \frac{(\alpha+\beta)}{n} \begin{bmatrix} n \\ \alpha \end{bmatrix} \begin{bmatrix} n-\alpha \\ \beta \end{bmatrix} q_l^{-\beta} \theta_l^{-\alpha} \cdot (1 - \overline{q}_l - \overline{\theta}_l)^{n-\beta-\alpha} \tag{B-1}$$

where $\overline{q}_l$, $\overline{\theta}_l$ are the modified error and erasure probabilities derived from (41), (42), respectively, i.e., $\overline{\theta}_l = \theta_l^2$. Clearly, we have to have two erasures in the same bit location if we are to have an erasure resulting finally two TH frames to have (according to the erasure modification of Fig. 4.5, while

$$\overline{q}_l = \mu_l (1 - \theta_l)^2 \tag{B-2}$$

It is clearly seen from (B-1), (B-2), that the erasure modification logic of Fig. 4.5 decreases the erasure probability and increases the probability of bit errors (since we replace erasures from one TH slot by demodulated bits that might be in error from the other TH slot).

In the combined erasure-error case (that of $P_{3,l}$, $P_{4,l}$ of Fig. 4.6), the decoded bits of the erasure decoder is taken as long as the number of erasures per code word (n bits) is less than or equal to e above. If the number of erasures exceeds e, the decision device takes the result of the error-detection decoder.

It is easily seen that the symbol is always correct if no more than $(n - k)$ erasures occur in the decoder input. This is due to the assumption of perfect side information and no background noise. If more than $(n - k)$ erasures occur, the output of the combined decoder will be the output of the error correction decoder (Fig. 4.6).

In the first case the probability of BCH decoding symbol error is given by

$$f_{1,l} = \sum_{\alpha=0}^{e} \binom{n}{\alpha} \theta_l^{\alpha} (1 - \theta_l)^{n-\alpha} \sum_{\substack{\beta=1 \\ e+1 \le 2\beta+\alpha \\ n \le \alpha+\beta}} \frac{\alpha + \beta}{n} q_l^{\beta} (1 - q_l)^{n-\alpha-\beta} \qquad \text{(B-3)}$$

where the probability of having e or less erasures out of n bits is given by the polynomial term of the first summation (over α) and the term in the second sum gives the probability of the erasure decoder being unable to correct more than (e) bits (β errors and α erasures) where the constraint $e \geq (2\beta + \alpha)$ is satisfied (to cause decoding errors). On the other hand, if the applicable TH slot has a high amount of multiaccess interference such that the number of erasures is $> e$, we obtain

$$f_{2,l} = \sum_{\alpha=e+1}^{n} \binom{n}{\alpha} \theta_l^{\alpha} (1 - \theta_l)^{n-\alpha}$$

$$\cdot \sum_{\substack{\beta=1 \\ (t+1)\le(\beta+\alpha \\ \beta\le\alpha \\ n-\alpha\ge\gamma}} \sum_{\gamma=1}^{n} \frac{\beta+\gamma}{n} \binom{\gamma}{\beta} \mu_l^{\beta} (1-\mu_l)^{\alpha-\beta}$$

$$\cdot \binom{n-\alpha}{\gamma} q_l^{\gamma} (1-q_l)^{n-\alpha-\gamma} \tag{B-4}$$

where μ_l is given by (25) and the binomial coefficient involving μ_l gives the probability of β bits in error when the erasure is declared. q_l is given by (42) and the involved binomial term gives the probability of γ bits the erasure is not declared $(n - \alpha)$ is the number of bits where the erasure is not declared $(n - \alpha - \gamma)$ is the number of bits received correctly, and the decoder makes an error (giving rise to $f_{2,l}$) when $(\beta + \gamma)$ exceeds t. Now the performance of the third and fourth decoders of Fig. 4.6 (the parallel decoders) is represented by the probability of symbol decoding error probability, i.e.,

$$P_{3,l} = P_{4,l} = f_{1,l} + f_{2,l} \tag{B-5}$$

In all cases the probability of bit error decoding follow by easily from symbol errer (either $P_{1,l}$, $P_{2,l}$, $P_{3,l}$, $P_{4,l}$)

$$P_b = \frac{2^{k-1}}{2^k - 1} P_s \tag{B-6}$$

where $P_s = P_{1,l}$, *or* $P_{2,l}$, *or* $P_{3,l}$, *or* $P_{4,l}$ depending on the case studied. In the results of Chapter 4 $2^k - 1 = 127$ so $k = 7$

$$P_b \approx \frac{1}{2} P_s \tag{B-7}$$

It is to be noted that all the presented results of the Chapter 4 are for the case of word and packet errors, bit errors not shown in the Figures.

APPENDIX C

The Doppler Effect

The Doppler frequency is a function of the relative velocity of the receiver and transmitter and of the frequency transmitted. To clear this let consider a radar with a frequency of $f = 1/T_0$, where T_o is the period of the transmitted wave, and a target moving at a constant speed, v toward the radar at time $t = t_o$, let $R = R_o$ be the target range, and assume at t_o the peak of the wave is A. At time $t = t_o + T_o$, the peak is B, at this time, let the target's range is $R = R_1$. The time necessary for the point A to travel from the radar to the target is Δt

$$\Delta t = \frac{R_0 - v\,\Delta t}{c} \tag{C-1}$$

or

$$\Delta t = \frac{R_o}{c + v}$$

where v is the target constant speed, c is the wave's speed (the speed of the light. The total round trip takes $2\Delta t$, and the point A returns to the radar at time

$$t_1 = t_o + \frac{2R_o}{c + v} \tag{C-2}$$

and for point B at time

$$t_2 = t_o + T_o + \frac{2R_1}{c + v} \tag{C-3}$$

since t_1 and t_2 are the time of arrival of two peaks of the wave, the period of the received wave, T'_o, is $t_2 - t_1$, or

$$T'_o = T_o - \frac{2(R_o - R_1)}{c + v} \tag{C-5}$$

From (C-5) it can be seen, the period (frequency) of the received wave decreases (increases) from the period (frequency) of the transmitted wave due to scattering from a moving target. This is the Doppler effect.

In Chapter 3 Doppler effect was taken by adding a prespecified frequency offset Δf from the carrier frequency. The Doppler representation we adapted [9], [18] (i.e. the Doppler is represented by adding or subtracting (Δf) a small frequency increment to the carrier (ω_c).

APPENDIX D

Matched Filters

The concept of matched filter is a very general notion. A filter matched to a given input signal is an optimum filter for signal reception when the received signal is corrupted by AWGN. The filter is optimum in several senses, this include maximizing the output signal-to-noise ratio, and maximizing the accuracy of parameter estimation (parameters such as delay, Doppler frequency, and signal amplitude). A matched filter to an input signal $s_i(t)$ with spectrum $S_i(f)$ is defined in terms of the matched filter transfer function $H(f)$ and the corresponding impulse response function $h(t)$ as follows:

$$H(f) = GS_i^*(f)\, e^{-j2\pi fT} \tag{D-1}$$

and

$$h(t) = Gs_i^*(T - t) \tag{D-2}$$

where G is gain (or loss) of the filter, T is a fixed delay through the filter, and $H(f)$ is the Fourier transform of $h(t)$. The asterisk refers to the conjugate form. The basic relationships stated in (D-1) and (D-2), assuming unity gain and fixed time delay of zero through the filter, are

$$H(f) = S_i^*(f) \tag{D-3}$$

and

$$h(t) = s_i^*(-t) \tag{D-4}$$

Complex quantities are implied throughout. The transfer function of a filter matched to any signal, except for a linear phase versus frequency slope, is

proportional to the conjugate of the spectrum of the signal. The matched filter impulse response, except for a fixed delay, is proportional to conjugate of the time inversion of the signal.

For the detection of signals in colored (nonwhite) noise of $S_n(f)$ it is known that if a white noise signal with power spectral density $\frac{1}{2}$ is passed through a filter with transfer function $H(f)$, the power spectral density of the output will be $S_o(f) = |H(F)|^2 \frac{1}{2} N_O$. Suppose we imagine that the colored noise at the receiver input is the result of passing white noise with power spectral density of unity through a filter with transfer function $H_c(f)$, where the subscript c denotes (channel). Thus

$$S_n(f) = 1\,|H_c(f)|^2 \tag{D-5}$$

At the receiver we can imagine making the noise, $n(t)$, white again by passing the signal plus noise through a filter with transfer function of magnitude

$$|H_w(f)| = \frac{1}{|H_c(f)|} = \frac{1}{\sqrt{S_n(f)}} \tag{D-6}$$

where the subscript w stands for (whitening). we note that $S_n(f) \geq 0$ for all f, so there is no problem with taking the square root. We will not worry about the realizability of $H_w(f)$ we assume zero phase response for convenience.

The signal portion of the input is distorted in passing through the whitening filter. Now instead of having $s_1(t)$ or $s_2(t)$, the tow received signals, we have $\tilde{s}_1(t)$ or $\tilde{s}_2(t)$, where

$$\mathbf{F}[s_1(t)] = \tilde{\mathbf{L}}_1(f) = \mathbf{L}_1(f)\mathrm{H_w}(f) = \frac{\mathbf{L}_1(f)}{\sqrt{\mathrm{S_n}(f)}} \tag{D-7}$$

and

$$\mathbf{F}\,[se_2(t)] = \tilde{\mathbf{L}}_2(f) = \mathbf{L}_2(f)H_w(f) = \frac{\mathbf{L}_2(f)}{\sqrt{S_n(f)}} \tag{D-8}$$

The advantage of this approach is that we know the form of the optimum receiver for white noise. Thus, we simply proceed it by the whitening filter, and the optimum receiver for colored noise is the cascade of the whitening filter and the optimum receiver for white noise. The transfer functions of $\tilde{s}_1(t)$ and $\tilde{s}_2(t)$ matched to filters are

$$\tilde{\mathbf{L}}_i^*(f)\,e^{-j2\pi Tf} = \mathbf{L}_i^*(f)\,\frac{e^{-j2\pi Tf}}{\sqrt{S_n(f)}} \tag{D-9}$$

where $i = 1, 2$. When cascade with the whitening filter, we obtain filters with the transfer functions

$$H_i(f) = \mathbf{L}_i^*(f)\,\frac{e^{-j2\pi Tf}}{\sqrt{S_n(f)}} \tag{D-10}$$

where $i = 1, 2$.

APPENDIX E

Parallel Decoding

Starting by describing the technique as presented by [12] and then its modification for the case in chapter 4.

At the demodulation decoding system shown in Fig.(E-1). First the signal is de-hopped and demodulated. Where the output of the de-hopper is a sequence of L diversity receptions for each of the n code bits. Side information regarding the presence of interference is extracted from the de-hopper and demodulator. The L diversity receptions of a given symbol are employed along with the side information to form the decision statistic. The side information is used to attach flags to unreliable diversity receptions. The diversity combiner forms the square-law combination of all unflagged diversity receptions. In case of at least one of the diversity receptions is not flagged, the decision device will be presented with a noise-free bit. If all of the diversity reception of a particular bit i have been flagged, the diversity combiner output is the square-law combination of all L diversity receptions and the decision device is presented with a noisy symbol. A (hard) binary decision must be made on the symbol, and it is fed into the error-correction decoder. For any bit in which all diversity receptions are flagged, the erasure-correction decoder sees only an erasure.

In Chapter 4 we don't consider the L diversity combining before decoding as in [12], rather we attach flags (erasures) to BCH bits as in Fig(4.4) independently (i.e. $L = 1$). The fact that we have 2 time hopping slots for each, is utilized later after decoding, this is the main difference. The following analysis mainly applies to the case of Chapter 4.

A BCH (n, k) code will correct up to $e = n - k$ erasures out of n bits or up to $t = (n - k)/m$ errors out of n symbols. In general it will correct any combination of ϵ erasures and τ errors provided that $2\tau + \epsilon$ does not exceed $n - k$ (see [10], and in practice, the erasure correction decoder of Fig.(F-1) should probably correct a small number of errors that might be caused by low-level background noise or other interference on the channel.

The error correction decoder input contains no erasures; it is a sequence of binary bits in the case of Chapter 4, from the output of the decision device $G_1(u)$, $G_2(u)$ of Fig. 4.3. The input to the erasure correction decoder has an erasure in each position, where the erasure threshold is exceeded ($D_1(u)$, $D_2(u)$ in Fig. 4.3), and a binary bit in each position where the threshold is not exceeded The erasure system counts how many erasures it makes, and if the number does not exceed e, the erasure correction decoding algorithm produces the correct answer (see Appendix G). The erasure correction decoder does not attempt to decode if the number of erasures exceeds e. If there are too many erasures, the erasure correction decoder defaults to the error correction decoder, who does not haretle erasures (i. e. side information is lost) . The error correction decoder is continually receiving the output of the decision device and attempting to decode. Most of the time it can decode, and its output will agree with the output of the erasure correction decoder. An important property of bounded distance decoding of BCH codes is that with high probability, it will default rather than decode into an incorrect codeword when the number of errors exceeds t. Thus, with high probability, the receiver will know if the two decoders have decoded correctly or not.

Appendix B shows the decoding bit error probability using the above parallel decoding in the different cases of erasure handling presented in Chapter 4.

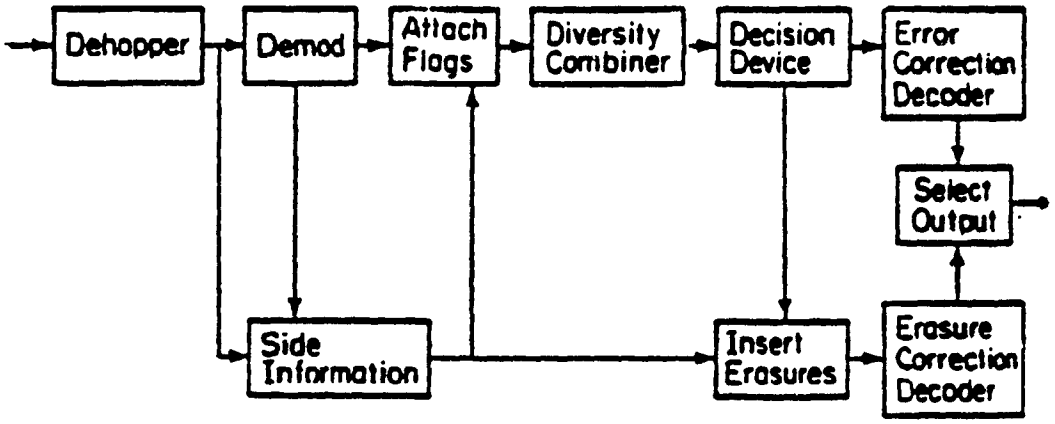

Fig. (E-1):- Demodulator/Decoder block diagram [12]

APPENDIX F

Definition of Binary BCH Codes

BCH codes are a large class of cyclic codes that include both binary and non-binary alphabets. Binary BCH codes may be constructed with parameters

$$n = 2^m - 1$$
$$n - k \leq mt$$
$$d_{\min} = 2t + 1$$

where m ($m \geq 3$) and t are arbitrary positive integers. This class of binary codes provides the communications system designer with a large selection of block lengths and code rates. In Chapter 4 an (127, 71, 10) BCH code was selected where $m = 7$ and $t \approx 9$ bits of this code, tepecally message size is in power of 2 so we have to feed the difference between 71 and 64 with zeros when we form messages, to feed the encoder. However our affective code rate is $\frac{64}{127} \approx 0.5$, actually those dame bits can be used at the decoder, in our results we did not perssume this improvement. Also we will not concerned actually with the algebraic struction of the BCH codes, we will only concerned with their error correction behavior (i.e. $t = 9$), we did not look in their obligations

A nonbinary block code consists of a set of fixed-length code words in which the elements of the code words are selected from an alphabet of q symbols. denoted as $\{ 0, 1, 2, \ldots, q - 1 \}$. Usually, $q = 2^m$ so that m information bits are mapped into one of the q symbols. The length of the nonbinary code word is denoted as n and the number of information symbols encoded into a block of n symbols is denoted as n. The minimum distance of the nonbinary code is

APPENDIX G

Correction of Errors and Erasures in BCH and RS codes

The BCH decoding algorithm does not generalize to utilize demodulator soft decision in a direct fashion (decoder works on samples received signal in noise as interference .. etc as oppressed to the case of hard decision where the decoder works on demodulated bits or symbols depending on the case). The only approaches that have been used require multiple application of the hard decision decoding algorithm. In the special case of demodulator erasures, an algebraic decoding approach is possible such as Berlekamp algorithm which is beyond the scope of this thesis (see [11]. That is , if the code is defined over the field $GF(q)$, then the demodulator is assumed to have the normal q outputs pulse as $(q+1)th$ output corresponding to an erasure. The erasure output is assumed to contain absolutely no information about which of the q possible symbols was actually transmitted. Unfortunately, this decoding algorithm does not provide significant additional gain on the Gaussian channel. It is of benefit, though, on certain interference channels where the interference may be detected and treated as erasures. Assume the code has minimum distance d and a received word contains e erasures, then the e (erased) positions can be ignored in the decoding process. However, even ignoring these positions, all code words will differ in at least $d - e$ of the remaining positions allowing correction of up to

$$t_m = \left[\frac{d - e - 1}{2} \right]$$

channel error is addition to the erasures. Thus, all combinations of v channel

errors and e erasures are correctable providing that

$$2v + e < d$$

The algorithm for erasure and error correction with binary BCH codes goes as follow. Assume that a BCH code is designed to correct t errors, and that the received word contains e erasures. The decoding algorithm ,first replace the e erased position with zeros and decode the resulting word using the standard BCH decoding algorithm. Second, replace the e erased positions with ones and decode in the same fashion. Finally, select from the two code words obtained, the one corresponding to the smallest number of errors corrected outside the e erased positions. This algorithm allows results in correct decoding when (G-2) is satisfied. Assume that when the e erasures are replaced by zeros, $e^* \leq e/2$ channel errors are introduced in those e positions making a total of $v + e^* \leq t$ errors which are guaranteed correctable when $2v + e \leq 2t$. On the other hand, if $e^* > e/2$ then only $e - e^* < e/2$ channel errors are introduced when replacing the e erasures by ones. In this case the resulting pattern of $v + (e - e^*) < t$ errors is also correctable. Correction of erasures is more difficult with nonbinary BCH codes.

Based on the above one might imagine the large complexity and time consented in handling erasures by using RS codes since for type (127, 71) code, 127 decoding ties are needed may be more. So for handling erasures we straightly recommend BCH codes, to try all possibilities we need (W^N) where W is number of errors, N is alphabet size.